"ELECTROACTIVE POLYMERS AND BIOSYSTEMS:
NEW DIRECTIONS IN ELECTROACTIVE POLYMER MATERIALS FOR
BIOMIMETIC AND INTERACTIVE PROCESSES"

JULY 30 – AUGUST 3, 2001

IL CIOCCO (LUCCA, TUSCANY, ITALY)

FINAL PROGRAM and EXTENDED ABSTRACTS

Organized by:

CENTRO INTERDIPARTIMENTALE DI RICERCA"E. PIAGGIO",
UNIVERSITY OF PISA, ITALY

Supported by:

OFFICE OF NAVAL RESEARCH INTERNATIONAL FIELD OFFICE (ONRIFO)
and
DEFENSE ADVANCED RESEARCH PROJECT AGENCY (DARPA)

REPORT DOCUMENTATION PAGE

Form Approved OMB No. 0704-0188

1. AGENCY USE ONLY (Leave blank)	2. REPORT DATE	3. REPORT TYPE AND DATES COVERED
	August 2001	July 30-August 3, 2001 Final

4. TITLE AND SUBTITLE

Electroactive Polymers and Biosystems: New Directions in Electroactive Materials for Biomimetic and Interactive Processes. Held in Lucca, Italy on July 30 – August 3, 2001. Final Program and Extended Abstracts.

5. FUNDING NUMBERS

6. AUTHOR(S)

7. PERFORMING ORGANIZATION NAME(S) AND ADDRESS(ES)

Centro Interdipartimentale di Ricerca :E. Piaggio"
University of Pisa
Pisa, Italy

8. PERFORMING ORGANIZATION REPORT NUMBER

9. SPONSORING/MONITORING AGENCY NAME(S) AND ADDRESS(ES)

Office of Naval Research,
European Office
PSC 802 Box 39
FPO AE 09499-0039

10. SPONSORING/MONITORING AGENCY REPORT NUMBER

11. SUPPLEMENTARY NOTES

This work relates to Department of the Navy Grant issued by the Office of Naval Research International Field Office. The United States has a royalty free license throughout the world in all copyrightable material contained herein.

12a. DISTRIBUTION/AVAILABILITY STATEMENT

Approved for Public Release; Distribution Unlimited.

12b. DISTRIBUTION CODE

A

12. ABSTRACT (Maximum 200 words)

The workshop, held in Lucca, Italy, 30 July – 3 August 2001, was sponsored by ONR-IFO and DARPA and was organized by the University of Pisa, Italy. Its aim was to evaluate the progress in research and assessment of new frontiers in the field of electroactive polymers and their potential applications in biomimetics and various other interactive processes. Presentations and topics were organized into six topical areas: (1) Biomimetics, (2) Molecular Actuators, (3) Neural Communications, (4) Biostructure and Tissue Engineering, (5) Artificial Sensors and Biosensors, and (6) Robotics and Biomechantronics.

13. SUBJECT TERMS

ONRIFO, Foreign reports

15. NUMBER OF PAGES

16. PRICE CODE

17. SECURITY CLASSIFICATION OF REPORT	18. SECURITY CLASSIFICATION OF THIS PAGE	19. SECURITY CLASSIFICATION OF ABSTRACT	20. LIMITATION OF ABSTRACT
UNCLASSIFIED	UNCLASSIFIED	UNCLASSIFIED	UL

**"ELECTROACTIVE POLYMERS AND BIOSYSTEMS:
NEW DIRECTIONS IN ELECTROACTIVE POLYMER MATERIALS FOR
BIOMIMETIC AND INTERACTIVE PROCESSES"**

JULY 30 – AUGUST 3, 2001

IL CIOCCO (LUCCA, TUSCANY, ITALY)

FINAL PROGRAM and EXTENDED ABSTRACTS

Organized by:

**CENTRO INTERDIPARTIMENTALE DI RICERCA "E. PIAGGIO",
UNIVERSITY OF PISA, ITALY**

Supported by:

**OFFICE OF NAVAL RESEARCH INTERNATIONAL FIELD OFFICE (ONRIFO)
and
DEFENSE ADVANCED RESEARCH PROJECT AGENCY (DARPA)**

COMMITTEE:

Scientific Director:
Danilo De Rossi (Center "E. Piaggio", University of Pisa, Italy)

Organizing Committee:
Arti Ahluwalia (Center "E. Piaggio", University of Pisa, Italy)
Len Buckley (Naval Research Laboratory, Washington, DC, USA)
Ben Mattes (SFST, Santa Fè, NM, USA)
Alberto Mazzoldi (Center "E. Piaggio", University of Pisa, Italy)
Phil Parrish (ONRIFO, London, UK)
Carlos Sanday (Naval Research Laboratory, Washington, Dc, USA)
Randy Sands (20504 Riggs Hill Way, Brookeville, MD, USA)
Steve Wax (DARPA, Defense Science Office, Arlington, Va, USA)

OBJECTIVE

This workshop is a venue of scientists from all over the globe involved in the fields of electroactive polymer, biomimetics, and bioengineering to explore new avenues of research and new applications involving natural and artificial systems. Researchers will be brought together to share ideas and techniques and learn about new results, thereby creating new collaborations, synergies and cross fertilizations. Another important objective of this meeting is to formulate criteria for the future integration of electroactive materials into new devices which exploit their intrinsic biomimetic and/or bio-interactive properties.

VENUE OF THE WORKSHOP:

"IL CIOCCO"
CENTRO TURISTICO INTERNAZIONALE
CASTELVECCHIO PASCOLI,
LUCCA,
ITALY

TEL: ++39-0583-7191
FAX: ++39-0583-723197

OVERVIEW

INTRODUCTION

A workshop for evaluation of progress in research and assessment of new frontiers in the field of electroactive polymers and their potential applications in biomimetics and various other interactive processes was held at Il Ciocco, Italy. The workshop was sponsored by ONR-IFO and DARPA, and was organized by the University of Pisa, Italy. The presentations and discussions were organized into six topical areas.: (1) Biomimetics, (2) Molecular Actuators, (3) Neural Communications, (4) Biostructure and Tissue Engineering, (5) Artificial Sensors and Biosensors, and (6) Robotics and Biomechatronics.

The workshop was organized to highlight the potential benefits of cross-disciplinary approach in this emerging field. A collection of speakers from various disciplines including medicine, biology, physics, polymer chemistry, materials and electronic engineering. The following provides highlights of the topics presented and discussed at the workshop.

BIOMIMETICS

Andre Dittmar of INSA-Lyon gave an overview of living issues which have evolved to act as sensors, actuators, structures in the micrometer and nanometer scales. Understanding the nature and function of these nature-made systems makes possible the development of microtechnics, signal processing and artificial intelligence. Professor Dittmar indicated a number of research frontiers and challenges which need to be solved. They include energy storage, high efficiency light emission, self-repair, multiple sensing, energy transmission, three-dimentional circuit design and biocompatibility. Success of nature developed over millions of years teaches us to utilize a multidisciplinary approach to replicate many of the processes in the nanometer scale.

Electroactive polymer gels offer great potential for biomimetics. The shape and volume changes resulting from electroactivity provide opportunities for direct conversion of chemical energy to mechanical work. George Jeronimidis of Reading University, UK has conducted several studies on the application of this class of polymers as actuators and vibration control devices. The polymer gels have one major deficiency and that is low stiffness. This prevents the effectiveness of force transmission, although the gels provide large displacements. Jeronimidis suggests integration of fibers to the gel to improve its force generation. He suggests that the fiber network, similar to muscles and plant cells, confines the swelling of the gels. The partial confinement magnifies the force, providing an effective conversion of chemical energy to mechanical work. Of course several issues such as hysterisis, response time, etc. need to be carefully examined. This study is an excellent example of learning from nature to fabricated man-made systems.

The topic of advanced textiles as a communication platform was presented by Holcombe, CCCSIRO, Australia. In addition to serving as a passive protector against elements with properties such as unidirectional sweat transport, thermal insulation and water repellency, the fabrics can be designed as wearable electronics for communications, computing and for monitoring physiological functions. Efforts are directed to design fabrics using non-woven, weaving and knitting technologies to produce 3-D structures of conductive grids and breathable membranes as substrates for printed circuits. Efforts are directed to study the integration of fabrics and conducting polymers.

JFV Vincent of University of Bath, in collaboration with reasearchers at the University of Reading, is developing a new type of gel-based robotic actuator capable of producing low translational speeds with low forces. The artificial system mimics biological systems used by sea cucumbers, brittle stars, starfish sea lilies and sea urchins. These animals have internally distributed

hydrostatic systems with total pressure generators associated with each tube foot. The tube feet are extended by internal pressures and retracted by the muscles. The researchers have developed a composite model to describe the control system and have fabricated cylindrical composite gels with embedded electrodes to produce movement, similar to the individual tube foot. The objective of the project is to produce an array of gel composites like a flying carpet which will act as a mobil surface to transport objects in predetermined directions.

T. Yamauchi and co-workers at Nagaoka University Japan have designed electroactive polymer gel membranes to act as bio-reactors utilizing the effects of electric fields on the change in volume and shape for transport of solutes and solvents through the pore channels. They have designed a system where the polymer gels act as chemical valves. These chemical valves could be used as bio-reactors through which the permeation of biochemical products can be controlled by the applied electric field.

B. Picasso of the University of Cagliari with his coworker A. Manuello, have conducted an interesting study on fish locomotion, both through a computational modeling approach as well as conducting experiments to measure propulsion of a fish by an oscillating tail. His work was motivated to understand Gray's Paradox (1936) which has stimulated significant research on the mechanics of fish locomotion. Experimentally, they have built a small scale prototype of a robotic fish using electroactive polymers and a test rig to measure all relevant parameters for propulsion. They have tested their results using a classical air foil theory based mathematical model developed by Lighthill. They have demonstrated quantitative agreements between the theoretically predicted thrusts and the experimental results. The study has potential use for marine application. A coordination of efforts in this area conducted at MIT, NRL and several other institutions would be most valuable.

MOLECULAR ACTUATORS

Dr. Baughman of the Honeywell Corporation (who has accepted a faculty position at the University of Texas-Dallas) presented results of an interesting study using carbon nanotubes and their potential application for artificial muscles, energy storage and energy harvesting. He is examining the use of carbon tubes as electromechanical actuators. He has demonstrated 50 times higher stress generation capability compared to natural muscles and 10 times higher actuator strain compared to high modulus ferroelectrics. Their best results to date show nanotube's youngs modulus of 10 Gpa and strain of 0.17%. They have also demonstrated that charge injection nanotubes can act as: (1) supercapacitors capable of charging and discharging in less than 20 ms, (2) actuators for microfluidic valves and (3) thermo-electrochemical cells for harvesting thermal energy with ten times higher thermopower than the high performance thermoelectrics.

Makoto Suzuki of Tohoku University, Japan has been studying the mechanism of protein motors since 1994. He has published a number of papers on the subject in the Journal of Physical Chemistry (1996, 1997) and other technical periodicals. The effort is directed towards studies of behavior of actin and myosin motor proteins which is known to generate a force for muscle contraction. By introducing a small change in the hydrophobicity gradient, he has shown a force generation of 5 pN, at a velocity of 108 μm/s with a step length > 60 nm. These very small protein motors can work effectively in a large thermal fluctuation environment.

Microrobots designed using polymer actuators were described by Olle Inganäs of Linköping University, Sweden. He has developed microminiaturized actuators of 10 μm dimension using bilayers of gold and polypyrrole. The devices provide electrochemically controlled motion in micrometer scales and are compatible with biological fluids. These devices can be used for moving

valves in microfluidic systems, electrical actuation and recording from nerve cells and for artificial muscles.

John Madden and coworkers at the Massachusetts Institute of Technology, USA are working on maximizing electro-mechanical conversion of conducting polymers for application in valves in human systems. One potential application is to replace defective bladder valves. The requirements for such a valve are compatibility with biological fluids operation under a pressure of 20 kPa and a force of about 2N, work/cycle of 0.01J, a time constant of 10s, a life of 5 years and a fatigue life of 100,000 cycles. They have designed on the molecular level a modified polypyrrole called polypyrroleand calixarene bithiophene which exhibits significantly improved efficiency.

Roy Kornbluh and coworkers at SRI International, USA are designing novel dielectiric elastomers to serve as actuators to engineer a muscle. An actuator must reproduce the features of a natural muscle with equivalent power and energy density, stress and strain resistance, speed of response, efficiency, controllability and mechanical impedance. A muscle is multifunctional, acting as an energy absorber and a variable stiffness structure, and contains sensing elements for motion control. Tests on dielectric elastomers show several important attributes of natural muscle. Kornbluh and coworkers have fabricated different designs such as flat actuators, diapharagms and tubular rolls. They have examined several biomimetic robot functions such as inchworm robots, serpentine manipulators and insect like walking robots. Their work is continuing with a focus on biomimetic features such as preflexive control, elastic energy storage and embedded proprioceptive feedbacks. They are looking at potential applications in micro devices, loudspeakers, pumps, rotary motors and oscillators. A very similar yet distinct-effort is being conducted by a group headed by Benjamin Mattes at Santa Fe Science and Technology, New Mexico, USA, to evaluate the electrochemical behavior and electromechanical actuation of polyaniline in non-acqueous electrolytes. This type of actuator relies on the effects of electrochemical stimuli on the change of the oxidation level of the polymer and hence the volume. Mattes et. al. have conducted bending actuation measurements of gilded polyaniline films partially immersed in a propylene carbonate electrolyte.

An interesting and thought stimulating paper was presented by Mohsen Shahinpoor, University of New Mexico, USA, on ionic polymer-conductor composites as potential candidates for biomimetic sensors, robotic actuators and artificial muscles. He has designed novel conducting polymer composite sheets with nanometer scale water particles. These polymer composites oscillate with a widely varying frequency in response to an applied voltage under 2V. The oscillation of these polymer sheets has a lifting capability equivalent to 40 times their weight.

Keld West and coworkers at the Risø National Laboratory, Denmark, are working on polypyrroles doped with alkyl benzene sulfonates. These conducting polymers are highly stable in aqueous systems and can be electrochemically oxidized or reduced in a reversible manner. This redux change is accompanied by a volume change in the polymer. They report actuation strains of 10% obtained by architecturing the electrodes in a corrugated configuration with the axis of the corrugation perpendicular to the actuation direction such that the electrodes are stiff in this direction and complaint in the actuation direction.

Leon Kane-Maguire and co-workers of the University of Wollongong, Australia, are studying the nature of attachment of biologically active molecules such as DNA and ATP to conducting organic polymers. They have evaluated the optical absorptance of the biologically active dopants in polyanilines in various pH conditions, changing from 3 to 6.

NEURAL COMMUNICATION

Ferdinando Mussa-Ivaldi, Northwestern University Medical School, USA, presented a highly challenging topic on connecting brains to robots: to create a machine capable of imitating a human brain. The challenge is that the nervous system of the simplest organism still outperforms the most advanced digital computers. The major obstacle to incorporating neural elements in machines is in our lack of understanding of the functions of brain tissues. He has made some remarkable progress in designing a mobile robot which acts as an artificial body that delivers sensory information to neural tissue and receives command signals from it. The experiment involves a robot and the brain of a sea lamprey (a fish). When the light sensors of the robot see a light source, they transform it to an oscillating voltage. Two stimulation electrodes are connected to two sides of a lamprey's brain. Two other probes collect the response signals from the brain to the spinal cord. The results are promising. His next study is on adaptive behavior, i.e. how does the brain computer gains experience.

Research on patterning the vertebrate retina was presented by Lucia Galli-Resta, Institute of Neuro Fisiologia, CNR, Italy. She is in the early stages of studying this complex research topic. Together with Arti Ahluwalia's group at Centro Piaggio, she is developing an understanding of the assembly of monolayers of orderly arranged functional photo receptors on a micro patterned substrate. The goal is to model retinal pathologies where vision is lost as a result of photo receptor degeneration.

Massimo Grattarola is a member of a sizable group of researchers working in the Neural and Bioelectronic Technology Department of the University of Genoa, Italy. The knowledge gained in the fields of physics (1800-2000), electronics (1950-2000) and biology is utilized to create a new field of research that the authors call Neuroengineering. Understanding the role of 10^{11} neurons x 10^{4} synapses or 10^{15} parallel nodes would lead to the recognition of brain plasticity, advances in neuroscience and new computer architecture. Development of thin-film based planar and 3-D arrays of microelectrodes to be coupled in vitro to a population of cultured neurons is the basis of this study.

J. U. Meyer and co-workers at the Fraunhofer-Institute for Biomedical Engineering, Germany (hhtp://www.medico.network.com) are engaged in microfabrication and micropatterning of 102 µm thick polyimide foils with embedded microelectrode arrays, conductive tracks and interconnects to be used as implantable devices for interfacing neural structures. The goal of this effort has been to build implantable devices for the retina and peripheral nerves. This work is referenced in a recent Scientific American Article: "Your bionic future", Fall 1994.

BIOSTRUCTURES AND TISSUE ENGINEERING

Gerald Pollack of the University of Washington, USA has been studying how nature produces motion, probing into the fundamentals of cell functions and examining how polymer-gel phase transitions can produce various types of movements typical of cell behavior. Among the many mechanisms discussed, the polymer-gel water affinity, that may account for the expansion to produce actuation, could have other potential application: Could this phenomenon be used for water storage? And, if reversible, could the stored water be recovered? This could provide a drinking water supply for trekkers in remote locations. Dr. Pollack has written a book on the subject which was published recently (www.cellsandgels.com) titled "Cells, gels' and the Engine of Life".

Pollack provided a detailed overview of several concepts of cell motion, cell growth and muscle contractions based on phase transitions.

Arti Ahluwalia and Giovanni Vozzi at the Interdepartmental Research Center "E.Piaggio", University of Pisa, Italy, are working on various methods related to tissue engineering using bioerodable polymers. The goal of their project is to engineer 2-D and 3-D neural arrays. Their approach takes advantage of a pressure activated nanosyringe glass and one of the approaches demonstrated by George Whitesides of MIT.

David Beebe of the University of Wisconsin, USA, is taking an approach alternate to the silicon-based IC-derived processing technology to fabricate microfluidic systems. His approach is using organic materials and liquid phase photopolymerization to design microvalves. He claims that the novel fabrication methods is simple, rapid and much more cost effective. Use of hydrogels is key to his processing approach.

G.G. Wallace, University of Wollongong, Australia is investigating the nature of biocommunication and the use of organic electrodes (replacing metals) to monitor and manipulate biosystems. Thus far all studies have been conducted using metal electrodes which are not necessarily compatible with biological fluids. He has fabricated polypyrrole electrodes containing antibodies, enzymes, DNA and living cells for communication at the molecular level. In yet another project he is developing anew class of wearable fabric based on sensors capable of monitoring strains and pressure in situ and in real time. Use of telemetry provides remote interrogation.

Danilo De Rossi of the Interdepartmental Research Center "E.Piaggio", University of Pisa, Italy, presented a thought provoking lecture on biomimetic and tissue engineering. He suggested that modern engineers are similar to latter day alchemists, trying to transform materials into living artefacts. The problem, he implied, was one of definition and the ability to generate static patterns with superimposed space and time dependent oscillations.

ARTIFICIAL SENSORS AND BIOSENSORS

Nicolas Franceschini of the Laboratory of Neurobiology, France is working on photoreceptors based on a critical analysis of fly optics. Flies are very small creatures which use a group of smart sensors for navigation in unknown environments and avoidance of obstacles. The photo receptor optical signals are processed on-board using 6000 pixels and about one million neurons. This level of performance is significantly advanced compared to mobile robots. Through a basic understanding of the principles involved in motion detection and using a simple neuron combined with a single photoreceptor cell on a retinal mosaic, they have designed a robot that will visually guide itself. They have demonstrated that the same principles of motion detection can be used by a flying robot to follow rough terrain. Their photo receptors consist of 25 μm lenses with 50 μm focal length packages in hexagonal arrays. The well arranged photo receptors are placed 50 μm behind each 1 μm diameter lens. Dr. Francesechini has published a number of papers on the subject and written a chapter in "Intelligent Vehicles II, Eds. M. Aoki and I. Masaki, p. 47-52 (1996).

Giulio Sandini of the University of Genova, Italy has constructed a humanoid robot. He has named it "Babybot". His group has developed a sensory motor technology for use with elastic actuators and controls, retina-like visual sensors, image stabilization and eye-head coordination. Babybot has two eyes, two ears and arms. It can move its arms and extend to touch an object. The arm, in coordination with inertial sensors, converts visual information (position of the objects in the image plane) to motor controls. These functions require eye-head coordination.

Another technology is being developed by Danilo DeRossi and his group at the University of Pisa, Italy to design high tech dressware by integrating electroactive polymer fibers into wearable garments. These garments will be capable of mechanical actuation and strain sensing. By coupling of these new classes of fabric with transistors and batteries, one could achieve functions such as sensing, actuating and processing and work in concert with human manipulative and gestural functions with the advantage of comfort and non-invasivness. One of the challenges is to develop multisensors embedded in synthetic material to provide information about the chemistry and physics of the environment. In a living system each sensor provides information on multiple variables in contrast with manufactured systems which usually respond to a single variable.

Paul Calvert at the University of Arizona, USA is working on constructing artificial bones made of a polymer and hydroxiappatite using freeform technology and imbedded sensors. Another approach is to use ink-jet printing technology to construct 5 layers of epoxy and 5 layers of amines. The goal of this project is to embed a large number of sensors in a synthetic system which can provide information on its surroundings.

Two papers on biosensors were presented by Krishna Persaud of UMIST, Manchester, UK working with a group from the University of Pune, India and Marco Mascini, University of Florence, Italy. The two approaches are distinct. One relates to the development of optical biosensors using Tiron-immobilized polypyrrole films to measure enzymes and the other relates to the development of DNA biosensors for detection of genetic disorders, polymorphism and pathogen microorganisms. Results of this effort were recently published (Biosensors and Bioelectronics 15 (2000) and Anal. Chim. Acta 418 (2000) 1-9).

Professor Dermot Diamond, Dublin City University, Ireland, presented a lecture on "smart fabrics" focussed on integration of autonomous devices which require very low power and can provide wireless communication to a remote point. He calls it "ubiquitous sensing". In addition to sensors capable of identifying selective species, accurate monitoring and wireless transmission to a base station, additional requirements include intimate contact with body fluids, a non-invasive approach for extended period sampling and in-situ calibration. A number of chemical and biological sensors have been designed including those from JPL and Kiser. Refer to a book on the subject published by Kinwer.

ROBOTICS AND BIOMECHATRONICS

An increasing demand for minimally invasive surgery and therapy has enhanced the need for miniature medical tools with improved diagnostics and flexibility. This need has brought a new set of engineering challenges to design machines in sizes ranging between 10 mm and 10 μm. P. Dario and his group at the Scuola Superiore Sant' Anna, Pisa, Italy are studying this topic. The emphasis of this effort is to design and build miniature devices for colonoscopy and neuroendoscopy. One of the major challenges is to design high-sensitivity microactuators effective in small dimensions and compatible with the human system. Micro motors do not have enough torque. Shape memory alloys require unacceptable high currents and piezoelectric materials have low a stroke and need high voltage. Electroactive polymers provide a unique solution to these issues.

Dario presented two case studies: one on the development of a microendoscopy system for inspection of the entire gastrointestional tract and the other on the design of a microendoscope with a hydrodynamic actuator.

A new laboratory called the Media Lab Europe was established in 2000 for nanostructure research to provide technology solutions for the future (for additional information: www.medialabeurope.org). The Laboratory is affiliated with MIT, USA and Trinity College, Ireland. It is a non-profit organization. The group is working on several issues including a design of a nanoscale FET, polymer nanotube composites for strong lightweight material, a full page display for the blind, and use of nanotubes as electrodes and sensors. The activity is very new and the projects highly ambitious.

Progress on a human-like android face was reported by Professor Danilo DeRossi of the University of Pisa, Italy. The objective is to understand human facial expressions as related to various facial muscle movements and use of electroactive polymers (acrylic VHB3M) and sensors to mimic the movements. The Laboratory is developing a human-like android equipped with linear actuators and a multisensing acquisition system to detect rheological properties of food. Their design goal is to develop facial expressions of the android which will mimic human response to food. Ultimately they hope to mimic facial expressions such as for pain, tiredness, fear and sleepiness.

The workshop was a good mix of studies of fundamental properties of electroactive polymers and of the novel applications of this class of materials to engineer various functions to meet future societal needs. Recognizing the progress made on many fronts of this research topic, the sponsors, such as DARPA and ONR, should continue their support of several successful projects to completion.

A list of speakers and their affiliation is attached for reference at the end of the book.

PROGRAM:

Time	Monday_30/07	
12.00	**Reception**	
13.00	**Lunch**	
16.00	**Registration,** **Welcome Lecturers by organizers and sponsors:** (D. De Rossi, P. Parrish, R. Sands)	
	Biomimetics **Chairpersons**: B.B. Rath, B. Picasso	
17.00	A. Rudolph, pag. 16	Bridging the gap across living and non living systems (A. Rudolph)
17.20	A. Rudolph	
17.40	A. Dittmar, pag. 17	Living being concepts and mechanisms, a source of ispiration for biomedical applications (A. Dittmar, G. Delhomme)
18.00	G. Jeronimidis, pag 24	Coupling between active polymer gels and fibre structures for tailored functionality (G. Jeronimidis)
18.20		
18.40	**Coffee break**	
19.00	J.F.V. Vincent, pag. 29	A biomimetic two-dimensional conveyor system (T. Yamauchi, J.F.V. Vincent, D. Shanley, F. Davies, A. Bowyer,
19.20	P. Chiarelli, pag. 33	Elastodynamics of hydrogels as bipahsic model of natural soft tissue (P, Chiarelli)
19.40	T. Yamauchi, pag, 35	Electroactive polymer gel application for bio-reactor (T. Yamauchi, K. Seki, K. Oshima, M. Shimomura, S. Miyauchi)
20.00	B. Picasso, pag. 42	Fish and ships: can fish inspired propulsion outperform traditional propeller based systems? (B. Picasso, A. Manuello, M. Ruggiu)
20.30	**Dinner**	

Time	Tuesday_31/07	
	Molecular Actuators **Chairpersons:** P. Calvert, A. Mazzoldi	
09.00	R. Baughman, pag. 45	Carbon nanotube charge transfer complexes for artificial muscles, energy storage and energy harvesting (Ray Baughman)
09.20	M. Suzuki, pag. 46	Protein motor mechanism: affinity gradient force model (M. Suzuki)
09.40	O. Inganas, pag. 50	Polymer actuators on microscale: microrobot and cell trappers (O. Inganas)
10.00	J.D. Madden, pag. 56	Towards conducting polymer organisms (J.D. Madden P.G. Madden, P.A. Anquetil, H. Yu, T.M. Swager, I. W. Hunter)
10.20	R. Kornbluh, pag. 61	Engineering muscles: artificial muscles based on dielectric elastomer actuators (R. Kornbluh, R. Pelrine, Q. Pei, S. Stanford, S. Oh, J. Eckerle, R. Full, K. Meijer, M. Rosenthal)
10.40	**Coffee break**	
11.00		
11.20	M. Shahinpoor, pag. 67	Ionic polymer-conductor composites (IPCC's) as biomimetic sensors, robotic actuators and artificial muscles (a brief review) (M. Shahinpoor)
11.40	K. West, pag. 71	Optimisation of the actuator properties of polypyrrole doped with alkylbenzene sulfonates (K. West, L. Bay, S. Skaarup)
12.00	L.A.P. Kane-Maguire, pag. 75	Polyanilins doped with adenosine-5 triphosphate and DNA (L.A.P. Kane-Maguire, D.A. Recce, L. G. Stirman, G.G. Wallace)
13.00	**Lunch**	

(continue Tuesday_31/07)

	Neural Communication **Chairpersons:** J. Uwe Meyer, M. Grattarola	
17.00	F.A. Mussa-Ivaldi, pag. 81	Connecting brains to robots: new perspectives for medicine, engineering and information technology (F.A. Mussa-Ivaldi, S.T. Alford, V. Sanguineti, K.M. Fleming, A. Karniel, B.D. Reger)
17.20	F.A. Mussa-Ivaldi	
17.40	F.A. Mussa-Ivaldi	
18.00	L. Galli-Resta, pag. 85	Wiring the vertebrate retina: global patterning from short range cellular interactions (L. Galli-Resta, E. Novelli, G. Resta)
18.20	M. Grattarola, pag. 90	Neuroengineering: bioartificial networks of real neurons (M. Chiappone, M. Grattarola, M. Pisciotta, M. (B.) Tedesco, A. Vato, F. Davide)
18.40	**Coffee break**	
19.00	J. Uwe Meyer, pag. 99	Microfabrication and micro patterning of biocompatible polyimide-foils with embedded metal thin films and PDMS co-material for neural interfaces devices. (J. Uwe Meyer, M. Schuettler, T. Stieglitz)
19.20	J. Uwe Meyer	
19.40	J. Uwe Meyer	
20.00		
20.30	**Dinner**	

Time	**Wednesday_01/08**	
8.30	**Departure from Il Ciocco: All day excursion to San Gimignano and Siena**	
20.00	**Return to Il Ciocco**	
20.30	**Dinner**	

Time	Thursday_02/08	
	Biostructures and Tissue Engineering **Chairpersons:** G. Wallace, A. Ahluwalia	
09.00	G. Pollack, pag. 105	Cell, gels and engines of life: a fresh paradigm for biological motion (G. Pollack)
09.20	G. Pollack	
09.40	G. Pollack	
10.00	R. Cancedda, pag. 114	Bone marrow stromal cells and their use in regenerating cartilages and bone tissue (R. Cancedda, R. Quarto, B. Dozin, M. Malpeli, A. Muraglia, M. Mastrogiacomo, A. Banfi, G. Bianchi)
10.20	A. Ahluwalia, pag. 115	Tissue engineering: methods for guiding cell disposition (A. Ahluwalia, F. Bianchi, D. De Rossi, A. Previti, G. Vozzi)
10.40	**Coffee break**	
11.00	G. Vozzi, pag. 119	Microfabricated biopolymer scaffolds tested in static and dynamic environments. (G.Vozzi, A. Ahluwalia, A. Previti, F. Bianchi)
11.20	D.J. Beebe, pag. 120	Organic microfluidic systems and components (D.J. Beebe)
11.40	G.G. Wallace, pag. 121	Biocommunications from the molecular to the whole-body level using novel organic electrodes (G.G Wallace)
12.00	D. De Rossi, pag. 128	Biomimetic materials and structures: past and present (D. De Rossi)
12.20	B.R. Mattes, pag. 135	Electrochemical behavior and electromecahnical actuation of polyaniline in non-aqueous electrolytes (B.R. Mattes) *(Presentation pertains tosession on molecular actuation)*
13.30	**Lunch**	
	Artificial Senses and Biosensors **Chair persons:** K. Persaud, M. Mascini	
16.30	N. Franceschini, pag. 137	From fly vision to robot vision (N. Franceschini)
17.00	G. Sandini, pag. 139	Sensory motor technologies: from biology to artificial systems (and viceversa) (G. Sandini, G. Metta, F. Panerai, L. Natale, R. Manzotti)
17.20	A. Bicchi, pag. 142	Tactile flow: does it exist, is it useful, and how? (A. Bicchi, P. Scilingo)

(continue Thursday_02/08)

17.40	P. Calvert, pag. 143	Forming active structures with embedded sensors (Y. Yoshioka, P. Calvert, M. Ghaemi)
18.00	B. Holcombe, pag. 151	Textiles as communications platform (B. Holcombe)
18.20	D. De Rossi, pag. 155	Active dressware: wearable haptics systems (D. De Rossi, F. Lorussi, A.Mazzoldi, P.Orsini, E.P. Scilingo)
18.40	**Coffee break**	
19.00	R.A. Bissel, pag. 159	Conducting organic polymer gas sensors - QSAR studies of sensor performance (R.A. Bissel, K. Persaud, P. Travers)
19.20	K-. Persaud, pag. 168	An optical biosensor employing tiron-immobilised polypyrrole films for estimating mono-phenolase activity (K. Persaud, R. Narayanaswamy, S. Dutta, S. Padye)
19.40	M. Mascini, pag. 173	DNA biosensor for the detection of toxicants (M. Mascini)
20.00	D. Diamond, pag. 177	Measuring biochemical parameters on-line: key challenges and future potential (D. Diamond)
20.30	**Dinner**	

Time	**Friday_03/08**	
	Robotics and Biomechatronics **Chair persons:** N. Francheschini, A.Bicchi,	
09.00	P. Dario, pag. 188	Design, actuation and fabrication issues in microendoscopy (P. Dario, A. Menciassi, C. Stefanini)
09.20	P. Dario	
09.40	P. Dario	
10.00	M. in het Panhuis, pag. 190	Nanostructures Group at Media Lab Europe, technologies and solutions for the future (M. in het Panhuis, A. Minett)
10.20	E.P. Scilingo, pag. 194	Haptic devices for minimally invasive surgery (E.P. Scilingo, A. Bicchi, D. De Rossi)
10.40	G. Pioggia, pag. 199	An android head to taste substances and to endow expressivity (D. De Rossi, G. Pioggia)
11.00	**Coffee break**	
11.20		
11.40	**DISCUSSION**	
12.00		
13.00	**Lunch**	
14.00	**Departure to Pisa by bus**	

EXTENDED ABSTRACTS

Bridging the gap across living and non living systems

Alan Rudolph
DARPA, Defense Science Office
3701 North Fairfax Drive
Arlington
VA 22203-1714
USA

Tel: ++1-703-696-2240
Fax:
E-mail: arudolph@darpa.mil

(text not available at time of printing)

Living Being Concepts and Mechanisms, a Source of Inspiration for Biomedical Applications

André DITTMAR and Georges DELHOMME

Microcapteurs et Microsystèmes Biomédicaux, INSA Lyon, Bât. Léonard de Vinci, CNRS LPM
20 avenue Albert Einstein, 69621 Villeurbanne Cedex, France
Tél : +33 (0) 4 72 43 89 86 Fax : +33 (0) 4 72 43 89 87 Email : dittmar@univ-lyon1.fr

Abstract - Microtechnologies offer the new possibility of designing and building sensors and actuators in dimensional scale close to that of living tissues or even to single cells.

The world of microtechnology between micrometers (or less) and millimeters, is governed by laws which differ from those valid for human size. Superficial tension, boundary layers, electrostatic effects, surface state, diffusion capillary forces ... are preponderant for this size, whereas they are weak or negligible at macroscopic scale.

Living tissues have been using "micro" and "nano" technologies for several hundred million years. They are models for the design of sensors, actuators, structures, organizations and concepts. We have to study this field, keeping in mind that nature does not give us "blue prints" "ready to copy".

The new knowledge of nature associated to the new possibilities in microtechnics, signal processing, artificial intelligence and materials... make possible a new approach in designing and research.

Many problems in man-made objects are not solved : energy storage, light emission with high efficiency, self-repairing, multi sensing, energy transmission, 3D designing in circuitry, biocompatibility actuators and sensors...

All these needs and trends are particularly strong in the Biomedical Engineering field.

We have to look to future with our own vision : with a large vision for the detection of movements, trends... and simultaneously with narrow field for an accurate analysis.

Nature gives us indications for the multidisciplinary approach.

This new approach is "in fine" reasonable : all the solutions of nature have been severely tested for thousands and millions years.

From the most elementary organisms to the most developed, life has designed a multitude of functions, systems, sensors, actions and software :

Functions Easily Perceptible :

Research of **energy** and **materials** for **development**, **reproduction**, **functioning** ...

- **Locomotion** (earth, air, water),
- **Detection** of shape, colors, height, taste, contact, vibration,
- **Defense and attack**, dissimulation, orientation, ...
- **Elementary actions** : mechanical, movement, running, jumping, catching, gripping, sowing, cutting, grinding, aspiring, blowing.

Functions of the Internal Mechanisms of Living Beings, Less Obviously Perceptible :

Countless regulation mechanisms : physical, electronical, thermal, chemical, mechanical, etc...and **signal processing** concerning **internal body functions**.

Immersed in the natural environment, humans follow three ways to satisfy their needs

- **use of natural resources** by taking advantage of their characteristics and specificities,
- **creating devices entirely thought by man** with no obvious anterior reference,
- **creating devices inspired from nature** for performing non existing functions in man or for improving them.

The creation of "man-made" or "man-designed" devices is not based exclusively on one of these processes but rather on their combination.

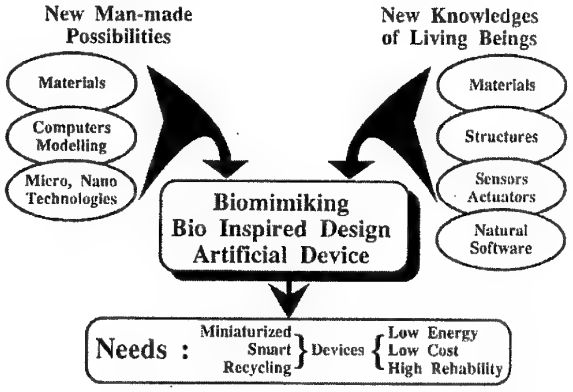

At this beginning of millennium, new trends are emerging for the definition and the design of man-made objects. For the harmonization of the relationship of man and its products, with nature, the objects have to be more and more miniaturized, smart and recyclable, and also they have to use low energy to be low cost and highly reliable. The most part of these characteristics corresponds to those of living beings.

At the present time, men have at their disposal, new and high knowledges of living beings and new possibilities for designing and building :

- **new knowledges** on nature, on its material structures, sensors, actuators, software, ...
- **new possibilities** : men have created new materials, sometimes better than those of nature, news devices for calculation and modelling. And now with micro and nano technologies men are able to build and work **at the same scale** as nature.

The **biomimicking approach** or the **bio inspired designing** is more a **global strategy of thought and creativity than a technique for copying nature**.

So we **HAVE TO LOOK TO NATURE** who has designed hardwares, softwares, macro and nano technologies, and a multitude of sophisticated concepts : **they are a useful source of inspiration for us.**

New possibilities are offered :

- by signal processing, computing, memory, software, modelling,...
- by designing and building new materials , new molecules,
- by microtechnologies and nanotechnologies : sensors, actuators and systems can be designed and built at scale close to that of living tissues or even to single cell.

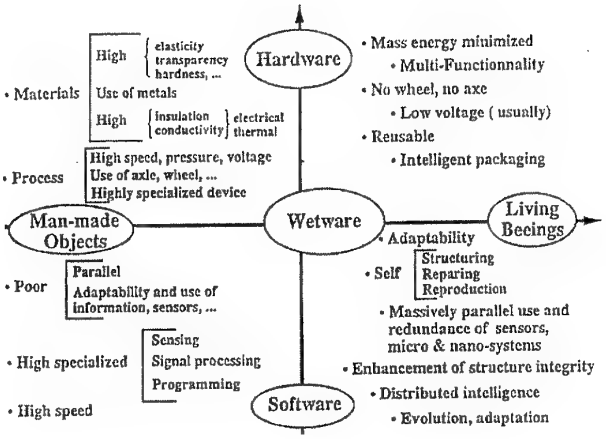

Living and non living beings

The frontier between living and non living beings is very mobile. Life is a pattern in space-time rather than a specific object (P. Marchal - 1995) **"Living beings embed a self-description a copy of which is used during reproduction. They are able to perform autonomous morphogenesis. They include a metabolism for energy supply"**. They are able to modify themselves to take into account : **Individual** modification of beings : **"adaptation"** (short term) ; **Species** modification of beings : **"evolution"** (long term).

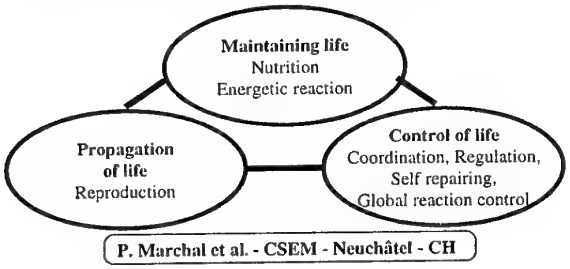

Contrarily to man-made sensors, actuators, systems, living beings are working with a wet and salt medium. A lot of obligations but also of possibilities are directly related to the use of water, which properties are numerous. Generally each part of living tissues is supplied with energy by using blood microcirculation, fluid and molecules diffusion.

Information is transmitted by nervous systems (otho- and para-sympathetic systems). But many interactions are existing between these 2 systems. The microcirculation can be modulated by **the nervous system** ... and information can be transmitted by the vascular system **using hormones.** For a long time in man-made systems, energy and information used the same line (electricity, fluides, mechanics...). But today the trend and specially with computer science is to use a **line (bus) for information** and a **line for energy,** as in nature.

This general diagram tries to give an idea of the main concepts and characteristics of man-made objects and living beings as well as its :

- **"Hardware"**, components, materials, etc...
- **"Software"** : sensing, signal processing, etc...

In living tissues, **hardware and software are often merged** resulting in distributed intelligence, adapting systems, intelligent packaging...

HETEROGENEITY OF ORGANISMS AND LIVING TISSUES

Tissues and organisms are rarely homogeneous, even they are observed at different scales.

They are composed of layers, membranes, cells, channels, using for each function the appropriate components, materials and sizes.

- A thermography of the whole body shows a heterogeneous distribution of skin temperature (scale 1 m).
- A histological slice of tissues shows also a heterogeneity of shapes, components, size... whereas its scale is 10^{-5} meter.

This "heterogeneity" gives an account of the complexity of living systems, and the optimization of its components in every **dimension scale** of its organs.

LIVING BEINGS : A HUGE QUANTITY OF COMPONENTS

The human body is composed of about 60 000 billions cells ($60\ 10^{12}$) and of course each one contains hundreds of mitochondrias (A. Giordan 1996).

Several hundred thousands of chemical reactions occur at the same time in the tissues of the body. These chemical reactions, often interacting concurrently, has to be controlled precisely and fastly for that sensors are used massively for local feed-back and information exchanges.

Measurements and information exchanges are one of the basic principles used in living beings

OPTIMIZING THE USE OF ENERGY AND MATTER

The living tissues are governed by the principle of energy economy. The human brain (about 100 billions neurons) works with less than 15 watts, i.e. 10 microwatt/mm^3.

The real 3D "organisation" of the brain is a way to save energy and time. One neuron can establish 200 000 connections with other neurons (average value).

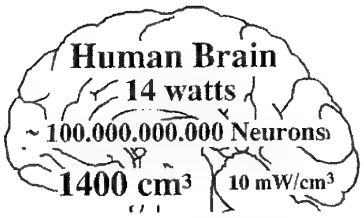

Average value of engine displacement of European cars

How the heterogeneity and the huge quantitiy of components of tissues are taken into account in Living Beings ?

Several solutions, concepts and mechanisms are used :

- **The massively parallel use of sensors** at each scale and level for the measurement of pressure, temperature, concentration, pH ...
- **The information of the sensors** can be used to pilot a local regulation, or exchanges with other sensors or its immediate neighbouring. It can be also sent to the **central nervous system** for several sorts of signal processing, giving **conscious or unconscious sensation**.
- **Usually the local information** of sensors is compared with **complementary** informations for improving reliability.

SENSORS, DETECTION, SENSATION, REGULATION, FEED-BACK

The massively parallel use of sensors : except some exceptional cases, sensors are not used alone but by hundreds, thousands, millions ....

There are many possibilities for classifying the sensors in living beings :

- **basic principle** : chemical, optical, mechanical, thermal...
- **location** : at the surface of the skin / inside the body
- **the function** : detection of odor, taste, noise, movement, colour...

For **avoiding a too long and abstract classification,** it is perhaps more useful to study **some real cases.**

SENSORS IN HUMAN SKIN

The skin is the functional interface between the human body and its environment medium. For that reason, sensors are particularly numerous in skin. The thickness of skin is about 1 mm. The merkel discs (sensors in the skin) are used in quantities, allowing :

- **mapping** : to characterise a surface, to detect the direction of a strain, etc...
- the safety and the reliability of measurements.

THE TISSUE HETEROGENEITY :

In Living Tissues, sensors are used in massive quantities 1000, 100 000 with a lot of redondencies, giving information related to complete areas or volumes (mapping). A simple fly wing contains hundreds of sensors on its surface and on its edges to send information on air stream lines or speed. The sensor density is related to the local functional importance.

The **shapes** of the various structures are also **optimized for measurement.** Such an interactivity between structure measurements and function results in a simple, fast and efficient signal processing.

In the skin, there are several sorts of sensors, each one having a specific function. The **"packaging"** of the sensor **participates actively** to the specificity of its signal.

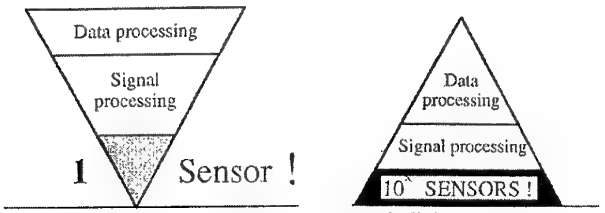

A. Dittmar 2000

In artificial systems (designed and built by human) few sensors are used. Signal and data processing are sophisticated.

In "**natural sensing**" in living systems, a lot of sensors are used. Signal processing is basically simple but sensors are mutually connected and informed. This method is more **"robust"**.

Multi-sensors

The measurement carried out by a **single sensor** is often not **sufficiently relevant,** due to the inhomogeneity of tissues and the specificity of the patient's response to illness or to stimuli.

Moreover the selectivity of biomedical sensors can be weak. All these facts need the design of **Multi-sensors** or **Matrix-sensors** using complementary principles (chemical, optical, thermal...). The multi-sensors have the supplementary advantage of simplifying use : a single device instead of 4 to 6 ... multi-sensors decreases invasivity, pain, infection risks...

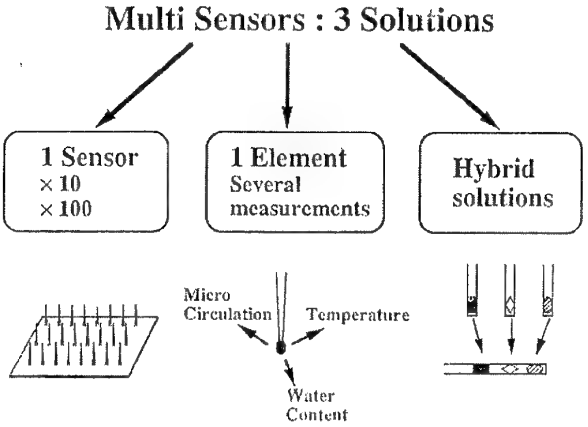

Living beings use the 3 types of multi-sensors :

- **Same sensors** used massively in parallel.
- **Sensors able to measure several parameters,** (pressure and temperature for example) ; Usely these sensors are used in parallel to increase their selectivity.
- **Hybrid** sensors using several sensors or elementary principles in the same unity.

Two powerful natural sensors have been studied and used to build man-made devices :

- **The retina of insects** and its system was studied by Francescini (1997) and Arreguit (1996).

- **The artificial nose** was designed using chemically interacting materials, a matrix and a neural network strategy, D'Amico (1997).

Local signal processing of sensors

The output signal of sensors is converted into spikes (1 ms duration) frequency modulated, because there are no metallic (or high electric conductivity) wire in living tissues.

The signal transmission is carried out by nerves, which use an active mode of propagation in which the analog transmission is not allowed.

The relationship stimulus/spike frequencies is not often linear, but it is composed of a threshold, a "S" curve and a saturation or an asymptote. But other signal processing are used, for example, in the pressure sensors of the skin :

This example shows that the signal of a natural sensor is processed "in situ".

The typical response is known as **"on" response** and **"off" response.** So with this type of sensors, only the **beginning** and the **end of the stimulus** is detected and transmitted.

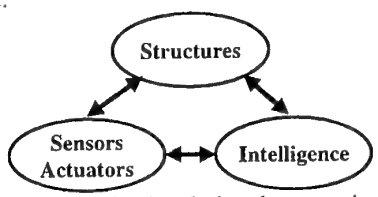

As for sensors with local signal processing, usually a large part of information of structure is processed locally. Structures, sensors, actuators and "intelligence" are merged closely.

The concept of separate sensors and signal processing is replaced by a distributed intelligence associated to a central decision making (brain).

FEEDBACK : USED AT ANY SCALE, IN PHYSICAL, CHEMICAL, OPTICAL .... NATURAL DEVICES

Feedback is used for many purposes :

- **Maintaining** at a constant level : pression, temperature, pH...
- **Dynamic control of actions** : movements, forces,
- **Adaptation to local conditions.**

The bone structure

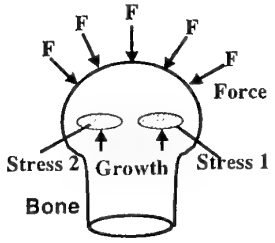

The bone structure is an equilibrium between continous "**self-destruction**" and continous growth or "building" process. Thousands of mirosensors are located inside bone for the **measurement of local stress**. When a local stress is high, the sensors give a signal to **increase the local bone growth**... so the local growth is related to local stress and the bone matter is placed in the force lines in optimized quantities.

In bones, matter is placed in the force lines in optimized quantities.

Roots find the direction of water

The growth of the root is higher on the side of dry soil... so the root turns in direction of wet soil. Moreover, an area with a low water content is induced around the root .... So this area can be detected by an other root. By this way, there is a sort of **exchange of information** betwen roots and they can optimize their **"3D functional distribution"**.

A similar process is existing for the growth of leaves and branches in which light is the leading parameter (equivalent to water in the case of root).

This use of **local feedback results** in the capability of adaptation and in high reliability. **Sometimes this property is called "local", "elementary" or "primitive" intelligence.**

The new trend in Biomedical Engineering and specially in surgery is to include sensors in tools, in clamps, in gloves for providing feedback to surgeon. Thus the quality of the surgeon gesture and action can be improved.

Detection

The detection is one of the most important functions in living beings. It is used in all the main tasks and functions of their life.

Detection of : odours, light, colours, shapes, movements, infra-red, sounds, ultra-sounds, infra-sounds, vibration, electric and magnetic fields, heat, chemical, mechanical, optical ... properties.

The detection is used to find food, ways, partners for reproduction,... and also for survival by early detection of danger and "enemies".

The sensitivity of the natural sensors is astonishing for its very high sensitivity and selectivity :

- **Butterflies** are able to detect some molecules per m^3,
- **Eyes** some photons,
- **Penguins and bats** are able to detect and localize the sound of their own "children" among thousands of individuals.

THE SIZE : a variable by itself : true for 1 mm, wrong for 1 µm

The world of microtechnology is governed by laws which differ from those valid for human size.

- **Superficial tension, boundary layers,**
- **Electrostatic effects, surface state**
- **Diffusion, capillary forces, bilayer effects...**

are preponderant for this size, whereas they are weak or negligeable at macroscopic scale. Due to these facts, the shape proportions and designs used in micromechanisms are specific to these sizes, living tissues, organisms and microorganisms use profusely the possibilities offered by their small size : for this reason they have to be considered as sources of inspiration for microtechnologies.

The components of living tissues **are designed and built at the optimal scale and size** for taking benefit of phenomenons which are **"scale dependant"**. The examples are numerous :

Muscles : a population of micro actuators

Muscles are composed of muscular fibers which are themselves composed at the subcellular level of a serie of

sarcomeres which are connected end to end. The sarcomere is the basic contractile unit, composed of a parallele array of myosin fibers in the middle, interdigitating with two arrays of actin fibers at either ends. The activation of this device result in a contraction (about 25 to 30 % of its initial lenght).

1 myosin filament = 530 pN (when stimulated).

Different sizes .... same actuator : (Myosin)

As the phenomenon of electrostatic attraction is conversely proportional to the square of the distance, the natural micro-actuators were designed at a small scale. With a larger scale high voltage would be necessary but it was not **possible in a wet medium** and the voltage difference between the inside and the outside of a cell is about 80 mV.

In consequence, a single microactuator was designed and used as well in insects, fishes, small (mouse) or large mammals (elephant). Big muscles are built with a large number of the basic actuators (5,7 10^{14} myosin filaments per square meter of cross-sectional area). C.J. Pennycuik (1992)

The same strategy is used nowadays in microtechnologies for the design of interdigitized structures as well for microactuators or microsensors : the accelerometers are composed of interdigitized structures, the effect of each one is not suffisant ... so they are used by 10, by 100... in the same way as natural devices.

Microcirculation

The size of vessels is adapted for their efficiency : the vascular system is in charge of 2 functions :

• **the transport** of blood to tissues for bringing oxygen and glucose by **arteries, by vein** after working in tissues.

• **the exchange** of glucose, CO2, lactate, ... using capillaries (small vessels Ø 8 to 10 µm).

The capillaries assume with efficiency the exchange function, due to their large surface for exchange and the small thickness of their wall. The transition from large vessels to capillaries is progressive as shown in the figure of the kidney vascularization. The strategy is arborescent and can also be considered as partially Fractal.

The 3D organisation of capillaries is complex and rich in concepts (in human brain, the average value of distance between capillaries is about 30 µm). Nowadays microsystems use a "multilayer 2D design" instead of a real 3D design. The real 3D design saves energy, distance communication, volume... But for the moment, it is not completely available due to technology and concepts limits. The vascular organisation is a good model of distribution taking continuously into account the local needs.

THE BILAYER STRUCTURE

The bilayer structure is used in plants and in animals. Some plants have bilayer systems which can change of form or accumulate mechanical energy (by strain) by using changes in temperature or humidity of the environment medium. The wild geranium uses a sort of catapult using bilayer structures to spread out its seed.

The bilayer structures can be either actuators or sensors, using physical, thermal, electrical, chemical, piezzo effects. They are compatible with many devices and can be :

• **Energy taken into the medium** (self moving),

• Energy brought from distance.

Bilayers in microsystems

Thermal bilayers structures are used for several years in microsystems for sensors or actuators.

- Micro thermal bilayers are used **as sensors** for the detection of enzymatic reaction in an artificial nose.
- Micro thermal bilayers are used also as component of an array of small actuators simulating the cilliaries of living beings. These arrays are used for the displacement of small objects in 2 dimensions.

THE WHEEL : an excluded solution in living tissues

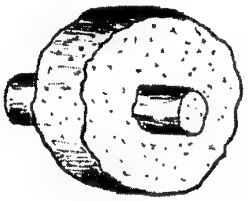

Among myriad examples of processes, devices, mechanisms designed by Nature, we have to note that **wheels and axles are not used in living tissues** (L.T.). In L.T., a single articulation has a rotation limited to 90°. Some articulations composed of several elements, as wrist or neck, have a rotation close to 1/2 turn.

An accepted explanation links this phenomenon with the fact that L.T. have usually the ability of **self-repairing**. But **self-repairing** involves the possibility to bring **materials** at the right place, using the vascular system.

The discontinuity induced by **wheels** and **axles** does not allow this solution. For the same reasons, turbine and propellers are not used inside living tissues. Naturally, there are some exceptions, a tail of a bacteria for example,... but its life is very short without possibilities of self repairing.

Consequences :

- **for locomotion (earth, air, water)**, wheel, turbine, propeller, screw are not used ; the movements are basically alternative,
- **for the propulsion of liquids and matters**, no turbine, no piston are used. This function is carried out by means of peristaltism (oesephagus, intestine ...) or by variable volume cavities (heart, uterus, glands ...), A. Dittmar (1996).

AERODYNAMISM AND HYDRODYNAMISM

The speed and the agility of **swimming or flying animals** are often largely higher than that of human ; and certainly men have tried early in our history to copy, to mimick,... so high performances, Icarus is undoubtly the most famous. But for a very long time, and still nowadays, the external appearance, easily perceptible was the main source of inspiration. Since 10 to 20 years ago, the researchers pay attention to animals, which are able to high speed with low energy (a dream).

A detail observation of these animals shows that a basic rule of aero and hydrodynamism : "the smoother surface is the best one" was not totaly exact .

- The **shark skin is not famous for its smooth touch** whereas sharks are remarkable for their swimming speed. **The rugosity of their skin** and its orientation is optimized in each location for reducing drag for their average speed.

- The **dolphin skin**, its neurophysiology, have been studied in details and one important and recent result of this study is due to S.H. Ridgway and D.A. Carter (1993). " ... the dolphin's nervous system detects changes in pressure on its skin surface.

However, these results only suggest that the dolphin's skin may reduce drag by moving synchronously with small vibrations impinging on its surface ... drag may be decreased by decreasing the pressure gradian in the adjacent water layer.

Bio-inspired devices and systems are developed to reduce drag noise and energy. This is particularly important in large boats and in submarines for reducing energy cost, noise and consequently the possibilities of detection.

AN EFFICIENT STRATEGY

The focusing of the **fish eyes** is obtained by the displacement of the crystalline lens as in classical cameras or projectors. In **birds and mammals** (more recent in the evolution of the crystalline lens), the focusing action is obtained by the **deformation**. The new type of focusing action is obtained with only 25 µm deforming lens shape instead of 3 mm with the conventional type, N. Kawahara, DENSO (1997).

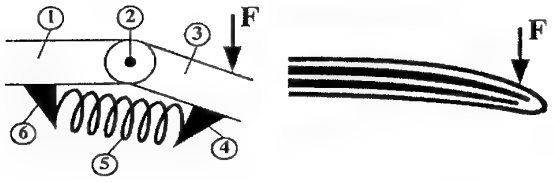

MULTI ELEMENT :	MULTI LAYER :
Articulation	Shape Memory
Spring	Composite
...	Self Repairing
Large Amplitude Movement	Low Amplitude Movement

The same strategy, **substitution of displacement by deformation**, is used for mirrors, P. K. C. Wang, 1996.

In many cases, in living beings, the deformation of structure is used with benefits.

- Smooth surface, friction reduction...
- New materials, composites are more and more used in this way.

THE INTELLIGENT PACKAGING

Red blood cells : a micropackaging increasing efficiency.

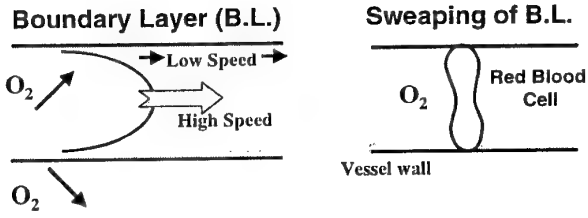

In human blood vessel, oxygen is carried by hemoglobin inside small packages : **RED CELLS .**

Advantages : the boundary layer (against the vessel wall) which decreases the exchanges, is swept by the red cells. Moreover the pressure increase due to red cells increases the transmural pressure and then the exchanges through the wall of vessels.

Paradoxically, the solution which consists to **put hemoglobin** in small packages increases the efficiency of exchanges. In living tissues, the packaging of a device generally participates actively to its function. The "intelligent" or "smart" packaging is typical of living beings.

THE ACTIVE PACKAGING

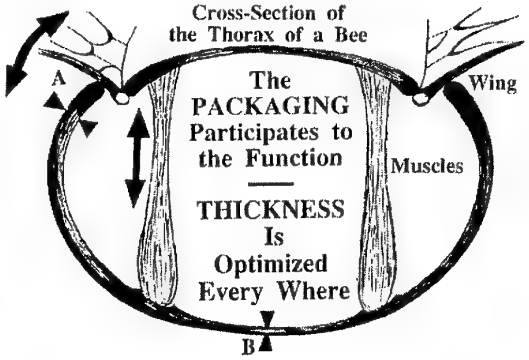

The **packaging** of living tissues is the interface with the environment medium. It is in charge of several functions, the most important of wich is the protection : physical, thermal, chemical, viral, bacteriological... and from predators.

FUNCTIONAL CONVERGENCES

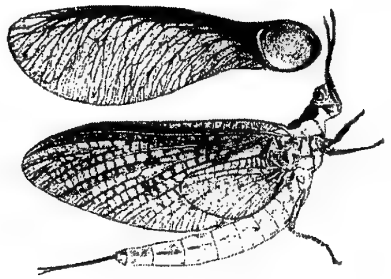

Sometime we can observe striking similarities or ressemblances between the shapes and the principles of plants and animals or between two species, insects and mammals. In this case, there is a good probability for finding optimized solutions.

The wings of the ephemera and the wings of the maple seeds plants have closely the same shape and the same internal structure, the paws of the mole (mammals) and that of the "mole crikett" have closely the same shape. The **commun point** is the adequation of the solution for flying in the air in one case and digging out galleries in the ground in the other case.

IS IT ALLOWED TO COPY NATURE ?

Certainly... but nature has to be considered as a source of inspiration. The classic error consists in the copy of the external appearance without understanding the real functions of this appearance and its limits.

The history of science and inventions is full of counter examples of biomimicking.

The mimick of horse feets or legs was not the good solution for locomotives !

"Eole" (invented by Adder in 1891) was the first airplane of the history. It uses for its first fly (50 m long about) wings directly inspired of that of bats. These wings marvellously built using bamboo were rather adapted for **beating wings** than fixed wings !

CONCLUSION

It is not possible in this document to "scan" a suffisant number of examples of the incredible and countless devices, mechanisms, processes... designed by nature.

The new knowledges of nature associated to the new possibilities in microtechnics, signal processing, artificial intelligence and materials... make possible a new approach in designing and research.

Many problems in **man-made objects** are not solved : energy storage, light emission with high efficiency, self-repairing, multi sensing, energy transmission, 3D designing in circuitery, biocompatibility actuators and sensors...

All these needs and **trends are particulary strong in the Biomedical Engineering field.**

We have to look to future with our own vision : with a large vision for the detection of movements, trends... and simultaneously with narrow field for an accurent analysis.

Nature gives us indications for the multidisciplinary approach.

This new **approach is "in fine" reasonable** : all the solutions of nature have been severely tested for thousands and millions years.

ACKNOWLEDGEMENT :

This work has been done with the support of ONRIFO

REFERENCES

Arreguit X., Debergh P., Photonic microsystems based on artificial retinas, Europto - SPIE, vol. 2783, Besançon, France, 10 p., 10-15 juin 1996.

Borroni-Bird C., What can seamless electro-mechanical vehicles learn from nature, Proc. International Congress on Transportation Electronics, Convergence, Dearborn, Michigan, USA, pp. 3-16, 1996.

D'Amico A., Di Natale C., Polesse R., Macagnano A., Davide F., Faccio M., Ferri G., Advances in electronic noses, World Congress on Medical Physics and Biomedical Engineering, Nice, France, pp. 87, 1997.

De Rossi D., Canepa G., Magenes G., Germagnoli F., Caiti A., Parisini T., Skin-like tactile sensor arrays for contact stress field extraction, Materials Science and Engineering, Vol. C1, pp. 23-36, 1993.

Delhomme G., Newman W.H., Roussel B., Jouvet M., Bowman H.F., Dittmar A., Thermal Diffusion Probe and Instrumentation System for Tissue Blood Flow Measurement : Validation in Phantoms and in vivo Organs, IEEE Trans. on BME, Vol. 41, n° 7, pp. 656-662, 1994.

Deussen N., Scientists are finding that in some branches of technology Mother Nature knows best, in Bionics, Lufthansa Bordbuch, pp. 51-57, January 1996.

Dittmar A., Delhomme G., Living Tissue Mecanisms and Concepts as Models for Biomedical Microsystems and Devices, 1st Annual International IEEE-EMBS Special Topic Conference on Microtechnologies in Medicine & Biology October 12-14, 2000, Lyon, France.

Dittmar A., Concepts and mechanisms of living organisms : examples for sensors, actuators and microtechnics, Course on Microengineering in Medicine and Biology, Comett Euro-BME, EPFL, Lausanne, Switzerland, October 5-7, 1994.

Dittmar A., Depeursinge C., Microtechnics, Microsensors and Actuators in Biomedical Engineering, First International Symposium on Andrology Bioengineering and Sexual Rehabilitation, AMBERS 95, Le Louvre, Paris, France, pp. 119-123, 5-7 July, 1995.

Franceschini N., Insect Vision : from Microelectrodes Analysis to Robot Synthesis, World Congress on Medical Physics and Biomedical Engineering, Nice, France, pp. 86, 1997.

Giordan A., Voici venue l'ère de la physionique, le vivant pour une nouvelle approche des organisations, La Recherche, Vol. 284, pp. 81-86, février 1996.

Gupta B., Goodman R., Jiang F., Tai Y.C., Analog VLSI system for active drag reduction, MicroNeuro 96.

Kawahara N., Development of inspection micromachine, Joint Seminar Japan-France on micromachine / MST, Besançon, France, 30th June-1st July 1997.

Marchal P., Mange D., Bio-inspiration, auto-organisation et systèmes complexes, Polyrama, n° 101, pp. 18-20, octobre 1995.

Moin P., Kim J., Les superordinateurs analysent la turbulence, Pour la Science, n° 233, pp. 46-52, mars 1997.

Pennycuick C.J., Newton Rules Biology, A physical Approach to Biological Problems, in Oxford University Press, New-York, 1992.

Ridgway S.H., Features of Dolphin Skin with Potential Hydrodynamic Importance, IEEE Engineering in Medicine and Biology Magazine, Vol. 12, n° 3, pp. 83-88, September 1993.

Smela E., Inganas O., Lundstrom I., Controlled Fording of Micrometer-Size Structures, Science, vo. 268, pp. 1735-1738, 23 June 1995.

Srinivasan A.V., Smart Biological Systems as Models for Engineered Structures, Materiels Science and Engineering, vol. C4, pp. 19-26, 1996.

Electroactive Polymers and Biosystems: New Directions in Electroactive Polymer Materials For Biomimetic and Interactive Processes. Lucca, 30th July- 3rd August, 2001

COUPLING BETWEEN ACTIVE POLYMER GELS AND FIBRE STRUCTURES FOR TAILORED FUNCTIONALITY

George Jeronimidis, Centre for Biomimetics, Department of Engineering, Reading University, Whiteknights, Reading, UK

Introduction

Active, and especially electro-active, polymer gels provide new opportunities for developing smart tailored actuation which can mimic biological processes [1-4]. Their capacity for large volumetric swelling in response to external stimuli such as temperature, pH, electrical fields, etc., can be harnessed and controlled for specific end-uses and applications. Current actuation technology is based either on high modulus – low strain materials, such as piezoceramics and magnetostrictors, or on components, such as hydraulic, pneumatic or electromagnetic devices. The former are capable of working at high stresses but low strains, the latter can produce large strains or displacement but at comparatively low stresses. The only materials capable of delivering both high forces and large displacements are shape memory alloys. In fact, a study on the performance indices of mechanical actuators [5] shows that there is a gap between the high stress-low strain and the low-stress – high strain groups. By themselves, owing to their chemical and physical properties, active polymer gels fall typically in the low stress (low force) –high strain group, together with muscle. Isotropic volumetric free swelling can be very large indeed, with swelling ratios of 10-12 [4] but omni-directional; differential free swelling can induce bending but, owing to the very low elastic modulus of the materials, the forces which can be generated are very limited. Anisotropic behaviour and increase the force-generation potential of electro-active polymer gels can be achieved is the free swelling potential of the gel is partially confined to extract mechanical work in a tailored fashion. There is an analogy with the free expansion of a gas which, unless confined and restricted by some "container", will not provide useful work.

Biological actuation

There are two basic mechanisms for mechanical actuation in biology, one based on muscle contraction, the other based on the generation of high turgor pressures inside plant cells. Muscle contraction depends on the specific molecular "ratchet" type

interaction between actin and myosin molecules, leading to the sliding filaments model [6]. Turgor pressure inside plant cells depends on the differences in the water chemical potential across the biologically active membrane which can control the passage of ions and hence alter the osmotic potential and the internal pressure. The anisotropy of muscle contraction is due primarily to the directionality of the sliding filaments, which occurs at the nanoscale. The anisotropy of actuation in plants manifests itself either at the level of a cell (micro-scale) via the shape of the cell and the orientation of cellulose fibres in it, or at the level of a tissue, via interactions between cells of different shapes, aspect ratios and cell wall thickness [7].
Although muscles and plant cell walls appear to have little in common as actuation devices there are similarities and common features which can inspire a biomimetic approach to the design of bespoke actuators based on electro-active polymer gels. Both systems share the following:

- Organised and extremely heterogeneous an hierarchical structures capable of swelling by drawing in solvent;
- Rate of swelling as a diffusion-controlled process;
- Swelling potential partially confined by a fibrous structure made of flexible but high modulus fibres – collagen in muscle, cellulose in plant cells;
- Anisotropic swelling resulting from interactions between swelling element and confining structure;
- Direct conversion of chemical energy into mechanical energy.

Integration of active polymer gels and fibrous structures

Fibrous composite structures are ideally suited to provide the coupling between the swelling potential of a gel and the conversion of chemical energy into mechanical work [8]. The gel acts essentially as the "motor" and the fibrous structure confines the volumetric expansion, generating tensile stresses in the fibres and producing global deformations of the structure. The response can be tailored by the arrangement of fibres in the confining structure and can be designed to generate large forces at small displacements or, vice-versa, large displacements at low forces. An example of this is shown in Figure 1 where an acrylamide gel is enclosed in a cylindrical braided fibrous structure with an initial fibre angle of about 20^0 from the cylinder axis. The length is approximately 100 mm and the diameter 12 mm. As the gel swells with water, the structure shortens, the diameter increases ad work is done in lifting the masses.

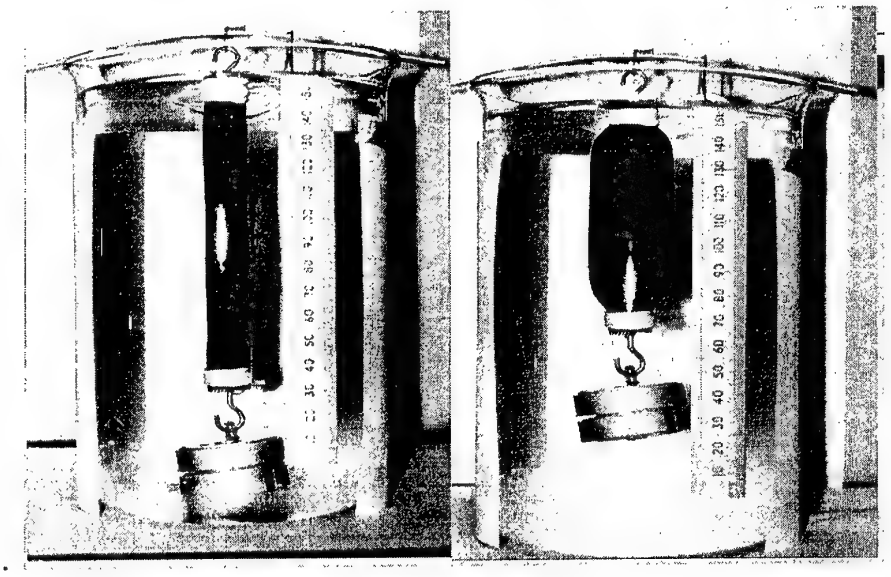

Figure 1. Anisotropic deformation of active polymer gel-fibrous structure combination due to swelling

The opposite effect, i.e. lengthening, of the cylinder would be obtained if the initial fibre angle in the braid were changed from 20^0 to 70^0, say. The response of such a system can be modelled, using Finite Elements for example, to optimise fibre angles, deal with complex geometries and predict deformation and force generation levels as well as intrinsic structural stiffnesses of the systems. Figure 2 shows the undeformed and deformed shape of a structure similar to that of Figure1. The swelling of the gel is simulated using thermal expansion on incompressible elements with a swollen Young's modulus measured experimentally. The diffusion process can also be simulated using heat-transfer which is governed by the same type of differential equation.

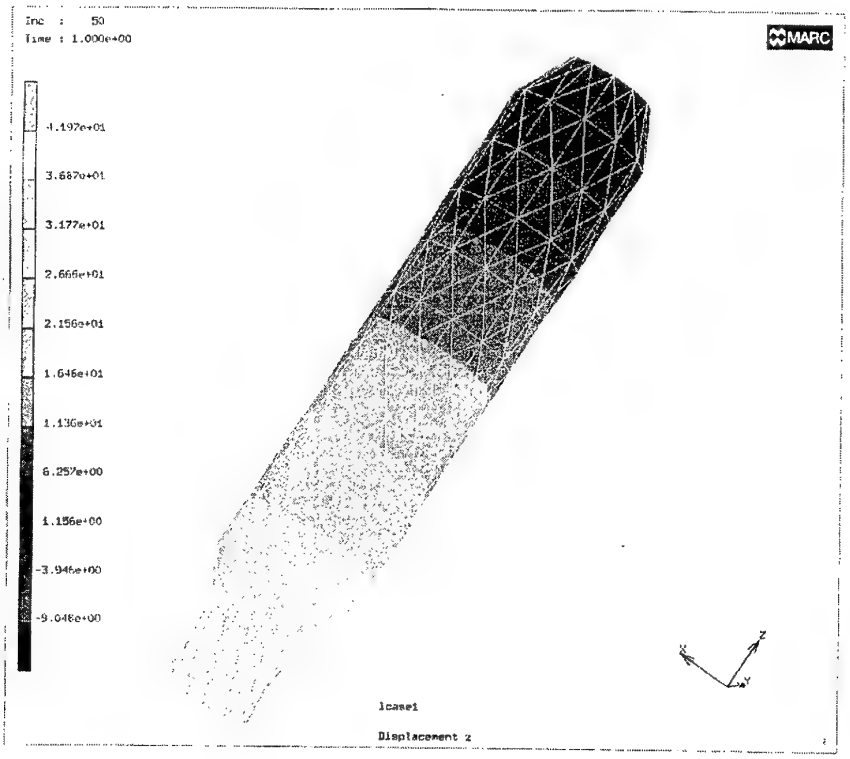

Figure 2. Finite Elements model of the deformation of an active polymer gel-fibrous braided structure

The maximum swelling potential of the gel is reached when the volume enclosed by the reorienting fibre structure, cylindrical in the above examples, reaches its maximum which corresponds to a fibre angle of about 55^0 from the cylinder axis [9]. When the system reaches this stage it acts as a very stiff element. If the deformation induced by the swelling gel is suppressed from the start (analogous to the isometric condition in muscles), large reacting forces are generated, up to several hundred newtons for typical dimensions of 100 mm inn length and 10 mm in diameter.

Altering the fibre pattern can be used to induce bending during swelling, via the addition of axial low extensibility fibres in the braid, for example, or twist about the cylinder axis – by having right-hand and left-hand fibrous helices in the braid of different extensibility or different diameter.

Conclusions

Used in combination with fibrous structures, active polymer gels can cover a very extensive range of actuator response, from high force – low deformation to high deformation – low deformation. Coupled deformation modes are also possible, depending on the fibre architectures used, as well as variable stiffness behaviour.

Electro-active polymers can add greatly to the basic passive swelling behaviour of a gel by enhancing swelling rates and improve the reversibility of swelling/de-swelling, as well as offering the possibility of more controllable systems. Although diffusion rates on the centimetre scale or above are slow, the speed of response can be improved by decreasing the size of the electro-active polymer gel / fibrous structure combination down to millimetre size or below and coupling mini-actuators is parallel or series, according to needs, i.e. restructuring the system mimicking the arrangement of active muscle fibres in muscle.

The author wishes to thank J.F.V. Vincent, M. Adeogun and S. Patel for helpful discussions and information.

References

1. DeRossi, D., Kajawara, K., Osada, Y. and Yamauchi, A. (1991) *Polymer Gels – Fundamentals and Biomedical Applications.* Plenum, New York.
2. Gong, J.P., Nitta, T. and Osada, Y. (1994) Electrokinetic Modeling of the Contractile Phenomena of Polyelectrolyte Gels. One-dimensional capillary Model. *J. Phys. Chem.* **98**, 9583-9587.
3. T. Fernandez-Otero (2000) Biomimicking materials with smart polymer gels. In *Structural Biological Materials: Design and Structure-Property Relationships.* M. Elices, Ed., 189-220.Pergamon, Oxford.
4. Tanaka, T., Nishio, I, Sun, S-T and Ueno-Nishio, S. (1982) Collapse of gels in an electric field. *Science,* **218**, 467-469.
5. Huber, J.E., Fleck, N.A. and Ashby, M.F. (1997) The selection of mechanical actuators based on performance indices. *Proc. Roy. Soc. Lond.* A, **453**, 2185-2205.
6. McMahon, T.A. (1984) *Muscles, Reflexes, and Locomotion.* Princeton University Press.
7. Simons, P. (1992) *The Action Plant.* Blackwell, Oxford.
8. Jeronimidis, G. (1996) Integration of active polymer gels and fibre composite structures for "smart" actuation. In *5th Symposium on Intelligent Materials, The Society for Non-Traditional Technology, Intelligent Materials Forum,* Tokyo, 17-19.
9. Clark, R.B. and Cowey, J.B. (1958) Factors controlling the change of shape of some worms. *J. Exp. Biol.*, **35**, 731-748.

A biomimetic two-dimensional conveyor system

T Yamauchi*, JFV Vincent, D Shanley, FJ Davies** and A Bowyer
Department of Mechanical Engineering, University of Bath
*Department of Bioengineering, Nagaoka University of Technology, Japan
** Department of Chemistry, The University of Reading

Abstract

From video films of starfish (*Asterias rubens* L.) moving along the glass wall of an aquarium, the movement of the tube feet was investigated during locomotion. The step cycle of the tube feet is not very different when the starfish is moving in vertical and a horizontal directions along the wall. However the phases of the cycle are variable suggesting that the control is relatively broad. The time for each cycle is directly related to the size of the animal.
As part of the development of this locomotory system into a novel type of conveyor system, the movement of the feet was modelled showing that, depending on the type of control system considered, the smoothness of locomotion depends on the number of feet in contact at any one time with the object being moved.
The final phase of the project will be to produce gel columns which will be mounted on a control board like the pile of a carpet and be separately addressable to produce waves of bending, hence move objects placed on the top of the carpet structure.
Key words: starfish, *Asterias*, tube feet, locomotion, transport, composite gel.

Introduction

Starfish move across the sea bed using tube feet which are extended hydraulically and retracted using muscles. Each tube foot is connected to an ampulla (a local reservoir) and a hydrostatic network which extends throughout the organism (Fig 1). The movement of the tube feet is coordinated, at least in part, by the central nerve system. The starfish extends the tube foot forward attaching the disk to the ground and contracting the foot (traction theory) or the tube foot acts as a lever and propels the animal forward (lever theory). Kerkut (1953) suggested that starfish climb upon a vertical surface using the traction mechanism and that the tube feet act as levers to give locomotion on a horizontal surface.
We are interested in this system for a number of reasons. The coordination of the tube feet controlled by a central system could be developed into new technology such as a new type of actuator for a transport system. Biomimetic engineering using soft materials has been studied in various research fields such as chemical, material and medical science (Osada *et al.* 1992, Osada and Ross-Murphy 1993). Nevertheless, there is little research work involving the coordination of soft materials under the control of a central system, or asking whether peripheral control (giving emergent behaviour) might not offer advantages. Additionally, most of the gel systems which have been suggested to date have not offered much in the way of practical application due to a combination of low available force for actuation and slow speed of movement. One solution to these problems is to use a large number of small actuators.
In the present work we report on a simple investigation of the movement of the starfish tube feet and develop the observations towards a new concept in gel technology.

Materials and Methods

Starfishes, *Asterias rubens* L. were collected near the Isle of Cumbrae, Scotland. They were kept in a circulating sea water aquarium at 15°C and fed on mussels (*Mytilus edulis*).
The starfish on a vertical surface of glass wall of the aquarium were videotaped with a digital

video camera within ten days of their arrival. The locomotion of the starfish and the movement of the food by the starfish vertically and horizontally along the glass wall were analyzed from the video images. The weight of the starfish in sea water was measured using strain gauge connected to strain indicator.

A simple computer model was developed using Mathematica to investigate the sensitivity of the temporal profile of the total force that the tube feet exert when a starfish is moving to the level of control in the stepping of individual feet and also to the number of feet involved in motion. The starfish has about 1000 feet of which 50% are active at any one time, therefore 500 feet need to be considered. Each model foot has a cycle of a duration which is repeated with new values taken from the distributions determined from observation. The force (and therefore energy) profile of individual foot movement was taken from Kerkut (1953). Using a number of energy / force profiles for each foot and knowing the position of all 500 feet within the distributions at any one time, the temporal profile of total force or energy for the whole starfish can be calculated.

The gel systems used to model the movement of starfish feet used conventional chemistry. Cylinders of PVA/PAA gel, usually about 5 mm in diameter and 10 mm long, were made with strips of more highly conducting polypyrrole gel down the sides. These were stimulated at a range of V/cm values.

Results

The starfish stretches a tube foot forward and attaches it to the substrate then contracts the foot pulling the body forward. When the foot is orthogonal to the substrate it is shortest; as the step continues it elongates again. Finally, the foot detaches from the substrate and returns to the position at the start of the cycle. The starfish can move in any direction on the plane, although there is a marked tendency for one of the five arms of the starfish to lead.

We divided the step cycle into three timed phases;

- First phase (t_p): From when the tube foot attaches to the wall to when it is vertical
- Second phase (t_e): From when the tube foot is vertical until it detaches
- Final phase (t_r): From when the tube foot detaches until it returns to its initial point

We took measurements from 2 starfish (Table 1 showing the times for the three phases with standard deviation) with arms of length 6 cm (series 1) and 8 cm (series 2). The letters, a,b, and c, refer to the direction in which the starfish was moving (a – upwards; b – horizontal; c – downwards). The standard deviation of most readings is about 30% of the mean. The times for the larger starfish are about twice those of the smaller; crudely the volume ratios will be about 1:2.4. The percentage error in the mean (=standard deviation / mean x 100) is about 30%. The body speed was dominated by the frequency of step cycle by the tube feet.

For the mathematical model, a short period was introduced between the recovery and attachment phases to allow for entrainment of the foot with the rest of the population. The percentage error in the mean of the distribution of total force exerted by all the feet was calculated, and compared with time whilst varying the mean and variance of individual foot phase parameters. We investigated sensitivity to the variance and mean value in t_p and t_e and the sensitivity to the number of active feet. The total force generated by the feet is relatively insensitive to variation in both the mean and variance of the separate phases of foot stepping t_p and t_e. These results are for a constant energy model. In assuming a constant force there is no clear pattern in the sensitivity of total force to the mean or variance of phases t_p and t_e. However the distribution of total force with time is very sensitive to the number of active feet. The fewer feet active at any one moment the higher the percentage error in the distribution of force with time which means that the variance is large relative to the mean.

Discussion

The three phases of the step cycle do not vary with the direction in which the feet are moving the starfish, and therefore presumably the direction in which the feet are loaded, although the error on the timing is rather large at about 30% of the mean. This may because the sample of times was not very large (20 for each reading) or because the timings themselves are very variable. Originally we thought that the recovery would occur over a much broader spread of time than the propulsive phases, thinking that recovery would not be entrained or co-ordinated in any way whereas the propulsive phases would at least be entrained by contact with a stiff substrate moving past the foot at a constant speed. However, it seems that all parts of the cycle are equally lax in temporal control. This is confirmed by the mathematical model which shows large variation in all the timings. This can happen only if the tube feet are stretched by differing amounts so that the step length is variable.

We are still trying to produce a gel actuator which will move sufficiently fast (Fig 2). This may be a function of the shape as much as the size and chemistry of the gel. Currently we use cylinders, which give the least surface area per unit volume – precisely what we do not want in order to increase water transfer! Other shapes will offer increased rates of diffusion of swelling water into and out of the gel without compromising the capacity of the gel to produce a force as it bends. We are also exploring the use of different materials for embedded electrodes within the gels, or perhaps even metal deposited onto the surface of the gel, putting the layer into bending rather than stretching when the gel itself bends.

The modelling and analysis of locomotion shows that co-ordination between the feet may not be an important issue: speed probably is but the movement of the feet can be entrained by contact with a stiff substrate.

Acknowledgements

We thank Mr. T. Jenkinson, Dr. E. A. Robson, Prof. G. Jeronimidis and other members of the Centre for Biomimetics at University of Reading for their help and advice. T. Yamauchi was funded by the Japanese Society for the Promotion of Science and the Royal Society.

References

Kerkut G A (1953). The forces exerted by the tube feet of the starfish during locomotion. *Journal of Experimental Biology* **30**, 575-583.

Osada Y, Okuzaki H, and Hori H (1992). A polymer gel with electrically driven motility. *Nature* **355**, 242-244 .

Osada Y and Ross-Murphy S B (1993). Intelligent gels. *Scientific American* **268(5)** , 82-87 .

Table 1 – Time taken by tubefeet of each of two starfish for different phases of movement

	t_p	t_e	t_r
1st starfish - upwards	2.0 ± 0.65	3.4 ± 1.36	5.6 ± 2.16
1st starfish - horizontal	3.55 ± 0.94	5.2 ± 1.24	5.9 ± 1.21
1st starfish - downwards	3.05 ± 1.96	6.95 ± 2.96	5.85 ± 1.18
2st starfish - upwards	4.55 ± 1.73	10.7 ± 3.24	9.6 ± 2.68
2st starfish - horizontal	8.1 ± 3	10.75 ± 3.08	9 ± 3.08
2st starfish - downwards	6.7 ± 2.08	14.5 ± 3.82	6.7 ± 2.08

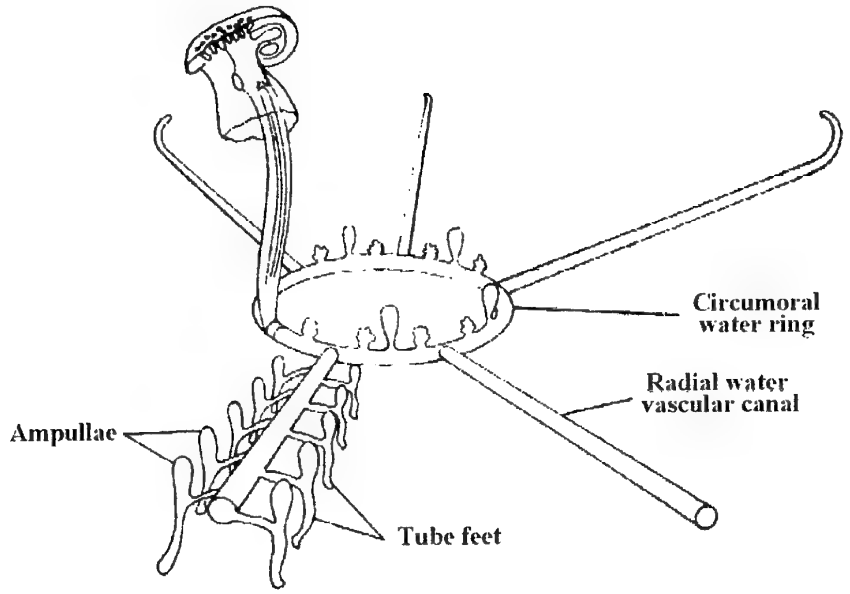

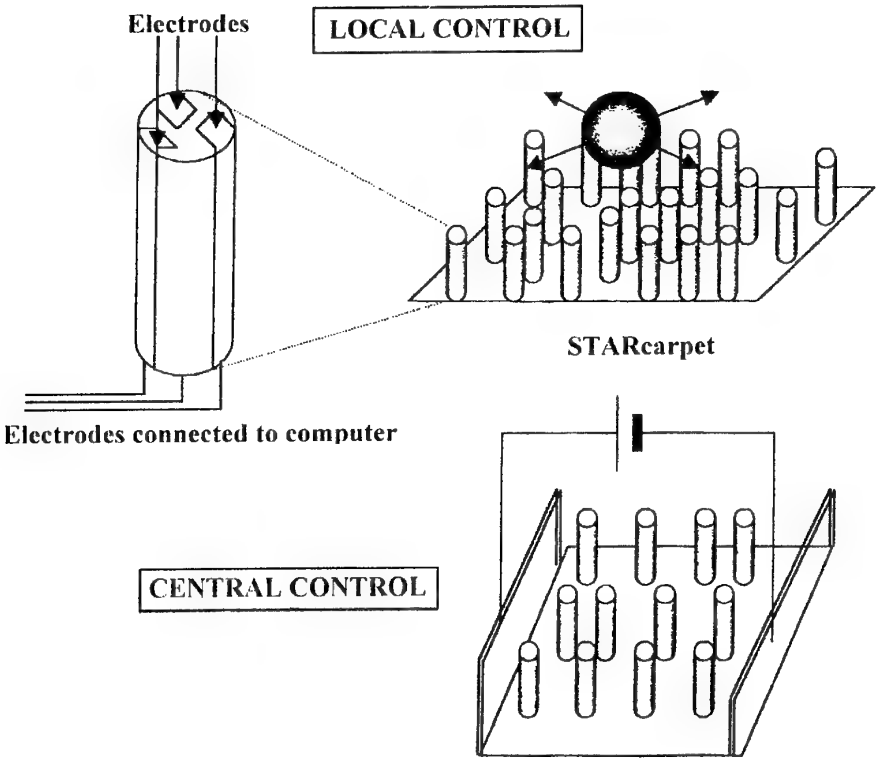

Figure 1 (top). The water vascular system of a starfish. There are ampullae and tube feet on each canal, about 100 in all. There may be several rows on the underside of each arm.
Figure 2 (bottom). Diagram of the Shear Traction *Asterias rubens* carpet showing two possible modes of actuation and control.

ELASTODYNAMICS OF HYDROGELS AS BIPHASIC MODEL OF NATURAL SOFT TISSUES

Piero Chiarelli

CNR-Institute of Clinical Physiology
and
Centro "E. Piaggio", Faculty of Engineering
University of Pisa

Macromoleular materials of synthetic origin are of ubiquitous use in modern technology. The peculiar rheological properties and energy transduction characteristics of selected polymeric systems make them an high priority target for the development of functional materials. As a parallel scientific and technical endeavour, biomimetic materials, structures and systems are emerging as tools that will enable engineering sciences to broaden their classical methods and techniques.
This lectures reports tutorially about rheological properties of polymer hydrogels with reference to selected implementations of a biomimetic character.
Interest in synthetic hydrogels is stimulated by their remarkable physical, chemical and mechanical properties, their commercial applications and their ability to mimic the behavior of the biological gels. Hydrogels are sensitive to a wide range of environmental stimuli; they also exhibit a wide range of responses. Their intrinsic compliance, high water content and ability to interconvert electrical, chemical and mechanical energy make them suitable for use as skin-like tactile sensors or muscle-like actuators. The sensitivity of their volume and hydraulic permeability to solvent composition, temperature and pH make them suitable as controllable macromolecular separation membranes and drug-delivery systems.
Moreover, some synthetic hydrogels mimic the properties of natural extra-cellular matrixes. Soft natural tissue have a solid polymeric matrix made up of collagen, elastin, muchopolysacharides, whose interstices contains water with small ions, nutrients, proteins and other solutes: living organism need both solid rheological properties and molecular or ion diffusion as in fluids. Hence the bi-phasic structure is a basic element of biological systems that have a proper form with good rheological properties and allows convective-diffusion process. Moreover the contemporary presence of a solid and fluid phase make possible the realisation of new phenomena that cannot happen both in a solid and a fluid structure; these are: compressive shock adsorption such as in cartilage abruptly submitted to a load, streaming potentials such as in compressed dermis and bone, proteins filtration such as in lymphatic system, elastic modulation of cardiac walls by means of its fluid content, etc.; all those phenomena can be ascribed to the relative motion of fluid within a solid matrix. Looking at the fluid component in soft biologiacal tissue we observe that it ranges from 80% in cartilage, to 60-70% in dermis, arterial wall, tendons and ligaments, down to 20% in bone and to 10% in dentin. Other tissues have a very low cellular component and are basically natural gels; among those they are

vitreous body, synovial fluid, cornea etc. Recently the rheological properties of white and grey brain tissue and of chromosomes have been explained in terms of bi-phasic elasticity.

The viscoelastic relaxation with presence of streaming potential and interstitial fluid pressure in a bi-phasic structures will considered. A creep elongation of an arterial wall submitted to a pressure beat and the streaming potential in dermis generated by in uniaxial confined compression tests will discussed..

Electro-active Polymer Gel Application for Bioreactor

Takeshi Yamauchi, Kaori Seki, K. Oshima, Masato Shimomura and Shinnosuke Miyauchi

Department of Bioengineering, Nagaoka University of Technology
1603-1 Kamitomioka, Nagaoka 940-2188, Japan
Phone: +81-258-47-9426 Fax: +81-258-47-9400

Abstract

Glucose oxidase (GOD) and glucose isomerase (GIR) were covalently immobilized on a electro-active polymer gel membrane composed with poly (vinyl alcohol)-poly (acrylic acid) (PVA/PAA) and it was investigated that the permeability of substrates and products of biochemical reaction through these enzymes immobilized gel membrane under applied electric fields.

The amount and specific activity of GOD immobilized on the electro-active polymer gel membrane are 1.1 mg/g-product and 145 U/mg-GOD, respectively. D-glucono-δ-lactone was effectively permeated through the GOD immobilized membrane under applied electric fields. Increased with applied electric field from 0 V to 6V, the amount of D-glucono-δ-lactone through the membrane was also increased in. The conversion fromβ-D-glucose to D-glucono-δ-lactone was determined by the ratio with the total amount of D-glucono-δ-lactone and β-D-glucose which permeated through GOD immobilized PVA/PAA membrane. The value of conversion fromβ-D-glucose to D-glucono-δ-lactone was ca. 80% under each electric field. On the other hand, the amount and relative enzyme activity of GIR immobilized electro-active polymer gel membrane were as same as those of GOD, though the value of the conversion fromβ-D-glucose to D-fructose under the electric field was very low compared with that of GOD.

Introduction

Polyelectrolyte gels undergo significant changes in their volume or shape under the influence of electric fields. When electric fields were applied to polyelectrolyte gels in such a way that their dimensions were kept constant without allowing for any change in shape, isometrically contractile stress was generated in the gel and this expanded the pore channels through which solutes and solvents could permeate. This unique specificity of polymer gel is known as chemical valve [1].

Polymer gels have been also useful support materials for immobilized enzymes and superior to maintenance of water to keep enzyme activities. Many studies have been reported on the method of immobilized enzymes such as absorbed, matrix-entrapped, micro-capsuled, and covalently bound in polymer gels. Immobilization of enzyme to chemical valve would construct a new type of bioreactor through which permeation of biochemical products can be controlled electrically.

In the present work, glucose oxidase and glucose isomerase which catalyzed glucose for biochemical reaction were covalently immobilized in the electro-active polymer gel membrane composed with poly (vinyl alcohol)-poly (acrylic acid) (PVA/PAA) and

permeability of substrates and products of biochemical reaction through enzymes immobilized gel membrane under applied electric fields.

Experimental

Materials

PVA (Mw=17,000; Kurare Chemical Co., Japan) and PAA (Mw=25,000; Wako Chemical Co., Japan) were commercial products. The GOD used (EC 1.1.3.4, Type I, from *Aspergillus sp.*) was supplied by Toyobo Co., Ltd., which had an activity of 594 units mg-1. The GIR used was supplied by Nagase Biochemicals Co., Ltd., which had an activity of 2 units mg^{-1}. Peroxidase used (EC. 1.11.1.7, type I, from horseradish) was supplied by Sigma Chemical Co., which had an activity of 120 units mg^{-1}.

Immobilization of enzyme on the PVA/PAA composite membrane

Preparation of the PVA/PAA composite gel membrane was reported before using the iterative freezing-thawing method [2]. Immobilization of enzyme on the PVA/PAA composite membrane was carried out as follows:

A mixture of 200 mg of the PVA/PAA, 40 mg of enzyme and 20 ml of 0.1 M phosphate buffer (pH 6.5) were placed into a flask and stirred for 5 min. Subsequently 100 mg of condensing agent (1-cyclohexyl-3- (2-mropholinoethyl) carbodiimide metho-*p*-toluensulphonate) was added and stirring was continued. After 18 h of stirring, the reaction product was washed with distilled water several times and filtrated *in vacuo*. This procedure of immobilization was carried out at 4 °C. The product was stored at 4 °C in 0.1 M phosphate buffer, pH 7.6. The amount of immobilized enzyme was estimated by using Folin – Ciocalteu phenol reagent after alkaline copper treatment, according to the direction of Lowry [3].

Enzyme activity measurements

The enzyme activity of immobilized GOD was measured by colorimetric method based on the procedure of Trinder [4]. In the dark bottle, 32 mg of 4-aminoantipyrine and 2.6 mg of peroxidase were dissolved in 200 ml of 0.1 M phosphate buffer, and a 0.1 M phenol solution (4 ml) was added: solution 1. β-D-glucose solution of 1.0 mM was prepared and allowed to stand for 12 h or more at room temperature: solution 2. Avoiding direct sunlight, 5.0 ml of solution 1 and 0.5 ml of solution 2 were kept a given temperature and mixed with GOD-bound polymer gel membrane, and incubated at 30 °C for 1h. The mixture was cooled to 0 °C and incubated for 5 min. The enzyme activity of immobilized GOD was determined by measurement of absorbance at 505 nm by using a Shimazu UV-310PC spectrophotometer.

The enzyme activity of immobilized GIR was measured by colorimetric method based on the procedure of. Dishes [5]. 0.15g of cystein was solved in 10 ml hydrochloric acid solution: solution 3. 0.12g carbazole was added in 100ml of alcohol. (solution 4). 2ml ofβ-D-glucose solution was mixed with GIR-bound polymer gel membrane, and incubated at 60 °C for 0.5h. Added Solution 3 in 1ml of the mixture and cooled to 0 °C . After cooling, solution 4 and 6ml of sulfuric acid solution were added to mixture with stirring for 30 min at 40 °C. The enzyme activity of immobilized GIL was determined by measurement of absorbance at 560 nm by using a Shimazu UV-310PC spectrophotometer.

Permeation Experiments

The permeability of glucose through the membrane was investigated at room temperature using the permeation cell. The cell consisted of two connected compartments; one side with a 100 mM phosphate buffer (pH 6.8, 100 ml) containing 50mM β-D-glucose and the other side containing the same buffer (100 ml) without the glucose. The membrane, having an effective area of 0.8 cm^2, was fixed tightly between the two sides. Circular platinum mesh electrodes with a diameter of 1 cm were placed in both the source and receiving phases separated by the membrane. The electrodes were connected to a DC source (Model PAB18-3A, Kikusui electronics. corp., Japan). The amount of β-D-glucose through the gel membrane was measured using by Somogyi-Nelson method. 0.5ml of solution in permeation cell, 1.0 ml of Somogyi solution was added and incubated at 100 °C for 15 min. After cooling at 0 °C, 1ml of Nelson solution was added with 10 ml distilled water. The amount of β-D-glucose was determined by measurement of absorbance at 540 nm by using spectrophotometer. The amount of D-glucono-d-lactone, which was products of enzyme reaction, was measured by using colorimetric method described as GOD activity measurements. The amount of D-fructose was measured by using high performance liquid chromatography (830-RI, Nihon Bunko Co., Ltd.).

Results and Discussion

Immobilization of GOD on the PVA/PAA composite membrane

The amount and enzyme activity of enzymes immobilized PVA/PAA membrane are given in Table I.

The amount of immobilized GOD and GIR to PVA/PAA gel membrane was 1.1 and 1.0 mg/g, respectively. Relative activities, which compared with the enzyme activity of native and immobilized enzyme, are also same value. The amount of GOD immobilized to PVA/PAA membrane was seven times as that of PVA membrane (Data is not shown). These results indicated that GOD and GIR in PVA/PAA gel membrane was bound to carboxyl group of PAA gel membrane covalently and kept 10- 20 % of its enzyme activity.

Table I The amount and enzyme activity of enzymes immobilized PVA/PAA gel membrane

	Amount of immobilized enzyme mg / g-gel membrane	Specific activity U / mg-enzyme	Relative activity %
Glucose oxidase	1.1	145	20
Glucose isomerase	1.0	0.09	12

ß-D-Glucose permeation characteristics

In the previous study, it was suggested that application of the electric field brought about the formation of pore channels within the PVA/PAA membrane[2]. Diffusion coefficient of β-D-glucose through the gel membrane was calculated from the time profile of β-D-glucose permeation by following expression:

$$D = \frac{Q\ L}{t\ A\ \Delta C}$$

where Q is amount of substrate in receiving phase, L is thickness of gel membrane, t is time, A is effective area of gel membrane, and C is the concentration of substrate in source phase.

. Increased with applied voltage from 0 V to 6V, the amount of β-D-glucose permeation was increased in. Difusion coefficient of β-D-glucose at 6V is ten times larger than that of 0V (Table II). This result indicated that application of an electric field brought about the formation of pore channels within the PVA/PAA membrane. Increased with applied voltage between the electrodes, the pore channels were extended and promoted permeation of β-D-glucose through the PVA/PAA membrane. The amount of glucose permeation through the PVA/PAA membrane was able to control by the electric field and this would be considered to construct new type bioreactor. The enzyme immobilized PVA/PAA gel membrane would control the permeation of products that produced by enzyme reaction when substrates transported through the membrane.

The diffusion coefficient of β-D-glucose through the gel membrane was increased 6 times with the mole fractions of PAA from 0 to 0.25 (Data is not shown). It is also estimated that polyelectrolyte gels were undergoing significant changes in their volume under electric field to their surroundings.

Table II Permeability of PVA/PAA gel membrane for β-D-glucose under the electric fields

Applied voltage V	Diffusion coefficient ($\times 10^6$) cm^2/ s
0	0.2
2	0.7
4	1.2
6	2.1

Molar ratio of PAA in gel membrane was 0.25

Products permeation characteristics

GOD is highly specific for β-D-glucose and D-glucono-δ-lactone is produced by the enzyme reaction

GOD (FAD) +β-D-glucose → GOD ($FADH_2$) + D-glucono-δ-lactone

Increased with applied voltage from 0 V to 6V, the amount of D-glucono-δ-lactone through the membrane was also increased in. Diffusion coefficient of β-D-glucose at 6V was ten times larger than that of 0V (Table III). This result indicated that GOD immobilized PVA/PAA membrane can control the permeation of products that produced by enzyme reaction applied the different voltage. Figure 1 shows the initiation and termination control of permeation of products by the electric field.
The conversion fromβ-D-glucose to D-glucono-δ-lactone was determined by the ratio with the total amount of D-glucono-δ-lactone andβ-D-glucose which permeated through GOD immobilized PVA/PAA membrane. The conversion of β-D-glucose to D-glucono-δ-lactone was ca. 80% under each electric field.

Table III Permeability of PVA/PAA gel membrane for D-glucono-δ-lactone under the electric fields

Applied voltage V	Diffusion coefficient $(\times 10^6)$ cm^2/s
0	0.2
2	0.3
4	1.0
6	2.1

Molar ratio of PAA in gel membrane was 0.25

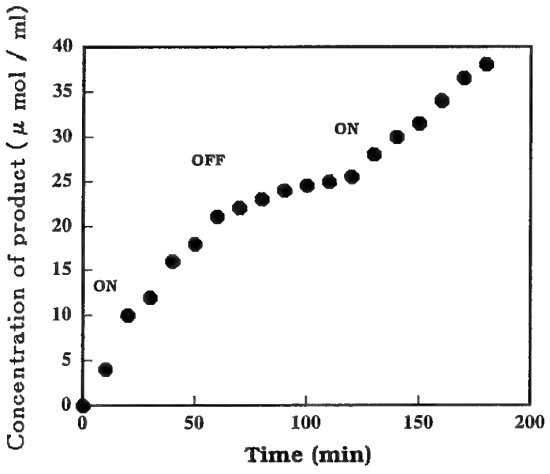

Figure 1 The initiation and termination control of products permeated through glucose oxidase immobilized gel membrane. Applied voltage: 6V

GIR is highly specific forβ-D-glucose and D-fructose is produced by the enzyme reaction

$$\beta\text{-D-glucose} \rightarrow \text{D-fructose}$$

Figure 2 shows the permeability of GIR immobilized PVA/PAA membrane for D-fructose. The amount of products was increased during application of the electric field (300v/cm). Compared with that of GOD immobilized gel membrane, it takes substantial time to convert the substrates to products. The conversion ratio was estimated at *ca.* 5 %. The amount of immobilized enzyme and relative enzyme activity of GOD and GIL were same value, though the enzyme activity of GOD was thousands times larger than that of GIR. Application of electro-active membrane for membrane type of bioreactor, the enzyme activity would be played role the important part for the ability of reactor.

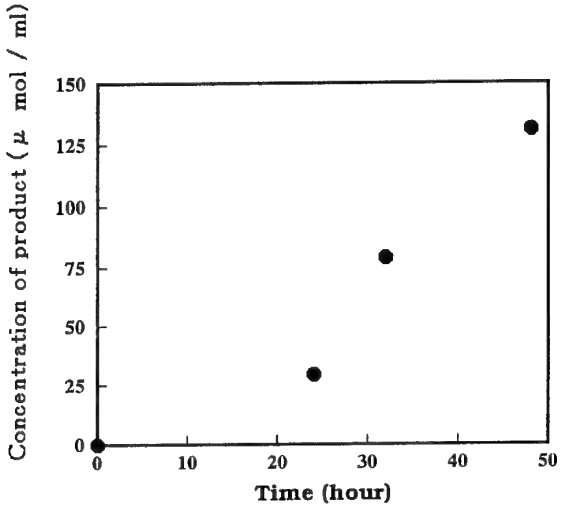

Figure 2 Permeation of product through glucose isomerase immobilized PVA/PAA gel membrane. Applied voltage: 6V

Conclusion

Glucose oxidase and glucose isomerase were covalently immobilized in the electro-responsive polymer gel membrane and investigated in the permeability of substrates and products of biochemical reaction through enzyme immobilized gel membrane under applied electric fields.

The amount and specific activity of GOD immobilized PVA/PAA membrane were 1.1 mg/g-product and 145 U/mg-GOD, respectively. D-glucono-δ-lactone was effectively permeated through the GOD immobilized membrane under applied electric fields. The increased with applied voltage from 0 V to 6V, the amount of D-glucono-δ-lactone through the membrane were also increased in. Conversion from β-D-glucose to D-glucono-δ-lactone was determined by the ratio with the total amount of D-glucono-δ-lactone and β-D-glucose, which permeated through GOD, immobilized PVA/PAA membrane. The value of conversion from β-D-glucose to D-glucono-δ-lactone was ca. 80% under each electric field.

The amount and relative enzyme activity of GIR immobilized electro-active polymer gel membrane were as same as those of GOD, though the value of conversion from β-D-glucose to D-fructose was very low compared with that of GOD under the electric field.

References

(1) Y. Osada and M. Hasebe, *Chemistry Letters*, 1285-1288 (1985)
(2) T. Yamauchi, E. Kokufuta, and Y. Osada, *Polymer gels and Networks*, 1, 247-255 (1993)
(3) O. H. Lowry, et al., *J. Biol. Chem.*, **193**, 265-275 (1951).
(4) P. Trinder, *Ann. Clin. Biochem.*, **6**, 24-27 (1969)
(5) Z. Dishe and E. Borenfreund, *J. Biol. Chem.*, **192**, 583-587 (1951).

Fish and ships: can fish inspired propulsion outperform traditional propeller based systems?

B. Picasso, A Manuello Bertetto, M. Ruggiu
Dipartimento di Ingegneria Meccanica,
Università di Cagliari, Italy.

Abstract

Fish propulsion mechanism is becoming a major research topic. Effort is aimed at understanding the reasons for the high swimming performances of marine creatures and investigating the possibility of applying fish-like propulsion to surface and underwater vehicles.
In this paper, two mathematical models were applied to predict thrust in oscillating tail propulsion. The first one was based on the classical treatment of M.J. Lighthill , the latter on the numerical integration of the dynamic and cinematic equations of the tail fin, modelled as an high efficiency hydrofoil . A fish robot prototype and a thrust measuring equipment were developed in order to assess the accuracy and reliability of the analytical models used. The model simplifications and assumptions were analysed and discussed.

1 Introduction

Natural selection ensured that the propulsion systems evolved in fish are highly efficient. Their remarkable swimming abilities could inspire innovative and efficient designs to improve the ways that man-made systems operate in the aquatic environment. Some mobile marine robotic devices are currently being developed to assess the potential and study the propulsive cinematic patterns utilised by fish and other aquatic animals [1], [2], [3], [4].
The wake left behind the fin is an array of discrete vortices of alternating sign, generated as the caudal fin moves, producing a backward water jet. The structure of the wake is reversed compared to the drag-producing Karman vortex street, typically observed in the wake of objects moving in a fluid [11]. Interesting examples are reported in the [12-16] web sites.

2 Mechanics of Motion and Analytical Models

Lighthill [8] classifies fish by the propulsion point of view in two large families, anguilliform (eel like) and carangiform. His model of the mechanics of fish propulsion is still largely used. In using Lighthill's results we have assumed that the fish tail was made of a peduncle connecting the tail fin to the fish body. Only the contribution of the hydrofoil shaped tail fin to the thrust is considered in the model.

3 The Robot and the test rig.

The robot fish [4] consists of four parts: a cylindrical aluminum body of 160 mm diameter, a front fiberglass nose, a rear conical part containing the motor and transmission, and the tail. The motor is powered by two Pb-batteries (12V, 1Ah) located in the central section. The drive is controlled by a microcontroller. The mechanical transmission consists of a couple of bevel gears and a toothed belt . The tail is made of polycarbonate and its shape was replicated from a real tuna tail fin.. The tail motion frequency was varied until a maximum of 3 Hz. The robot is immersed in a water canal and fixed to an instrumented strut. The thrust was obtained as the decrease in drag force due to the fin oscillation.

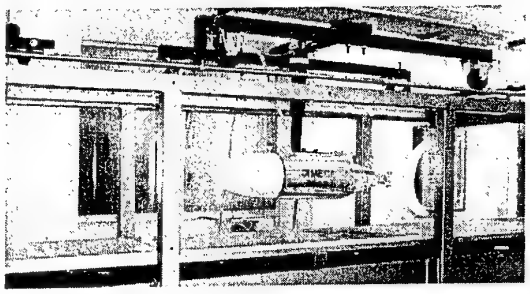

4 Numerical Model

The robot kinematics and dynamics were simulated using a commercial code[18] based on the numerical integration of the motion equations. The fish was modeled as a four body system, the fish body, the dynamometer, the peduncle hinged to the fish body and the hydrofoil hinged to the peduncle. The fish body is modeled as an elliptical pure mass, the dynamometer as a spring-dashpot unit whose stiffness and damping parameters were measured.

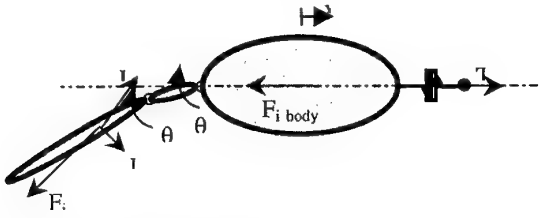

Figure 2: Numerical model

5 Thrust Measurement

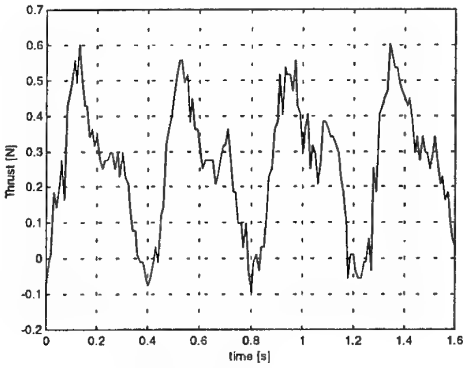

Numerous tests were performed in order to measure thrust exerted by the robot at different frequencies and amplitudes of the tail motion and different water speds. As an example in figure 5 the thrust curve vs. time at f=1.25Hz and amplitude A=25° is shown. In table 1 below the mean value of the thrust is given,for a watervelocity of 0.2 m/s, together with the corresponding predicted values.

Figure 3 : Thrust vs time curve

Table 1 Experimental and calculated average thrust values

f (Hz)	0.8	0.8	0.8	0.8	1.25
α (deg)	12.5	20	30	40	12.5
θ	0.268	0.270	0.278	0.288	0.171
h (m)	0.0324	0.0513	0.075	0.0964	0.0324
Lighthill	0.13	0.31	0.681	1.12	0.32
Our Model	0.178	0.256	1.9	2.6	0.30
Test results	0.175	0.25	0.39	0.19	0.26

It can be observed that Lighthill model and ours give fair predictions of the thrust force provided the semi amplitude of the tail oscillation remains under 20°. For larger amplitudes the basic assumptions made for

both models are not valid any more. In this case a more complex three dimensional CFD non-stationary analysis is required.

6 Conclusions

A strong research endeavour is needed to reach a full understanding of the real potential of fish inspired propulsion for marine applications. In this paper it has been shown that relatively symple models can be used to predict the average thrust values produced by an oscillating fin. Moreover the implementation of a fully instrumented test rig permitted to get a fruitful insight on many aspects of the propulsion mechanics. The applicability of the models used seems to be limited to small angular oscillations, say less than 20°of half angular amplitude. Further investigations are planned to to develop improved models of extended applicability.

Bibliography

[1] D. Barrett, M. Grosenbaugh, and M. Triantafyllou, "The optimal control of a fexible hull robotic undersea vehicle propelled by an oscillating foil," in *Proc. 1996 IEEE AUV Symp.*, pp. 1–9.

[2] N. Kato and M. Furushima, "Pectoral fin model for manuever of underwater vehicles," in *Proc. 1996 IEEE AUV Symp.*, pp. 49–56.

[3] I. Yamamoto, Y. Terada, T. Nagamatu, and Y. Imaizumi, "Propulsion system with exible/rigid oscillating fin," *IEEE J. Oceanic Eng.*, vol. 20, pp. 23–30, 1995.

[4] B. Picasso, A. Manuello Bertetto, M. Ruggiu, "Development of a robotic Fish for Surface and Underwater Inspection: an Experimental Study on the Mechanics of Oscillating Tail Propulsion", in *Proc. 9th International Workshop on Robotics in Alpe-Adria-Danube Region RAAD 2000*, pp. 227-232.

[5] P.W. Webb, "Form and function in fish swimming," *Sci. Amer.*, vol. 251, pp. 58–68, 1984.

[6] M.J. Lighthill, "Note on the swimming of slender fish", *Journal of Fluid Mechanics*, vol. 9, 1960.

[7] M.J. Lighthill "Hydromechanics of aquatic animal propulsion", *Journal of Fluid Mechanics*, vol. 44, 1969.

[8] M.J. Lighthill "Aquatic Animal Propulsion of High Hydromechanical Efficiency", *Journal of Fluid Mechanics*, vol. 44, 1970.

[9] M.J. Lighthill, "Large amplitude, elongated body theory of fish locomotion", in *Proc. R. Soc. Lond. Ser. B. Biol.Sci., pp.* 125-138, 1971.

[10] Garrick I.E., "Propulsion of A Flapping And Oscillating Airfoil", *NACA Technical Report 567, 1936.*

[11] G. S. Triantafyllou, M. S. Triantafyllou, and M. A. Grosenbauch, "Optimal thrust development in oscillating foils with application to fish propulsion," *J. Fluids Struct.*, vol. 7, pp. 205–224, 1993.

[12] http://www.cee.hw.ac.uk/~sfakios/html/describe.htm
web page of Heriot-Watt University (Edinburgh – Scotland)

[13] http://www.erc.caltech.edu/Research/Reports/mason1full.html
web page of Caltech - Center for Neuromorphic Systems Engineering

[14] http://dimeca.unica.it/labrob.html
DIMECA University of Cagliari Italy robotic lab web page

[15] http://web.mit.edu/towtank/www/tuna/brad/tuna.html
MIT web page Massachusetts USA

[16] http://robby.caltech.edu/~kristi/
Caltech web page California USA

[17] http://draper.com/tuna_web/vcuuv.htm
Draper Laboratories web page

[18] Working Model 2D user's Manual

CARBQN NANOTUBE CHARGE-TRANSFER COMPLEXES FOR ARTIFICIAL MUSCLES, ENERGY STORAGE, AND ENERGY HARVESTING

Ray H. Baughman, Honeywell nt.

Our early theoretical work predicted that carbon nanotubes could be used for electromechanical actuators that provide order-of-magnitude advantages over any competing technology in work density per cycle and stress generation capabilities, while operating at over an order-of-magnitude lower voltage than ferroelectrics. This dream of a game-changing actuator technology based on giant double-layer charge injection into carbon nanotubes is being realized in our DARPA funded programs. We use three fundamentally different types ot actuator mechanisms: band-structure-related expansion of individuai nanotubes, electrostatic double-layer repulsion, and pneumatic sheet expansion. Using the former mechanism, we demonstrated 50 times higher stress generation capability than natural muscle and 10 times higher actuator strain and gravimetric work capacity than for high modulus ferroelectrics. Like natural muscles, our large artificial muscles are assemblies of billions of individuai nano-scale actuators, while our nanoscale machines can potentially utilize a single nanometer-diameter fiber. We also use double-iayer charge injection into carbon nanotubes to made super capacitors that charge and discharge in less than 20 ms, chemicaliy driven nanotube actuators for microfluidic valves, and thermo-electrochemical cells for harvesting thermai energy that have ten times higher effective thermopower than the highest performance thermoelectrics. The presentation will describe theoretical and experimental results, as weii as the novel methods that we have developed for materials synthesis and fabrication.

Protein motor mechanism: Affinity gradient force model

Makoto Suzuki

Graduate School of Engineering, Tohoku University
Aoba-yama 02, Sendai City, 980-8579 Japan
Phone/Fax +81-22-217-7303, msuzuki@material.tohoku.ac.jp

Abstract
Actomyosin is a natural nano-machine which generates force up to 5pN per myosin motor domain S1 and moves with a relative speed of 10μm/s. The working stroke per S1 per one ATP hydrolysis was evaluated as at least 60nm by Yanagida (1985) which lead to the loose coupling (LC) model by Oosawa (1986). This paper describes a linear motor model for actomyosin based on an affinity gradient force and affinity transition of protein surface. This model can successfully predict the experimental facts, such as the magnitude of driving force, the force-velocity relation by Edman(1988) and long-powerstroke movement, which were hardly explained by well-known swinging-crossbridge models.

Introduction

A skeletal muscle fiber generates tensile force as high as 0.5 MPa within 0.1s. This force and the response speed enable animals quick, limber and dexterous movement. Actomyosin is a motor protein complex which converts chemical energy of ATP (adenosine triphosphate) hydrolysis into mechanical work, therefore it is the molecular engine of muscle fiber. F-actin is a linearly polymerized filament of G-actin (Mw:42300) which size is 5nm. Myosin filament is a bipolar bundle of myosin molecules which have a tail and two identical motor domains called S1 which binds with ATP and hydrolyze it, then drives F-actin at 10μm/s at no-load. This speed is high enough to produce most of animals' movement. S1 domain can generate force as high as 5 pN [Ishijima et al.(1994)]. The ATP hydrolysis rate (actin activated ATPase rate) of S1 is 10 s^{-1} in solution. In vitro motility experiment by Harada et al. (1987) showed that a short F-actin of 40nm long can slide at 6 μm/s which is caused by only a few S1. Assuming that at most ten S1 molecules acted on a 40nm F-actin, the ATP hydrolysis rate may be about 100 s^{-1}. As a conclusion F-actin filament must travel 60nm per 1ATP hydrolysis reaction. It is 12 times longer than G-actin size and 4 times longer than S1 size.

Bases of new driving mechanism

To construct a driving model of actomyosin satisfying the facts noted above, one cannot depend only on a structure change of S1, which is well-known the swinging-leverarm model [Rayment (1993) , Sutoh, et al. (1998)]. Thus, we consider that F-actin cannot be only a rail of S1 and should act as an active device to carry S1 for long distance using a part of energy transferred from S1-ATP complex. How can such an energy transfer be possible? What is the high energy state of protein molecule? To discuss these problems we here start from the basic energetics.

ATP is called a high energy molecule because of its steric unstable stracture between β-P (phosphorus) and γ-P. By hydrolysis reaction of ATP the chemical energy may be used to break considerable secondary bonds between the nucleotide and the protein or in the inside of protein. Breaking such secondary bonds coresponds to an enthalpy increase. It may not be preferable in nature. But at the step from the M.ATP complex state to the M.ADP.Pi complex state $\Delta H>0$, $\Delta S>0$, $\Delta C_p<0$ was observed by calorimetric study[Kodama, (1985).]. In water ATP molecules dissociate very slowly at neutral pH. There is a large energy barrier. How can the energy barrier be reduced in a protein molecule?

One solution has been given by dielectric analysis of myosin S1 solution [Suzuki, (1997)]. The study showed a reduction of the hydrophobic hydration, which is proportional to the hydrophobic surface area, of S1 molecule at the M.ADP.Pi state and a hydrophobicity recovery at M.ADP state. The surface of S1 at M.ADP.Pi state is less hydrophobic than that at M.ADP state. In addition liquid chromatographic study [Gopal and Burke, (1997)] showed the surface hydrophobicity decrease of S1 at the step. It indicates that hydrophobic interaction at the S1 surface increased at the step. Thus, $\Delta S>0$ is realized by dehydration of protein, and ΔH is compensated by $-T\Delta S$.

Thus, the reduction mechanism of barrier height from M.ATP to M.ADP.Pi can be understood as the secondary bond breaking inside the protein with ATP (which corresponds to $\Delta H>0$) is promoted by hydrophobic interaction at the surface of S1 (which corresponds to $\Delta S>0$). Such a hydrophobicity change of protein surface upon some chemical reaction may be rather general mechanism in protein-protein interactions. Here we propose a new theory of force generation of actomyosin by refining the rough idea [Suzuki, 1994].

Affinity gradient force

Let us consider a hydrophobic substrate in water. When a protein molecule with a surface-exposed hydrophobic area approaches to the substrate the protein molecule (P) can attach to the substrate (S) with contact area A and diameter L. Let the free energy change of contact be ΔG_c. If ΔG_c is negative the interaction is attractive (positive affinity). So we define the surface affinity to P as $-\Delta G_c$. Consider a plane substrate S which surface has positive affinity to P then the contact free energy change is $\Delta G_{c1}(<0)$. If the affinity of P to S became negative by some stimulation, such as by chemical reaction or light irradiation, put the contact free energy change as $\Delta G_{c2}(>0)$. If the stimulation was given to the left half surface of the center position of P, P should translocate toward right. The free energy change of the translocation is $[\Delta G_{c1}-\Delta G_{c2}]$. Then the driving force F is written as

$$F = [\Delta G_{c2}-\Delta G_{c1}]/L.$$

This consideration can be extended to general substrate surface having hydrophobic moieties and polar or ionic groups. Extending this equation to a continuum form by introducing $\Delta G_c(x)$, the equation is written as

$$F = - \partial \Delta G_c (x)/\partial x,$$

where x is the center position of P and the surface affinity of S to P varies continuously as a function of x. ΔG_c is also a function of other parameters such as temperature, ionic strength of solution and so on.

The substrate surface can be stimulated by an energy transfer from P which undergoes chemical reaction such as ATP hydrolysis. In actomyosin the chemical energy of ATP hydrolysis is first released in myosin S1and finally transferred to actin to pull the load. It is important to note that the transferred energy from S1 to one actin just interacting is not necessarily all of hydrolysis energy of one ATP which is about 20kT. This idea gives a physical image of the loose coupling model proposed by Oosawa et al.(1986).

Linear motor model

Based on the affinity gradient force introduced above we constructed a linear motor model. X is the left-edge position of motor (S1) in the x-axis which is the long axis of F-actin. We put the lattice length as d. The contact length L is a function of ΔG_c. When the surface of F-actin at X <x<X+d is stimulated to become negative affinity to S1 ($\Delta G_{c2}(>0)$), driving force F is generated. Using a molecular friction coefficient γ and a load F_w the equation of motion of X becomes that

$$dX/dt = (F - F_w)/\gamma.$$

Introducing a time constant τ for the transition of the surface affinity ($-\Delta G_c$) when a stimulation A was applied,

$$\partial\Delta G_c/\partial t = (A - \Delta G_c)/\tau, \quad \min(\Delta G_c)=\Delta G_{c1}, \max(\Delta G_c)=\Delta G_{c2},$$

where $A=A_0u(x,X)$, and $u(x,X)=0$ for $x<X-d$ and $X+2d<x$, $u(x,X)=1$ for $X <x<X+d$, $u(x,X)=(x-X+d)/d$ for $X-d<x<X$, and $u(x,X)=(X+2d-x)/d$for $X+d<x<X+2d$. And

$$F = - (L/L_0)\partial\Delta G_c/\partial x,$$

where L is the contact length and a function of ΔG_c as

$L= L_0$ for $\Delta G_c <\Delta G_{c1}/ n$ or $\Delta G_c >\Delta G_{c2}/ n$,

$L= L_0/ n$ for $\Delta G_{c1}/ n < \Delta G_c <\Delta G_{c2}/ n$.

Here n was introduced to realize a sharp transition of surface force.

Fig.1 shows the force velocity relation of the present linear motor model using affinity gradient force and the experimental data on a muscle fiber given by Edman (1988). The parameters used in the model were n=6, γ=1.15μNs/m, $[\Delta G_{c2}-\Delta G_{c1}]/(L_0)$=3pN, d=1nm, τ=80μs, and $A_0=\Delta G_{c2}$, which gave a sliding speed around5μm/s. The experimental contraction velocity is approximately hyperbolic and becomes zero above $F_w=0.65F_{max}$. The present model could predict the feature, specially the sudden decrease above $F_w= 0.6F_{max}$, although there is a deviation at low F. If we assume that the friction coefficient between actin and myosin is a function of velocity v with a factor exp(-av) the experimental curve can be perfectly fitted.

The magnitude of driving force

The possible driving force by this model can be estimated from the contact free energy change ΔG which is close to the interfacial tension from 5 to 50 mJ/m^2. The value 50 mJ/m^2 corresponds to the interface between water and liquid hydrocarbon. Using the contact area between F-actin and S1 of $5nm^2$ and the contact width L=2nm,

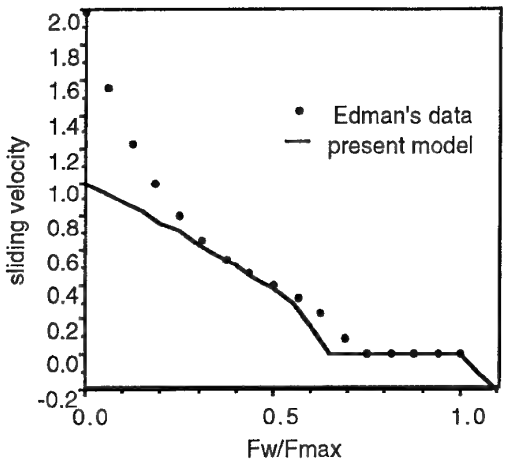

Fig.1 Force-velocity relation

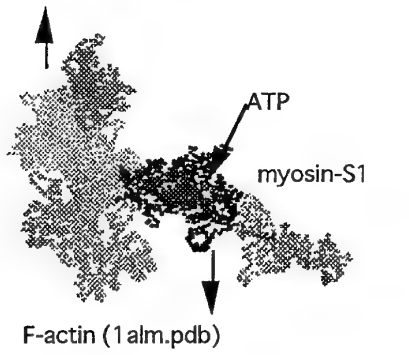

Fig.2 Actomyosin motor

which are just posible values as shown in Fig.2, we obtain the force F more than 10 pN calculated by $[\Delta G_{c2}-\Delta G_{c1}]/L= [5(mJ/m^2)x5(n\ m^2)]\ /2(nm)$. This value is close to the experimental value 5pN given by Ishijima et al. The maximum energy to step 5nm with 10pN is about 12kT, which is a large portion of 20kT of ATP hydrolysis.

Conclusion

The linear motor model using the affinity gradient force and surface transition of F-actin by interacting with myosin motor domain S1 and ATP, could explain the experimental facts such as the magnitude of generated force 5pN, the force-velocity relation of muscle fiber and possible to explain the high sliding velocity 10μm/s.

Acknowledgment

The author thanks to Dr. Kodama and Dr. Yanagida for helpful discussions, and thanks to Monkasho for the grant #11167203.

References

Yanagida, T, Arata, T. Oosawa, F., Nature, 316, 366-369 (1985)
Higashi-Fujime, S., J. Cell Biol., 101,2335-2344 (1985).
Ishijima,A., Harada,Y., Kojima, H., Funatsu, T., Higuchi, H. and Yanagida, T., Biophys. Res. Commun., 199, 1057-1063 (1994).
Oosawa, F, Hayashi, S.,Adv. Biophys., 22, 151-183 (1986).
Edman, K.A.P., J. Physiol., 404, 301-321 (1988).
Harada, Y., Yanagida, T., Nature, 326, 805-808 (1987).
Rayment, I. Et al., Science, 261, 58-65 (1993) ,
Suzuki, Y., Yasunaga, T., Ohkura, R., Wakabayashi, T., Sutoh, K., Nature, 396, 380-383 (1998)
Kodama, T., Physiological Reviews, 65, 467-551 (1985).
Suzuki, M., Shigematsu, J., Fukunishi, Y., Harada, Y., Yanagida, T. and Kodama, T., Biophys. J., 72, 18-23 (1997).
Gopal, D., Burke, M., Biochemistry, 35, 506-512 (1997).
Suzuki, M., Polymer Gels and Networks, 2, 279-287 (1994).

Polymer actuators on microscale: microrobot and cell trappers

O. Inganäs, Biomolecular and organic electronics, IFM,
Linköping University, Linköping, Sweden

We are currently pursuing the development of polymeric actuators for biological studies and biomedical uses, a field that still is in its infancy. The genomic and proteomic revolution presently changing our worldview does to a large and increasing degree rely on data generation from genes or proteins, on biochips using small oligomers of DNA, RNA, or polypeptides. These microarrays are all utilizing microtechnology, in this case for microsensors in an array format. The use of micromachined structures in the ongoing revolution will only loom larger in the future; the data flow will only increase enormously as the quest of proteomics, to measure the protein profile and protein-protein interactions in cells along their life path, is expanding. Microarrays have been crucial in the sequence of the human genome; we expect microactuators to play an important part as more and more detector functions are miniaturized to allow massive data extraction from minuscule sample volumes. Most samples coming from the biological realm are based on aqueous solutions in one or another of the steps. Microfluidics in aqueous environments will therefore be essential to the operation of micromachined biological sensors. Therefore microacutators operating in aqueous environment may enable this technology. This is where our polymer actuators come in.

On much larger dimensions, medical practice is being transformed by the increasing emphasis on minimizing trauma during surgical procedures, by using minimal invasive surgery. Tools for this purpose should eventually be adequately chosen from a broader range of technologies than offered by the classical small size mechanical tools operated by hand. This is an field of medical technology where polymer actuators may offer some reward.

The actuators we use are all based on the doping induced volume change in a conjugated polymer[1] a volume change that is controlled by the applied potential on a polymer electrode in a electrochemical cell. The electrochemical reactions driven by the redox

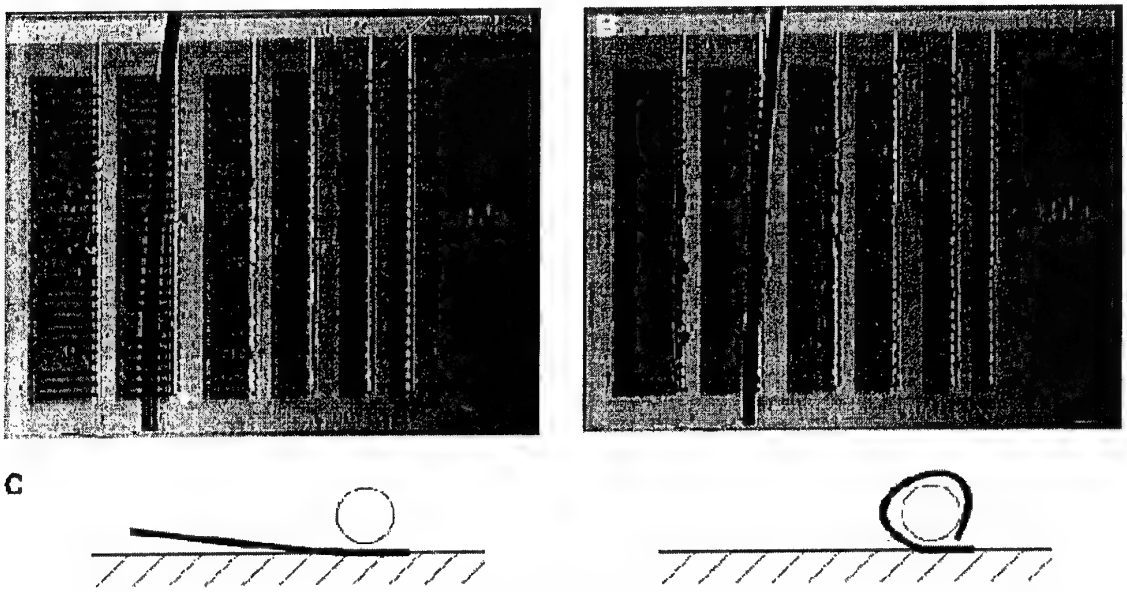

Photo 1. Photographs of polypyrrole/gold bilayer fingers uncurled and curled. The fingers are 20 µm wide and 50, 100, 150, 200, 250 and 300 µm long, and hold a fiber of 30 µm diameter. See Jager et.al, *Science* 290(2000) 1540., also Smela et.al.

process of the conjugated polymer includes both ion and electron transport through and transfer between between the three different phases of electrode (current collector), electroactive polymer and electrolyte[2-11]. Upon oxidation/reduction of the polymer electrode, subsequent charge compensation is effected by ion transfer from or to the electrolyte. This ion transfer is a dominant part of the volume change effected in the polymer layer. The rather moderate volume change in this layer is converted into larger geometrical changes by building bilayer assemblies, where an active polymer layer is laminated to a inactive supporting layer. The volume change is now converted to a bending of the bilayer, visible by simple measurements.

We have built simple and more elaborate micromuscles on dimension from 10 to 1000 μm in lateral size[11-16]. The bilayers used are typically gold/polypyrrole, with thickness in the range of ≈0.1 μm. The lateral geometries are defined by photolithographically controlled materials deposition on top of a silicon or glass chip, which act as our carrier substrate. The polymer is generated by electrochemical polymerisation on top of a gold surface. The substrate with structures is then immersed in an aqueous electrolyte and actuated by electrochemical reduction and oxidation, to set the muscle free from the substrate and then to drive the movement of the assembly. The assembly may be simple bilayers of gold and polypyrrole, which give rise to curling and uncurling fingers, much longer than wide(Photo 1). The thickness of the micromachined structures here described are typically 0.1 to 1 μm; they are therefore exceedingly slender and may be bent to a very large degree. The curling and uncurling of fingers may be used to hold objects as shown where rows of individual bending bilayer roll up or roll out, and thus can be used to hold onto cylindrical objects. The fiber used in the photo is a synthetic fiber, but similar devices may be used to hold onto blood vessels inside the body,

The flexible muscles may be combined with stiffer elements, such as plates or stiff beams, to build more elaborate structures. A first example is that of microboxes which can be assembled by actuation of a number of flexible muscles /actuators joining hard plates that forms the surface of the box. Here all muscles are simultaneous actuated; if we make possible the sequential activation, we may use a first muscle to move the "base" of the next muscle, thus making possible more elaborate movements.

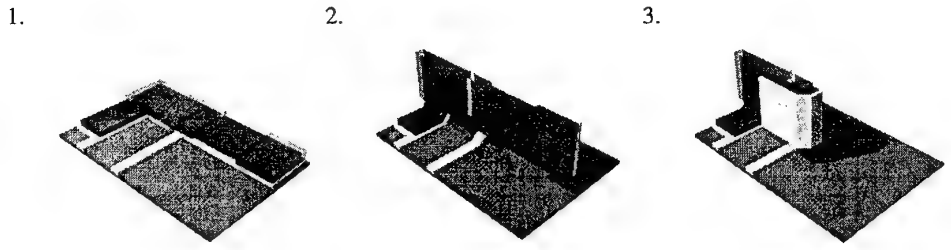

Figure 1 A sketch of the movement. (1.) After the fabrication the device is laying on the surface. (2.) By activating the first microactuator, the device rotates from the surface in a perpendicular state. (3.) By activating the second actuator the tip bends 180 °. By cycling the voltage on the second actuator, the tip bends and straightens. Not shown is the third actuator that should lock the whole device. After [15]

Photo 2 Two pictures of the movement of the tip. To be able to see better, we have bent the whole device at a small angle instead of setting it perpendicular to the surface. Actuator 1 bent the tip. Actuator 2 controlled the angle with respect to the surface of the device. Actuator 3 was there in order to move a plate with a slit over the device in other to lock it in the perpendicular state and thus supply some strength to the device. Here actuator 3 is bent almost flat [15]

With more elements. more complex movement is possible, as in conventional macroscopic machine design. A more complex structure is that of a microrobot capable of gripping and moving small objects in an electrolyte. Here we use up to 5 individually controlled micromuscles to control the movement of the hand imitation, where three fingers are simultaneously activated to hol the object, and where two joints (mimicking the elbox and the wrist) are used to bring about the larger movement. So far we have used this device to move synthetic objects, such as the glass ball shown in Photo 3; we plan to use the microrobot to manipulate cells.

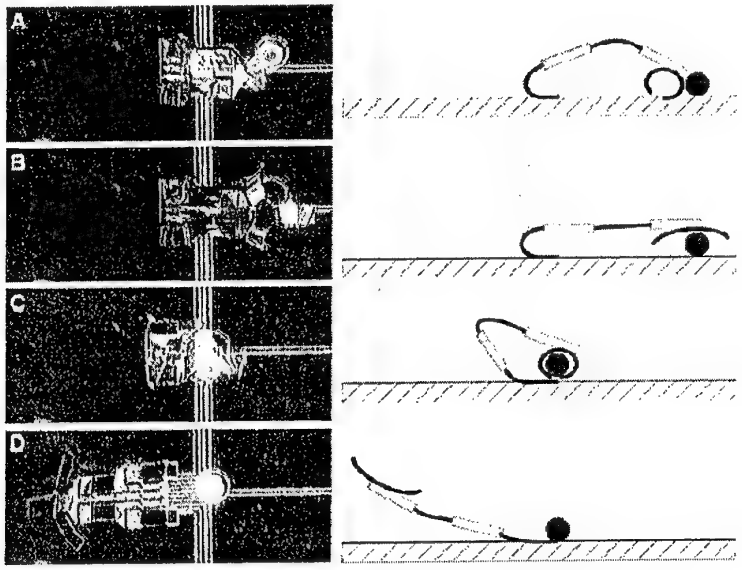

Photo 3 (A through D) A sequence of pictures (left) show grabbing and lifting of a 100-mm glass bead and schematic drawings of the motion (right). In this case, the arm has three fingers, placed at 120¡ from each other. The pictures do not illustrate the fact that the bead is actually lifted from the surface before it is placed at the base of the robot arm. We have illustrated this in gray in the second sketch to the right. [14]

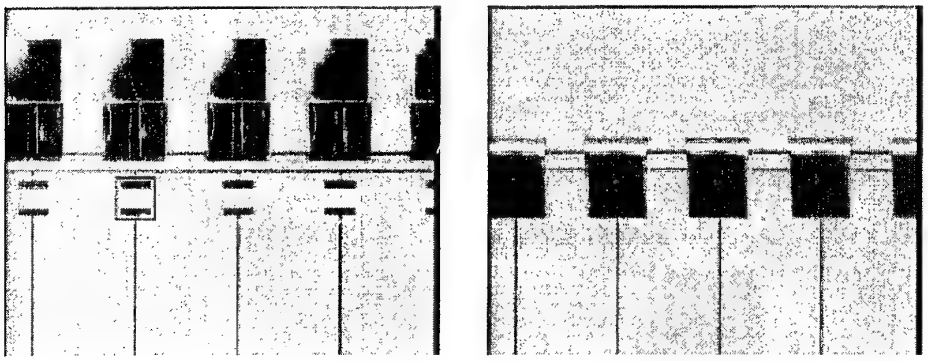

Photo 4. Four opened (a) and closed (b) cell clinics. The contours of the second microvial from marked with a black line. Each microvial (100x100x20mm 3) is equipped with two electrodes.

We are currently incorporating sensors into micromachined structures equipped with these actuators, in order to be able to interrogate the state of cells confined within a small volume, something we name the cell clinic.. An example is shown where the impedance between two micromachined interdigitated gold electrodes is measured in the presence of biological cells. Here we have chosen cells from *Xenopus laevis*, cells which also act as chromophores. Aggregation of pigments within the cell can be induced by external stimuli, and may be observed in optical microscopy. We therefore attempt to correlate the state of aggregation of the pigment to the impedance signal from a few cells confined on the microelectrode with in a small cell clinic. So far we are not using the closed cell clinic, but attempt to establish an experimental protocol which will allow us to study individual cells confined in clinics

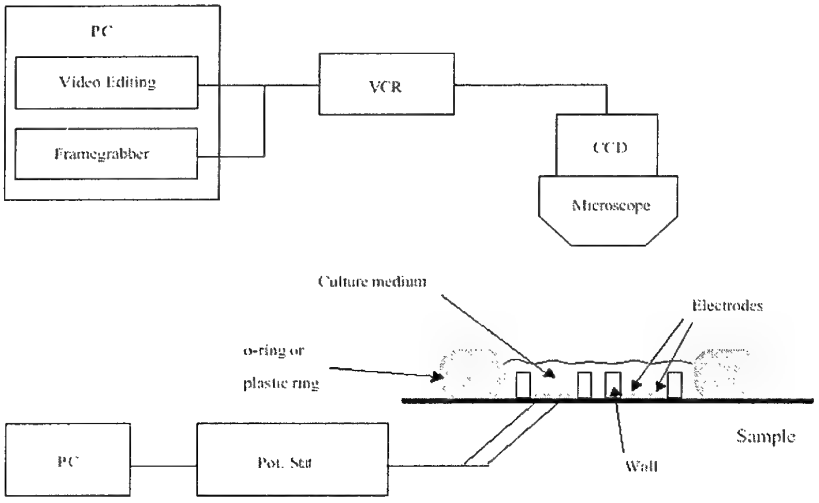

Figure 2. Scheme of the experimental setup for cell clinic studies (not scaled).

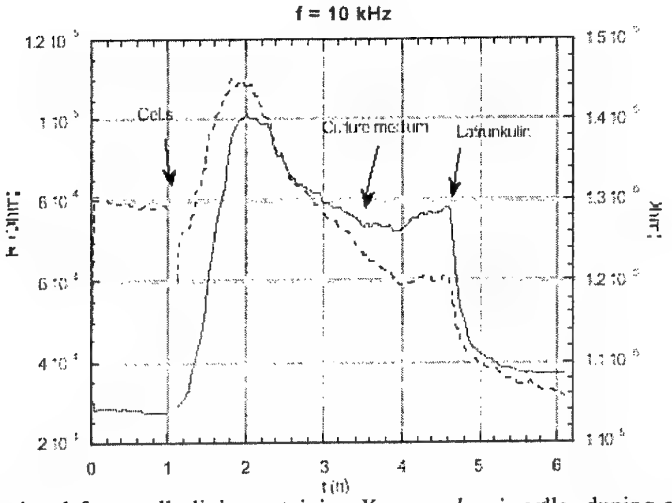

Figure 3. Impedance signal from cell clinic containing *Xenopus laevis* cells duning stimulation with the substance latrunculin, interacting with the actin polymerisation controlling the movement of pigment, as observed in Photo 5.

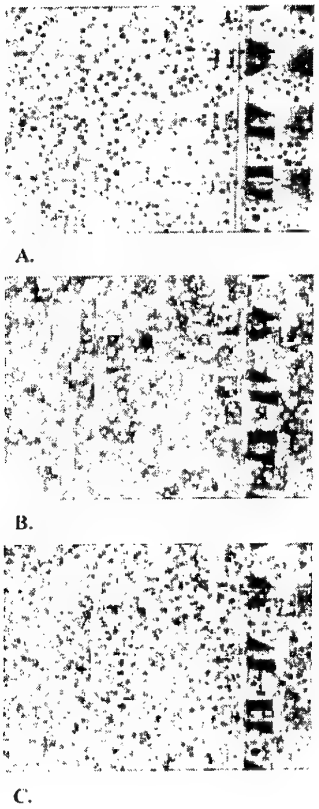

Photo 5. Representative images of *Xenopus Laevis* melanofores in cell clinic a) shortly after addition of cells and b) after the cells have attackhed to the clinic surfaces and the pigments are dispersed and c) afer stimulation with latrunculin which causes aggregated pigment granules.

In summary, we are pursuing the development of polymer actuators compatible with biological fluids , with dimensions comparable to the cell or structure which is to be interrrogated. These novel tools may come to have their use in massive cell screening, as valves in microfluidic systems or for mechanical stimulation of cells. They may also offer interesting alternatives as tools inside the body.

Acknowledgements: The work reported here has been done by Edwin Jager, Elisabeth Smela, and Charlotte Immerstrand , in collboration with numerous coworkers. The work has been done with the support from NUTEK, and from SSF through the graduate school Forum Scientum. We acknowledge the support of ONRIFO for this summer school.

References:

1. R. H. Baughman, L. W. Shacklette, R. L. Elsenbaumer, E. J. Plichta,C. Becht, in *Molecular Electronics* P. I. Lazarev, Ed. (Kluwer Academic Publishers, Dordrecht, 1991) pp. 267-289.
2. Q. Pei and O. Inganäs, *Adv. Mater.* **4**, 277-278 (1992).
3 Q. Pei and O. Inganäs, *J. Phys. Chem.* **96**, 10507-10514 (1992).
4 Q. Pei and O. Inganäs, *J. Phys. Chem.* **97**, 6034-6041 (1993).
5 Q. Pei, O. Inganäs,I. Lundström, *Smart mater. Struct.* **2**, 1-6 (1993).
6 Q. B. PEI and O. INGANAS, *SYNTHETIC METALS* **57**, 3730-3735 (1993).
7 Q. B. PEI and O. INGANAS, *SYNTHETIC METALS* **57**, 3724-3729 (1993).
8 T. F. Otero and J. M. Sansinena, *Bioelectrochemistry and Bioenergetics* **38**, 411-414 (1995).
9 M. R. Gandhi, P. Murray, G. M. Spinks,G. G. Wallace, *Synth. Met.* **73**, 247-256 (1995).
10 A. Della Santa, D. D. Rossi,A. Mazzoldi, *Synth. Met.* **90**, 93-100 (1997).
11. R. H. Baughman, *Synth. Met.* **78**, 339-353 (1996).
12. E. Smela, O. Inganäs, Q. Pei,I. Lundström, *Adv. Mater.* **5**, 630-632 (1993).
13. E. Smela, O. Inganäs,I. Lundström, *Science* **268**, 1735-1738 (1995).
14. E. W. H. Jager, O. Inganäs,I. Lundström, *Science* **288**, 2335-2338 (2000).
15. E. W. H. Jager, O. Inganäs,I. Lundström, *Adv. Mater.* **13,** 76 (2001).
16. E. W. H. Jager, E. Smela and O. Inganäs,, *Science* **290**, 1540 (2000).

TOWARDS CONDUCTING POLYMER ORGANISMS

John D. Madden, Peter G. Madden, Patrick A. Anquetil, Hsiao-hua Yu*, Timothy M. Swager*, and Ian W. Hunter

Massachusetts Institute of Technology

MIT Mechanical Engineering, Room 3-147,

***MIT Department of Chemistry**

77 Massachusetts Ave., Cambridge, MA 02139

Abstract

In Nature, systems are created from the cellular level to build machines with complex structures and behavior. Nature's structures, largely fabricated from organic materials (amino acids, lipids, carbohydrates, nucleic acids), are able to sense, compute, store energy and convert energy to motion. Rather than separately manufacturing and assembling systems (as in existing engineering system construction) nature grows systems by 3D cofabrication. Intrinsically conducting polymers offer a material basis set of similar which promises to enable a similar diversity of function[7]. For example, conducting polymer actuators exert maximum stresses of 35 MPa, 100 times greater than mammalian skeletal muscle. Conducting polymer wires can carry currents of over 10^7 A/m^2 (similar to copper wire). Polypyrrole supercapacitors (for energy storage and recovery) achieve very high charge densities (10^5 F/kg). Strain gages, transistors, photo detectors, solar cells, chemical sensors, batteries and many other devices have been constructed from conducting polymers. The challenge is to integrate these elements to form highly integrated, all-polymer devices.

An advantage of employing conducting polymers as a materials basis set is the availability of a powerful actuator technology[8-11]. Conducting polymer actuator materials such as polypyrrole and polyaniline convert chemical or electrical energy into work. However, a disadvantage to date has been that the proportion of input energy that is transformed into mechanical work is relatively small, and usually less than 1 %. We present strategies for improving efficiency in existing conducting polymers, and for designing polymers at the molecular level such that electro-mechanical conversion is maximized.

Introduction

In seeking to emulate Nature, humankind has relied on a diverse set of material types (metal, ceramics, semiconductors) to mimic the different functions of a life system. Most of the materials used in active devices are low in molecular weight, and isotropic. An alternative approach which promises simpler manufacturing and assembly is to mimic Nature's use of high molecular weight anisotropic materials.

We use the material class of conducting polymers to build actuators (muscles), transistors (computation), wires (information transmission and energy delivery), supercapacitors (energy storage), and strain gages (position sensing) thereby building most of the elements needed for creating a biomimetic lifelike system.

Traditional polymers are electrically insulating. In a conducting polymer, the polymer backbone structure is conjugated (alternating single and double bonds). These polymers are semiconductors, whose conductivity can be made near metallic by changing oxidation state. Changing oxidation state not only leads to changes in conductivity, but also in dimension, color, and charge content – these effects being made use of to create transistors, chemical sensors, actuators, electrochromic windows, capacitors and batteries, among other devices. A number of polymer subcomponents are now described.

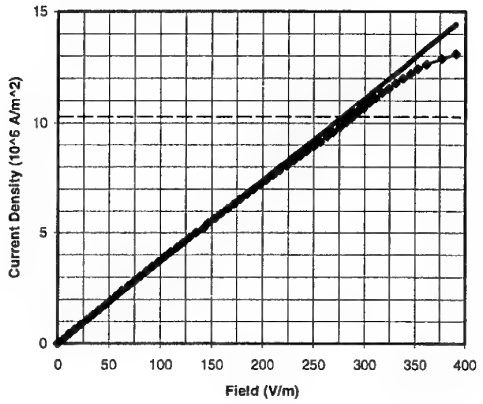

Figure 1: Measured current density vs. electric field for polypyrrole. The maximum current density of $13 \cdot 10^7$ A/m^2 is greater than the generally quoted maximum current density of 10^7A/m^2 for copper wire (dashed line). The slope of current density vs. electric field is the conductivity of the sample (37000 S/m). PPy sample grown at –40 °C, 2.5 mm by 10 μm by ~50 mm long.

Conducting Polymer Wires

The densities of most metals (e.g. copper 8910 kg/m^3, silver 10500 kg/m^3) are high compared to organic materials (typically 1000 to 2000 kg/m^3). We have found that conducting polymers are able to equal or exceed the current carrying capacity per unit mass of metals such as copper and silver.

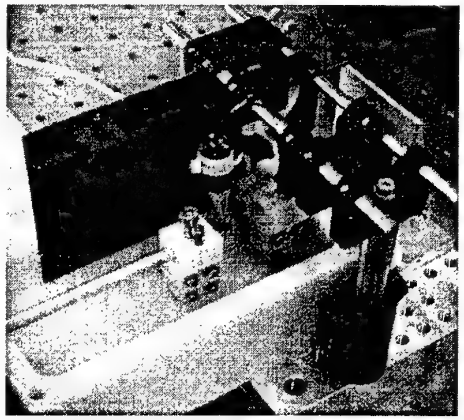

Figure 2: Photograph of a conducting polymer actuator test platform.

In Figure 1, the current density in a polypyrrole strip is plotted as a function of electric field. The strip was destroyed at a current density of 1.3 x 10^7 A/m^2, slightly higher than the typically quoted maximum safe current density of 10^7 A/m^2 for copper wire[1].

High current carrying capacity is of particular interest in electric motors. Where moving parts are involved, the current density per unit mass is a useful figure of merit, as it determines motor bandwidth. The densities of copper and silver are more than 7 times higher than conducting polymers, making conducting polymers very competitive for use in motor windings. Conducting polymers are also potentially cheaper and biodegradeable.

Strain Gages

Strain gages provide a mechanism for measuring position or force. When a material is stretched it becomes longer and generally the cross-sectional area decreases. In a conductive material, the dimensional changes affect the electrical resistance as well.

We have fashioned strain gages from polypyrrole (PPy) strips and tubes. These conducting polymer strain gages have several properties that open new applications where traditional strain gages are impractical. In particular, because they are made of flexible plastic, the PPy gages can undergo maximum strains of several percent whereas silicon or metal film gages are limited to ~0.1 or 0.2%. PPy gages can also be used in applications that not only require large strain but that also require bending or flexing of the gage itself. In much the same way, the mammalian muscle spindles transduce position yet are as flexible as the muscle fibers themselves. Gage factors for polypyrrole range from 0.25 in unstretched polymer to 5 in stretch aligned films.

Conducting Polymer Actuators

Nature has evolved actuators that convert chemical energy to mechanical energy. Mammalian skeletal muscle exerts 350 kPa and undergoes contractions of up to 20% at rates as high as 100%/s. Muscle is flexible and highly modular.

Conducting polymer actuators exert forces per cross-sectional area of up to 35 MPa, over 100 times the force per cross-sectional area of skeletal muscle[2]. So far, the maximum strain we have measured is 7% and contraction rates reach 3%/s.

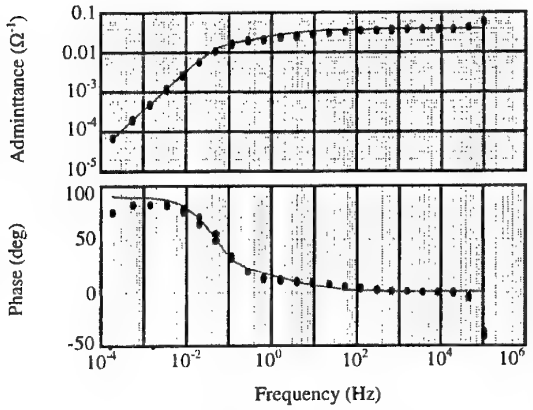

Figure 3: Electrochemical impedance of a polypyrrole muscle. The solid line was fit to the data by varying only a single parameter. Experimental data is extremely well described by the model between 10^{-3} Hz to over 10^{4} Hz. (Admittance is for a polypyrrole strip 8.5 μm thick).

Figure 2 is a photograph of a typical actuator test platform as used in our laboratory. A polypyrrole film and a counter electrode sit in an electrochemical bath. As the voltage between the electrodes is changed, ions are driven into or out of the polymer electrode, causing it to expand or contract.

At constant stress, the amount of expansion or contraction is proportional to the amount of charge transferred:

$$\varepsilon = \alpha \cdot \rho$$

where ε is the strain, ρ is the charge transferred per unit volume, and α is the strain to charge ratio. α is experimentally measured and is roughly related to the size of the ions ($\alpha \sim 10^{-10}$ m^3·C^{-1}).

In order to predict the strain rate, we have developed a model relating the current flow into the polymer to the potential applied to the cell[3]. Expressed as a function of the Laplace frequency variable $s = j\omega$, the admittance Y is:

$$Y(s) = \frac{s}{R} \cdot \frac{\frac{\sqrt{D}}{\delta} \cdot \tanh\left(\frac{a}{2} \cdot \sqrt{\frac{s}{D}}\right) + \sqrt{s}}{\frac{\sqrt{s}}{RC} + s^{3/2} + \frac{\sqrt{D}}{\delta} s \cdot \tanh\left(\frac{a}{2} \cdot \sqrt{\frac{s}{D}}\right)}$$

where R is the resistance of the solution and contacts, C is the double layer capacitance of the solution polymer interface, δ is the thickness of the double layer, D is the diffusion coefficient of the ions in the polymer, and a is the thickness of the polymer.

One of the important limits to speed of the polymer is the diffusion rate of ions into the solid material. As a result, thinner films have faster response because the diffusion distance is smaller. As we aim for better performance, we have been electrochemically growing films as thin as 8 μm.

A measured electrochemical admittance is shown in Figure 3. The model for admittance (solid line) was fit to the data with one free parameter. As can be seen from the plot, the model predicts the frequency response of the polymer over more than seven orders of magnitude.

Polymer Conformation Changes

While the conducting polymer actuators based on ion intercalation between the polymer chains give impressive performance, the strain is still significantly smaller than that of muscle. New conducting polymers with large free volumes are being designed and synthesized to undergo conformational changes resulting in 10 to 20% strains. In this case the active properties of the conducting polymer are intrinsic to the polymer backbone[4] rather than depending on ion and solvent intercalation.

These novel polymers hold the promise of generating strains of 20% or more at stresses in excess of 0.5 MPa. A number of candidate thiophene based molecular conducting polymers actuators are synthesized and characterized in our laboratories. One compound under study features an accordion like polymer formed by calix[4]arene flexible hinges separated by conducting thiophene rods (Figure 4). In this particular compound, actuation results from π-π stacking of thiophene oligomers upon oxidation, producing a reversible molecular displacement (**Errore. L'origine riferimento non è stata trovata.**). The novel polymer composites have been successfully synthesized and their active and passive mechanical properties are currently being evaluated.

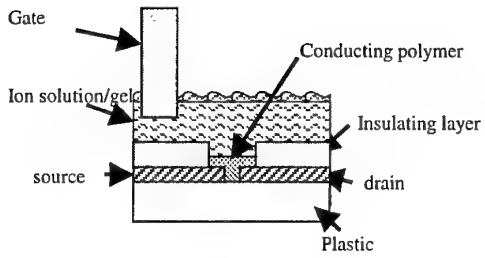

Figure 5: The conducting polymer electrochemical transistor. The source to drain resistance is changed by raising or lowering the gate potential to drive ions into or out of the active region of conducting polymer (exposed to the solution).

Electrochemical Transistors

If the ion content (or the doping level) of a conducting polymer is reduced far enough, the conductivity begins to drop dramatically. With no doping at all the backbone of conducting polymers becomes insulating and no current can flow.

Wrighton first made use of this property of conducting polymers to make transistors[5]. Conducting polymer is grown across a gap between two electrodes. By driving ions into or out of the polymer, the resistance between the two electrodes can be changed, analogous to the operation of a FET transistor (Figure 5).

We have built conducting polymer transistors based on polyaniline doped with chloride. In our transistors the source to drain resistance changes by over two orders of magnitude, and should increase by a further two orders by limiting leakage currents through the electrolyte.

With transistors we can construct the logic, amplifiers, and feedback loop circuits that are needed to create an intelligent biomimetic system. Computations can also be performed. Signals from sensors can be combined and analyzed. The output from a strain gage can be amplified to drive a muscle creating a simple reflex loop.

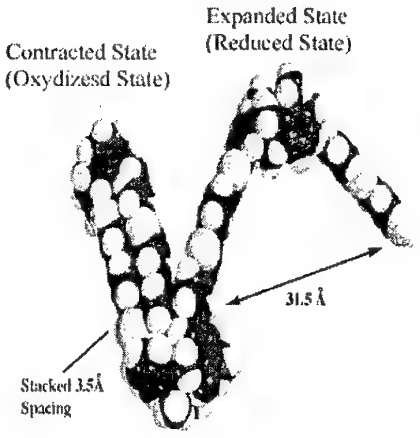

Figure 4: Structure of a molecular actuator. The calix[4]arene bithiophene monomeric compound. The left side of the figure represents the molecule in its contracted state (oxidized) and the left side its expanded state (reduced).

Supercapacitors

Animals store energy in the form of sugars and complex carbohydrates. Engineered biomimetic systems also need to store energy. At low frequencies, and over a certain range of potentials, conducting polymers behave as supercapacitors, able to store significant amounts of charge.

The insertion of ions into conducting polymer systems as they are doped and undoped takes place over the bulk volume of the material rather than just at the surface and as a result, a very large amount of charge can be stored per unit volume. Figure 3 is a plot of the electrochemical admittance of a strip of conducting polymer. At frequencies below 0.1 Hz, the behavior of the polymer is almost purely capacitive, with the very high capacitance of 10^5 F/kg. A strip of material of around 10 mm square by 1 mm thick has a capacitance of near 1 F.

A conducting polymer supercapacitor could be used for energy storage for biomimetic systems, either as a local source of energy within a muscle or as an energy storage for the biomimetic system as a whole.

Conclusions

Conducting polymers offer a great range of capabilities for future biomimetic applications. We have developed conducting polymer muscles, strain gages, transistors, and supercapacitors to be components of future biomimetic systems.

Looking to the future, systems that integrate the multiple functions of conducting polymer will enable us to build truly biomimetic systems from the molecular scale.

Acknowledgements

This research was supported by the Office of Naval Research program for Biomimetic Robotics (grant number N00019911022).

---

[1] See for instance: National Electric Code Handbook, Delmar Publishers, 1993.

[2] Madden, John D., Cush, Ryan A., Kanigan, Tanya S., Hunter, I.W, "Fast Contracting Polypyrrole Actuators", *Synthetic Metals*, 113 (2000) 185-192; Madden, John D., Madden, Peter G., Hunter, Ian W., "Characterization of polypyrrole actuators: modeling and performance", *Proceedings of SPIE 8th Annual Symposium on Smart Structures and Materials: Electroactive Polymer Actuators and Devices*, Yoseph Bar-Cohen, Ed., SPIE Press, 12 pages, 2001 (in press); Madden, John D. Conducting Polymer Actuators, Ph.D. thesis, MIT 2000.

[3] Madden, J. "Conducting Polymer Actuators", Doctoral Dissertation, Massachusetts Institute of Technology, 2000.

[4] Marsella MJ and Reid RJ. "Toward Molecular Muscles: Design and Synthesis of an Electrically Conducting Poly[cyclooctatetrathiophene]", *Macromolecules*, 32 (1999) 5982-5984.

[5] E.Lofton, J.Thackeray, M.Wrighton, "Amplification of Electrical Signals with molecule-based transistors", *J. Phys. Chem.* 90 (1986) 6080-6083; E.Jones, O. Chyan, M. Wrighton, "Preparation and characterization of molecule-based transistors with a 50-nm source-drain separation with use of shadow deposition techniques", *J. Am. Chem. Soc.* 109 (1987) 5526-5528.

[7] T. A. Skotheim, R. L. Elsenbaumer, J. R. Reynolds, *Handbook of Conducting Polymers,* 2nd ed., Marcel Dekker, New York, 1998.

[8] *ELectroactive Polymer (EAP) Actuators as Artificial Muscle*, Yoseph Bar-Cohen, Ed., SPIE, Bellingham, WA, 2001.

[9] A. Mazzoldi, A. Della Santa, D. De Rossi, "Conducting polymer actuators: Properties and modeling", *Polymer Sensors and Actuators*, Y. Osada and D. E. De Rossi, Eds., Springer Verlag, Heidelberg, 1999.

[10] E. W. H. Jager, O. Inganas, I. Lundstrom, "Mircrorobots for Micrometer-Size Objects in Aqueous Media: Potential Tools for Single-Cell Manipulation", *Science* **288**, pp. 2335-2338, 2000.

[11] R. H. Baughman, "Conducting Polymer Artificial Muscles", *Synthetic Metals* **78**, pp. 339-353, 1996.

Engineering a Muscle: Artificial Muscle Based on Dielectric Elastomer Actuators

Roy Kornbluh*, Ron Pelrine, Qibing Pei, Scott Stanford, Seajin Oh, Joe Eckerle
SRI International
Robert Full, Kenneth Meijer, Marcus Rosenthal
University of California at Berkeley

Introduction

Just as the motion capabilities of biological creatures are critically determined by the actuation characteristics of natural muscle, the motion capabilities of robots are critically determined by the characteristics of their actuators. To achieve desirable biomimetic motion, actuators must be able to reproduce the important features of natural muscle such as power and energy density, stress and strain, speed of response, efficiency, controllability, and mechanical impedance. It is a mistake, however, to consider muscle as only an energy output device. Muscle is multifunctional. In locomotion, for example, muscle often acts as an energy absorber (brake) and a variable-stiffness structural or shock-absorbing suspension element. Additionally, muscle contains many sensing elements that play an important role in motion control. Pneumatics and hydraulics are often employed to make up for the limitations of electromagnetic actuators; however, these approaches introduce additional complexity and difficulty in control. Electroactive polymers (EAPs) have been the focus of much recent attention as the potential basis for electrically controllable "artificial muscle" actuators. Electroactive polymer technology based on the electric-field-induced deformation of elastomeric polymer dielectrics with compliant electrodes is particularly promising.

Basic Principles of Operation

All actuators based on *dielectric elastomer* technology operate on the simple principle that when a voltage is applied across compliant electrodes, the polymer shrinks in thickness and expands in area [Pelrine et al. 1998]. The observed response of the film is caused primarily by the interaction between the electrostatic charges on the electrodes [Pelrine, Kornbluh, and Kofod 2000]. Simply put, the opposite charges on the two electrodes attract each other, while the like charges on the electrodes repel each other. This basic structure is shown in Figure 1a. The pressure and strain response is roughly proportional to the square of the applied field [Pelrine et al. 1998, Kofod et al. 2001].

Strains over 100% have been observed in both acrylic and silicone elastomers [Pelrine et al. 2000]. The corresponding specific energy density (a measure of the amount of work a given amount of material can perform) exceeds that of any other field-activated material. Figure 1b shows the large strain responses that are possible with dielectric elastomers. As with other field-activated actuators, dielectric elastomers can be efficient and fast [Kornbluh et al. 2000]. Dielectric elastomers also can operate well over a wide range of temperature and humidity. [Kornbluh et al. 2001]

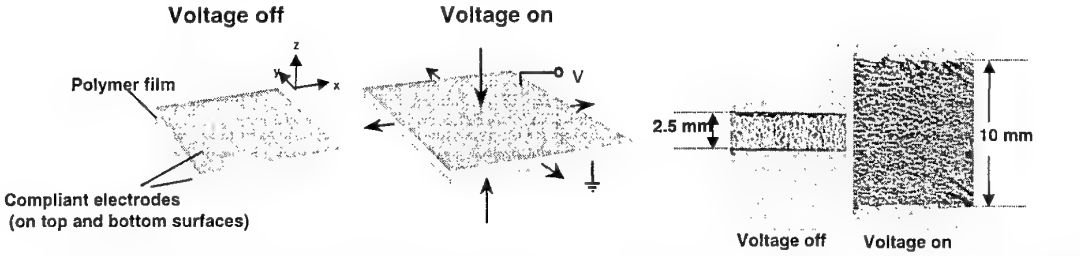

(a) Functional element of dielectric elastomer actuators

(b) Acrylic film undergoing more than 300% linear strain

Figure 1 Dielectric Elastomer Basic Operation and Performance

* Roy Kornbluh, SRI International, 333 Ravenswood Avenue, Menlo Park, CA 94025, USA. Ph: 001-650-859-2527,
e-mail; roy.kornbluh@sri.com

The deformation of polymer film can be used in many ways to produce muscle-like linear actuation. For example, the film and electrodes can be formed into a tube, rolled into a scroll, supported by a frame, or laminated to a flexible substrate to produce bending. The best configuration depends on the application and properties of the film. Figure 2 shows three types of linear *artificial muscles*. Two are based on essentially flat structures that can be stacked to produce greater force. Rolled actuators with a mass of 15 g have produced more than 5 N of force and 5 mm of stroke (20% strain).

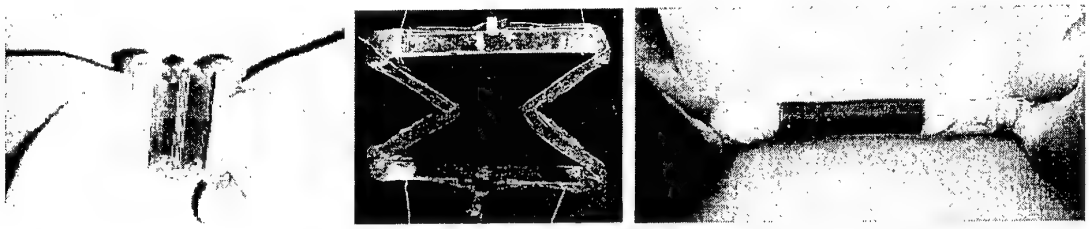

(a) Multilayer double bowtie with acrylic film (b) Bowtie with silicone film (c) Rolled actuator with acrylic film

Figure 2 Linear Artificial Muscles

Actuators can operate unilaterally against a load or can be grouped to operate antagonistically or in push-pull mode. It has recently been shown that the change in the capacitance of a rolled actuator can repeatably and accurately indicate the change in length of the actuator itself. Like natural muscle, these artificial muscles can therefore be said to incorporate proprioceptive sensory capabilities.

Biomimetic Robot Applications

Dielectric elastomer artificial muscles have been incorporated into a variety of biomimetic robots, each of which exploits one or more unique capabilities of the actuator. These robots include a snake-like manipulator, an insect-inspired walking robot, an insect-inspired flapping wing flyer, and an inchworm-like propulsion mechanism. These robots are shown in Figure 3.

At this point the robot of Figure 3a can walk only slowly and over even terrain. Improvements in the driving electronics and in the strength and durability of the muscles themselves are needed to increase the robot's mobility. Nonetheless, this robot is significant because it is believed to be the first self-contained walking robot that is powered by EAP actuators. More details on this robot are given by Eckerle et al. [2001]. The robot also can serve as a testbed to assess the advantages of muscle-like actuation. In particular, we hope to exploit the viscoelastic behavior of the muscles to enable robots to reject disturbances due to obstacles or uneven terrain, much as preflexes in the musculoskeletal system of a cockroach help it to run over uneven terrain in a stable manner and without large disturbances of its torso [Dickinson et al. 2000].

The large strain capability of the dielectric elastomer actuators can be exploited to make structurally simple joints for a snake-like manipulator (Figure 3b). Large numbers of such joints can be connected in series, for great dexterity: such manipulators can work in cluttered environments. A further advantage is the inherent compliance of the actuators, which would enable them to tolerate accidental contact with objects.

Robotic platforms using the inchworm-like propulsion system (Figure 3c) could eventually be used to make small robots for tasks such as inspection in narrow pipes. This inchworm uses electrostatic clamps that enable it to travel over both vertical and horizontal surfaces. The inchworm takes advantage of the large strain capability of a dielectric elastomer EAP roll. It also shows the multifunctionality of dielectric elastomer materials. The inchworm can function without a separate rigid supporting skeleton, as do many biological creatures such as worms.

The design of the flapping-wing mechanism (Figure 3d) was inspired by the mechanics of the many flying insects whose wings are driven indirectly by muscles located in their thoraxes. These muscles flex the

exoskeleton and move the wings, which are attached to the exoskeleton. In the same way, a bundle of artificial muscles can flex a plastic exoskeleton with wings attached. The flapping-wing mechanism exploits resonance to increase the energy output of the muscle and increase the efficiency of the mechanism. Insects and hummingbirds also exploit resonance [Dickinson and Lighton 1995; Alexander 1988]. The eventual goal is to make simple and robust flying platforms that can be used for reconnaissance in cluttered environments. Flapping-wing flight offers potential advantages over conventional flyers based on rotors, in slow speed thrust-to-power ratio and stability. To eliminate noise, lightweight and powerful electric actuation is needed. Dielectric elastomer EAPs, incorporated into a biomimetic flapping mechanism, can form the basis of such an electric flapping-wing propulsion system.

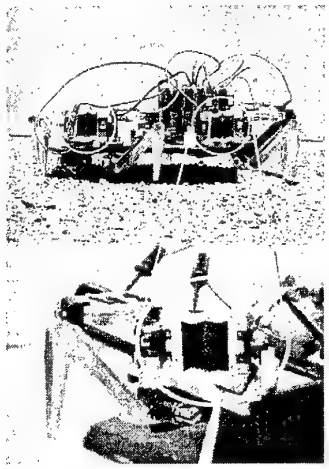

(a) Insect-inspired hexapedal walker (top) with two multilayer actuators per leg (bottom).

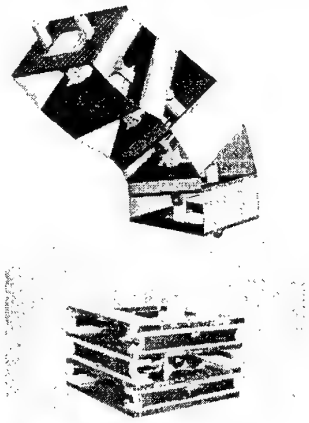

(b) CAD representation (top) and photograph (bottom) of section of a snake-like manipulator with a pair of actuators for each segment.

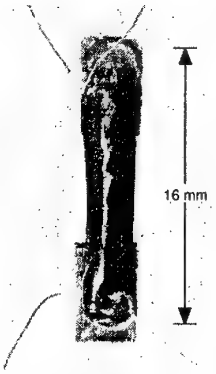

(c) Inchworm-like propulsion system for a small robot with a silicone roll and electrostatic clamps.

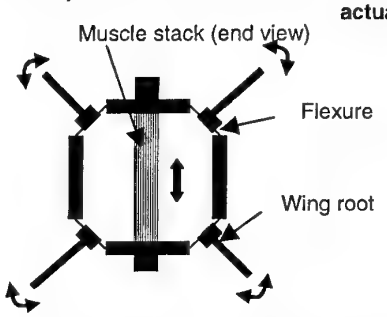

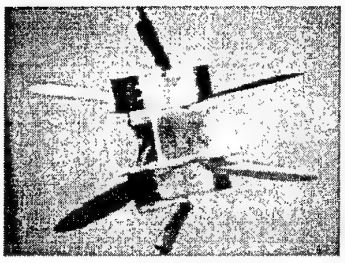

(d) Schematic (left) and photograph (right) of an insect-inspired flapping mechanism with a multilayer silicone bowtie actuator stack.

Figure 3 Biologically Inspired Robots Incorporating Dielectric Elastomer Artificial Muscles

Thus far we have focused on applications in which muscle does mechanical work to move or modulate the impedance of an appendage or body segment. In many instances, natural muscle has other functions. For example, muscle inflates and deflates the lungs to enable us to breathe. Muscle also acts as a valve in numerous places in the body. Muscle changes the shape of the lens of the eye and controls the amount of light that passes through the eye. Muscle changes the shape of our lips or eyebrows to allow us to express emotion. Muscle erects hairs when a creature is frightened or cold, to change its appearance or thermal properties. Dielectric elastomer actuators have been demonstrated in many of these applications [Pelrine et al. 2001].

Is It a Muscle? Results of Experiments

The above examples illustrate that dielectric elastomers can exploit some of the desirable properties of muscles, but other, more objective measurements are needed. A collaboration between investigators at SRI who are working on developing artificial muscle, and biologists at the University of California at Berkeley who are studying the performance of natural muscle and its role in animal locomotion has allowed for such objective measurements. Engineers who study actuators or actuator materials often use parameters such as free strain (maximum stroke) or blocked stress (maximum or isometric force) to characterize actuators. However, many factors can affect the results of such studies. Factors such as loading conditions, frequency of contraction, nonlinear force vs. stroke, and force vs. velocity behavior affect the actual output of muscle. We must therefore use other characterization techniques. For example, work loop techniques can be used to characterize muscle undergoing cyclic contraction [Josephson 1985]. In a work loop, the activation level of a muscle as function of time and stroke is duplicated, and the force produced is measured.

Work-loop techniques can yield useful metrics such as total work produced per cycle, and maximum force and average power. Work-loop and other muscle characterization techniques have revealed that dielectric elastomer artificial muscle does fall within the range of natural muscle performance for several parameters [Full and Meijer 2000; Full and Meijer 2001]. Figure 4a shows that the stress and strain of dielectric elastomers can match the stress and strain of natural muscle. Figure 4b shows that the work and power output also falls within the range of natural muscle.

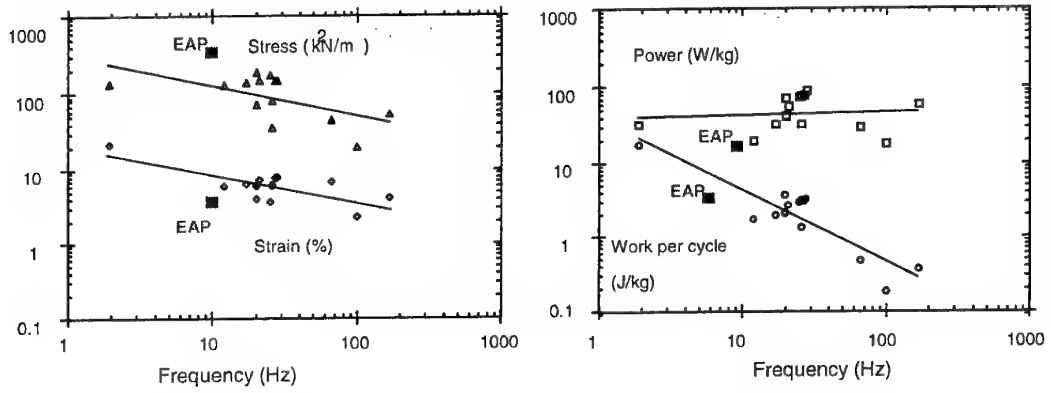

[Source: Full and Meijer [2001]

Figure 4 Stress And Strain Of Natural Muscle in a Variety of Invertebrate Species. The measured performance of dielectric elastomer actuators (EAPs) is also shown.

In applications where the muscle must function also as a spring or energy-absorbing element, it is also useful to compare the passive (unactivated or at a constant level of activation) behavior of natural muscle with that of dielectric elastomers. Figure 5 shows that the passive behavior of dielectric elastomers can duplicate that of a natural muscle (in this case, a leg muscle from a cockroach). The stiffness and damping of the dielectric elastomer actuator is similar to those of the natural muscle.

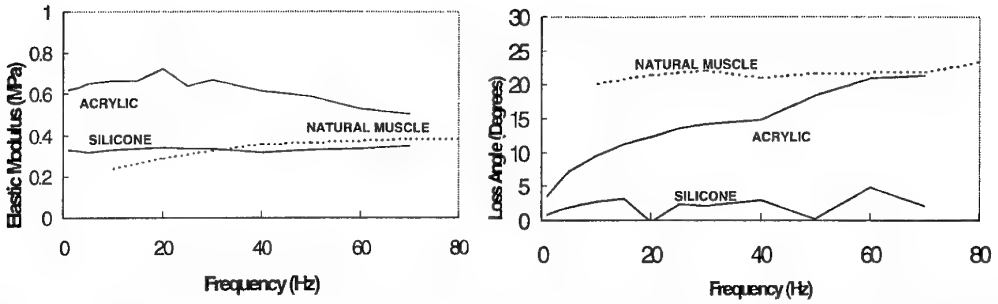

Figure 5 Comparison of the Passive Visoelastic Properties of Natural Muscle (Cockroach Leg Muscle 177c) with those of Dielectric Elastomer EAP Materials

It should be noted that the work-loop measurements of the dielectric elastomer actuators were not performed under conditions of maximum voltage or optimal loading, so their actual performance could be much greater.

While we can declare that dielectric elastomer actuators are like natural muscle in some respects, they are of course not like natural muscle in many others. We have noted that natural muscle has certain nonlinear time-variant behaviors that are not necessarily duplicated by the actuators. Obviously, EAPs differ from natural muscle in that the energy source is electrical rather than chemical. Some less obvious characteristics of natural muscle that artificial muscle might emulate in order to reproduce the desirable motion of biological creatures include the degradation of performance with fatigue, the ability to self repair, sensitivity to temperature, the ability to be consumed to provide energy, structures composed of large number of fibers operating in parallel, and diverse performance of individual muscle fibers. Of course, it is important to note that muscle is only part of a motion actuation system that also includes the nervous, sensory, and skeletal systems. The importance of all these other features and systems issues to the development of useful biomimetic robots has yet to be determined. However, by exploiting the similarities in performance to natural muscle that have already been demonstrated, we may be able to develop robots that emulate many of the desirable motions of biological creatures.

There remain several technical challenges to the implementation of artificial muscles based on dielectric elastomer actuators in practical robotic devices. Efficient and lightweight high-voltage driving circuits must be developed. Durability in extreme environments must be defined through continued experimentation. Nonetheless, dielectric elastomer actuators offer unique properties that may well earn them the name *artificial muscle*.

Acknowledgements

The development of dielectric elastomer artificial muscle actuators and the application of the technology to large biomimetic robots was supported by the Defense Advanced Research Projects Agency (DARPA) under contracts DABT63-98-C-0024, N66001-97-C-8611, and DAAG55-98-K-0001, and by the Office of Naval Research (ONR) under contracts N000-14-96-C-0026, N00174-99-C-0032 and N00014-00-C-0497. Much of the basic dielectric elastomer technology was developed at SRI International under the management of the Micromachine Center of Japan, in the Industrial Science and Technology Frontier Program, Research and Development of Micromachine Technology of METI (Japan), and supported by the New Energy and Industrial Technology Development Organization. Work performed at the University of California, Berkeley was supported by ONR MURI contract N00014-98-0747 and DARPA-ONR contract N00014-98-1-0669. The authors thank Dr. Anna Ahn for the use of preliminary data on insect muscle. The authors also wish to acknowledge the staff at SRI and the University of California who have helped make possible the results presented here.

References

Alexander, R. 1988. *Elastic Mechanisms in Animal Movement*, Cambridge University Press, Cambridge, UK, pp. 56–69.

Dickinson, M., and J. Lighton. 1995. "Muscle Efficiency and Elastic Storage in the Flight Motor of Drosophila," *Science* 268, pp. 87–90.

Dickinson, M.H., C.T. Farley, R.J. Full, M.A.R. Koehl, R. Kram, and S. Lehman. 2000. "How Animals Move: An Integrative View," *Science* 288, pp. 100–106.

Eckerle, J., J.S. Stanford, J. Marlow, Roger Schmidt, S. Oh, T. Low, and V. Shastri. 2001. "A Biologically Inspired Hexapedal Robot Using Field-Effect Electroactive Elastomer Artificial Muscles," to be published in *Proc. SPIE, Smart Structures and Materials 2001: Industrial and Commercial Applications of Smart Structures Technologies*, Vol. 4332.

Full, R., and K. Meijer. 2000. "Artificial muscle versus natural actuators from frogs to flies," *Proc. SPIE, Smart Structures and Materials 2000: Electroactive Polymer Actuators and Devices*, Vol. 3987, ed. Y. Bar-Cohen, pp. 2–9.

Full, R., and K. Meijer. 2001. "Natural Muscles as an Electromechanical System," *Electroactive Polymer (EAP) Actuators as Artificial Muscles—Reality, Potential and Challenges*, ed. Y. Bar-Cohen, SPIE Press, pp. 67–83.

Josephson, R.K. 1985. "Mechanical power output from striated muscle during cyclic contraction," *J. Exp. Biol.*, Vol. 114, pp. 493–512.

Kofod, G., R. Kornbluh, R. Pelrine, and P. Sommer-Larsen. 2001. "Actuation response of polyacrylate dielectric elastomers," in *Proc. SPIE, Electroactive Polymer Actuators and Devices*, Vol. 4329, presented at the Smart Structures and Materials Symposium 2001, Newport Beach, California (4–8 March).

Kornbluh, R., R. Pelrine, J. Joseph, R. Heydt, Q. Pei, and S. Chiba. 1999. "High-Field Electrostriction of Elastomeric Polymer Dielectrics for Actuation," *Proc. SPIE, Smart Structures and Materials 1999: Electroactive Polymer Actuators and Devices*, Vol. 3669, ed. Y. Bar-Cohen, pp. 149–161.

Kornbluh, R., R. Pelrine, Q. Pei, S. Oh, and J. Joseph. 2000. "Ultrahigh Strain Response of Field-Actuated Elastomeric Polymers," *Proc. SPIE, Smart Structures and Materials 2000: Electroactive Polymer Actuators and Devices (EAPAD)*, Vol. 3987, ed. Y. Bar-Cohen, pp. 51–64.

Kornbluh, R., R. Pelrine, Q. Pei, and V. Shastri. 2001. "Application of Dielectric EAP Actuators," *Electroactive Polymer (EAP) Actuators as Artificial Muscles—Reality, Potential and Challenges*," ed. Y. Bar-Cohen, Ch. 16, pp. 457–495, SPIE Press.

Pelrine, R., R. Kornbluh, J. Joseph, and J. Marlow. 1998. "Analysis of the Electrostriction of Polymer Dielectrics with Compliant Electrodes as a Means of Actuation," *Sensors and Actuators A: Physical* 64, pp. 77–85.

Pelrine, R., R. Kornbluh, and G. Kofod. 2000. "High-Strain Actuator Materials Based on Dielectric Elastomers," *Advanced Materials 2000,* Vol. 12, No.16, pp. 1223–1225.

Pelrine, R., R. Kornbluh, Q. Pei, and J. Joseph. 2000. "High-Speed Electrically Actuated Elastomers with Over 100% Strain," *Science*, Vol. 287, No. 5454, pp. 836–839 (4 February).

Pelrine, R., P. Sommer-Larsen, R. Kornbluh, R. Heydt, G. Kofod, Q. Pei, and P. Gravesen. 2001. "Applications of Dielectric Elastomer Actuators," *Proc. SPIE (Electroactive Polymer Actuators and Devices, 2001)*, also to be published in *Smart Structures and Materials Symposium 2001*, Vol. 4329, Newport Beach, California (4–8 March).

Ionic Polymer-Conductor Composites (IPCC's) As Biomimetic Sensors, Robotic Actuators and Artificial Muscles (A Brief Review)

Mohsen Shahinpoor
Artificial Muscle Research Institute, School of Engineering and School of Medicine
The University of New Mexico, Albuquerque, NM 87131
Environmental Robots Incorporated, Albuquerque, NM 87108

ABSTRACT

This extended abstract will briefly review the state-of-the art and fundamental properties and characteristics of Ionic Polymeric-Conductor Composites (IPCC's) as biomimetic sensors, robotic actuators and artificial muscles. It will further address the current manufacturing techniques, mechanical, electrical and electronic characteristics of IPCC's in both sensing and actuation, phenomenological modeling of the underlying sensing and actuation mechanisms in IPCC's, and the potential application areas for IPCC's, respectively. In particular, medical applications of IPCC's to cardiovascular problems in connection with congestive heart compression/assist devices, drug delivery and fluid drainage systems in connection with micro-pumps and ophthalmological problems in connection with vision refractive errors will be discussed.

1-INTRODUCTION

It is now well documented that ionic polymers (such as a perfluorinated sulfonic acid polymer, i.e. Nafion™) in a composite form with a conductive metallic medium (herein, called Ionic Polymer-Conductor Composites, IPCC's) can exhibit large dynamic deformation if placed in a time-varying electric field (see Figure 1) [1-6]. Conversely, dynamic deformation of such ionic polymers produces dynamic electric fields (see Figure 2). A recently presented model by de Gennes, Okumura, Shahinpoor, and Kim [5] describes the underlying principle of electro-thermodynamics in ionic polymers based upon internal ionic transport and electrophoresis. It is obvious that IPCC's show a great potential as soft robotic actuators, artificial muscles, and dynamic/static sensors and transducers in micro-to-macro size scales.

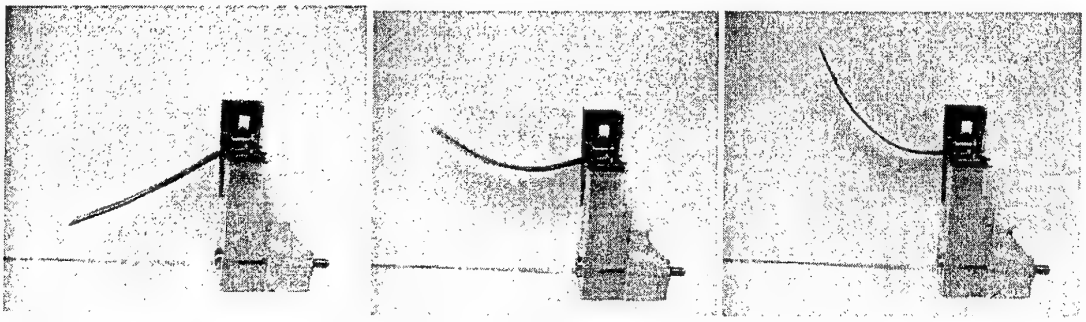

Figure 1. Successive photographs of an IPCC strip that shows very large deformation (up to 4 cm) in the presence of low voltage. Note that Δt=0.5 sec, 2 volts applied. The sample is 1 cm wide, 4 cm long, and 0.2 mm thick.

Manufacturing of an IPCC starts with Ion Exchange Membranes (IEM) via. metal compositing by means of chemical reduction processes. The term *Ion Exchange Membranes* refers to materials designed to selectively pass through ions of a single charge (either cations or anions). They are often manufactured from polymers that consist of fixed covalent ionic groups. The currently available IEM are:

(i) Perfluorinated alkenes with short side-chains terminated by ionic groups [typically sulfonate or carboxylate (SO_3^- or COO^-) for cation exchange or ammonium cations for anion exchange (see Figure 3)]. The large polymer backbones determine their mechanical strength. Short side-chains provide ionic groups to interact with waters being served as the passage of appropriate ions. A popular product is Nafion™ of Du Pont Co.

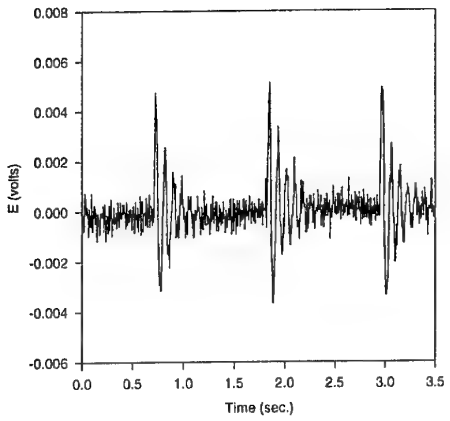

Figure 2. A typical sensing response of an IPCC. It shows dynamic sensing response of a strip of an IPCC (a thickness of 0.2 mm) subject to a dynamic impact loading in a cantilever configuration. A damped oscillatory electric response is observed which is highly repeatable with a high bandwidth of up to 1000's of Hz. Such direct mechanoelectric behaviors are related to the endo-ionic mobility due to imposed stresses. This implies that, if we impose a finite solvent (=water) flux, $|Q|$, not allowing a current flux, J=0, a certain conjugate electric field, $\vec{E}$, is produced that can be dynamically monitored as discussed later in Section 3.

(ii) Styrene/divinylbenzene-based polymers in which the ionic groups have been substituted from the phenyl rings where the nitrogen atom to fix an ionic group. These polymers are highly crosslinked and are rigid. Ionic groups are high and analogous to gels. A popular product is CR/AR series of Ionics Inc.

In Nafion™ there are relatively few fixed ionic groups. They are located at the end of side-chains so as to position themselves in their preferred orientation at some extent. Therefore, it can create hydrophilic nano-channels, so called *cluster networks.* Such a fact is completely different in nature relative to stylene/divinylbenzene-based ones that are primarily limited by crosslinking, ability of the IEM to expand (due to hydrophilic nature).

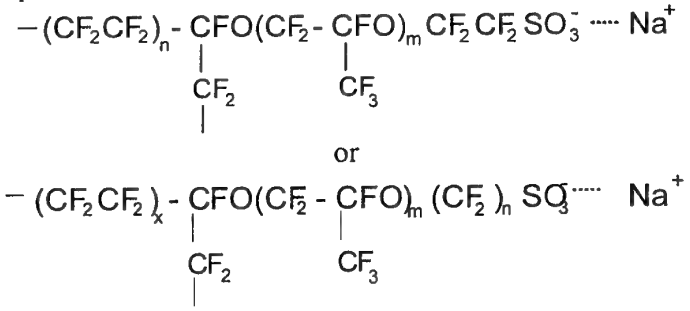

Figure 3. Perfluorinated sulfonic acid IEMs.
The counter ion, Na^+ in this case, can simply replaced by other ions.

2-MANUFACTURING TECHNIQUES

The preparation of ionic polymer-metal composites (IPCC's) requires intense laboratory work. The current state-of-the-art IPCC manufacturing technique [1-6] incorporates two distinct preparation processes: *initial compositing process* and *surface electroding process.* Due to different preparation processes, morphologies of precipitated platinum are significantly different. The initial compositing process requires an appropriate platinum salt such as $Pt(NH_3)_4HCl$ in the context of chemical reduction processes. The principle of the compositing process is to metalize the inner surface of the membrane by a chemical-reduction means such as $LiBH_4$ or $NaBH_4$. The IEM is soaked in a salt solution to allow platinum-containing cations to diffuse through the thin membrane *via* the ion-exchange process. Later, a proper reducing agent such as $LiBH_4$ or $NaBH_4$ is introduced to platinize the membrane. The platinum layer is buried submicron deep (typically 1-20 μm) within the IPCC surface and is porous. The fabricated muscles can be optimized for producing a maximum force by changing multiple process parameters including time-dependent

concentrations of the salt and the reducing agents (applying the Taguchi technique to identify the optimum process parameters seems quite attractive [10]). The primary reaction is,

$$LiBH_4 + 4\left[Pt(NH_3)_4\right]^{2+} + 8OH^- \Rightarrow 4Pt^o + 16NH_3 + LiBO_2 + 6H_2O \qquad (1).$$

In the subsequent surface electroding process, multiple reducing agents are introduced (under optimized concentrations) to carry out the reducing reaction similar to Equation (1), in addition to the initial platinum layer formed by the initial compositing process. In general, the majority of platinum salts stays in the solution and precedes the reducing reactions and production of platinum metal. Other metals (or conducing mediums) also successfully used include palladium, silver, gold, carbon, graphite, and nanotubes.

3-PHENOMENOLOGICAL LAW

A recent study by de Gennes, Okumura, Shahinpoor, and Kim [5] has presented the standard Onsager formulation on the underlining principle of IPCC actuation/sensing phenomena using linear irreversible thermodynamics: when static conditions are imposed, a simple description of *mechanoelectric effect* is possible based upon two forms of transport: *ion transport* (with a current density, J, normal to the material) and *electrophoretic solvent transport* (with a flux, Q, *we can assume that this term is water flux*). The conjugate forces include the electric field, $\vec{E}$, and the pressure gradient, $-\nabla p$. The resulting equation has the concise form of,

$$J = \sigma\vec{E} - L_{12}\nabla p \qquad (2),$$

$$Q = L_{21}\vec{E} - K\nabla p \qquad (3),$$

where σ and K are the membrane conductance and the Darcy permeability, respectively. A cross coefficient is usually $L_{12} = L_{21} = L$, believed to be on the order of 10^{-8} $(ms^{-1})/(volts\text{-}m^{-1})$. The simplicity of the above equations provides a compact view of underlining principles of both actuation and sensing of IPCC. So, we can illustrate it simply in Figure 4.

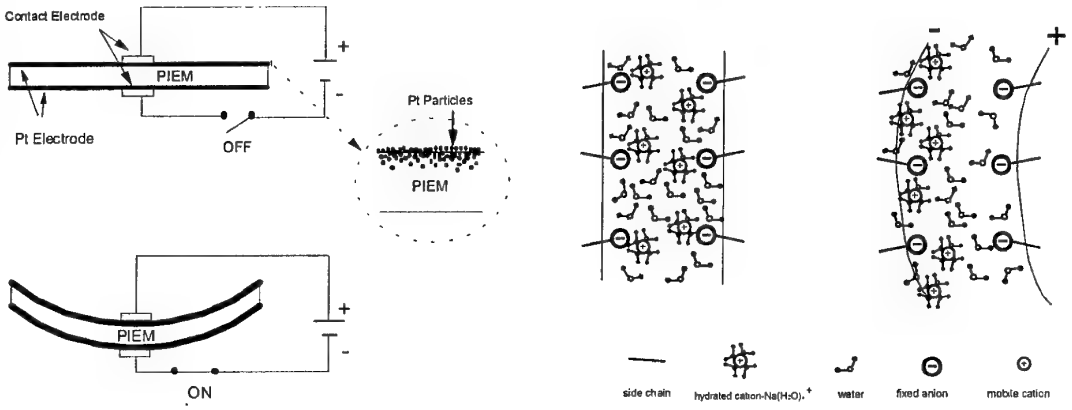

Figure 4. A schematic of the typical IPCC artificial muscle and its actuation principle.

4- Biomedical Applications and Future Challenges

In this extended abstract, the fundamental properties and characteristics of Ionic Polymeric-Metal Composites (IPMCs) as biomimetic sensors, actuators and artificial muscles are briefly presented in a summary form. It is obvious that the successful commercialization of the IPMC is highly dependent upon further improvement of its thermodynamic efficiency and force density generation. In particular, the dimensional scale-up of the IPMC is of a major factor enhancing its useful forces. The ultimate goal of using the IPMC as soft biomimetic sensors and actuators can be clearly envisioned upon the successful development of three-dimensional systems of IPMC's to be used as electrically controllable/deformable three-dimensional smart structures. In future communications, we will discuss our effort to achieve these challenges. In connection with biomedical applications, one can mention the potential of such IPCC

materials to help cardiovascular problems associated with congestive and ischemic hearts, implantable micro-diaphragm pumps for drug delivery and fluid drainage problems as well as applications in ophthalmology in connection with refractive errors of the human eye as well as glaucoma and other ophthalmological disorders such as retinal detachment. Esoteric application of such IPCC artificial muscles can also be expanded to facioscapulohumeral muscular dystrophy problems such as ptosis or the eye-lid droop syndrome as well as artificial epiglottis, larynx and vocal cords. Figure 5 depicts an schematic of a recently fabricated and successfully tested micro-pump equipped with a diaphragm made with an IPCC muscle.

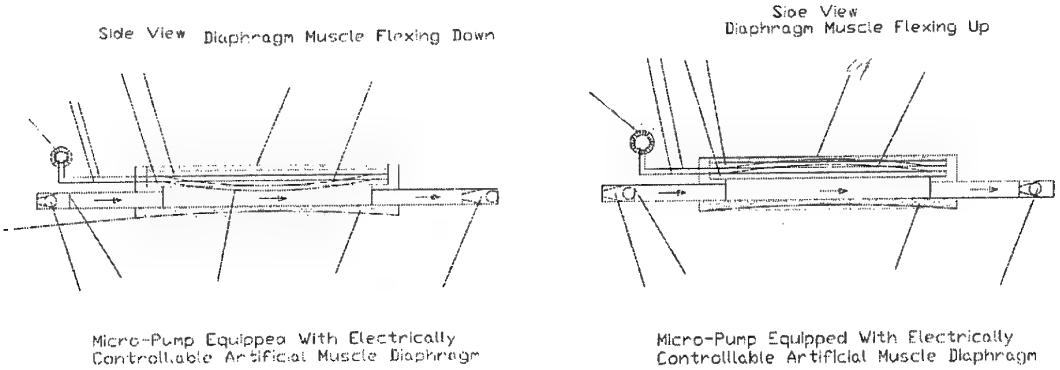

Figure 5- Schematic of a micro-diaphragm pump equipped with a flexing IPCC muscle sheet

5-ACKNOWLEDGEMENTS

This work was partially supported by U.S. NRL/DARPA. The authors thank the laboratory work done by Environmental Robots, Inc. and the Artificial Muscle Research Institute of the University of New Mexico.

6-REFERENCES

1. M. Shahinpoor, D. Adolf, D. Segalman, and W. Witkowski, "Electrically Controlled Polymeric Gel Actuators," *U.S. Patent* # 5,250,167, October (1993).
2. M. Shahinpoor and M. Mojarrad, "Soft Actuators and Artificial Muscles," *U.S. Patent*, # 6,109,852, August (2000).
3. M. Shahinpoor, Y. Bar-Cohen, J. O. Simpson, and J. Smith, "Ionic Polymer-Metal Composites (IPMC) as Biomimetic Sensors and Structures-A Review," *Smart Materials and Structures*, **7**, pp. 15-30 (1998).
4. M. Shahinpoor and K. J. Kim, "The Effect of Surface-Electrode Resistance on the Performance of Ionic Polymer-Metal Composites (IPMC) Artificial Muscles, *Smart Materials and Structures*, **9**, pp. 543-551 (2000).
5. P. G. de Gennes, K. Okumura, M. Shahinpoor, and K. J. Kim, "Mechanoelectric Effects in Ionic Gels," *Europhysics Letters*, **50(4)**, pp. 513-518 (2000).
6. K. J. Kim, M. Shahinpoor, and A. Razani, "Preparation of IPMCs for Use in Fuel Cells, Electrolysis, and Hydrogen Sensors," *Proceedings of SPIE 7th International Symposium on Smart Structures and Materials*, **3687**, pp. 110-120 (March 2000).
7. M.Shahinpoor, "Ion-Exchange Membrane-Metal Composite As Biomimetic Sensors and Actuators, " Book Chapter, Chapter 12, in Polymer Sensors and Actuators, Edited by Y. Osada and D. De Rossi, Springer-Verlag-Heidelberg, pp.325-359, (2000)
8. M. Shahinpoor," Potential Applications of Electroactive Polymer Sensors and Actuators in MEMS Technologies,", SPIE Smart Materials & MEMS Publication No. 4234-40, pp. 450-459, (2000)

Optimisation of the Actuator Properties of Polypyrrole Doped with Alkyl Benzene Sulfonates

Keld West,
The Danish Polymer Centre, Risø National Laboratory, DK-4000 Roskilde, Denmark

Lasse Bay and Steen Skaarup,
Department of Chemistry, Technical University of Denmark, DK-2800 Lyngby, Denmark.

Introduction

Polymer actuators offer the prospect of a soft and noiseless response - quite different from traditional piezoelectric or electromechanical actuators. These properties make polymer actuators well suited for biomimetic devices and the development of more efficient polymer actuators will be instrumental in the development of new applications inspired by nature. The similarity in responses is the reason for polymer actuators being nicknamed *"artificial muscles"* despite the actuation principles utilised in polymer actuators are quite different from those in natural muscles.

In the Danish "ARTMUS" project two types of polymer actuators are being developed: actuators based on dielectric elastomers and conducting polymers, respectively. The original goals set for the project are now close to being met [1] by the dielectric elastomer actuators that have shown very large strains (175%), fast response (10 Hz) and high power densities. The drawback is the high voltage (kV) required to drive these field-dependent actuators. Actuators based on conducting polymers are charge-dependent and can be operated by voltage differences of a few volts or less. They are, however, relatively slow, and the achievable strain is much smaller than with dielectric elastomers. Conducting polymer actuators nevertheless have demonstrated impressive performances in micro-devices [2- 4]. The present communication reports results of the effort to optimise a specific type of conducting polymers (polypyrrole doped with alkyl benzene sulfonates) as the active element in medium size (cm-scale) actuators.

Actuation Principle

The conducting polymer polypyrrole (PPy) doped with large anionic detergents has an unusual high stability in aqueous media. PPy can be reversibly oxidised and reduced electrochemically. The changes in redox state are accompanied by changes in volume that can be utilised for actuation.

The volume change can be separated into an *intrinsic* part stemming from changes in bond lengths and conformation of the polymer on reduction/oxidation, and a part due to an *osmotic effect* causing solvent molecules to move in and out of the polymer in a number far in excess of those bound in the solvation shell of the mobile ion.

In a previous paper a thermodynamic description of the osmotic expansion is worked out [5]. The model was compared with measurements on films made from PPy doped with

dodecyl benzene sulfonate (DBS). Experiments show that the expansion decreases as the concentration in the surrounding electrolyte was increased. Comparison with theory led to the conclusion that a considerable part of the total expansion of PPy-DBS is due to the osmotic effect, and that the osmotic effect must be taken into account when interpreting and designing actuator experiments. Figure 1 shows how the amplitude of the expansion is larger in dilute electrolytes as expected from the osmotic model.

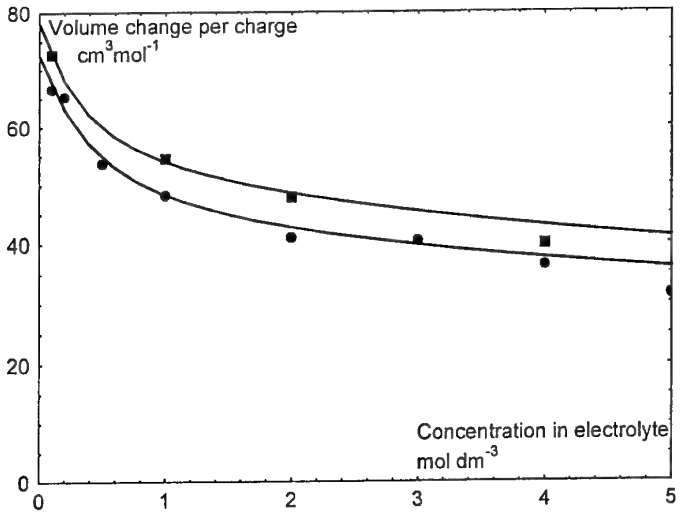

Figure 1: Expansion of two different PPy-DBS strips when the potential is swept between –0.85 V and 0.3 V vs. SCE in NaCl solutions of different concentrations. The expansion is recalculated as volume change per charge on the polymer backbone. Curves are fitted to the model for osmotic expansion [5].

Whereas osmotic expansion only depends on the electrolyte and the mechanical properties of the polymer, the intrinsic expansion will be dependent on the chemistry of the specific polymer in question. We have undertaken a systematic study of the influence of the dopant ion on physical properties and expansion of PPy polymers. Figure 2 shows the expansion of a series of 10 μm × 5 mm × 10 mm PPy films doped with different alkyl benzene sulfonate anions. The x-axis shows the length of the alkyl chain, ranging from 1 in p-toluene sulfonate to 22 in p-(11-docosyl) benzene sulfonate (DCBS). The shorter alkyl groups are linked to the benzene ring in the *n*-position, whereas the longer chains are linked in an intermediate position as the corresponding linear isomers have very low solubilities in water. Results for two different isomers of DBS are shown on the graph: p-(2-dodecyl) benzene sulfonate, (2D)BS, and p-(6-dodecyl) benzene sulfonate, (6D)BS. The highest expansion (and contraction), which is almost 4 % in the configuration used here, is obtained with p-(n-octyl) benzene sulfonate (OBS). Doping of PPy with p-(n-hexyl) benzene sulfonate (HBS) or smaller anions gives less elongation. An important reason is the smaller dopant ions being partially mobile, leading to opposite cation and anion motion and thus to a smaller total length change. With the largest anions, p-(8-hexadecyl)benzene sulfonate (HDBS) and DCBS, the charge that can be redox cycled is low: for HDBS only 0.1 e^- per monomer, and for DCBS only 0.03 e^- per monomer can be cycled, while it for the other dopant ions is between 0.15 and 0.2 e^- per monomer.

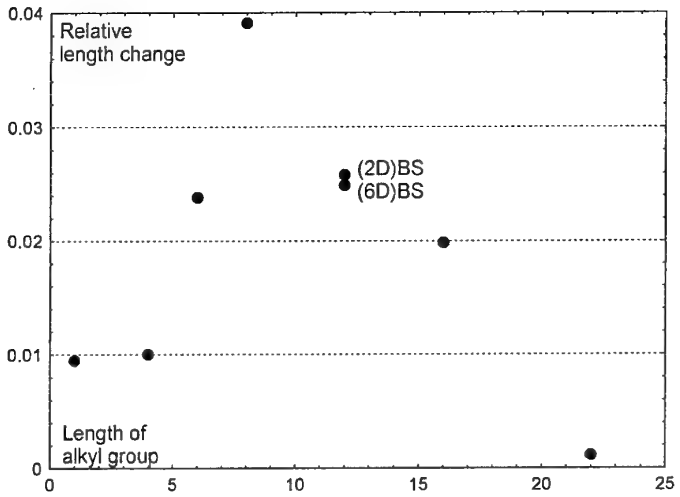

Figure 2: Maximum expansion of PPy-alkyl benzene sulfonate films on changing the potential from 0.2 V *vs SCE* (oxidised) to –0.85 V *vs SCE* (reduced state). The length of the alkyl chain is indicated on the x-axis.

Limitations

It is mainly transport processes that limit the speed of a conducting polymer actuator. For micro-actuators, where the active polymer is deposited onto a conducting (gold) layer, the speed is limited by ion diffusion across the thickness of the polymer layer. The time-constant for this process is given by:

$$\tau = \frac{\ell^2}{D} \qquad (1)$$

where D is the diffusion coefficient, and ℓ is the thickness of film. For micro devices, this time constant is quite low, and responses measured in seconds or fractions of seconds are reported. As the time constant increases with the square of the length of the diffusion path, it is important on upscaling to larger devices, that one dimension of the active polymer element is kept in the μm-range,

In order to better exploit the strain and force capability in larger devices, it is desirable to operate conducting polymer actuators in a configuration as the one shown schematically on figure 3, where a polymer strip or fibre is contacted electrically in one end and suspended in an electrolyte. The length change of the polymer strip can then act directly on the load with much smaller losses than in bender configurations.

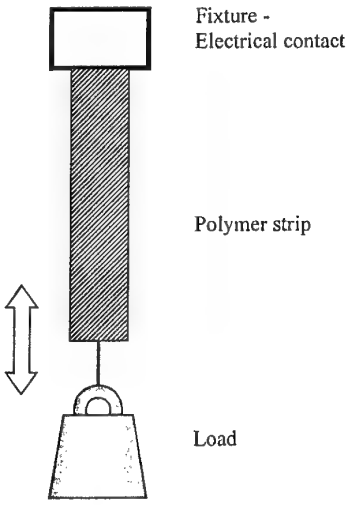

Figure 3: Schematic diagram of free-standing polymer actuator

This configuration, however, imposes additional kinetic limitations to the speed of the device stemming from charge transport along the length of the conducting polymer element. The result of these limitations is that the potential imposed on the polymer only propagates along the length of the strip with a finite velocity. This is illustrated on figure

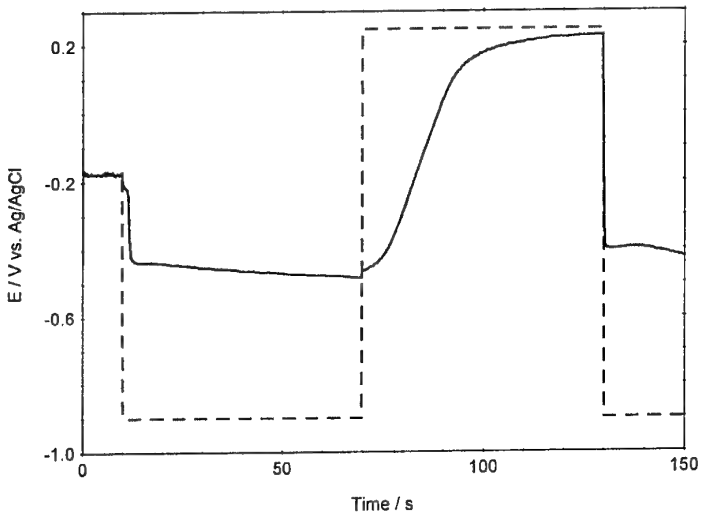

Figure 4: Potential applied to a 10 μm × 3.6 mm × 7.3 mm PPy-DBS strip (dashed line), and potential measured at the opposite end of the strip (solid line).

4 showing data from an experiment where a potential was applied to one end of a PPy-DBS strip while the potential in the other end was monitored.

On oxidation, the set potential is approached with a time constant of 10 – 20 s, mainly due to the delayed charge transport in the transmission line formed by the resistivity of the conducting polymer and the redox capacity. Phenomenologically this charge transport process is equivalent to a diffusion process and the time constant will increase with the square of the length of the strip. On reduction the set potential is approached very slowly. This is in part due to the rapid increase in resistivity when the polymer is reduced, and in part to oxygen reduction competing with discharging of the redox capacity [7]. In order to overcome these limitations it is important to increase the conductivity of the active polymer element – preferably independently on its redox state! One way to accomplish this with a minimised restriction of the motion of the polymer is to apply a compliant electrode to one surface of the polymer strip. Using a corrugated gold electrode (10 μm period, 5 μm amplitude) we have achieved strains exceeding 10 % with PPy-DBS, and made a multi layer actuator capable of lifting 200 g.

References

1. P. Sommer-Larsen, J. Hooker, G. Kofod, K. West, M. Benslimane, and P. Gravesen, *SPIE's 8th Ann. Int. Symp.: Smart Structures & Materials*, Newport Beach, CA, USA, March 2001.
2. E. Smela, O. Inganäs, I. Lundström, *Science* **268** 1735 (1995).
3. E.W.H Jager, E. Smela, O. Inganas, I. Lundstrom, *Synthetic Metals*, **102**1309 (1999).
4. E. Smela, *J. Micromech. Microengn.*, **9** 1 (1999).
5. L. Bay, T. Jacobsen, S. Skaarup, and K. West; *J. Phys. Chem. B*, in print (2001).
6. E. Smela, N. Gadegård; *Advanced Materials* **11** 953 (1999).
7. L. Bay, K. West, N. Vlachopoulos, and S. Skaarup, *SPIE's 8th Ann. Int. Symp.: Smart Structures & Materials,* Newport Beach, CA, USA, March 2001.

Polyanilines Doped With Adenosine-5´-Triphosphate and DNA

Leon A.P. Kane-Maguire, David A. Reece, Laura G. Stirman and Gordon G. Wallace
Intelligent Polymer Research Institute, Department of Chemistry, University of Wollongong, Northfields Ave., Wollongong, NSW 2522, Australia.

INTRODUCTION

There has been considerable recent interest in the attachment of biologically-active dopants to conducting organic polymers[1-3]. Potential applications for these composite materials include their use as novel, selective biochemical sensors or as systems for the controlled release/incorporation of drugs via redox switching of the conducting polymer backbone. Most studies to date have involved polypyrrole or polythiophene substrates. Only limited studies of the incorporation of biologically-active dopants onto polyaniline (PAn) have been reported, perhaps in part because of constraints imposed by the acid conditions usually needed for generation of the conducting emeraldine salt forms.

Adenosine-5´-triphosphate (ATP, **1**) is one of the most important biological molecules in animal and plant metabolism. Hydrolysis of its triphosphate group provides the major source of energy within cells. We now report that it may be readily incorporated as a dopant into polyaniline to give green, electroactive PAn.ATP films via the electropolymerisation of aniline in aqueous 0.50 M HCl containing added ATP as its di-sodium salt. Circular dichroism (CD) measurements showed the films to be highly optically active in the visible region, suggesting that the chiral ATP dopant induces a preferential one-handed helical structure onto the polyaniline chains.

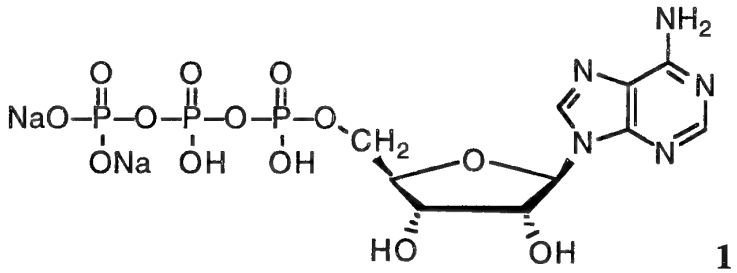

1

We have also found that *DNA* can be similarly incorporated onto polyaniline at pHs between 4-6. Interestingly, the electrochemically deposited Pan.DNA films were optically inactive in the visible region. This suggests that the polyaniline chains cannot track along the helical backbone of the high molecular weight DNA substrate.

EXPERIMENTAL

Aniline (Aldrich) was distilled and stored in a freezer under nitrogen prior to use. Adeninine-5´-triphosphate, di-sodium salt **1** was purchased from Aldrich, while DNA (from salmon sperm) was obtained from Sigma. The pH 4 phosphate buffer was prepared by adjusting the the pH of a 0.10 M NaH_2PO_4 solution with conc. HCl. UV-visible-near infrared spectra of the PAn.ATP and Pan.DNA films were recorded on a Cary 500 spectrophotometer, while circular dichroism (CD) spectra were

measured using a Jobin-Yvon Dichrograph 6. Cyclic voltammetric studies of these films were carried out in a three-electrode cell with a platinum mesh auxiliary electrode and Ag/AgCl as the reference electrode. A small (1.5 mm diameter) platinum working electrode was used and a sweep rate of 50 mV/sec. Electrospray mass spectra were recorded with a Quattro (VG Biotech) mass spectrometer.

Emeraldine Salt Film Preparations.- The same electrochemical instrumentation was employed for the deposition of the emeraldine salt films, except that an ITO-coated glass (Delta Technology) working electrode was used in order to permit subsequent spectroscopic characterisation. An aniline concentration of 0.20 M was employed for all polymer film growth experiments.

(i) ***PAn.ATP films*** were deposited *potentiodynamically* by scanning the potential between -0.2 and +1.0 V at 50 mV/sec) from aniline solutions containing 0.50 M HCl and either 0.01 M or 0.04 M Na_2ATP. *Potentiostatic* deposition of PAn.ATP films was investigated using 0.04 M Na_2ATP/0.50 M HCl and an applied potential of +0.80 V (*vs* Ag/AgCl). Films of thickness suitable for uv-visible-near infrared and CD spectral studies could be thus grown within 2 min. At higher applied potentials (0.90 and 1.00 V), shorter polymerisation times (60 and 30 sec, respectively) were only necessary. *Galvanostatic* growth of PAn.ATP films was also carried out, using 0.04 M Na_2ATP/ 0.50 M HCl as electrolyte and a constant current density of 2 mA/cm^2 (deposition time120 sec).

(ii) **PAn.DNA films** were similarly electrochemically grown, using a DNA concentration of 0.10% (w/v) and a pH of 4 or 6. For *potentiodynamic* polymerisation, the potential was swept between –0.2 and +1.0 V with a cycle rate of 50 mV/sec. *Potentiostatic* polymerisation used an applied potential of +1.0 V, while current densities between 1 and 5 mA/cm^2 were used for *galvanostatic* deposition.

RESULTS AND DISCUSSION

(a) Pan.ATP Films.- Sweeping the potential of a 0.2 M aniline/ 0.04 M Na_2ATP solution between -0.2 and +1.0 V with [HCl] $\geq$ 0.50 M led to the rapid deposition of green emeraldine salt films on a Pt working electrode. Cyclic voltammograms during polymer growth exhibited increasing currents with successive sweeps, confirming the deposition of conductive polymeric films (eg. Figure 1 for a film grown on platinum from 0.04 M ATP / 0.50 M HCl). The first anodic wave in this cyclic voltammogram showed a peak at ca. + 0.9 V, corresponding to the oxidation of the aniline monomer to its radical cation. The current/voltage profiles observed in subsequent scans were typical of previously reported[4] PAn.HA emeraldine salts. An oxidation peak at ca. +0.2 V can be attributed to the oxidation of the deposited PAn from leucoemeraldine to the emeraldine salt state, while a second oxidation peak at ca. +0.7 V is consistent with further oxidation to pernigraniline.

Although films grew from less acidic solutions ([HCl $\leq$ 0.3 M), the films were pale brown in colour and were non-conductive, as shown by the very low current passed during successive potential sweeps. All subsequent electrochemical approaches to the target PAn.ATP salts were therefore carried out with Na_2ATP in 0.50 M HCl.

The UV-visible-near infrared spectrum of an analogous polyaniline film *potentiodynamically* grown from 0.04 M ATP/0.50 M HCl onto an ITO-coated glass electrode, shown in Figure 2a, is consistent with an emeraldine salt. On the basis of earlier studies by MacDiarmid et al[5], the presence of both a

shoulder at ca. 800 nm and strong near-infrared absorption (λ_{max} ca. 1250 nm) suggests that the polyaniline chains adopt a mixture of "expanded coil" and "compact coil" conformations. Conclusive evidence for the incorporation of ATP into the emeraldine salt came from the corresponding circular dichroism spectrum (Figure 3a). This exhibited bisignate CD bands at ca. 390 and 470 nm associated with the absorption band at 430 nm, as well as strong ellipticity above 600 nm associated with the film's high-wavelength polaron absorption band at 800 nm. We believe that the chiral ATP dopant induces a preferential one-handed helical conformation onto the PAn chains, giving rise to the recorded optical activity.

The intensity of the CD spectra for potentiodynamically deposited PAn.ATP films was markedly dependent upon the concentration of ATP used in the polymerisation mixture. For example, a film grown from 0.01 M ATP/ 0.50 M HCl exhibited much reduced optical activity, the ellipticity of the negative CD band at 475 nm decreasing from the -45 mdeg observed above with 0.04 M ATP) to -5 mdeg. This observation is consistent with increasing competitive incorporation of ATP as a dopant into the PAn chains with increasing [ATP]. On the other hand, the scan rate during potentiodynamic electropolymerisation was found to have only a moderate influence on the uv-visible and CD spectra of the deposited emeraldine salt films.

Potentiostatic polymerisation was subsequently found to be the most effective method to deposit highly optically active PAn.ATP. Films grown from aniline/ATP/HCl solutions at a constant potential of 0.8 V onto ITO-coated glass electrodes again exhibited uv-visible-near infrared spectra typical of emeraldine salts, eg. Figure 2b for a film grown from 0.04 M ATP / 0.50 M HCl. However, this latter spectrum exhibited considerably less absorption in the near- infrared region than the potentiodynamically grown film in Figure 2a , suggesting a more "compact coil" character.

Significantly, the potentiostatically grown PAn.ATP films showed (Figure 3b) markedly higher optical activity than those grown potentiodynamically (Figure 3a). Even higher optical activity was achieved by growing the PAn.ATP films at more positive potentials. For example, increasing the applied potential from + 0.8 to +1.0 V led to PAn.ATP films with chiral anisotropy factors, g ($=\Delta\varepsilon/\varepsilon$), as high as 1.94 %. These exceptional g values suggest that PAn.ATP films grown potentiostatically possess high diastereomeric purity. The high chiral induction by the ATP dopant presumably arises from strong stereoselectivity in the interaction of its numerous H- and ionic- bonding sites with amine (NH) and radical cation ($NH^{+\cdot}$) centres on the PAn chains. *Galvanostatically* deposited PAn.ATP films exhibited CD bands with intermediate intensities, eg. Figure 3c for a film grown with a constant current density of 2 mA/cm^2 for 120 sec.

Alkaline De-doping of PAn.ATP Films.- The electrochemically grown PAn.ATP films could be readily converted to their corresponding emeraldine base (EB) forms via treatment with aqueous 1.0 M NH_4OH. The films changed colour from green to blue within seconds. Their uv-visible spectra recorded after 15 min of alkaline treatment confirmed conversion to emeraldine base, exhibiting characteristic absorption bands at ca. 620 and 320 nm. The CD spectra of these EB films showed

them to be strongly optically active, confirming that racemisation did not occur in the solid state during the alkaline de-doping.

A negative ion electrospray mass spectrum of the aqueous NH_4OH solution after alkaline de-doping of the above PAn.ATP film showed the presence of $[ATP-H]^-$ (m/z 506) ions, confirming at least partial release of ATP from the polyaniline matrix upon alkaline treatment. This feature, together with their electroactive character, suggests that the PAn.ATP materials may have potential as new agents for the controlled release of ATP or for the separation/synthesis of enantiomerically pure chemicals.

(b) Pan.DNA Films could be similarly deposited on ITO-coated glass working electrodes using either potentiodynamic, potentiostatic or galvanostatic polymerisation of aniline (0.20 M) in the presence of 0.10 % (w/v) DNA. In each case their UV-visible-near infrared spectra confirmed the formation of emeraldine salts, exhibiting the expected characteristic peaks at ca. 310 nm (π-π^*) and 450 nm (polaron band), together with a higher wavelength polaron band. For example, a PAn.DNA film grown *potentiodynamically* at pH 6 exhibited high wavelength bands at 800 and ca. 1500 nm (Figure 4). This suggests that the PAn chain is a mixture of "compact coil" and "extended coil" conformations.

The position and intensity of the high wavelength bands were sensitive to the polymerisation conditions. For example, a PAn.DNA film *potentiodynamically* deposited at pH 4 showed little evidence of the 800 nm localised polaron band, suggesting a more "extended coil" conformation. Longer deposition times also led to red shifts for the high wavelength polaron band. Similarly, for PAn.DNA films *galvanostatically* deposited at pH 4, the position of the high wavelength band red shifted from 920 to 1050 nm when the current density was increased from 2 to 5 mA/cm^2.

Cyclic voltammograms of PAn.DNA films were also consistent with their formulation as emeraldine salts. However, surprisingly, the films showed no circular dichroism bands in the visible region. This lack of chiral induction contrasts with the above PAn.ATP films and suggests that the PAn chains cannot track uniformly along the helical backbone of the large DNA dopant.

Acknowledgements

The Australian Research Council, ONRIFO and DARPO are thanked for support.

References

1 M. Pyo and J.R. Reynolds, *Chem. Mater.*, **8** (1996) 128.
2 A. Guiseppe-Elie, G.G. Wallace and T. Matsue, Chapter 34 in *Handbook of Conducting Polymers, 2nd Ed.,* T.A. Skotheim, R.L. Elsenbaumer and J.R. Reynolds, Eds., Marcel Dekker, Inc., New York, USA, 1998.
3 J.N. Barisci, A.J. Hodgson, L. Liu, G.G. Wallace and G. Harper, *React. Funct. Polymers*, **39** (1999) 269, and refs. cited therein.
4. A.A. Syed and M.K. Dinesan, *Talanta*, **38** (1991) 815, and refs. cited therein.
5 Y. Xia, J.M. Wiesinger and A.G. MacDiarmid, *Chem. Mater.*, **7** (1995) 443.

Fig 1. CV during potentiodynamic growth of PAn.ATP on Pt (0.2 M aniline, 0.04 M ATP, 0.5 M HCl.

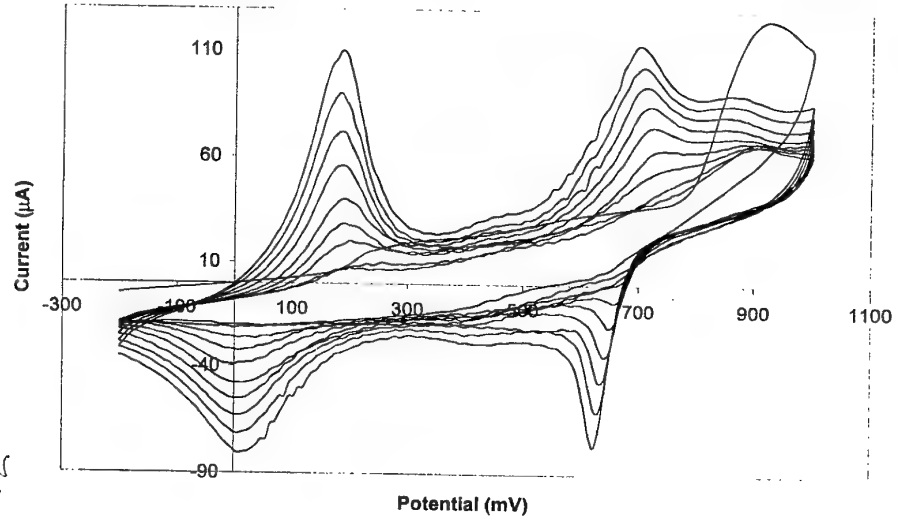

Fig 2. UV-Vis-NIR spectra of PAn.ATP films (a) Potentiodynamically grown (-0.2 to 1.0 V, 50 cycles/sec), (b) Potentiostatically grown (0.8 V for 120 sec).

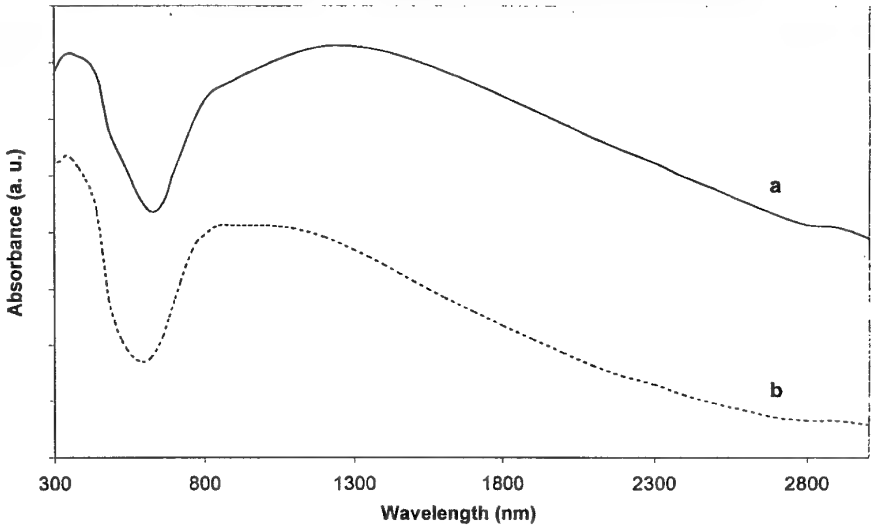

Fig 3. CD Spectra of PAn.ATP films grown (a) Potentiodynamically, (b) Potentiostatically (0.8 V, 120 sec), (c) Galvonostatically, 2 mA/cm^2 (120 sec).

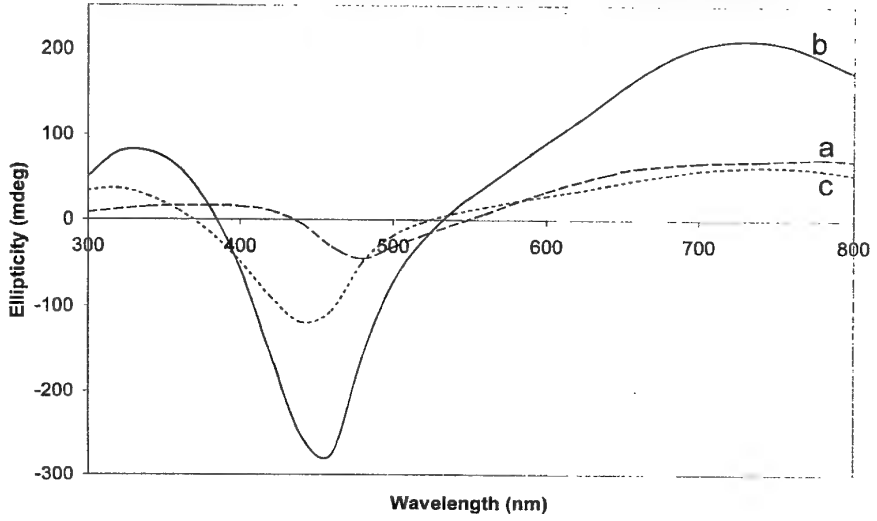

Fig 4. UV-Vis-NIR spectrum of PAn.DNA film grown by CV (-0.2 to 1.0 V, 5 cycles) at pH 6.

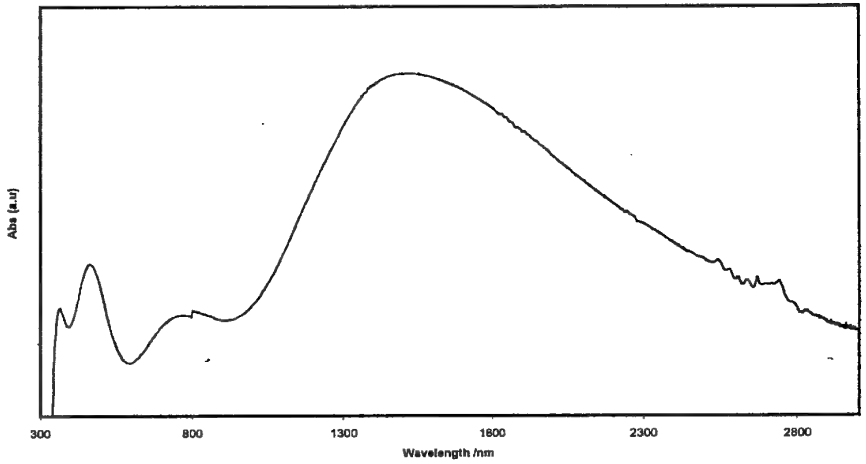

Fig 1. CV during potentiodynamic growth of PAn.ATP on Pt (0.2 M aniline, 0.04 M ATP, 0.5 M HCl.

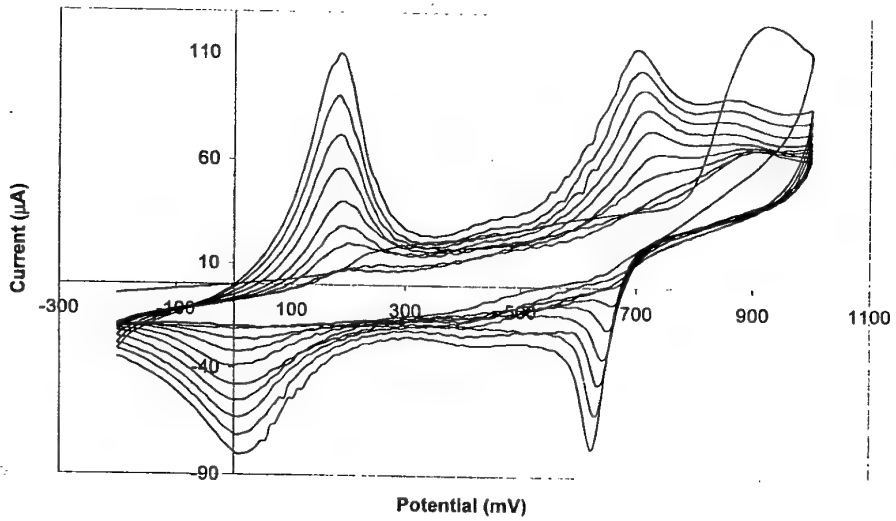

Fig 2. UV-Vis-NIR spectra of PAn.ATP films (a) Potentiodynamically grown (-0.2 to 1.0 V, 50 cycles/sec), (b) Potentiostatically grown (0.8 V for 120 sec).

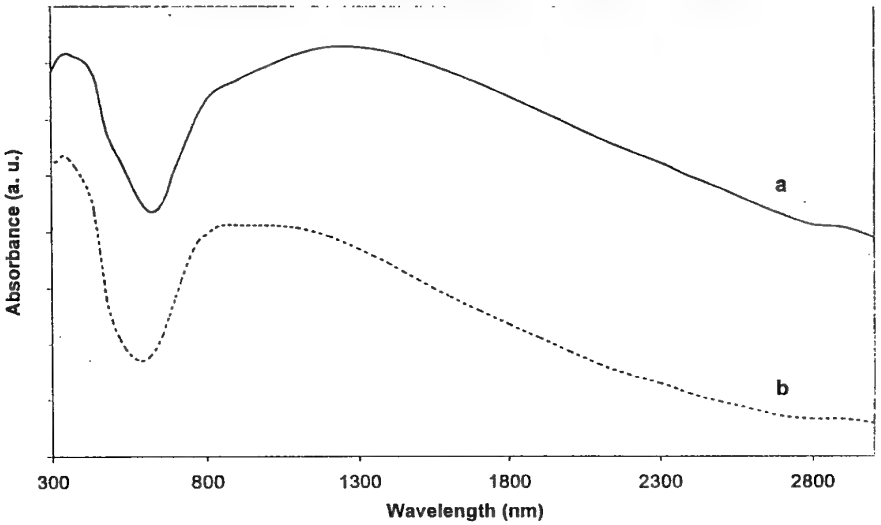

Fig 3. CD Spectra of PAn.ATP films grown (a) Potentiodynamically, (b) Potentiostatically (0.8 V, 120 sec), (c) Galvonostatically, 2 mA/cm^2 (120 sec).

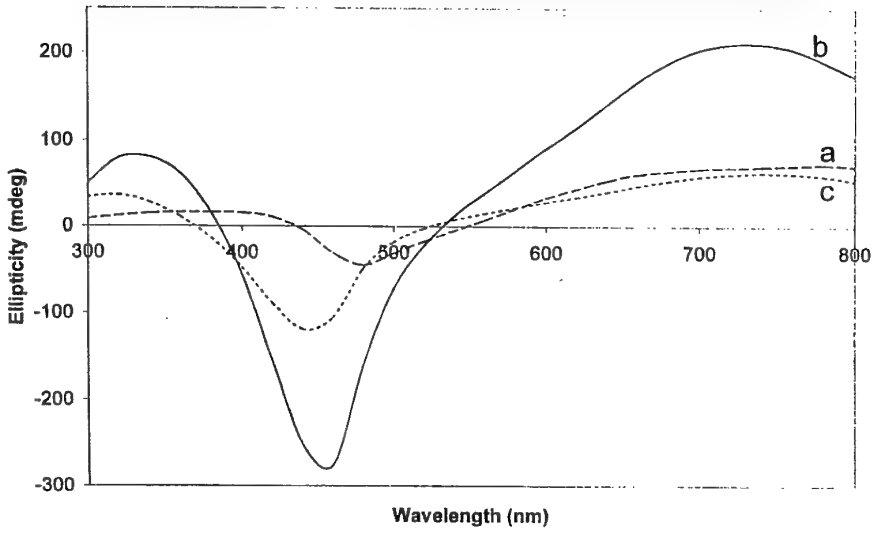

Fig 4. UV-Vis-NIR spectrum of PAn.DNA film grown by CV (-0.2 to 1.0 V, 5 cycles) at pH 6.

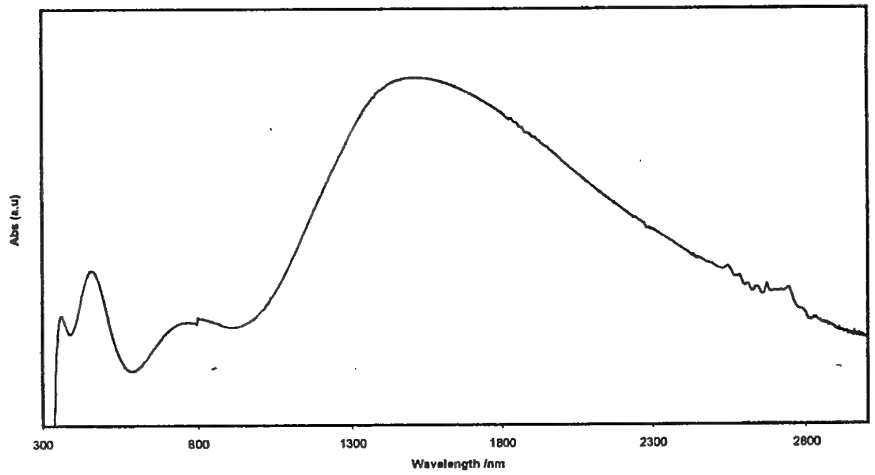

Connecting brains to robots: New perspectives for Medicine, Engineering and Information Technology.

Ferdinando A. Mussa-Ivaldi, Simon T. Alford, Vittorio Sanguineti, Karen M. Fleming, Amir Karniel, Bernard D. Reger

Northwestern University Medical School and
Rehabilitation Institute of Chicago

Introduction

The declared goal of early pioneers of computer science was to create machines capable to imitate the human brain. Researchers have adopted the reference to biology as a source of inspiration for creating artificial devices, particularly in the last two decades. More recently, a new perspective has emerged: the perspective of including biological elements within hybrid integrated systems (Jahnsen et al., 1999). The idea of using "neurobiology as a technology" is rooted on the observation that the nervous systems of the simplest organisms still outperform the most advanced digital computers. In addition, there have been important advances in the techniques for delivering stimulations to brain tissue and for recording the activity of large neuronal populations. These advances allow us to think of neural nets not just as simulations of biological properties but as possible operational descriptions of neural tissue.

At the moment, the major obstacle for the development of systems that incorporate neural elements is our own ignorance about how the brain tissue operates. But this limit should not prevent one from moving along this direction, as the creation of systems in which biological neurons interact with computers and artificial machines provides us with new tools for investigating the neurobiological underpinnings of computation.

Here, we describe one of such hybrid systems, which has established a bi-directional communication between the brainstem of a lamprey and a small mobile robot. We have developed this system as a tool for investigating the cellular mechanisms of learning in the sensory-motor system. In particular, we wish to explore the possibility of inducing controlled long-lasting changes in synaptic efficacy within the neural tissue so as to effectively "program" a desired response to the presentation of a light. If neural tissue can be considered as a biological computer and if we have an understanding of the mechanisms of neural plasticity, this goal should be within reach. On the other hand, the problems that we may encounter along this way may expose the gaps in our knowledge of the connection between cellular mechanisms and information processing in the brain.

In parallel with increasing our basic knowledge of neurobiology, the creation of devices that establish bi-directional communications with neural tissue has two applicative domains: (a) the creation of instruments – neuroprostheses – for the victims of disabling neurological illness (such as stroke, spinal cord injury and neurodegenerative disease) and (b) the creation of the technology and of the basic science necessary for the construction of devices that tap into biological resources for information processing. The last goal is suggested by the consideration that, as of today, biological tissue is far superior to technological artifacts, in particular for what concerns the ability to carry out adaptive control tasks with a self-repairing and self-renewing medium.

A hybrid system

The framework that we have developed (Figure 1) is a hybrid system, which establishes a two-way signal exchange between a mobile robot and brain tissue maintained alive in vitro from the reticular formation of the Lamprey- a primitive eel-like vertebrate. In this experimental arrangement, the brain and the robot are interconnected in a closed loop. They communicate through an interface that transforms (a) light information from

the robot's optical sensors into electrical stimuli to the lamprey's brainstem, and (b) recorded neural activity from two brainstem nuclei into motor commands to the robot's wheels.

The neural component.
We extracted and maintained the brain of anesthetized larvae of sea lampreys (Petromyzon marinus) in continuously superfused, oxygenated and refrigerated (9-11 C°) Ringer's Solution (NaCl, 100.0 mM; KCl, 2.1 mM; CaCl2, 2.6 mM; MgCl2, 1.8 mM; glucose, 4.0 mM; NaHC;O3, 25.0 mM).

We recorded extracellularly the activity of neurons in the reticular formation, a relay that connects different sensory systems (visual, vestibular, tactile) and central commands to the motor centers of the spinal cord. We placed two recording electrodes in the right and left Posterior Rhombencephalic Reticular Nuclei (PRRN). We also placed two unipolar tungsten stimulation electrodes among the axons of the Intermediate and Posterior Octavomotor nuclei (nOMI and nOMP in Figure 1). These nuclei receive inputs from the vestibular capsule and their axons form synapses with the Rhombencephalic neurons on both sides. The impedance of the stimulation electrodes ranged between 1 and 2 MΩ. Recording electrodes were glass micropipettes filled with 1M NaCl (1.5-10 MΩ). The recorded signals were acquired at 10kHz by a data acquisition board (National Instruments PCI-MIO-16E4) on a Pentium II 200MHz computer (Dell Computer Corp.).

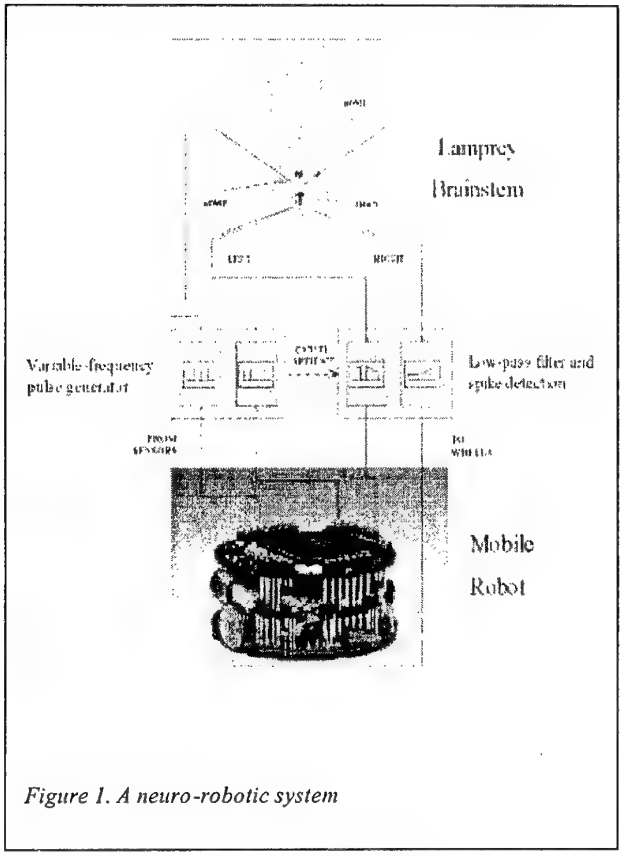

Figure 1. A neuro-robotic system

Electrode placement
While the axons of the nOMI remain on the same side of the spinal cord where they originate, those of the nOMP cross the midline. As a result, the activity of one vestibular capsule affects the reticulo-spinal (RS) neurons on both sides. We placed each stimulating electrode near the region in which the axons of the nOMI and nOMP cross. This placement of the electrodes also induced predominantly excitatory responses in the downstream neurons. The recording electrodes were inserted on either side of the midline, near the visually identified neurons of the PRRN.

The robot
The robot is the base Khepera module (K-Team). Its small size allows us to use a small workspace. A circular wall was constructed with a 2-foot diameter and then painted black to reduce the amount of reflected light. Placed along the circumference of the robot are eight

sensors each providing proximity and light intensity information. The sensors are located on opposite sides of the robot's midline at 10°, 45°, 85°, and 165° from the front position. Two wheels provide a means of locomotion for the small robot. Our computer system communicates with the robot through the serial port and a custom designed LabVIEW application. Eight lights are mounted at the edge of the robot workspace at 45° intervals. The lights are computer controlled using the digital outputs of our acquisition card. These lights generate the stimulus that elicit a phototactic response.

The interface

The interface acts as a simple interpreter between the neural signals and the robot control system. It is responsible for the transformation of the robot's light sensor information into vestibular inputs and then for processing in real time the neural activity of the reticulo-spinal nuclei and for translating it into motor commands for the robot.

The light intensity detected by the robot sensors determines the frequency at which the right and left vestibular pathways are stimulated. The weighted sum of the optical sensors on each side is multiplied by a gain factor, which determines the maximum stimulation frequency. We use the digital counter on the acquisition board to generate a train of biphasic current impulses. This pulse train is delivered to the neural preparation by the tungsten electrodes after passing through ISO-Flex stimulus isolators.

The spiking activity of the PRRN, as recorded near the axons, is analyzed through a five-step process. The signal picked up by the recording electrodes contains a combination of spikes, stimulus artifacts, excitatory and inhibitory postsynaptic potentials (PSP) and noise. To suppress the slow PSP components, this signal is first put through a high pass filter (cutoff at 200 Hz). The output of this filter contains high frequency noise, stimulus artifacts, and the spikes generated by multiple neurons in the vicinity of the electrode. Stimulus artifacts are canceled by zeroing the recorded signals over temporal windows of 4 ms following the delivery of each 200 μs stimulation pulse. The remaining signal is rectified, and a threshold is applied to separate the spikes from the background noise, under the assumption that the spike amplitude is much larger than the noise amplitude. The resulting train of spikes is put through a low pass filter (5 Hz), which effectively generates a rate-coded signal. The mean of this signal is used as a control signal for each of the robot's wheels.

The interface is calibrated so as to account for random differences between the recorded responses from the left and right side of the brainstem. The net intensity of the signal picked up by each electrode is affected by a number of uncontrollable factors, such as the actual distance from signal sources. To compensate for these random factors, we make the working assumption that when both left and right sides are stimulated at the same frequency, the same motor response should be obtained on each side of the robot.

Computational Neurobiology

The primary goal of this work is to create an instrument for exploring the computational properties of neural tissue. Modern Neuroscience includes broad variety of approaches to the nervous system, ranging from the study of molecules and cells to the research of information processing mechanisms. These different approaches are generally taken by separate research groups, using separate methods. We wish to develop a framework that may help filling this gap. The neuro-robotic system is an instrument for addressing computational questions in a neurobiological framework. Following some visionary idea set forth by Valentino Braitenberg

(Braitenberg, 1984), one can replace the biological tissue with a model and observe the resulting behavior. We have shown that this approach can provide the means for cross-validating model of neural connections based on electrophysiological data (Reger, Fleming, Sanguineti, Alford, & Mussa-Ivaldi, 2000). Different models of neural connectivity between stimulating and recording electrodes lead to different predictions of robot behavior in response to a source of light. A salient feature of neural connectivity is it may change as a function of past signal experience. The two main mechanisms of synaptic plasticity are long-term potentiation and long-term depression (Bliss & Lomo, 1973; Ito, 1989) . The neurorobotic system offers a unique opportunity to observe the effects of these synaptic changes on the robot's behavior by performing an operation that amounts to a "reversible alteration". This operation consists in changing the gain in the input pathway from the sensors (and/or in the output pathway to the wheels) and exposing the robot to this altered environment for an extended period of time. Then, the gain is restored to the original value and the alteration is removed. At this point, any persistent difference in behavior, compared to the initial behavior, would be an indication of a long-term plastic change that has been induced by the alteration. Our preliminary findings indicate that, following a reduction of one sensor input, the activities of the reticular neurons on the opposite side tend to become depressed. While these are encouraging observations, the main challenges are still ahead. To the extent that we really understand the neurobiological underpinnings of learning and memory, we should become able to operate on the neural tissue so as to obtain a pre-specified behavior of the robot in a way that is equivalent to the programming of an artificial controller. Such an accomplishment would open a new perspective in brain-machine interactions.

Acknowledgements
This work has been supported by the Office of Naval Research

References

Bliss, T., & Lomo, T. (1973). Long-lasting potentiation of synaptic transmission in the dentate area of the anaesthetized rabbit following stimulation of the perforant path. *Journal of Physiology (London), 232*, 331-356.

Braitenberg, V. (1984). *Vehicles*. Cambridge, Massachusetts: MIT Press.

Ito, M. (1989). Long-term depression. *Annual Review of Neuroscience, 12*, 85-102.

Jahnsen, H., Kristensen, B., Thiebaud, P., Noraberg, J., Jakobsen, B., Bove, M., Martinoia, S., Koundelka-Hep, M., Grattarola, M., & Zimmer, J. (1999). Coupling of organotypic brain slice cultures to silicon-based arrays of electrodes. *Methods: A Comparison to Methods in Enzymology, 18*, 160-172.

Reger, B. D., Fleming, K. M., Sanguineti, V., Alford, S., & Mussa-Ivaldi, F. A. (2000). Connecting brains to robots: an artificial body for studying the computational properties of neural tissue. *Artificial Life, 6*, 307-324.

Wiring the vertebrate retina: global patterning from short range cellular interactions

Lucia Galli-Resta[$], Elena Novelli[$], Giovanni Resta*

[$]Istituto di Neurofisiologia CNR, *Istituto di Matematica Computazionale CNR,
56100 - Pisa Italy

Most regions of the central nervous system derive their power of processing from a modular circuitry. A sequence of cell layers allows serial processing, while the positioning and connectivity of neurons within the layers supports parallel processing. Understanding how this organization develops out of undifferentiated regions of proliferating cells may be crucial to any strategy aiming at alleviating pathologies by artefact-neuronal interactions. Here we describe recent studies of the developing retina that provide new information for this search, showing how global patterning may just be the outcome of short-range intercellular interactions.

The brain bases its enormous power of processing on a modular organization. Different functional regions deal with different information, and within most regions serial and parallel circuits support the processing. Typical examples are the sensory pathways where the wiring of cells preserves maps of the external world. The circuitry of these regions is commonly a sequence of layers, through which serial processing flows, while the positioning and connectivity of neurons within the layers support parallel processing. This organization is found in the cerebral and cerebellar cortices, as well as in the retina [1].

These orderly neuronal architectures develop out of undifferentiated proliferative tissues, where cells divisions occur normally only in a border region, from where newly generated cells must then migrate to their final positioning[2]. DNA does not encode enough information to determine the absolute positioning of each single cell, or its connectivity, albeit these are crucial determinants of circuital functions. Recent studies of retinal development show the powerful strategy enforced by nature to deal with this issue, a strategy based on local interactions and the fact that all the cells of the same type are alike.

The retina is probably the region of the central nervous system where our tools to identify the different functional types of neurons are most advanced. Decades of anatomical and functional studies have unveiled a major organizing principle of the retinal architecture: cells are stacked in a sequence of layers, and neurons of the same type commonly form regular arrays, or mosaics, which orderly tile the layers[3,4] *(Figure 1)*. Investigating how this organization develops has long been hampered by the lack of markers allowing the early detection of different retinal cell types. This situation has now changed, and revealed an unexpected scene.

From fish to monkey, non-random arrays of like neurons are found early in retinal development, at times when new array cells must still be generated, or are still migrating towards the array layer[4]. Thus, positional constraints act on neurons at times when cell migration, death, proliferation and fate determination are also taking place, and are likely to interact with these developmental processes. The first example of such interplay was found when investigating how arrays maintain their order while incorporating new cells.

The case known in greatest details is the late phase of assembly of the mosaics of the cholinergic cells in the rat retina. These cell arrays are regular early in development, when they still have to accommodate about 30% more cells to reach their adult number. Yet, the geometry of cell positions within the array is the same throughout the days new cells arrive. This dynamic maintenance of order appears due to at least two factors: while new cells enter the arrays among the old ones, the retina grows, and array cells can move laterally within the plane of the layer[5]. Cell death could potentially also contribute to this game[4].

Which is the pattern of cell positioning in retinal arrays? Autocorrelation analysis, a technique that can detect patterns even if partially hidden by noise, has shown that many retinal arrays have the same basic geometry: cell spacing is based simply on an exclusion rule, by which no two array cells are ever closer than a fixed minimal distance. This minimal distance, or d_{min}, is typical of the cell type and is independent of the density of array cells. It is just the spatial range of the interactions between like cells and the local density of these cells that set the difference between the different mosaics. This is well exemplified by the mosaics of rod and S cone photoreceptors of the ground squirrel. The highly ordered S cones have simply a larger dmin than the rods, but this is enough for the S cones to form a precisely ordered array, while, at the same local density, the rods form an array that tiles the retina almost like a random distribution of cells[6] *(Figure 2)*.

These findings have important implications, as it is obvious that cells do not need to interact with anything but their surrounding like cells to enact a local exclusion rule. This prediction was verified by testing whether array cells could form their mosaics no matter what happens to cells of different types. The cholinergic mosaics provide again paradigmatic examples. One of the two cholinergic mosaics forms within the ganglion cell layer, which can be depleted of almost all other cells by optic nerve section at birth. This manipulation leaves the cholinergic array to develop in an almost empty layer rather than in the sea of different neurons that usually surrounds the cholinergic cells. Yet this array develops normally, which is even more remarkable when considering that the cholinergic neurons normally form synapses on the cells that were eliminated. Similarly, the cholinergic arrays are normal in transgenic models (the BCL-2 over-expressing mouse) where the retina contains many more cells than normal. Notwithstanding a conspicuous increment in the number of both their input and output cells, and the altered density of cells in the layers where they develop, the cholinergic neurons of this transgenic mouse are in

normal number, and form mosaics that are indistinguishable from normal[7]. Similar observations were made for other retinal mosaics[8]. Thus, retinal arrays appear to form independently of other cells.

Considered altogether, these studies allow us to trace a schematic and incomplete sequence of the developmental events leading to mosaic formation. Newly generated array cells migrate towards their final layer, and here recognize and interact with their like cells by means of signalling whose nature is currently unknown. The interactions controlling cell spacing are local and involve exclusively homotypic cells. Indeed, nothing but a local exclusion rule is enforced, by which no two array cells can be closer than a fixed minimal distance. This is enough for array cells to organize dynamically their relative positioning so that their array appears regularly organized and actively maintain this regular spacing as new cells join the array[5]. This occurs by means, at least, of lateral cell movement[5,9,10], but could also involve cell death[4]. Although all these steps have been elucidated only for a few mosaics, there are several indications that that this could be a general picture, as suggested by the generality of the d_{min} rule[4,11], as well as by the lack of correlation between cell spacing in different mosaics[8], an indicator of their mutually independent assembly.

Albeit still incomplete, this sequence of developmental events suggests that retinal arrays could be the building blocks of retina assembly, as they form early, and independently of one another. We can now reasonably speculate that, once cells are spatially organized in arrays of like neurons, then interactions between synaptic partners within a limited spatial range would be enough to wire the modular architecture of the retina. Indeed, when like cells form orderly arrays, each array cell is warranted a domain within the retina. If each array cell searches for synaptic partners within a limited spatial range, it will suffer little competition from other like cells, as each will be searching partners in a region centred on its own domain.

The capability of cells to recognize one another, and two sets of local rules (the spacing of like-neurons and the interactions with synaptic partners within a limited domain) could thus be sufficient to lay down the major characteristics of the retinal modular circuits: the parallel arrays of like neurons, and their serial connections according to a topographical order that preserves a map of the information as this flows through the sequential steps of retinal processing

Acknowledgment

Our work on retinal mosaics was supported by the CNR, the EC DGXII and the Telethon Foundation.

References

1. Kandel, E., Schwartz, J. & Jessel, T. M. (eds.) *Principles of Neural Science* (Elsevier, New York, 2000).

2. Gilbert, S. *Developmental biology* (Sinauer, Sunderland, MA, USA, 2000).
3. Wässle, H. & Boycott, B. B. Functional architecture of the mammalian retina. *Physiol Rev* **71**, 447-480 (1991).
4. Cook, J. E. & Chalupa, L. M. Retinal mosaics: new insights into an old concept. *Trends Neurosci* **23**, 26-34 (2000).
5. Galli-Resta, L., Resta, G., Tan, S.-S. & Reese, B. Mosaics of Islet-1 expressing amacrine cells assembled by short range cellular interactions. *J Neurosci* **17**, 7831-7838 (1997).
6. Galli-Resta, L., Novelli, E., Kryger, Z., Jacobs, G. & Reese, B. Modelling the Mosaic Organization of Rod and Cone Photoreceptors with a Minimal Spacing Rule. *Eur. J. Neurosci.* **11**, 1438-1446 (1999).
7. Galli-Resta, L. Local, possibly contact-mediated signalling restricted to homotypic neurons controls the regular spacing of cells within the cholinergic arrays in the developing rodent retina. *Development* **127**, 1499-1508 (2000).
8. Rockhill, R. L., Euler, T. & Masland, R. H. Spatial order within, but not between types of retinal neurons. *Proc. Natl. Acad. Sci.* **97**, 2303-7. (2000).
9. Reese, B. E., Harvey, A. R. & Tan, S.-S. Radial and tangential dispersion patterns in the mouse retina are cell-class specific. *Proceedings National Academy of Science, USA* **92**, 2494-2498 (1995).
10. Reese, B., Necessary, B., Tam, P., Faulkner-Jones, B. & Tan, S. Clonal expansion and cell dispersion in the developing mouse retina. *Eur J Neurosci* **11**, 2965-78 (1999).
11. Galli-Resta, L. Patterning the vertebrate retina: the early assembly of retinal mosaics. *Seminars Cell Develop Biol* **9**, 279-284 (1998).

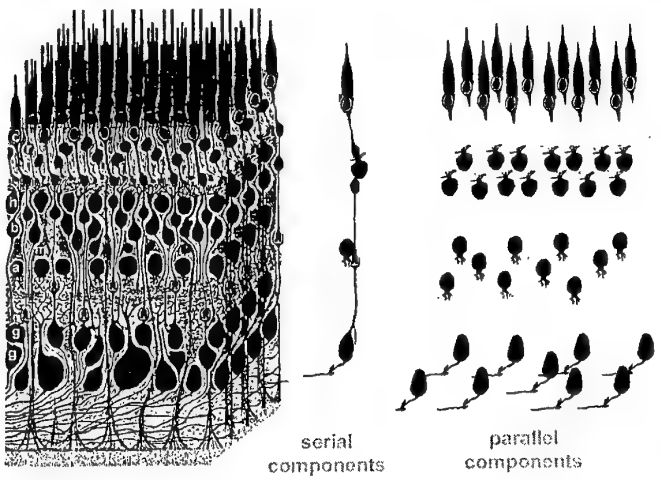

Figure 1: A scheme of the retinal modular circuitry: neurons are staked in layers, subserving serial processing, while the arrays of like neurons within the layers support parallel processing.

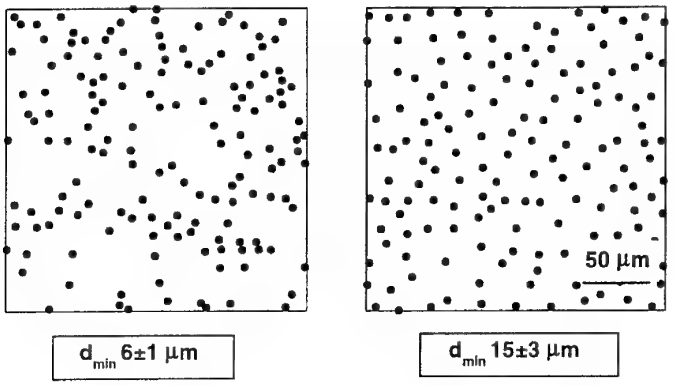

Figure 2: Most retinal neurons base their geometry on an exclusion rule by which no two array cells are ever closer than a fixed minimal distance. This minimal distance, or d_{min}, is typical of the cell type and is independent of the array cell density.

The figures show how at the same cell density, two different minimal distances give rise to two different arrays, one almost indistinguishable from a random distribution of cells (d_{min} =6±1 µm), the second tiles the place in a highly ordered fashion (d_{min} =15±3 µm). These two d_{min} corresponds to the values found for the rods and S cones of the ground squirrel retina.

Neuroengineering: Bioartificial Networks of real neurons

M. Chiappalone[1], M. Grattarola[1], M. Pisciotta[1], M. (B.) Tedesco[1], A. Vato[1]
F. Davide[2]

[1]Department of Biophysical and Electronic Engineering, University of Genoa, Italy
[2]Telecom Italia S.p.A., Rome, Italy

1. Introduction: Neuroengineering

Neuroengineering is a new field rapidly growing at the interface among Neuroscience, Micromachining and Information Technologies. Its main goal is to understand, modify and use brain plasticity in order to advance Neuroscience at the network level and to inspire new computer architectures. The scientific background embraces Bioengineering, Neuroscience, Electronics and Informatics and several different pathways are to be explored to reach the main goal, namely:

1. By interfacing *in vitro* networks of neurons to microelectronic transducer (i.e. bioartificial networks of real neurons)
2. By creating hybrid neuro-electronic systems
3. By developing neuro-prostheses
4. By computer simulating neural plasticity at the network level
5. By developing silicon (neuromorphic) neurons
6. By developing a new family of interfaces based on smart materials and other emergent technologies in order to allow self-organizing 3-dimentional structures

Here we will consider specific experiments referring to path 1 (i.e., bioartificial networks of neurons).

2. Materials: Bioartificial networks of real neurons

2.1 Primary cultures of neurons

Dissociated neurons were obtained from the spinal cord of chick embryos after 7-8 days of incubation. Neurons were seeded on microelectrode arrays covered with adhesion promoting molecules (Polylisyne, laminin). Electrophysiolocal signals were recorded after 15-20 days *in vitro* (DIV) into *NeuroBasal* medium, to allow the formation of synaptic connections among the cells.

2.2 Microelectrode arrays-MEAs

Nowadays, array of planar microelectrodes [1] are becoming a reliable tool in the framework of *in vitro* electrophysiology. Three main features make microelectrode arrays (MEAs) a valuable tool for electrophysiological investigations [2,3]: a) non-invasive measurements and therefore, under appropriate conditions, registration of neurons' activity for a long period of time (i.e., from several minutes up to several hours); b) multi-site recording and electrical stimulation; c) real-time monitoring of morphological and functional changes in the network over time.

There is only one disadvantage in using these devices, that is the difficulty in data interpretation, due to the extracellular recording (Fig. 1). It is possible to find more than one cell above a single microelectrode and the recorded signal can be the sum of the extracellular potentials coming from different neurons close to the same electrode.

Above the array the cells create a 2-dimensional network, far from the original structure they had *in vivo*, but mantaining some kind of link with it. In the stable conditions of culturing, they are free to generate a new neurobiological system, that is we want to investigate.

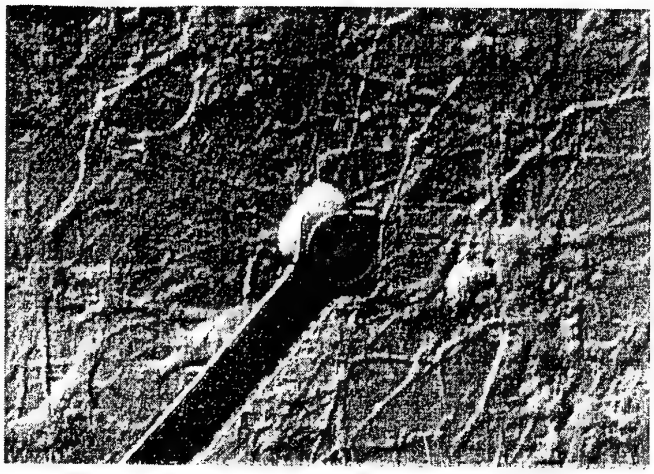

Fig. 1: A single neuron coupled to a single microelectrode of a planar array

Neurons can be grown as a random layer or can be chemio-mechanically guided over the substrate of microelectrode (Fig. 2).

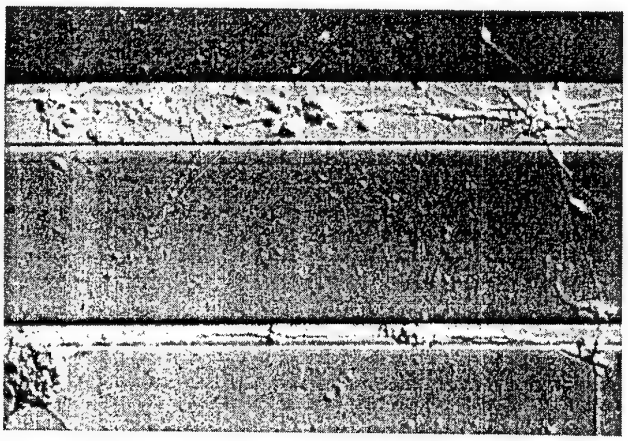

Fig. 2: A micromachined substrate for chemio-mechanical guidance of neuron arborisations.

2.3 Experimental set-up

An experimental set up, based on the microelectrode array and constituted by the following functional elements, was developed (Fig. 3):

- Microelectrode array, which is itself an interface between the biological and the electrical environment;
- Faraday Cage, to avoid electromagnetic interference;
- 8 channels amplifier and filtering stage (gain=100);
- Long term acquisition instrumentation: Digital Tape Recorder (BioLogic DTR-1802) with a maximum of 8 recording channels at the sampling frequency of 12kHz and GPIB Interface. Each channel is connected to the MEA via the amplification and filtering system. For an easier identification, we named them according to the labels on the DTR display: L1, L2, L3, L4, R1, R2, R3, R4.
- System for eventually network electrical stimulation (Scanner, Stimulation Interface, and Isolator);
- Oscilloscope for real time monitoring of signals;

- PC for off-line data management and equipped with National Instruments AT-MIO device, used for generating electrical stimuli in case of electrical stimulation experiments.

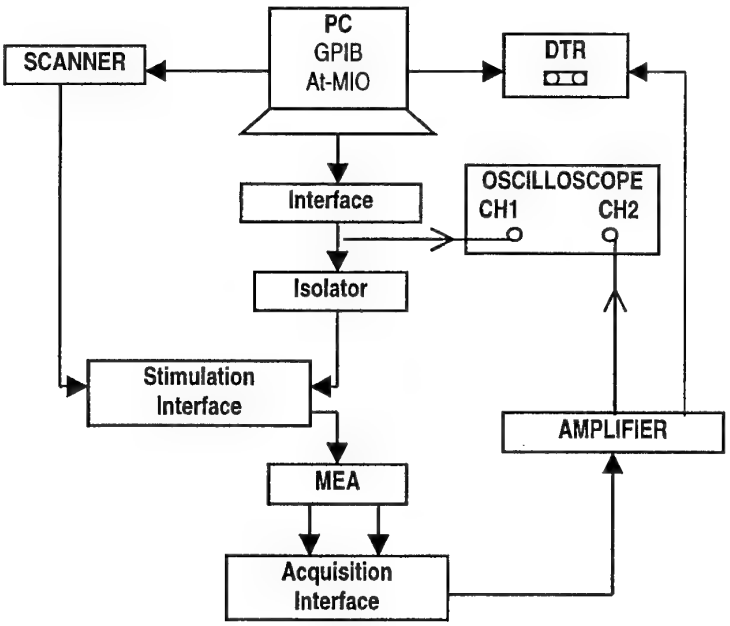

Fig. 3: Experimental set-up scheme

2.4 Chemical stimulation protocols

In order to investigate the role of AMPA receptor in the developing Central Nervous System, with specific reference to networks of spinal cord neurons, two experimental protocols were applied, using two different drugs:

1. CTZ , which acts blocking AMPA receptor desensitization, added at final concentration of 30μM.
2. NBQX, an antagonist of the AMPA receptor, added at a final concentration of 20 μM.

2.5 Signal Processing

Signals collected from a microelectrode array have typical amplitudes in the range 0.1-0.4 mV and are embedded in biological and thermal noise ranging from 5μV up to 10μV peak to peak. DTR was used with a sampling frequency of 12kHz with a resolution of 2 bytes per sample. That resulted in a large amount of data: about 240 MB for one experimental phase of 20 min acquisition, which are difficult to be processed with general-purpose commercially available processing tools. For this reason, custom software tools for data management and signal processing were developed (NSM-Neural Signal Manager).

Data formats were defined for both raw data and post-processed data and standard routines for graphical representation were implemented. The post-processed data are ascii file compatible with Microsoft® Excel or Microcal(TM) Origin® format.

Statistical analysis together with peak detection pre-processing techniques were developed.

Peak Detection The algorithm uses a floating window and a peak-to-peak threshold (absolute threshold). A mask is shifted along the raw signal and when a spike is detected the feature related to the signal is saved (see Fig. 4).

The Spike parameters are:

1) Window time length, set at 5 msec
2) Threshold value, set at 0.12 mV p-p

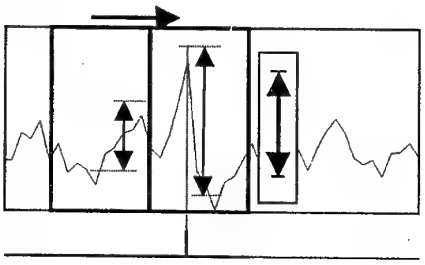

Fig. 4: Peak Detection Algorithm by means of a floating window and absolute threshold

The Peak detection produces an output file containing the following parameters:

- Time occurrence of single spike (ms)
- Amplitude peak-to-peak of spikes (mV)

Burst Detection The spontaneous activity obtained from cultured spinal networks ranges from apparent stochastic spiking to organized bursting, a condition which denotes synchronous activity of the cells. The description of network activity at burst level, analyzing the burst pattern in different pharmacological conditions, provides a vast amount of information about network behavior without having to deal with the complexities of spike analysis [4].

To investigate burst patterns, we developed an algorithm for their automatic detection, utilizing pre-processed data by the peak-detection algorithm. Data coming from the peak-detection are greatly reduced with respect to their complexity and to their original memory occupancy. A window is shifted along the processed signal and when a spike cluster is detected a graph is shown to the user. This graph represents the time of occurrence of spike clusters and their amplitudes in arbitrary units, which represent the sum of spikes amplitudes that belong to the same cluster. Before having a real burst detection, it is necessary to define a threshold level, which eliminates the spike clusters that cannot be considered as bursts.

The Burst parameters that we imposed are:

1) Window time length, set at 650 msec
2) Threshold level, set at 3500 units.

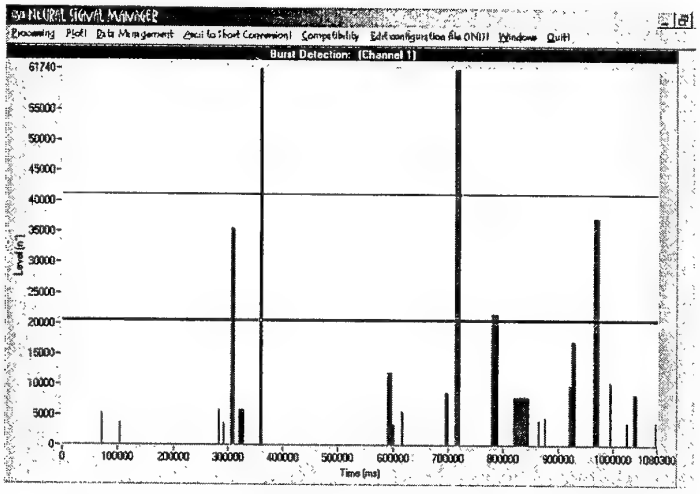

Fig. 5: The graph produced by InterBurst Interval software which represents the spikes cluster that could be considered as burst after the definition of a cutting threshold

The extracted features for each burst detected, saved on an Excel compatible file, are the following:

- Time of occurrence (min)
- Burst Duration (msec)
- InterBurst Interval – IBI (ms), defined as the time length between the end of a burst and the beginning of the next one.
- Burst amplitude (arbitrary units)

Once that bursts have been detected, it is also possible to calculate, following the algorithms implemented for single spike analysis, the Joint Inter Burst Interval (J-IBI) and the Cross – conditioned Inter Burst Interval (C-IBI), which hold the same definition as for the J-ISI and C-ISI, provided that now the event is the burst occurrence instead of the spike occurrence.

3. Results

3.1 Recorded signals

Fig. 6 shows an example of spontaneous activity recorded from one channel (i.e., one microelectrode) for about 15 minutes. Simply by eye inspection one can identify "evident" bursts (circle) and signals which look like single isolated events (left arrow).

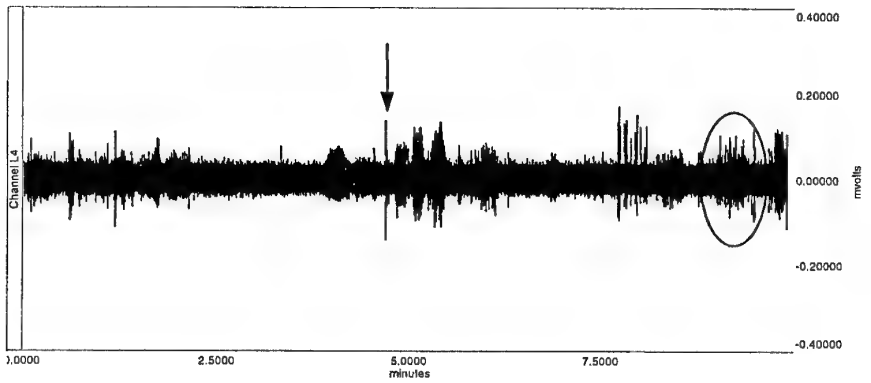

Fig.6: Spontaneous activity recorded from one microelectrode of the array: the circle holds an evident burst, the arrow indicates a single isolated event.

In presence of CTZ we find significantly different signals, in which burst frequency seems to be higher than in case of spontaneous activity, as shown in Fig. 7.

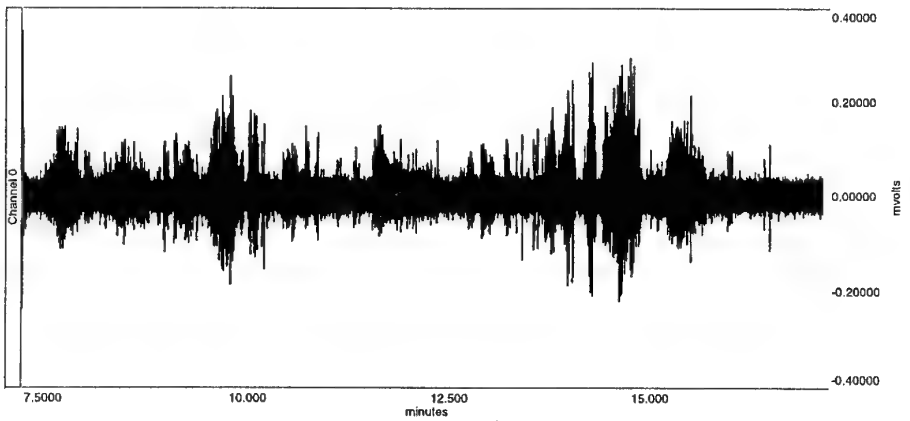

Fig.7: Electrophysiological activity recorded from one microelectrode of the array during EXP1, after CTZ treatment. Note how, only by visual inspection, there is an increasing of burst number respect the previous phase.

This is an expected behavior, because the blockade of AMPA receptor desensitization by cyclothiazide potentiates the responses of spinal cord neurones and therefore makes the synchronized activity much more evident.
Fig 8a) and 8b) show a 13 minutes registration in the presence of NBQX, the other drug used in our experiments.

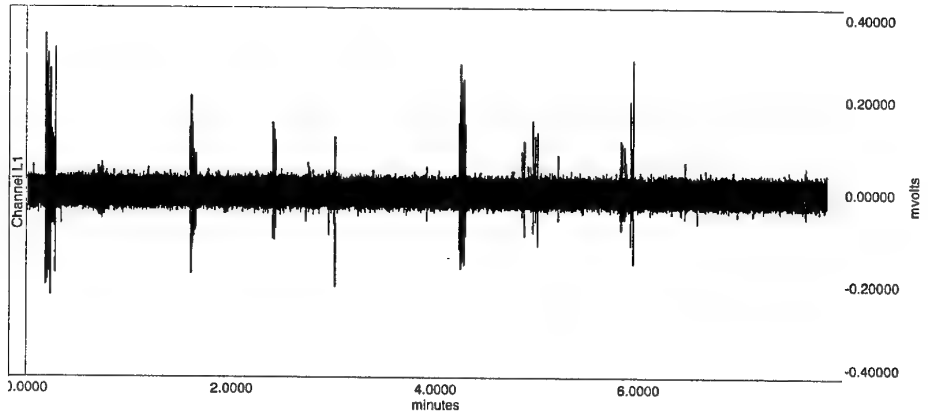

Fig. 8a): NBQX treatment, recording minutes 0-8

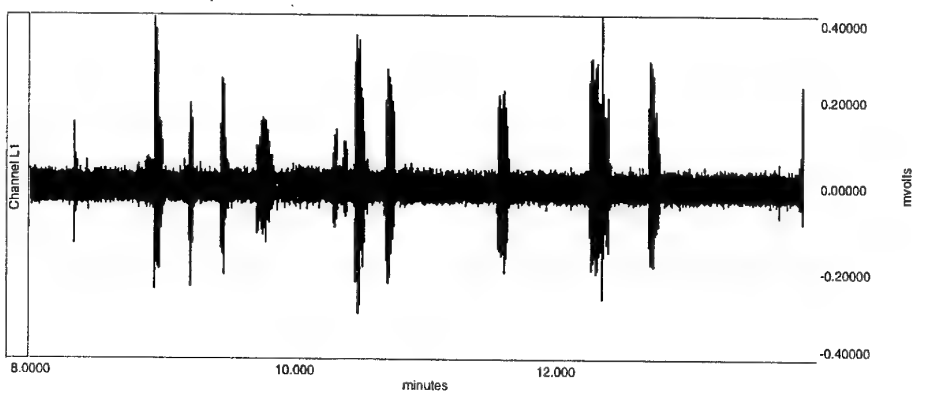

Fig. 8b): NBQX treatment, recording minutes 8-13

The signals in the presence of the neurotransmitter antagonist resulted to be significantly different from the control, but only in the first part of the acquisition (Fig. 8a). At the end of the drug treatment, the burst pattern seemed to be quite similar to the one in case of spontaneous activity (Fig. 8b), maybe trying respond at the drug presence recovering the initial condition [5].

3.2 Signal analysis results

In Fig.9 a bar graph shows the IBI mean value and the standard error, calculated using NSM tools for Burst Detection, for each channel during the two experimental phases of one experiments. For each channel the presence of CTZ causes a decreasing of the mean IBI, which means an improving of the electrophysiological bursting activity. At the same time, we can note a different behavior in the 8 channels, which denotes the importance of the multisite recording that only microlectrode arrays allow. For instance, in R1 and R3 the CTZ treatment has, in average, more effect than in the other channels.

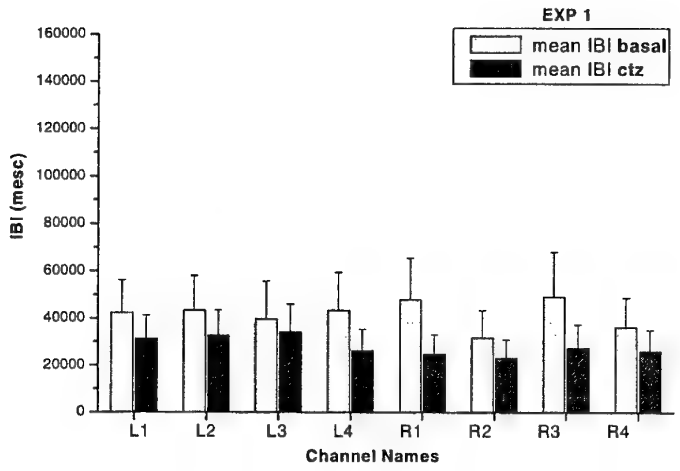

Fig. 9: Mean and standard error of IBI for each channel. Note how mean value of IBI decreases for each channel during CTZ treatment.

In Fig.10 a bar graph shows results for another experiment, in term of IBI mean value and standard error for all the channel set in control condition and CTZ treatment. Also in this case the treatment with CTZ causes an improving of bursting rate.

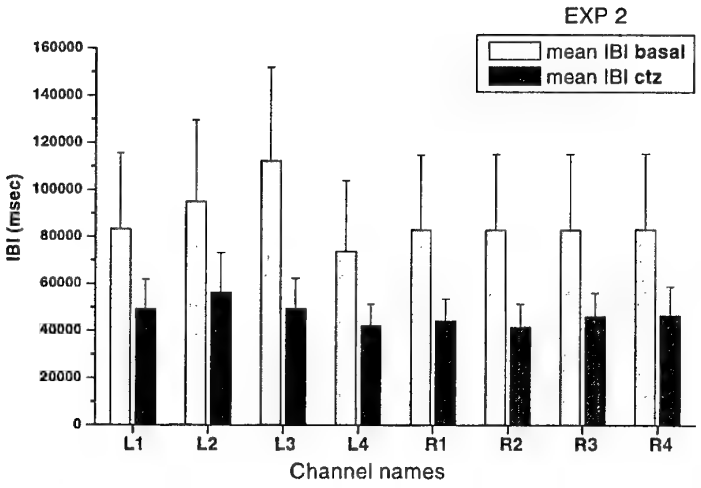

Fig. 10: Mean and standard error of IBI for each channel for another experiment. Also in this case mean value of IBI decreases for each channel during CTZ treatment.

The other applied protocol involved the use of another drug, NBQX [6]: in presence of the neurotransmitter antagonist the signal resulted to be different from the control in the first 8 minutes of acquisition, but in the second 5 minutes the burst pattern seemed to be quite similar to the one in case of spontaneous activity, as shown in Fig. 11. Also in this graph we represent the mean IBI in different experimental conditions: control, NBQX (0-8), first part, NBQX (8-13), second part.

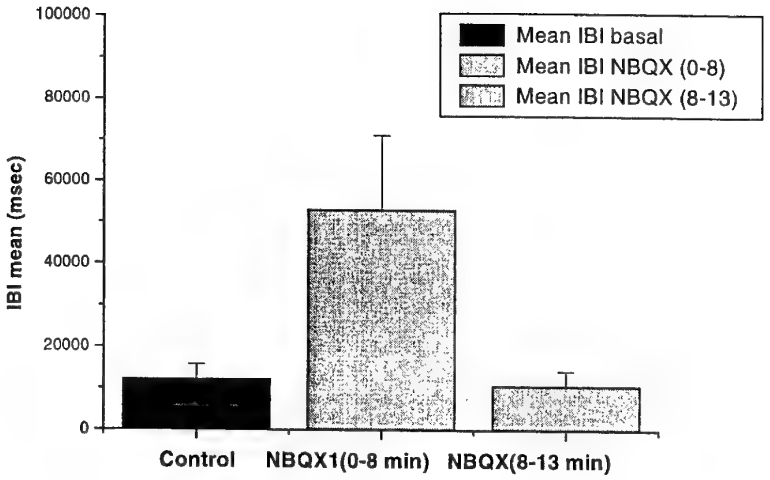

Fig. 11: Mean and standard error of IBI are represented for the three situation: Control, NBQX (0-8), NBQX(8-13). Note as the values for Control and NBQX (8-13) are similar, while they're very different in case of NBQX (0-8).

3. Prospects

4.1 Short term prespects

- Other experiments with the same protocol used for electrical and chemical stimulationDesign of new set-up components, to allow also 16 recording channel
- Developing new features for NSM sw tool, studying other algorithms for Burst Detection improving its performances
- Multichannel statistics for different experimental phases (C-ISI, C-IBI istograms)

4.2 Long term prospects

- Use of chemical and electrical stimuli to induce specific patterns of electrophysiological activity
- Close a feed-back loop with a roving robot
- ...
- ...
- ...
- To crack the brain information code
- Computers which learn by their own experience
- Implantable communication systems

5. References

[1] G. W. Gross: "Simultaneous single unit recording in vitro with a photoetched laser deinsulated glod multielectrode surface", IEEE Trans. Biomed. Eng., BME-26, 1979, pp. 273 – 279

[2] Y. Jimbo, A. Kawana, "Electrical stimulation and recording from cultured neurons using a planar array", Bioelectrochem. Bioeng.,vol. 40, pp. 193-204, 1992

[3] M. Bove, M. Grattarola, G. Verreschi :"In vitro 2D networks of neurons characterized by processing the signals recorded with a planar microtransducer array " IEEE Trans. Biomed. Eng, BME - 44, 1997, pp. 964 – 977

[4] G. W. Gross:"Internal dynamics of randomized mammalian networks in culture", Enabling Technologies for Cultured Neural Networks", Chapter 13, Academic Press, 1994.

[5] N. Chub , M. J. O'Donovan :"Blockade and recovery of spontaneous rhythmic activity after application of neurotransmitter antagonists to spinal networks of the chich embryo" The Journal of Neuroscience, 1, 1998, pp. 294 – 306.

[6] M. Chiappalone, F. Davide, M. Grattarola, S. Pasa, G. Maura, M. Marcoli, M.(B.) Tedesco: "Networks of spinal cord neurons cultured on microelectrode arrays: response to stimuli and homeostasis" Proceedings of the 2nd International Symposium on "Image and Signal Processing and Analysis", Pula, Croatia, June 19-21, 2001, pp. 645-649

7. Acknowledgments

Work supported by the National research Council of Italy (CNR) , Target project "Biotechnology" and by Telecom Italia S.p.A., protocol 0009989-01

Microfabrication and Micropatterning of Biocompatible Polyimid-Foils with Embedded Metal Thin Films and PDMS Co-Material for Neural Interface Devices

J.-Uwe MEYER, Martin SCHÜTTLER, Thomas STIEGLITZ
Fraunhofer-Institute for Biomedical Engineering, Ensheimer Str. 48, 66386 St. Ingbert, Germany
uwe.meyer@ibmt.fhg.de

ABSTRACT

This paper describes microfabrication and micropatterning of 10- 20 µm thin polyimide (PI) foils that serve as a flexible substrates with embedded microelectrode arrays, conductive tracks and interconnection structures. Microtechnologies were developed for generating double metallization layers and double-sided microelectrode arrangements onto the PI foil. An 'Microflex Interconnection (MFI)' was invented to interconnect bare chips with the PI foils. Three dimensional PI structures were accomplished when curing the PI on molded structures. In other designs, Polydimethylsiloxane (PDMS) was used as a co-material for cuff-like structures and biocompatible packaging. The described technologies were utilized for the development of implantable devices for interfacing neural structures. Among others, implantable microdevices have been built for stimulating the retina and peripheral nerves.

INTRODUCTION

Advanced microtechnologies offer new opportunities for the development of functional micropatterned material and active devices for implantation in the human body. Active biomedical implants employ electronic and technical systems to restore physiological functions that were destroyed or impaired either by disease or accidents. Smallest footprint, high functionality, highest reliability and biocompatibility are one of the most important requirements for active medical implants. The smaller the device the less invasive is the procedure of implantation. Examples of such active implantable devices include neural and muscular stimulators, implantable drug delivery systems, intracorporal monitoring devices and body fluid control systems. The active microimplants demand a high degree of device miniaturization without compromising on design flexibility and biocompatibility requirements.

In need for developing mechanically flexible devices that interface neural tissue under in-vivo conditions, we have developed a new class of implantable devices that are based on biocompatible, flexible, micropatterned polymer foils with embedded thin film microelectrodes and metallic structures for integrating bare microchips directly on the substrate. The applied materials and material compositions have been extensively tested for biocompatibility and biodegradation since the method was invented for biomedical applications. A novel high-density interconnection technology has been applied for microassembly of discrete microcomponents, termed 'Microflex Interconnection (MFI)'. The MFI technique is based on a rivet like approach that yields an electric and mechanic contact between the pads on the flexible polyimide substrate and the bare chips or electronic components. A implantable retina stimulator was built utilizing the devised technologies. Polydimethylsiloxane (PDMS) has been used as a co-material for cuff-shaped neural devices that interface peripheral nerves.

In the following, the technologies are introduced for micromanufacturing the flexible polyimide based microstructures and for assembling microelectronical chips onto it (Fig. 1). Examples for implantable neural interface devices are given, comprising microdevices for interfacing peripheral nerves and nerve cells from the retina.

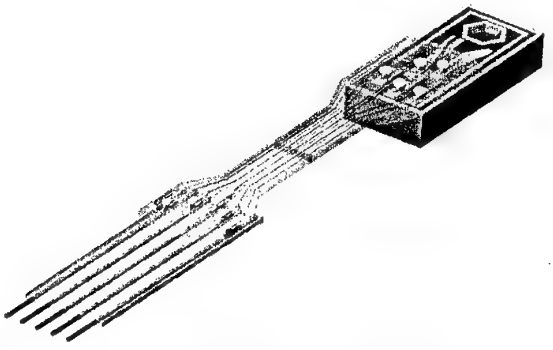

Fig. 1: Schematic of a hybrid assembled device consisting of ultrathin polyimide based flexible foil interconnecting a silicon chip and a cable.

APPLIED MICROTECHNOLOGIES AND MATERIALS

Micropatterning flexible polyimide foils

A special micromachining process has been developed for embedding platinum microstructures into 15 µm thin polyimide (PI) films. The flexible PI foils serve as carrier and insulation layers that hold the platinum/ gold/ iridium based microelectrodes, conductive lines, and interconnection pads. The process of the microfabrication of flexible microelectrode structure with integrated chip carriers has been previously described [1]. Fig 2 is sketching the micromachining process for fabricating the PI films with via holes, double layered conducting tracks, and contact pads [2].

Micromachining of PI allows the fabrication of neural interface devices adhering smoothly to the various shapes of the neural tissue. Concentric ring electrodes were fabricated employing a double metal layer insulated by a 5 µm PI layer. The microelectrode design for the retina is seen at various magnifications in the micrographs of Fig. 3.

Hybrid Chip Integration

A special microflex interconnection (MFI) technology has been developed to integrate bare silicon chips mechanically and electrically on the substrate without consuming any additional space for wiring [3]. The MFI technology enables high-density interconnects with a center to center pitch of contacting pads less than 100 µm. The MFI process is sketched in Fig. 7. The basic process of this new technology is utilizing a common thermosonic ball wedge bonder. The process is altered to form just the gold ball, which serves as a rivet that mechanically and electrically interconnects the thin PI foil with the bare chip (Fig. 4).

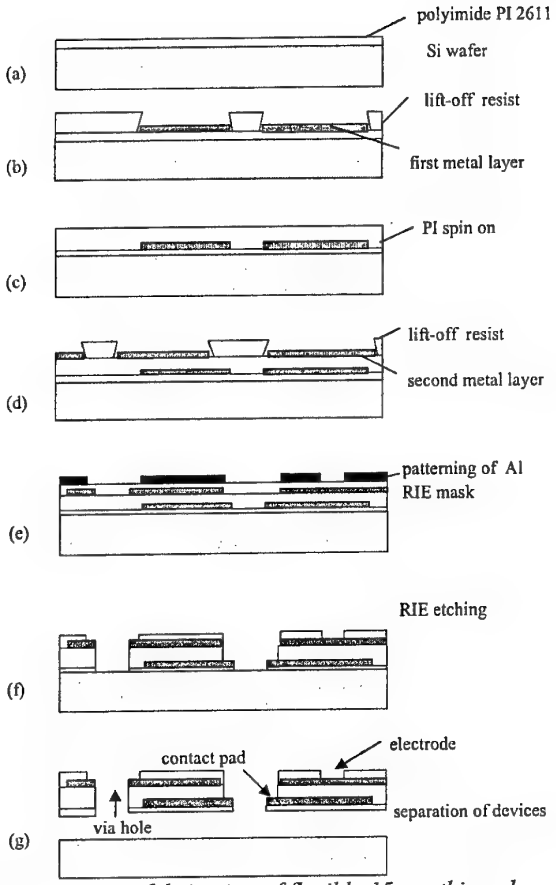

Fig 2: Microfabrication of flexible 15 µm thin polyimide film that serves as an insulator and carrier for microelectrode arrays, double metal conductor layers, and interconnecting pads.

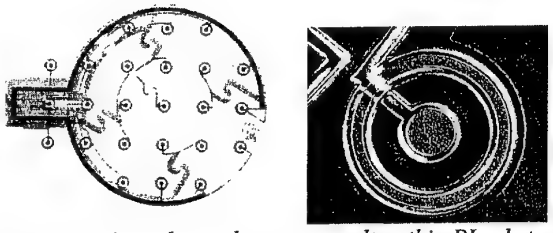

Fig. 3: Microelectrode array on ultra-thin PI substrate at 2 magnifications. The outer electrode ring (left) has a diameter of 4 mm.

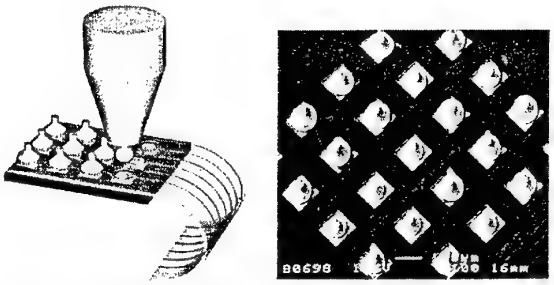

Fig. 4: Microflex Interconnection (MFI) technology. Left: Graphic that illustrates the forming of gold ball studs as rivets for connecting the bottom chip with the thin PI foil. Right: MFI based integration of stimulator chip on PI foil.

Surface mount devices (SMD capacitor, SMD diodes) and a receiver coil for signal and data transmission were soldered to corresponding contact pads on the PI foil. Complete neural devices including implantable multiplexers have been built on flexible foils using the MFI technology and hybrid assemblies (Fig. 5).

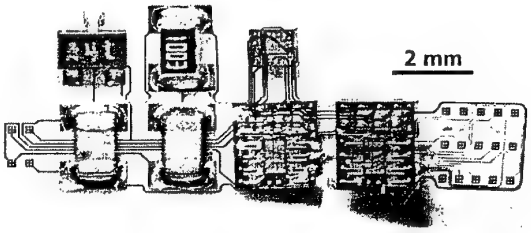

Fig. 5: A MFI based hybrid assembled multiplexer with interface structures for connecting to a 4-strand cable (left end) and to a microelectrode array (right end).

NEURAL INTERFACE DEVICES

Peripheral Nerve Devices

A new class of flexible, micromachined neural microelectrode devices has been developed for interfacing peripheral nerves in the living body. The thin film microelectrodes are embedded in micropatterned ultrathin, biocompatible polyimide substrates of various shapes. A major advantage of this flexible structures is the integration of microelectrodes, cables, and interconnects in one microfabrication process. No further wire bonding is needed. One of our first structures have been sieve electrodes for recording of compound action potentials in peripheral nerves. A sketch on regenerating nerves growing through the sieve structures is pictured in Fig. 6.

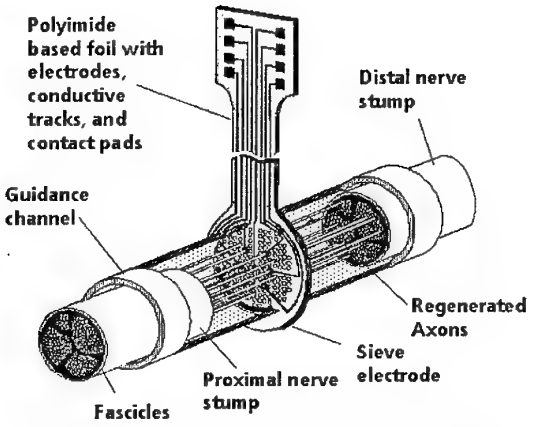

Fig. 6: Sketch of peripheral nerve axons growing through a thin polyimide structures with integrated interconnects

Fig. 7 shows a micrograph of the sieve electrode. Eight ring electrodes in the center and an outer counter electrode are deposited on the structure. The diameter of the structure with vias is about 2 mm. The sieve electrode is placed in a silicon tubing guidance channel which is seen around the electrode. A detailed description on the microfabrication of this kind of electrodes is given elsewhere [4]. The polyimide (PI) structures are about 10 – 15 µm thin depending whether one or two PI insulation layers are used.

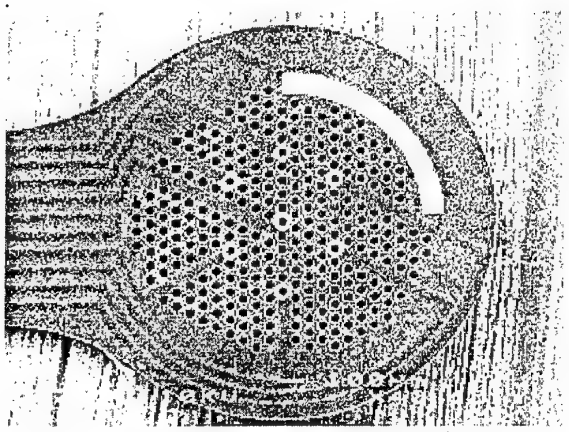

Fig. 7: SEM photo of a sieve microelectrode. Axons are growing through the 20-40 µm holes. The device houses seven electrodes with a centered via and one reference electrode

When dealing with anatomically intact peripheral nerves that lack electrical activation, e.g. as a consequence of spinal cord injury, neural devices are required that interface peripheral nerve bundles non-invasively. Cuff-electrodes are established interfaces to peripheral nerves. Most cuff electrodes are manufactured using silicone materials in combination with platinum foils, welded to stainless steel wires [5]. These devices are hand-crafted and strongly limited the number of channels embedded in the silicone. Their major drawback are the costs, that rise proportional to the number of stimulation sites due to the additional fabrication effort. We have developed a new class of cuff electrodes made of flexible, micromachined thin-film electrodes embedded into polyimide (PI) substrates of various shapes [6].

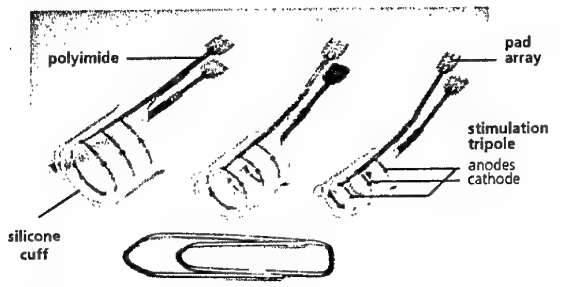

Fig. 8: Various designs of cuff microelectrodes for interfacing peripheral nerves. A method has been developed for integrating the thin film microelectrodes on polyimide with PDMS based cuffs.

Retina Stimulator

Patients that are blind due to photoreceptor degeneration caused by retinitis pigmentosa or macula degeneration are able to perceive light sensations after localized electrical stimulation in the retina. A retina implant sysxtems has been built comprising The whole system for a retina implant comprises several functional units (Fig. 9).

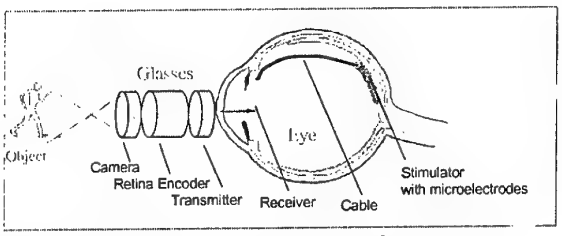

Fig. 9: Schematic of the retina stimulator system. (Graphic adapted from Buss, Univ. Duisburg)

The external part includes a high speed CMOS camera to generate the images. It sends the data to a portable box that includes the energy supply by (rechargeable) batteries and a signal processing unit called retina encoder. The retina encoder is used to simulate the spatio-temporal properties of the different layers of the retina. The encoder will process the signals from the camera and generates stimulus patterns for the ganglion cells. Those data are led to a telemetric unit for signal and data transmission to the implantable part of the system. A telemetry receiver in the eye will decode the data. A stimulator chip is responsible to select individual electrodes in a spatio-temporal pattern for current stimulation of the ganglion cells. A complete assemled system is shown in Figure 10.

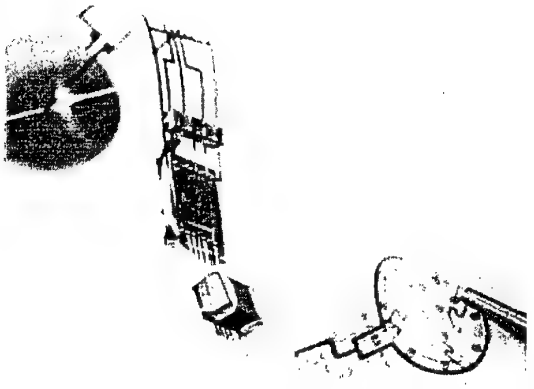

Fig. 10: A completely assembled epiretinal demonstrator illustrating the flexibility of the translucent carrier foil and the hybrid integration of chips and SMDs.

The assembled retina stimulator device will be implanted in the eye of cats and pigs. Previously, chronic implantation experiments have been performed in rabbits using devices without integrated electronic components [7]. Clinical and electrophysiological examinations through 6 month of follow up did not reveal any adverse effects. The implanted devices stayed stable without damaging the retina. In acute experiments it could be shown that 10 µA pulses with a period of 100 µs evoked electric cortical potentials in the visual cortex. Charge delivery at threshold varied between 0.1 and 0.3 nC/phase and charge densities ranged from 1 to 12 µC/cm^2 [8]. Chronic implantation experiments are underway for the long term stimulation of the retina via wireless signal and energy transmission into the eye.

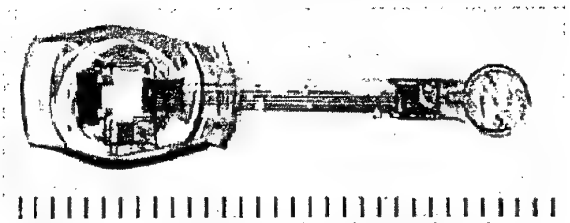

Fig. 11: A complete epiretinal implant packaged in silicone. The receiving electronics is housed in an intraocular lens made of silicone. The distance between two bars of the scale correspond to 1 mm.

DISCUSSION AND CONCLUSION

Microtechniques habe been developed to microfacture and to micropattern flexible, biocompatible polymer films with embedded metal thin films. A new class of neural interface devices has been developed utilizing these techniques. Implantable active neural devices have been designed to interface living tissue in the body. First tests in animals show promising results. While the shown electronic devices for neural interfaces are still awaiting clinical testing our research group has embarked on the development of biohybrid implants which integrate technical components with living material in one device. Work has started to cultivate embryonic spinal neural cells and co-cells on our flexible substrates with microelectrodes. Technologies and implantation procedures of the biohybrid assembly are designed to generate biological interconnects to the end organ, e.g. a muscle. Biohybrid interfaces hold the promise to combine genetic engineering with microelectronics for the development of novel biohybrid implants which will restore or substitute lost biological functions in humans.

ACKNOWLEDGMENT

This work has been supported by the European Commission and the German Ministry for Research (BMBF). The authors wish to thank all the scientific and technical stuff at IBMT for ther support in the demonstrated work. The authors also express their gratitude to all the national and European project partners who contributed to the successful outcome of the shown research.

REFERENCES

[1] Stieglitz, T., Beutel, H., Keller, R., and Meyer, J. U. Integrative design and hybrid assembly of a flexible retina implant system. 1, 474. 1999. Proceedings of the First Joint BMES/EMBS Conference. 1999 (Cat. No.99CH37015).

[2] Stieglitz, T., Beutel, H., Keller, R., Blau, C., and Meyer, J. U. Development of flexible stimulation devices for a retina implant system. 5, 2307-2310. 1997. Proceedings of the 19th Annual International Conference of the IEEE Engineering in Medicine and Biology Society (Cat. No.97CH36136).

[3] Stieglitz, T., Beutel, H., and Meyer, J. U. "Microflex"- A new assembling technique for interconnects. J.Intelligent Matrial Systems and Structures 11, 417-425. 2000.

[4] Stieglitz, T., Beutel, H., and Meyer, J. U. A flexible, light-weight multichannel sieve electrode with integrated cables for interfacing regenerating peripheral nerves. Sensors and Actuators A60, 240-243. 1997

[5] Veraart C, Grill WM, Mortimer TM, "Selective Control of Muscle Activation with a Multipolar Nerve Cuff Electrode", IEEE Transactions on Biomedical Engineering, Vol.40, 7:1993, pp.640-653.

[6] Schuettler, M, Stieglitz, T.: "18 polar Hybrid Cuff Electrodes for Stimulation of Peripheral Nerves", Proc. of the 5th Ann. Int. Conf. of the International Functional Electrical Stimulation Society, June 18-20, 2000, Aalborg/Denmark, pp. 265-268.

[7] Walter, P., Szurman, P., Vobig, M., Berk, H., Ludtke-Handjery, H. C., Richter, H., Mittermayer, C., Heimann, K., and Sellhaus, B. Successful long-term implantation of electrically inactive epiretinal microelectrode arrays in rabbits. Retina 19[6], 546-552. 1999.

[8] Walter, P. and Heimann, K. Evoked cortical potentials after electrical stimulation of the inner retina in rabbits. Arch.Clin.Exp.Ophthalmol. 238[4], 315-318. 2000.

Cells, Gels and the Engines of Life: A Fresh Paradigm for Biological Motion

Gerald H. Pollack, Dept. of Bioengineering, Univ. of Washington, Seattle WA 98195

The cell is a machine designed to carry out a multitude of tasks—all of which involve motion of some kind. Such tasks are currently described by a variety of mechanisms, seemingly devoid of any unifying theme.

Is there a unifying theme? If the cell is a gel, as commonly agreed, then a logical approach to the question of a common underlying theme is to ask whether a common underlying theme governs gel function. Gels do "function." They typically undergo transition from one state to another. Much like the transition from ice to water, this process is known as a phase-transition—a small change of environment resulting in a huge change in conformation.

Such changes can perform work. Just as the formation of ice has the power to fracture hardened concrete, gel expansion or contraction is capable of many types of work, ranging from solute/solvent separation, all the way to force generation (Fig. 1). Common examples of useful phase-transitions are the time-release capsule, in which a gel-sol transition releases bioactive drugs, the disposable diaper, where a condensed gel undergoes enormous hydration and expansion, and certain artificial actuators and muscles. Such behaviors are attractive in that a huge change of structure can be induced by a subtle change of environment (Fig. 2).

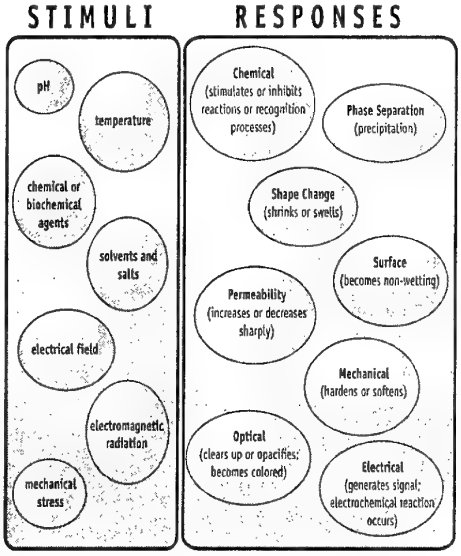

Figure 1. Typical stimuli and responses of polymer hydrogels. After Hoffman [1].

Like synthetic gels, the natural gel of the cell may have the capacity to undergo similarly useful transitions. The question is whether they do. This question is perhaps more aptly stated a bit differently, for the cell is not a homogeneous gel but a collection of gel-like organelles, each of which is assigned a specific task.

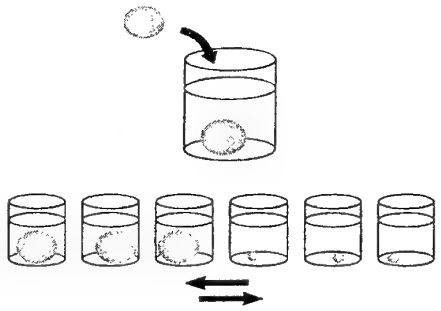

Temperature, solvent composition, pH, ions electric field, UV, light, specific molecues, orchemicals

Figure 2. Phase-transitions are triggered by subtle shifts of environment. After Tanaka et al. [2].

The more relevant question, then, is whether any/all such organelles undergo a phase-transition.

The short answer is yes—it appears that this may be the case. Pursuing so extensive a theme in a meaningful way in this short space is challenging, and for a fuller development I refer the reader to a recent book by this author [3]. In this venue I focus on a single aspect: the relevance of phase-transitions in the production of motion.

GELS AND MOTION

The classes of motion produced by phase-transitions fall largely into two categories, isotropic and linear. In isotropic gels, polymers are randomly arranged, and sometimes cross-linked. Water is held largely by its affinity to polymers (or proteins, in the case of the cell). The gel is thus well hydrated—and may in the extreme contain 99.97% water [4]. In the transitioned state, the polymer-water affinity gives way to a higher polymer-polymer affinity, condensing the gel into a compact mass and expelling solvent. Thus, water moves, and polymer moves.

Linear polymers also undergo transition—from extended to shortened states. The extended state is stable because it maximizes the number of polymer-water contacts and therefore minimizes the system's energy. Water builds layer upon layer [3]. In the shortened state the affinity of polymer for itself exceeds the affinity of polymer for water, and the polymer folds. It may fold entirely, or it may fold along a fraction of its length. As it folds, polymer and water both move. And, if a load is placed at the end of the shortening filament, the load can move as well.

Phase-transitions are inevitably cooperative: once triggered, they go to completion. The reason lies in the transition's razor-edge behavior: once the polymer-polymer affinity (or the polymer-water affinity) begins to prevail, its prevalence increases; hence the transition goes to completion. An example is illustrated in Figure 3. In this example, the divalent ion, calcium, cross-links the polymer strands. Its presence thereby shifts the predominant affinity from polymer-water to polymer-polymer. Once a portion of the strand is bridged, flanking segments of the polymer are brought closer together, increasing the proclivity for additional calcium bridging. Thus, local action enhances the proclivity for action in a neighboring segment, ensuring that the reaction proceeds to completion. In this way, transitions propagate toward completion.

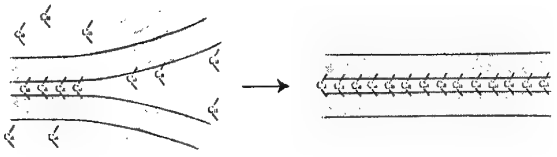

Figure 3. Calcium and other divalent cations can bridge the gap between negatively charged sites, resulting in zipper-like

The polymer-gel phase-transition can thereby produce different classes of motion. If the cell were to exploit this principle, it could have a simple way of producing a broad array of motions, depending on the nature and arrangement of constituent polymers. In all cases, a small shift of some environmental variable such as pH, chemical content, *etc.* could give rise to a cooperative, all-or-none response, which could produce massive mechanical action.

***

As representative examples of such action, we focus briefly on two fundamental cellular processes—secretion and contraction. The first involves an isotropic transition, the second a linear one. [Additional details on these (and other) mechanisms can be found in the above-mentioned book [3]].

Secretion

According to current views, the secretory vesicle is a kind of "soup" surrounded by a membrane—a miniature of the prevailing view of the cell itself. This soup contains no croutons, but a matrix of polymers plus the substance to be secreted. For discharge, the vesicle docks with the cell membrane as cell and vesicle membranes fuse, opening the interior of the vesicle to the extracellular space and allowing the vesicle's contents to escape by diffusion. Although attractive in its apparent simplicity, this mechanism does not easily reconcile with two lines of evidence.

One concern is that discharge is often accompanied by dramatic vesicle expansion. Isolated mucin-producing secretory vesicles, for example, undergo a 600-fold volume expansion within 40 ms [5]. Vesicles of Nematocysts, aquatic stinging cells, are capable of linear expansion rates of 2,000 μm/ms [6]. Such phenomenal expansion rates imply something beyond mere passive diffusion of solutes and water.

A second concern is the response to solvents. Demembranated vesicle matrices can be expanded and re-condensed again and again by exposure to various solutions. But the required solutions are anomalous. When condensed matrices from mast cells or goblet cells (whose matrices hydrate to produce mucus) are exposed to low osmolarity solutions—even distilled water—they remain condensed even though the osmotic draw for water should be enormous [7, 5]. But if small amounts of sodium (<10 mM) are added to these low osmolarity solutions, the matrices expand instantly. Such behavior does not follow classical expectations.

Gels, on the other hand, do not subscribe to the osmotic expectations of aqueous solutions. The vesicle matrix is the quintessential gel: it is built of tangled, highly anionic polymers, cross-linked by multivalent cations. Within this matrix, water is tightly held. The multivalent cation, in virtually all cases, is the bioactive substance to be released.

Given the gel-like nature of the matrix, and the above-mentioned anomalies, it is no surprise that investigators have begun looking for mechanistic clues within the realm of the phase-transition. One reason for pursuing the phase-transition route is that the secretory discharge happens or doesn't happen depending on a critical shift of environment—the very hallmark of the polymer-gel phase-transition. As the solvent ratio (either glycerol/water or acetone/water) is edged just past a threshold, or as the temperature edges past a threshold, goblet-cell and mast-cell matrices condense or expand abruptly—the transition thresholds in both cases lying within a window as narrow as 1% of the critical value [5]. Hence, the phase-transition's signature criterion is satisfied.

How such a system might work is as follows. When the condensed matrix is exposed to the extracellular space, sodium displaces the divalent cross-linker. No longer cross-linked, the polymer can satisfy its intense thirst, imbibing water and expanding explosively, like a jack-in-the-box [5]. Meanwhile, the displaced multivalent cation—the messenger—is discharged. Diffusion may play some role in release; but the principal

role is played by convective forces, for divalents are relatively insoluble in the layered water surrounding the charged polymers [8], and are therefore forcefully ejected. Hence, discharge into the extracellular space occurs by explosive convection.

Muscle contraction

As is now well known, muscle sarcomeres contain three filament types: thick, thin and connecting—the latter interconnecting the ends of the thick filaments with respective Z-lines. All three filaments are polymers: thin filaments consist largely of repeats of monomeric actin; thick filaments are built around multiple repeats of myosin; and connecting filaments are built of connectin (also known as titin), a huge protein containing repeating immunoglobulin-like (Ig) and other domains. Together with water, which is held with extreme tenacity [9], this array of polymers forms a gel-like lattice.

Until the mid-1950s muscle contraction was held to occur by a mechanism not much different from the phase-transition mechanism to be considered: protein folding. All major research groups subscribed to this view. With the discovery of interdigitating filaments in the mid-1950s, it was tempting to dump this notion, and suppose instead that contraction arose out of pure filament sliding. This supposition led Sir Andrew Huxley and Hugh Huxley to examine independently whether filaments remained at constant length during contraction. Back-to-back papers in *Nature*, using the optical microscope [10, 11] appeared to confirm this supposition. The constant filament-length paradigm took hold, and has held remarkably firm ever since—notwithstanding reports of thick filament or A-band shortening in more than 30 subsequent papers [12, 13]—a remarkable disparity of theory and evidence. The motivated reader is urged to check the cited papers and judge for him/herself.

With the emerging notion of sliding filaments, the central issue became the nature of the driving force, and the swinging cross-bridge model came to the forefront [14]. This mechanism explains many known features of contraction, and has therefore become broadly accepted [15, 16, 17, 18, 19]. It is now textbook material.

On the other hand, contradictory evidence is plentiful. In addition to the issue concerning the constancy of filament length (above), which conflicts with the pure sliding model, a serious problem is the absence of compelling evidence for cross-bridge swinging [20]. Electron-spin resonance, X-ray diffraction, and fluorescence polarization have produced largely negative results, as has high-resolution electron microscopy [21]. The most positive of these results has been an angle change of 3° measured on a myosin light chain [22]—far short of the anticipated 45°. Other concerns run the gamut from instability [23], to mechanics [12], structure [24, 25], and chemistry [26, 27]. A glance at these reviews conveys a picture rather different from the one in textbooks.

An alternative approach considers the possibility that the contractile mechanism does not lie in cross-bridge rotation, but in a paradigm in which all three filaments shorten. If

parallel filaments shorten synchronously, the event is global, and may qualify as a phase-transition We consider the three filaments one at a time.

Most obvious is the connecting filament. Shortening of the connecting filament returns the extended, unactivated, sarcomere to its unstrained length. Applied stress lengthens the filament. Shortening may involve a sequential folding of domains along the molecule, whereas stretch includes domain unfoldings—the measured length change is stepwise [28, 29]. Similarly in the intact sarcomere, passive length changes also occur in steps [30], implying that each discrete event is synchronized in parallel over many filaments.

Next, consider the thick filament. Thick filament shortening could transmit force through the thin filaments, thereby contributing to active sarcomere shortening. Evidence for thick filament shortening was cited above. Although rarely discussed in contemporary muscle literature, these observations are extensive: they have been carried out in more than 15 laboratories worldwide, and have employed electron and light microscopic techniques on specimens ranging from crustaceans and insects, to mammalian heart and skeletal muscle—even human muscle. Evidence to the contrary is relatively rare [31]. These extensive observations cannot be summarily dismissed merely because they are not often discussed.

Thick filament shortening could not be the sole mechanism underlying contraction, for if it were, the *in vitro* motility assay, which contains no filaments, could not work. On the other hand, the phenomenon is difficult to dismiss as irrelevant, as it is so commonly seen. Thick filament shortening could contribute directly to sarcomere shortening. It could be mediated by and alpha-helix to random-coil transition along the myosin rod [13]. The helix-coil transition is a classical phase-transition well known to biochemists—and also to those who have put a wool sweater into a hot clothes dryer and watched it shrink.

The thin filament may also shorten. There is extensive evidence that some structural change takes place along the thin filament [32, 33, 25]; also, see below. Crystallographic evidence shows that monomers of actin can pack interchangeably in either of two configurations along the filament—a "long" configuration, and a shorter one [24]. The difference leads to a filament length change of 10 - 15%. The change in actin is worth dwelling on, for although it may be more subtle than the ones above, it is possibly more universal, as actin filaments are contained in all eukaryotic cells.

Isolated actin filaments show prominent undulations. Known as "reptation" because of its snake-like character, the constituent undulations are broadly observed: in filaments suspended in solution [34], embedded in a gel [35], and gliding on a myosin-coated surface [36]. Such undulations had been presumed to be of thermal origin, but that notion is challenged by the observation that they can be substantially intensified by exposure to myosin [34] or ATP [37]; these effects imply a specific structural change rather than thermally induced change.

In fact, structural change in actin is implied by a long history of evidence. Molecular transitions had first been noted in the 1960s and 1970s [38, 39, 40]. On exposure to myosin, actin monomers underwent a 10° rotation [41]. Conformational changes have since been confirmed in probe studies, X-ray diffraction studies, phosphorescence-anisotropy studies and fluorescence-energy transfer studies, the latter showing a myosin-triggered actin-subdomain-spacing change of 17% [42].

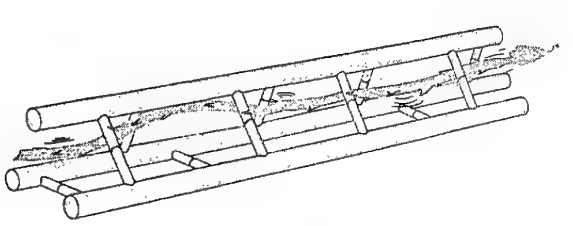

Figure 4. Reptation model. Actin filament snakes its way toward the center of the sarcomere, past myosin cross-bridges, which may well interconnect adjacent thick filaments [13].

That such structural change propagates along the filament is shown in several experimental studies. Gelsolin is a protein that binds to one end (the so-called "barbed" end) of the actin filament; yet the impact of binding is felt along the entire filament. Molecular orientations shift by 10°, and there is three-fold decrease of the filament's overall torsional rigidity [43]. Thus, structural change induced by point binding propagates over the entire filament. Such propagated action may account for the propagated waves seen traveling along single actin filaments—observable either by cross-correlation of point displacements [44] or by tracking fluorescence markers distributed along the filament [37, 45]. In the latter, waves of shortening can be seen propagating along the filament, much like a caterpillar.

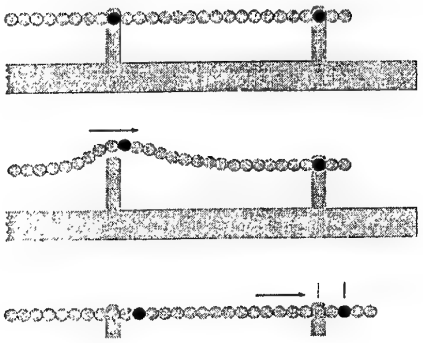

Figure 5. Reptation model predicts that each advance of the thin filament will be an integer multiple of the actin-monomer repeat along the filament.

Could such a propagating structural transition drive the thin filament to slide along the thick? A possible vehicle for such action is the inchworm mechanism (Fig. 4). By propagating along the thin filament, a shortening transition could propel the thin filament to reptate past the thick filament, each propagation cycle advancing the filament incrementally toward the center of the sarcomere.

Perhaps the most critical prediction of such a mechanism is the anticipated quantal advance of the thin filament. With each propagation cycle, the filament advances by a step (Fig. 5). The advance begins as an actin monomer un-binds from a myosin bridge; it ends as the myosin bridge rebinds an actin momomer further along the filament. Hence, the filament-translation step must be an integer multiple of the actin-repeat spacing (see Fig. 5). The translation step could be 1, 2.....or *n* times the actin-repeat spacing along the thin filament.

This extraordinary prediction is confirmed. The thin filament advances in steps (Fig. 6, 7); and, step size is an integer multiple of the actin-monomer spacing. This is true both in the isolated molecular system, where myosin molecules translate along actin [46], and in the intact sarcomere, where thin filaments translate past thick filaments [30, 47]. In the latter experiments, the striated image of a single myofibril is projected onto a photodiode array. The array is scanned repeatedly, producing successive traces of intensity along the myofibril axis. Hence, single sarcomere lengths can be tracked. The sarcomere-length change is consistently stepwise (Fig. 6). Analysis of many steps showed that their size is an integer multiple of the actin-monomer spacing (Fig. 7). Striking agreement of this result with the model's signature-like prediction lends support to the proposed thesis: the reptation mechanism or something very much like it seems to be involved in the contractile process.

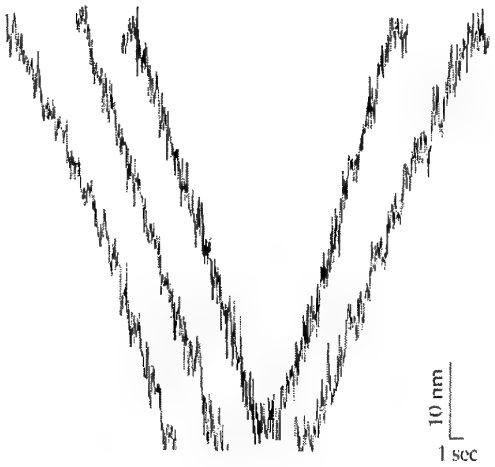

Figure 6. Time course of single sarcomere shortening in single activated myofibrils. From Yakovenko, Blyakhman, and Pollack, submitted.

In sum, contraction of the sarcomere could well arise out of contraction of each of the three filaments—connecting, thick and thin. Connecting and thick filaments appear to shorten by local phase-transitions, each condensation shortening the respective filament by an incremental step. Because these two filaments lie in series, filament shortening leads directly to sarcomere shortening. The thin filament appears to undergo a local, propagating transition, each snake-like cycle advancing the thin filament past the thick by an increment. Repeated cycles produce large-scale translation. (A similar process may occur in the *in vitro* motility assay, where the myosins are firmly planted on a substrate rather than in the lattice of filaments; the filament may "snake" its way along).

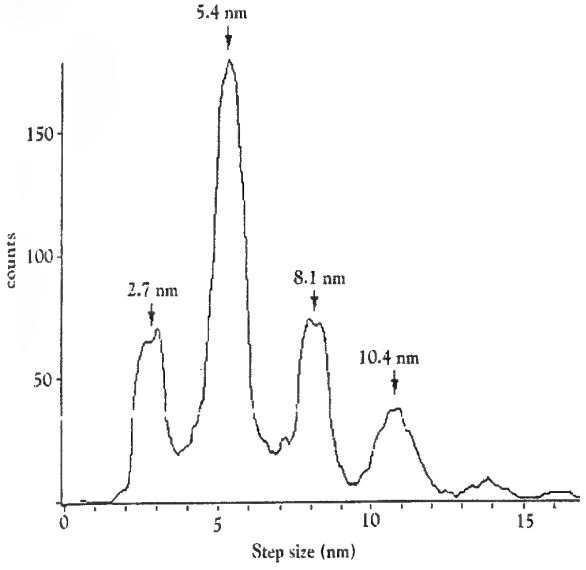

Figure 7. Analysis of steps in records such as those of Figure 6. Histogram peaks are separated by 1/2 of the 5.4 nm spacing between actin monomers. The half may arise because the filament's two strands are axially displaced by half of 5.4 nm. The axial repeat along the filament is thus 1/2 of 5.4 nm, or 2.7 nm—the same as the quantal step.

The incremental steps anticipated from these transitions are observable at various levels of organization, ranging from the single myofibrillar sarcomere [30, 47], to bundles of myofibrils [48], to segments of whole fibers [49]. Hence, the transitions are global—as the phase-transition anticipates. It is perhaps no surprise that phase-transitions arise in all three elements: This endows the system with an array of features that makes muscle the versatile and effective machine that it is.

CONCLUSION

Two examples of biological phase-transitions have been briefly presented, each generating motion of a different kind. Structures such as secretory vesicles undergo isotropic condensations and expansions, whereas filamentary bundles such as actin and myosin produce linear contraction. Linear contraction can also occur in microtubules: when cross-linked into a bundle, microtubules along one edge of the bundle are often observed to shorten [50]; this could mediate bending, as in a bimetal strip. Hence, diverse motions are possible.

Given such mechanistic versatility, it would not be surprising if the phase-transition were a generic mechanism for motion production, extending well beyond the examples considered here. This theme is developed in the above-mentioned book [3]. Phase-transitions are simple and powerful. They can bring about large-scale motions, induced by subtle changes of environment. This results in a kind of switch-like action with huge amplification. Such features seem attractive enough to imply that if nature has chosen the phase-transition as the common denominator of cell motion—and perhaps sundry other processes—it has made a wise choice.

REFERENCES

1. Hoffman, A. S. (1991). Conventionally and environmentally sensitive hydrogels for medical and industrial use: a review paper. Polymer Gels 268(5): 82-87.
2. Tanaka, T. Anaka, M. et al. (1992). Phase transitions in gels: Mechanics of swelling. NATO ASI Series Vol. H64, Springer Verlag, Berlin.
3. Pollack, G. H. (2001). *Cells, Gels and the Engines of Life: A New, Unifying Approach to Cell Function.* Ebner and Sons, Seattle.
4. Osada, Y. and Gong, J. (1993). Stimuli-responsive polymer gels and their application to chemomechanical systems. *Prog. Polym. Sci.* 18: 187-226.
5. Verdugo, P., Deyrup-Olsen, I., martin, A.W., and Luchtel, D.L. (1992). *Polymer gel-phase transition: the molecular mechanism of product release in mucin secretion?* NATO ASI Series Vol. H64 Mechanics of Swelling T.K. Karalis, Springer, Berlin, 1992.
6. Holstein, T. and Tardent, P. (1984). An ultra high-speed analysis of exocytosis: nematocyst discharge. *Science* 223: 830-833.
7. Fernandez, J.M., Villalon, M., and Vedugo, P. (1991). Reversible condensation of mast cell secretory products in vitro. *Biophys. J.* 59: 1022-1027.
8. Vogler, E. (1998). Structure and reactivity of water at biomaterial surfaces. *Adv. Colloid and Interface Sci.* 74: 69-117.
9. Ling, G. N., and Walton, C. L. (1976). What retains water in living cells? *Science* 191: 293-295.
10. Huxley, A.F., and Niedergerke, R. (1954). Structural changes in muscle during contraction: Interference microscopy of living muscle fibres. *Nature* 173: 971-973.
11. Huxley, H.E. and Hanson, J. (1954). Changes in the cross striations of muscle during contraction and stretch and their structural interpretation. *Nature* 173: 973-976.
12. Pollack, G.H. (1983). The sliding filament/cross- bridge theory. *Physiol. Rev.* 63: 1049-1113.
13. Pollack, G.H. (1990). *Muscle & Molecules: Uncovering the Principles of Biological Motion.* Ebner and Sons, Seattle, WA.
14. Huxley, A. F. (1957). Muscle structure and theories of contraction. *Prog. Biophys Biophys. Chem.* 7: 255-318.
15. Spudich, J.A. (1994). How molecular motors work. *Nature* 372: 515-518.
16. Huxley, H.E. (1996). A personal view of muscle and motility mechanisms. *Ann. Rev. Physiol.* 58: 1-19.
17. Block, S.M. (1996). Fifty ways to love your lever: Myosin motors. *Cell* 87: 151-157.
18. Howard, J. (1997). Molecular motors: structural adaptations to cellular functions. *Nature* 389: 561-567.
19. Cooke, R. (1997). Actomyosin interaction in striated muscle. *Physiol. Rev.* 77(3): 671-679.
20. Thomas, D.D. (1987). Spectroscopic probes of muscle cross-bridge rotaion. *Ann. Rev. Physiol.* 49: 641-709.
21. Katayama, E. (1998). Quick-freeze deep-etch electron microscopy of the actin-heavy meromyosin complex during the in vitro motility assay. *J. Mol. Biol.* 278: 349-367.

22. Irving, M., Allen, T. St.-C., Sabido-David, C., Craik, J.S., Brandmeler, B., Kendrick-Jones, J., Corrie, J.E.T., Trentham, D.R., and Goldman, Y.E. (1995). Tilting the light-chain region of myosin during step length changes and active force generation in skeletal muscle. *Nature* 375: 688-691.
23. Iwazumi, (1970). *A New Field Theory of Muscle Contraction.* Ph.D Thesis, University of Pennsylvania.
24. Schutt, C.E. and Lindberg, U. (1993). A new perspective on muscle contraction. *FEBS.* 325: 59-62.
25. Schutt, C.E. and Lindberg, U. (1998). Muscle contraction as a Markhov process I: energetics of the process. *Acta. Physiol. Scan.* 163: 307-324.
26. Oplatka, A. (1996). The rise, decline, and fall of the swinging crossbridge dogma. *Chemtracts Bioch. Mol. Biol.* 6: 18-60.
27. Oplatka, A. (1997). Critical review of the swinging crossbridge theory and of the cardinal active role of water in muscle contraction. *Crit. Rev. Biochem. Mol. Biol.* 32(4): 307-360.
28. Rief, M., Gautel, M., Oesterhelt, F., Fernandez, J. M. and Gaub, H. E. (1997). Reversible unfolding of individual titin immunoglobin domains by AFM. *Science* 276: 1109-1112.
29. Tskhovrebova, L., Trinick, J., Sleep, J. A., and Simmons, R. M. (1997). Elasticity and unfolding of single molecules of the giant muscle protein titin. *Nature* 387: 308-312.
30. Blyakhman, F., Shklyar, T., and Pollack, G. H. (1999). Quantal length changes in single contracting sarcomeres. *J. Mus. Res. Cell Motil.* 20: 529-538.
31. Sosa, H., Popp, D., Ouyang, G. and Huxley, H.E. (1994). Ultrastructure of skeletal muscle fibers studied by a plunge quick freezing method: myofilament lengths. *Biophys. J.*, 67:283-292.
32. Dos Remedios, C. G., and Moens, P. D, (1995). Actin and the actomyosin interface: a review. *Biochim. Biophys. Acta.* 1228(2-3): 99-124.
33. Pollack, G. H. (1996). Phase-transitions and the molecular mechanism of contraction. *Biophys. Chem.* 59: 315-328.
34. Yanagida, T., Nakase, M.. Nishiyama K., and Oosawa, F. (1984). Direct observation of motion of single F-actin filaments in the presence of myosin. *Nature* 307: 58-60.
35. Käs, J., H. Strey, and E. Sackmann (1994). Direct imaging of reptation for semi-flexible actin filaments. *Nature* 368: 226-229.
36. Kellermayer, M. S. Z. and G. H. Pollack (1996). Rescue of in vitro actin motility halted at high ionic strength by reduction of ATP to submicromolar levels. *Biochim. Biophys. Acta.* 1277: 107-114.
37. Hatori, K., Honda, H. and Matsuno, K. (1996). Communicative interaction of myosins along an actin filament in the presence of ATP. *Biophys. Chem.* 60:149-152.
38. Asakura, A., M. Taniguchi, and F. Oosawa. (1963). Mechano-chemical behavior of F-actin. *J. Mol. Biol.* 7: 55- 63.
39. Hatano, S. T. Totsuka, and F. Oosawa (1967). Polymerization of plasmodium actin. *Biochem. Biophys. Acta.* 140: 109-122.
40. Oosawa, F., Fujime, S., Ishiwata S., and Mihashi, K. (1972). Dynamic property of F-actin and thin filament. *CSH Symposia on Quant. Biol.* XXXVII: 277-285.
41. Yanagida and Oosawa, (1978) Polarized fluorescence from epsilon-ADP incorporated into F-actin in a myosin-free single fibre. *J. Mol Biol.* 126: 507-524.
42. Miki, M. and T. Koyama (1994). Domain motion in actin observed by fluorescence resonance energy transfer. *Biochem.* 33: 10171-10177.
43. Prochniewicz, E., Q. Zhang, P. A. Janmey, D. D. Thomas (1996). Cooperativity in F-actin: binding of gelsolin at the barbed end affects structure and dynamics of the whole filament. *J. Mol. Biol.* 260(5): 756-766.
44. deBeer, E. L., Sontrop, A., Kellermayer, M. S. Z., and Pollack, G. H. (1998). Actin-filament motion in the in vitro motility assay is periodic. *Cell Motil. and Cytoskel.* 38: 341-350.
45. Hatori, K., Honda, H., Shimada, K., and Matsuno, K. (1998). Propagation of a signal coordinating force generation along an actin filament in actomyosin complexes. *Biophys. Chem.* 75: 81-85.
46. Kitamura, K., Tokunaga, M. Iwane, A., and Yanagida. T. (1999). A single myosin head moves along an actin filament with regular steps of 5.3 nanometers. *Nature* 397(6715): 129-134.
47. Yakovenko, O., Blyakhman, F., and Pollack, G. H.: Sarcomere contraction occurs in reversible 2.7-nm steps. *Submitted*
48. Jacobson, R.C., Tirosh, R., Delay, M.J. and Pollack, G.H.: Quantized nature of sarcomere shortening steps. *J. Mus. Res. Cell Motility* 4:529-542, 1983.
49. Granzier, H.L.M., Myers, J.A. and Pollack, G.H.: Stepwise shortening of muscle fiber segments. *J. Mus. Res. & Cell Motility* 8:242-251, 1987
50. McIntosh, J. R. (1973). The axostyle of Saccinobaculus. II. Motion of the microtubule bundle and a structural comparison of straight and bent axostyles. *J. Cell. Bio.* 56: 324-339.

Bone Marrow Stromal Cells and their use in regenerating cartilage and bone tissue.

Ranieri Cancedda[1, 2], Rodolfo Quarto[1], Beatrice Dozin[1], Mara Malpeli[1], Anita Muraglia[1], Milena Mastrogiacomo[1, 2], Andrea Banfi[1, 2], Giordano Bianchi[1, 2].

[1] Centro di Biotecnologie Avanzate / Istituto Nazionale per la Ricerca sul Cancro, Genova, Italy.
[2] Dipartimento di Oncologia, Biologia e Genetica, Universita' di Genova, Italy.

Bone Marrow Stromal Cells (BMSC) can differentiate into different lineages: osteoblasts, chondrocytes, adipocytes and myocyte. We assessed the differentiation potential of 185 clones from human bone marrow cultures. The existence of fixed combinations of lineages (i.e. osteo-adipo-chondro, osteo-chondro and osteo-genic clones) and the sequential loss of lineage potential in tripotent clones suggests a model of predetermined BMSC differentiation. BMSC undergo limited mitotic divisions and do not express telomerase activity. Thus BMSC do not display full features of stem cells and should be regarded as early mesenchymal progenitors. A search for specific markers expressed by BMSC at the early progenitor stage is in progress.

Cartilage formation can be induced by TGFβ in high density BMSC "pellet culture" or in 3D cultures within a polymeric scaffold. We performed specific experiments to show that 1) once committed towards chondrogenesis in *vitro*, BMSCs, maintain the capacity to undergo further differentiation into osteogenic cells and 2) the sequence of changes observed in pellet cultures mimics the early steps of bone formation via cartilage models.

When implanted in immunodeficient mice, BMSCs combined with mineralized tridimensional scaffolds form a primary bone tissue highly vascularized. We used autologous BMSC/bioceramic composites to treat full-thickness gaps of tibial diaphysis in adult sheep. Gross morphology, x ray, histology, microradiography and SEM studies showed complete integration of ceramic with bone and good function recovery. Given these results, similar composites, whose size and shape reflected each bone defect, were implanted at the lesion sites of three patients. External fixation was used. Patients were followed for 18 to 32 months. An initial integration at the bone/implant interface was already evident one month after surgery. Bone formation progressed steadily during the following months. A full functional recovery of the treated limb occurred within 6 to 7 months after surgery.

Tissue Engineering: Methods for guiding cell disposition

Arti Ahluwalia, Francesca Bianchi, Danilo De Rossi, Antonino Previti, Giovanni Vozzi
Interdepartmental Research Center "E. Piaggio", University of Pisa, Italy
and CNR Institute of Clinical Physiology, Pisa, Italy

Introduction

The microscale patterning of organic materials is of fundamental importance for the realisation of a wide range of nano and micro-technology based devices and systems. Amongst the possible applications of micropatterning are tissue engineering, microactuators, multiparametric biosensing and micro-fluidics.

In the fields of tissue engineering and biosensing, several methods have been developed which permit spatially controlled adhesion of biomolecules and cells using for example photolithographic techniques or mechanical deposition with precision controlled motors.

As far as tissue engineering is concerned, it is clear that there is an intimate relationship between tissue structure and function. This is particularly evident for neural, hepatic, coronary and other complex tissues. Cells tend to organise themselves in a well-defined manner in space in order to correctly explicate their functions and to render the tissue, and the organ that it constitutes, a functional whole. Thus, guiding cells to take up a predetermined spatial organisation is considered to be one of the chief milestones in engineering complex tissues.

An important example of structurally organised tissue is neural tissue such the retina. The retina has a modular architecture and is made up of 3 main layers separated by interweaving layers of cell processes. Within their layers neurons of the same type commonly form non-random planar arrays known as mosaics [1]. The correct topographic development of a single layer of cells leads to correct connections between each layer, which then leads to a functional retina. Another important example of a tissue with a well-defined architectural organisation is the liver, in which hepatocytes form a close packed hexagonal structure interlaced with blood vessels and bile ducts. The efficient transport, exchange and collection of nutrients and wastes depends enormously on the exquisite organisation, at the cellular level, of the liver.

Whilst our current research is principally aimed at fabricating 3D scaffolds with highly controlled geometric parameters for applications in tissue regeneration, several other techniques or combinations of techniques are being investigated. It is in fact likely that combination of various techniques for modulating cell behaviour and their space-time disposition could lead to more efficient methods of engineering tissue. Among the methods currently being investigated at Centro Piaggio are :

- Syringe based microfabrication of polymer structures
- Soft lithography based methods
- Spatially selective chemistry
- Gene therapy based methods

Syringe Based Microfabrication

Syringe based microfabrication is used to fabricate 2 and 3 dimensional scaffolds of bioerodable polymers [2]. The system used, illustrated in figure 1a, is extremely simple and consists of a stainless steel syringe with a 20 μm glass capillary needle. A solution of the polymer in a volatile solvent is placed inside the syringe. The syringe has no plunger but is driven by filtered compressed air at a pressure of about 20 -150 mmHg, and is positioned by a 3 axis micropositioning system with a resolution of 0.1 micron.. The entire system including valves, pressure sensors and position controllers is interfaced to and controlled by a PC through a GPIB card. Linear structures with widths of 20 to 150 μm can be deposited, depending on the pressure applied to the syringe. The resolution of the deposition system combined with the dimensions of the syringe tip enables precise polymer patterns to be deposited on glass and silicone substrates and also permits selective placement of cells and adhesion ligands.

The system has been characterised and optimised and a simple model simulating the fluid-dynamics of the deposition process has been developed.

Using this technique we have developed a proprietary method for fabricating three dimensional structures. The 3D scaffolds produced have a lateral resolution of about 20 μm, and have been shown to promote adequate cell adhesion. We are currently in the process of analysing the physico-mechanical characteristics of these scaffolds, as well as their ability to support cell proliferation. An examples of a 3 D structures is shown in figure 1b.

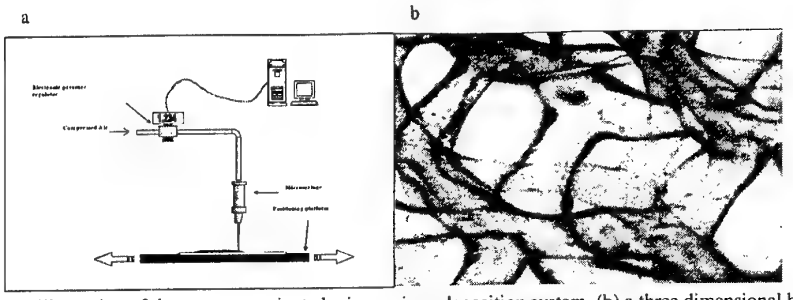

Figure 1: (a) Schematic illustration of the pressure activated microsyringe deposition system, (b) a three dimensional hexagonal scaffold of a polylactide/polycaprolactone blend. Magnification X40.

Micromolding

The other technique, developed in collaboration with the Microscale Tissue Engineering Laboratory, University of California, San Diego, is based on 'soft lithographic' approaches that utilize a Poly(dimethylsiloxane) (PDMS) mold and is depicted in Figure 2a. For this technique the first important step is the production of the silicon template that allows the fabrication of the PDMS mold. The details for the microfabrication of the photoresist master have been previously described [3].

PDMS prepolymer was prepared by mixing the commercially available prepolymer and catalyzer (Sylgard 184 kit, Dow Corning) in a 10:1 w/w ratio. The mixture was degassed under vacuum to eliminate bubbles created during mixing. The prepolymer solution was cast on the master and placed under vacuum once again to remove bubbles created by pouring, and then baked in an oven for two hours at 65 °C. After cooling and demolding the PDMS mold was then washed with 70% ethanol and sonicated for 5 minutes. Once the PDMS master mold was obtained, the PLGA solution was cast on the mold and placed under vacuum for 2 minutes to allow the polymer to fill the microchannels present in the mold and displace any air present. Excess PLGA was removed by passing a glass slide across the top of the mold, and the PDMS mold and polymer were baked for 30 minutes at 60 °C . After cooling, the PLGA pattern was peeled off with a pair of tweezers. It is also possible to construct laminated 3-dimensionalstructures by applying a mechanical load to a set of PLGA patterns stacked together and heating for 10 minutes at 60 °C. The lateral resolution of this method is about 30 m, and the resulting structures have been shown to promote adequate cell adhesion. An example of a 3 D structure fabricated by micromolding is shown in figure 2b.

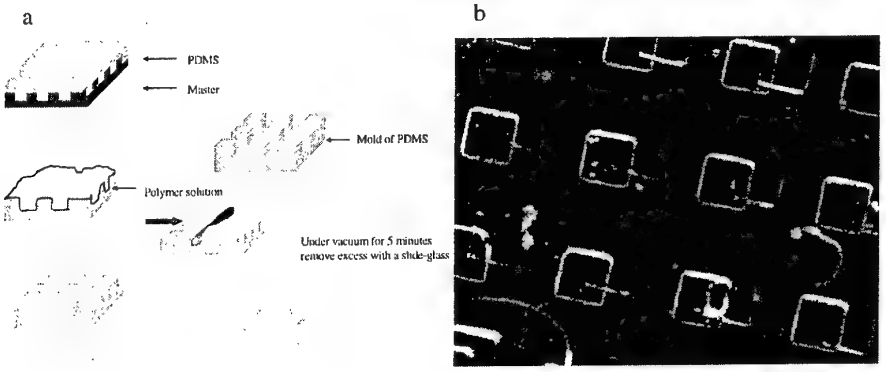

Figure 2: (a) Scheme illustrating the various steps of the micromolding technique, (b) a three dimensional square grid scaffold produced with the micromolding technique. Magnification X10.

Spatially selective chemistry

In order to direct cell adhesion on 2D structures, it is necessary to resort to surface derivatisation, as in most cases cells tend to spread uniformly on all surfaces. There are two general approaches used to demarcate cell adhesion. One is to render non-adhesive areas highly hydrophobic so as to exclude water, proteins and cells. The other method involves decreasing the water angle of contact of non-adhesive areas so that only water, to the exclusion of proteins is adsorbed. Whilst both methods have been used successfully, the relationship between cell type and surface properties for non-adhesion is not clearly understood.

When non biological scaffolds, such as the synthetic polymers commonly employed for tissue engineering, are employed, it is also necessary to enhance cell adhesion on these, since cell adhesion to most polymers such as polylactides and polyglycolides is often rather poor. This is usually done through the use of adhesion ligands such as fibronectin, collagen or RGD peptides. Covalent chemistry is often used to ensure strong protein-polymer interactions.

We have applied a number of surface derivatisation methods to our two dimensional microfabricated scaffolds. To determine the most effective method of demarcating cell adhesion, two dimensional hexagonal grids of a polylactide-polycaprolactone blend were subjected to various surface chemistry treatments to establish the most effective method of demarcating cell adhesion. In particular, to render the glass substrates underlying the polymer scaffolds anti-adhesive,

we coupled two types of hydrophobic silanes as well as two polyethyleneglycol (PEG) derivatives to the glass. Furthermore, in order to augment cell adhesion on the polymer scaffold, polylysine was covalently linked to the free carboxyl groups through the formation of amide bonds.
The results of the experiments indicate that in our experimental conditions, derivatisation with a hydrophobic silane, renders a surface more anti adhesive with respect to PEG. We also concluded that this effect is fairly independent of the length of the alkyl chain of the silane. Nevertheless, given time, even silane derivatised surfaces change their hydrophobic nature as proteins expressed by living cells modify their surface properties: a process commonly known as biofouling.
While surface derivatisation to spatially demarcate cell adhesion is necessary for 2 dimensional scaffolds, the 3D scaffolds produced by syringe deposition do not necessitate chemical treatment because the scaffolds are independent of a supporting substrate.

Conclusion

In summary, our objective is to guide cellular disposition using novel microfabrication techniques of biocompatible and bioerodable polymer scaffolds combined with surface chemistry and diffusion modulated exchange. To this end, we developed two novel methods, which can be used to construct structures with a wide range of potential geometries. These methods offer a valid alternative to the techniques currently being used to microfabricate tissue engineering scaffolds. Their resolution of approximately 20-30 microns is comparable or superior to that of other commonly employed methods. Furthermore, both techniques have been utilized to construct multilayer, 3-dimensional scaffolds that will constitute a valid help to study the cellular activities as adhesion, proliferation and motility. Current and future investigations are directed towards the study of cellular activities in dynamic environments and on the development of structures with spatially modulated diffusion gradients.

References:

[1] L. Galli Resta, Patterning the vertebrate retina: The early appearance of retinal mosaics, *Seminars in Cell & Developmental biology*, Vol. 9,1998:pp.279-284;
[2] G. Vozzi, A. Ahluwalia, D. De Rossi, A. Previti, Deposition of 2 and 3-D Polymer Scaffolds with a Well Defined Geometry for Application to Tissue Engineering, *Tissue Engineering* (2001, in press);
[3] G. Vozzi, CJ Flaim, A Ahluwalia, F Bianchi, and SN Bhatia, Microfabricated PLGA Scaffolds: A Comparative Study for Application to Tissue Engineering. *Materials Science & Engineering C,* (2001, in press).

Microfabricated biopolymer scaffolds tested in static and dynamic environments.

G.Vozzi, A. Ahluwalia, A. Previti, F. Bianchi

(text not available at time of printing)

ORGANIC MICROFLUIDIC SYSTEMS AND COMPONENTS

David J. Beebe
Dept. of Biomedical Engineering, UW-Madison
1410 Engineering Drive, rm 274 CAE BLDG
Madison, WI 53706-1608
Office: 608-262-2260 Lab: 608-262-3013 (rm 273), 262-5112 (rm 70)
FAX: 608-265-9239 e-mail: dbeebe@engr.wisc.edu
Cell: 608-516-9552 http://mmb.bme.wisc.edu/

While "simple" microfluidic systems have now been commercialized (e.g. Capillary Electrophoresis), achieving practical microfluidic systems capable of carrying out complex functionality has been elusive. Adapting silicon-based or IC-derived processes to creating microfluidic systems has met with limited success. I will discuss an alternative approach based on organic materials and liquid phase photopolymerization methods. Using responsive hydrogels and layered PDMS micromolding, we have demonstrated several novel valve designs (including bio-inspired designs). The fabrication processes are extremely simple, rapid and low-cost. Limitations include resolution and time response. In addition, I will discuss recent work demonstrating the ability to create very large liquid/gas interfaces within microfluidic channels via surface patterning.

DARPA WORKSHOP PRESENTATION - ITALY

Biocommunication From The Molecular To "Whole-Body" Level Using Novel Organic Electrodes

G. G. Wallace

Intelligent Polymer Research Institute, University of Wollongong,
Northfields Ave, Wollongong, NSW 2522, Australia

INTRODUCTION

The ability to monitor and modify biological function is a fascinating area of research facilitated in recent years by the discovery and development of new organic electrode materials. Studies in these areas allow us to monitor performance and determine mechanisms of failure in complex biosystems from the molecular to "whole-body" level. This information then provides a platform for the development of appropriate molecular technologies as well as training or rehabilitation routines that will enable us to avoid or repair such failures.

At the molecular level the advent of microelectrodes heralded a new era in biomonitoring, allowing the development of *in-vivo* techniques. These have proven particularly useful for investigations into brain activity in animals [1] or even probing electrochemical events within single cells [2]. Attempts to modify the behaviour of biological systems using electrical stimulation via simple metallic electrodes has also been of interest for some time. For example, the passage of small electrical currents has been shown to stimulate bone regrowth [3, 4]. More recently direct electrical stimulation has been shown to enhance wound healing [5] and been useful in tumor treatment [6]. These positive results though little understood have been achieved using electrodes metallic in nature and inherently incompatible with biological systems.

Due to the discovery of inherently conducting polymers (ICPs) by MacDiarmid, Shirakawa and Heeger [7] we are now poised to enter a new era of biocommunications. The organic nature of these electronic conductors provides a conduit (an organic electrode) that should enable more efficient communication with biosystems from the molecular to "whole-body" level.

These organic electronic conductors include the polypyrroles, polythiophenes and polyanilines. In the case of polypyrroles polymerisation can be achieved from neutral aqueous solution at low potentials. This enables diverse chemistries to be incorporated into the organic conductor. For example, the dopant in polypyrrole may be an enzyme, an antibody or even a whole living cell [8].

Simple polymerisation methods have also been used to coat fabrics with ICPs to produce mechanical sensors that can be utilised at the "whole-body" level [9]. These novel sensing systems enable information to be gathered in real time and remotely using appropriate telemetry units. The use of ICPs as organic electrodes capable of communicating (sensing/actuating) from the molecular to the "whole-body" level is discussed below.

The discovery and development of inherently conducting polymers (ICPs) has provided a unique molecular platform on which to build bioactive communication systems. The fact that the electronic properties of ICPs are highly sensitive to molecular interactions provides a molecular listening device capable of monitoring processes such as enzymatic or immunological reactions. Perhaps even more fascinating is that, when configured properly, ICPs can function as molecular wires providing stimuli to control biomolecular events. Both of these aspects of biomolecular communication are illustrated below by considering selected studies involving ICPs and some of the building blocks of life.

Molecular Monitors

Amino Acids: Previous work in our laboratories has utilised inverse thin layer chromatography to study the interactions of amino acids with conducting polymers [10]. The most interesting finding in these studies was that the location of charge rather than the total charge on the amino acid molecule, determined the degree of interaction with the polyaniline material.

Other work [11] has shown that varying the composition of the polymer by changing the dopant has a marked influence on the interaction (or at least signals arising from these) of amino acids with the ICP.

We [12, 13] and others [14-17] have also been interested in the design and development of intrinsically chiral ICPs and the interaction of these with chiral amino acids. Kaner et al. [16] have shown that chromatographic separation of D- and L-phenylalanine is possible via HPLC using optically active emeraldine base as the stationary phase. In our own laboratories, circular dichroism

spectral studies have demonstrated that optically active poly(2-methoxyaniline) POMA interacts differently with the enantiomeric amino acids, D- and L-phenylalanine, D- and L-histidine, and D- and L-leucine. We have also shown that chiral, electroactive membranes based on optically active polyaniline transport enantiomeric anions at different rates.

Proteins: The interaction of conducting polymers with proteins has been of interest. The effect of applied potential on these interactions has been investigated with a view to developing novel membrane separation techniques [18, 19]. It has been shown that the oxidation state of the conducting polymer dramatically affects protein affinity.

Redox Proteins: The electron transfer sites buried within redox proteins are not readily accessible on chemically inert metal electrodes [20]. However, a number of studies have shown that ICP - containing systems can be used to facilitate access to the electron transfer site of cytochrome c. Work by Cooper et al. [21] showed that the site could be accessed using a functionalised polypyrrole. In our labs we have shown that polypyrrole composites with Prussian Blue [22] or polypyrrole containing ferricyanide as dopant [23] are effective in mediating electron transfer processes with cytochrome c. More recently, the same mediator effect has been demonstrated with an inherently more stable polythiophene polymer that has ferrocene attached via a conjugated linker [24].

Enzymes: A number of enzymes have been either covalently attached or integrated (as dopants) into inherently conducting polymers (see ref 8 and references cited therein). The primary objective of these studies has been the development of enzymatic biosensors. However, perhaps the most intriguing results obtained relate to the apparent dependence of the enzymatic activity on applied potential when it is incorporated into the conducting polymer, providing a degree of regulation over the enzyme function. This phenomena has been noted both by our group [25] and previously by Aizawa [26].

Antibodies: Antibodies (Ab) have also been incorporated directly into ICPs as dopants. Initial experiments investigated the effect of applied potential on Ab-Ag (Antigen) interactions using an electrochemically controlled affinity chromatography set-up and demonstrated a clear effect [27]. This subsequently led to the development of Ab - containing sensors that utilise a pulsed potential routine to ensure sensitivity and reversibility in the Ab-Ag interaction [28]. The continued practical

application of this phenomena has proven difficult due to the inherent irreproducibility in the Ab immobilisation approach [29]. Research into this area continues.

Molecular Actuators

Living Cells: The ability to manipulate the growth/differentiation and eventually the performance of these fascinating molecular machines is perhaps the most important level of biomolecular communication. We [30, 31] and others [32, 33] have shown that biocommunication at this level is possible. In one study [30] it has been shown that intact red blood cells can be incorporated into a polypyrrole – polyelectrolyte composite. The ICP then functioned as a transducer enabling Ab-Ag interactions occurring in the red blood cell membrane to be monitored. In another study it has been shown that PC-12 cells can be cultured on polypyrrole - polyelectrolyte composites and that cell differentiation can be stimulated by the electrically generated release of growth promoters. More recently the effect of the oxidation state of the polymer [34] and the presence of fibronectin [35] have been investigated and shown to significantly influence cell growth.

"Whole-Body" (Mechanical) Monitors

Using the concept introduced by De Rossi [9] we have investigated a number of approaches to the preparation of ICP coated stretch fabrics (including Lycra). The parameters influencing the strain gauge performance (sensitivity, dynamic range and response time) have been investigated. A number of biomechanical applications are under investigation.

Mechanical ("Whole-Body") Actuators

The realisation of artificial muscles based on inherently conducting polymers still entices the scientific research community. At present, performance can exceed natural muscle in terms of force generation [36] but not elongation. It has recently been shown that the configuration of ICP based artificial muscles can have a dramatic effect on the force generation capabilities [37]. The development of fabrication technologies that allows us to mimic the hierarchical structure of human muscles will accelerate progress in this area. With this in mind we have been interested in the actuation capabilities of conducting polymer fibre structures [37].

CONCLUSIONS AND FUTURE DEVELOPMENTS

The quest to interact more efficiently with biosystems to obtain monitoring information related to system performance and to control that performance remains an exciting and increasingly viable area of research.

The diverse and often complex chemistry coupled with the mechanical electronic properties required of molecular conduits to achieve the above at a range of levels is available with ICPs. It appears that the practical realisation of the application of these materials will only be limited by the level of innovation in the areas of polymer processing and device fabrication.

The processing requirements are driven by the needs of fabricators. To enable the use of simple device fabrication, methods such as ink-jet printing or screen printing stable solutions or dispersions of ICPs are required. There has been much progress in these areas in recent years and further work is needed to expand the range of materials processable in biocompatible (aqueous) environments.

ACKNOWLEGEMENTS

The above is a summary of work carried out in conjunction with a range of collaborators as detailed in the publication list - I am extremely grateful to them all. I also acknowledge the continued support of the Australian Research Council in the form of a Senior Research Fellowship.

References

[1] Shibuki, K. Neuroscience Research 1990, 9, 69.

[2] Meulemans, A., Ponlain, B., Baux, G., Tauc, L. Anal. Chem. 1986, 58, 209.

[3] Ciezynski, T. Arch. Immun. Ther. Exp. 1963, 191, 11.

[4] Black, J. Orthopaedic Clinics of North America 1984, 45, 15 (and references cited therein)

[5] Karba, R. et al. Bioelectrochem. Bioenerg. 1997, 43, 265.

[6] Miklavcic, D. et al. Bioelectrochem. Bioenerg. 1997, 43, 253.

[7] Shirakawa, H., Louis, E.J., MacDiarmid, A.G., Chiang, C.K., Heeger, A.J. J. Chem. Soc., Chem. Commun., 1977, 578.

[8] Adeloju, S.B., Wallace, G.G. Analyst. 1996, 121, 699 (and references cited therein).

[9] De Rossi, D., Della Santa, A., Mazzoldi, A. Mat. Sci. Eng. C. 1999, 7, 31.

[10] Teasdale, P.R., Wallace, G.G. Polymer. Int. 1994, 35, 197.

[11] Akhtar, P., Too, C.O., Wallace, G.G. Anal. Chim. Acta. 1997, 339, 211 and 1997, 339, 201.

[12] Majidi, M., Kane-Maguire, L.A.P., Wallace, G.G. Polymer, 1994, 35, 3113.

[13] Strounina, E.V., Kane-Maguire, L.A.P., Wallace, G.G. Synth. Met. 1999, 106, 129.

[14] Havinga, E.E., Bouman, M.M., Meijer, E.W., Pomp, A., Simenon, M.M. J. Synth. Met. 1994, 66, 93.

[15] Moutet, J.C., Saint-Aman, E., Tran-Van, F., Angibeaud, P., Utille, J.P. Adv. Mater. 1992, 4, 511.

[16] Guo, H., Knobler, C.M., Kaner,R.B. Synth. Met. 1999, 101, 44.

[17] Pleus, S., Schwientek, M. Synth. Met. 1998, 95, 233, and references cited therein.

[18] Zhou, D., Too, C.O., Hodges, A.M., Mau, A.W.H., Wallace, G.G. React. Funct. Polym. 2000, 45, 217.

[19] Barisci, J.N., Lewis, T.W., Spinks, G.M., Too, C.O., Wallace, G.G. J. Int. Mat. Syst. Struct. 1998, 9, 723.

[20] Armstrong, F.A., Hill, A.A., Walton, N.J. Acc. Chem. Res. 1988, 21, 407.

[21] Cooper, J.M., Morris, D.G., Ryder, K.S. J. Chem. Soc. Chem. Commun. 1995, 697.

[22] Lu, W., Wallace, G.G., Karayakin, A.A. Electroanal. 1998, 10, 472.

[23] Lu, W., Zhao, H., Wallace, G.G. Electroanal. 1996, 8, 248.

[24] Chen, J., Too, C.O., Officer, D., Burrell, T., Swiegers, G., Wallace, G.G. (Submitted).

[25] Lu, W., Zhou, D., Wallace, G.G. Anal. Comm. 1998, 35, 245.

[26] Aizawa, M., Haruyama, T., Khan, G.F., Kobatake, E., Ikiriyama, Y. Biosens. and Bioelectronics 1994, 9, 601.

[27] Hodgson, A.J., Lewis, T.W., Maxwell, K.M., Spencer, M.J., Wallace, G.G. J. Liq. Chrom. 1990, 13, 3091.

[28] Sadik, O., Wallace, G.G. Anal. Chim. Acta. 1993, 279, 209.

[29] Barisci, J.N., Hughes, D., Minett, A., Wallace, G.G. Anal. Chim. Acta 1998, 371, 39.

[30] Campbell, T.E., Hodgson, A.J., Wallace, G.G. Electroanal. 1999, 11, 215.

[31] Hodgson, A.J., Gilmore,K., Small, C., Wallace, G.G., Mackenzie, I.L., Aoki, T., Ogata, N. Supramolecular Science 1994, 1, 77.

[32] Shinohari, H., Kojima, J., Yaoita, M., Aizawa, M. Bioelectrochem. Bioenerg. 1989, 22, 23.

[33] Schmit, C.E., Shastri, V., Vacanti, J.P., Langer, R. Proc. Nat. Acad. Sci. 1997, 94, 8948.

[34] Garner, B., Georgevich, A., Hodgson, A.J., Liu, L., Wallace, G.G. J. Biomed. Mat. Res. 1999, 44, 121.

[35] Garner, B., Hodgson, A.J., Wallace, G.G., Underwood, P.A. J. Mat. Sci. Mater. Med. 1999, 10, 19.

[36] Baughman, R.H., et al . Science. 1999, 284, 1340 (and refs cited).

[37] Hutchison, A.S., Lewis, T.W., Moulton, S.E., Spinks, G.M., Wallace, G.G. Synth. Met. 2000, 113, 121.

BIOMIMETIC MATERIALS AND STRUCTURES: PAST AND PRESENT

Danilo De Rossi

Centre Interdepartmental of Research «E. Piaggio», School of Engineering

University of Pisa, Italy

An old-rooted endeavour of man, i.e. fabrication of material and structures taking inspiration from nature, is again actively pursued under a renewed name: biomimesis.
This approach, once belonging to the realm of biological sciences, is based on the observation that, when one tries to embody our recognition criteria for biological organisms in an explicit list, nothing can be found on that list which cannot be mimicked by some inorganic system (1). Hence, a large variety of artifacts can be made, all possessing, to some extent, life-like features.
Biomiinetic arguments are today common reasoning in experimental studies about the "origin-of-life" and in "advanced robotics"; a relatively new entry pertains to the area of "materials science".

The "magic" and the "economic" as engineering factors

The development of embryonic technical areas very much depends upon the value bestowed to them by the leading social components of the time; those values should not be only identified with utility or cost effectiveness. The perception of their own role by operators involved in the development of the area has also an influence on the selection of style and subject of the study, as we may recognize through a few scattered historical remarks (2).
In the greek world the machine had a magic character since it opposes nature, it permits one to operate against nature and so, the engineer, "mechanician "or the *mekanopoiós,* being a creator of machines, is a wizard, a demon.
It is still true that in the ellenistic period the engineer is an ambigous he does not care for them character, even difficult to define: he although he knows geometry and mathematics, and of theories; neither does he operate as an artisan or a technician. Unable to place himself between "tékne" and "epistéme", since the radicality of the contradiction makes a mediation impossible, he becomes a pivot in the struggle against nature which he forces, through his knowledge, to produce wonders.
The motivation behind new technologies at the beginning of the modern era does not consist in conceiving, inventing and constructing machines because of their utility or economic value: this will only happen at a later moment, it will occur with the onset of the industrial revolution. The aim instead, consists, in accordance with the program of ascertainins of the true possibility of controlling and dominating nature, in constructing all possible machines, that is, all machines which can be conceived on the lines of new physics, in verifying the possibility of making something from something entirely different.
Nowadays, industrial society is a mass society, characterized by huge industrial enterprises and gigantic public administrations, standardized mass production methods and diffused conformism in mass media and life-styles. In this society utility/and cost-effectiveness is the engineering factor.
The oncoming information society seems to present the connotation of a society of individuals in which new technologies will cope with the already manifested tendency of our young generations to escape from conformistic life and to express individuality. All this will occur only through the emergence of a social and economic order based on decentralized power and responsibility of the individual (3).
I have no difficulty in foreseeing a role of the playful/magic engineering factor in the design of

man-machine interfaces and of small, individually supervised facilities for the computer-controlled generation of artifacts in this new information society.

Soft and hard biomimesis

There is little doubt that in the area of biomimetic engineering the two characters (useful/economic and playful/magic) described above coexist both in terms of personal motivation of operators and in the foreseeable results of ongoing research.
Biomimicking as a respectable branch of material engineering has been questioned on the basis of its predicted inadequacy to fulfill industrial process requirements, particularly in terms of "time-to-make" (4).
Stereolithography and related rapid prototyping techniques (5), exploiting the moving front biomimetic principle (6), with the potential capacity to operate as home-based production facilities may well vanquish that argument.
Beside this debate on time and economics, we have to underline the fact that this line of research looks at the materials to be prepared and the structures to be fabricated with the classical mechanistic/reductionistic attitude of physics. The analysis and synthesis of isolated parts, studied and prepared under the highest possible level of operator control, will eventually make available useful biomimetic materials and structures at a viable price. This we may call "soft biomimesis". Any student of biological science would realize soft biomimesis being as far from biology as Newtonian mechanics is.
On the other hand practitioners of "hard biomimesis" may find the pioneers of their discipline in the founders of "synthetic biology".
Synthetic biology was most lucidly defined and clearly reported in its first attemps by Stephan Leduc (7), but it only had approximately fourty years (from 1870 to 1910) of stunted life before falling into oblivion. Artificial
cells, osmotic creatures and membraneous precipitations, all made of inorganic compounds, were prepared showing almost all the observable attributes of living creatures with an astonishing degree of resemblance.
It is worth mentioning, however, that the very large majority of today's students of hard biomimesis do not use chemistry University laboratories, instead they operate with a computer keyboard to create "Artificial Life".
Artificial Life, as it is cultivated today, has its roots in computer programming and, beside using serial machines of the Von Neumann type, it attempts to generate life-like behaviours in their parallel, emergent nature. More than dealing with life-as-we-know-it, it deals with life-as-it-could-be or it-will-be (8).
We may say that Artificial Life has taken mostly the computational from contemporary science and technology aspects, with a minimum attention to other major advances such as the analysis of dynamic patterns, dissipative structures, self-assembly phenomena and other off springs of non-linear effects in physical chemistry.

The material breeder

As remarked before, a truly peculiar characteristic of living systems resides in the emergent nature of their behaviour, which *de-facto* prevents any a-priori deterministic reasoning about the structure and function of the entity to be generated.
If we attempt to adopt an hard biomimesis approach we definitely proceeds along the lines indicated by D. Parisi (10) and K. Kelly (11).
"A form of engineering truly inspired by biology should aim to construct artifacts which, when they leave the hands of the engineer, are not yet what they have to be, they will become so after a process of development. The

engineer does not create the artifact anymore, he just sets the suitable conditions for an artifact to develop and learn" (D. Parisi).
"Yet as we unleash living forces into our created machines, we loose control of them. They acquire wildness and some of the surprises that the wild entails. This, then, is the dilemma all gods must accept: that they can no longer be completely sovereign over their finest creations. The world of the made will soon be like the world of the born: autonomous, adaptable, and creative but, consequently, out of control". (K. Kelly).
Biology tells us that the emergent nature of the living systems originates from the distinction genotype/phenotype. The genotype is the complete set of genetic instructions. The phenotype is the physical organism, the structure emerging in space and time as a result of interpretation of the genotype code in a specific environment.
The process through which the phenotype develops in space and time, following genotype instructions, is called morphogenesis. The non-linear interactions between the objects specified by the genotype set the ground for a very rich variety of possible phenotypes. The price for this wealth of creatures resides in the impredictability with which phenotypes will finally emerge. Impredictability of genotype/phenotype systems prevents determination, by mere inspection, of which kind of phenotype will be produced by an arbitrary genotype. If we want to know the phenotype, we must test the genotype in a specific environment and let things go.
Now, my question is, in the context of biomimetic systems, how can we look for suitable artificial genotypes capable of generating life-like phenotypes?

The artificial genotypes

The search for the appropriate artificial genotype and the optimum conditions for the development of the living phenotype was pursued by man in the time of Alchemy which required to a proper state of spirit and the help of God.
Since the times the of fierce attack of Boyle in "The sceptical chemist" in 1661 and after the Royal Society's investigation (1783) of Dr. Pierce's claim of transmutation of mercury into gold, Alchemy has no links with science (12).
Instead, the search for artificial genotypes is actively pursued in the field of Artificial Life with the aim of generating immaterial creatures throug computer programming or, as it is called, "life-in silico" (13).
With this aim, at present, Artificial Life is not involved in any activity related to materials science and engineering and so, the connections with the area of biomimetic materials and structures are virtually non existent. All the equipment needed by Artificial Life practitioners is computers and peripherals requiring nowadays little economic investment and short time to run.
The search for artificial genotypes and appropriate "growing" conditions of life-like phenotype in hard biomimesis, on the other side, appears to be an extremely laborious and expensive operation with limited chance of success, at least in the near future. Such an enterprise would appear as a sort of a dream (you may even say a nightmare) in a period in which the value of dreams depends on the stock market value.

New tools

If the resuscitation of synthetic biology will prove to be possible, the words of Stephane Leduc may be worth remembering: "The synthesis of life is not going to be the sensational discovery evoked by the expression. If evolution occured as we presently believe, the synthesis of life can only originate through productions being intermediate between mineral and the life kingdoms, having no more than a few rudimentary attributes of life, to whom, laboriously, other ones will add to, and who we may say, will lead to a progressive evolution of the first productions of synthetic biology".

The physicochemical tools and our knoledge of phenomena of a biomimetic nature have increased in terms of quality and understanding from the times of Leduc: Even more profound is our knowledge of physics and chemistry, in the analysis of the characteristics of living systems and in some form of mathematics useful to describe them (14).
According to a materialistic vision, a biomimetic organism, as much as a living creature, may be described as a
spatially-confined entity of limited duration in time in which space-and time-resolved chemical processes driven by matter and energy flow operate purposefully (teleonomy); the entity has the capability of autonomous morphogenesis and invariant reproducibility (15). If we look at material details we realize that an organism, as a functional necessity, needs to be structured.
As underlined by Rowland and Blumenthal (16): "An annoying ambiguity attaches to the word "structure".
It traditionally refers to static spatial patterns that are near or at thermodinamical equilibrium. But the word has been extensively adapted in the temporal domain and in thermodynamics to apply to systems with recognizable
patterns mantained for finite periods, however brief or enduring. These patterns differ significantly, however, from the old space structure in their requirement of energy for their manteinance. Thus, the classical structure-function dichotomy in biology is blurred by the introduction of dissipative structures (dynamic patterns)".
Dissipative structures (17) and related far-from-equilibrium phenomena (18) all refer to the onset of anisotropic dynamic effects spontaneously generated by isotropic causes.
This is the key issue of morphogenesis and structure formation in hard biomimesis.
We may be in facing, here, governing or enabling phenomena which, in analogus to the prepattern concept in biological morphogenesis, may consent to "frozen-in" structures (static patterns) being the permanent record of the originating dynamic patterns (19). The generated static patterns will then form an influential skeleton for the development of newly operating dynamic patterns.
Oscillating chemical reactions and chemical waves (20), spatially periodic precipitations and other forms of patterning tools will operate in the support medium purposefully structured as a chemical (wave) guide, through appropriate local changes of material coefficients.
I will try to clarify this procedure through a possible implementation in my talk where a repertoire of potential artificial genotypes and an environment for phenotypes development will be illustrated.
At this early evolutionary stage of hard biomimesis we limit our selection criteria of emerging phenotypes to the attainment of a purposeful action.
Although I am aware that invariant reproduction (21) and autonomous morphogenesis (9) have been both demonstrated in inorganic material systems, I do not believe the implementation of these life-like features, when combined with the requirement of purposefulness, belongs to the domain of predictable operations. The converse in easier.

Rings in a brick

One attempt to exploit dynamic patterns from an engineering perspective deals with the preparation of systems ceramics using Liesegang rings (LR) (22). LR are forms of periodic precipitations that manifest themselves in a great variety of diffusive media permeated by suitable reactants (23). This form of patterns has been noted for a long time (24), although a detailed comprehension of their complex origin is still elusive (25).
It is worth mentioning that Leduc also made extensive studies on these phenomena and reported about interesting realizations of optical diffraction gratings made by silver arseniate LR in gelatine blocks (9). Leduc also reported evidence of guided chemistry with LR, proposing a close

analogy between refraction, diffraction, dispersion and interference in optics and LR propagation in structured diffusive media.

The state of scientific understanding at that time was not developed enough to permit the analogy to be pushed too far; however the wave like phenomena we may call "optochemistry" could prove to be rich in their theoretical and practical implications.

The toymaker and the butterfly wing

Hard biomimesis today is an activity of the *mekanopoios* more than the one of the economy-concerned engineer.

This consideration doesn't prevent the conception and eventual implementation of biomimetic structures endowed with the beauty and fascination of like-life behaviours, which are *per set* valuable characteristics. To be more specific, I refer to one of the most spectacular chromatic effects exploited by living creatures, i.e. submicron diffraction gratings (26). The hypotesis of Liesegang precipitation being responsible, though their diffractive properties, for the stripes of butterfly wings has been proposed a long time ago (27). Without being firmly disprooved, this hypothesis belongs to the inventory of rejected ideas. Many other models based on periodic solutions of reaction-diffusion equations have been proposed in time to account for patternig phenomena in morphogenesis (28). Most recently the possibility of a Turing mechanism (29) being responsible for stripes formation in sea angelfish has been convincingly supported (30).

However, it is not necessary here to enquire about the biological role of these phenomena, but of conceiving methods and techniques for generating hard biomimesis creations, as it has been attempted by using Belousov-Zabotinsky reaction-based genotypes to originate classes of phenotypes capable of restoring blurred visual images (31).

What ca we make of this rich background?

Play with new toys: patterning tools, growing media, and marvel at the butterfly-wing analogs emerging from them.

References

1) R. Rosen, "Life Itself. A comprensive inquiry into the nature, origin, and fabrication of life". Columbia Univ. Press, New York, 1991.

2) R. Rinaldi in a Introduction to: 1. Cohen "I robot nel mito e nella scienza", De Donato, Bari, 1981.

3) K. Seitz, "Europe: a technological colony?", Community Editions, Bruxelles, 1995.

4) I. Amato, "Meeting the call of the wild". Science, vol. 253, pp. 966-968, Aug. 1991.

5) P.J. Jacobs, "Fundamentals of stereolithography", Society of Manufacturing Engineers, Deaborn (MI), 1992.

6) A.H. Hener et al, "Innovative materials processing strategies: a biomimetic approach", Science, vol. *255,* pp. 1098-1105, 1992.

7) see M. Zeleny, G.J. Kiir, K.D. Hufford, "Precipitation membranes, osmotic growths, and synthetic biology" in Artificial Life, C.G. Langton (ed), Addison-Wesley Publ. Co, 1988.

8) 8)C.G. Langton, "Artificial Life" in - as 7).

9) 9)J. Leduc, "Theorie physico-chimique de la vie et generation spontanèes", A. Poinat Ed., Paris, 1910.

10) D. Parisì, "Il controllo perduto", Virtual, vol I, n. 3, 1993.

11) K. Kelly, "Out of control: The new biology of machines", Fourth Estate, London., 1994.

12) E.J. Holmyard, "Alchemy", Dover Publ. Inc, New York, 1990.

13) see the volumes of the serie of Proceedings of the Santa Fe Institute Studies in the Sciences of Complexity published by Addison-Wesley Pub. Inc. as Artificial Life I, II and III.

14) V.I. Arnoid, "Catastrophe theory", Springer Verlag, Berlin, 1992.

15) J. Monod, "Il caso e la necessità" EST Mondadori, Milano, 1970.

16) in "Dynamic patterns of brain cell assemblies» Neurosciences Res. Prog. Bull, vol 12 (1), pg. *54,* March 1974.

17) I. Prigogine, G. Nicolis "Self-organization in nonequilibrium systems", *3.* Wiley & Sons, New York 1977.

18) J.A.S. Kelso, M. Ding and O. Schoner: "Dynamic pattern formation: a primer» in "Principles of organization in organism" SF1 Studies in the Science of Complexity, Proc. Voi. XIII, J. Mittenthal and A. Baskin (Eds), Addison Wesley, 1992.

19) L.E. Scriven in 16) at pg 17.

20) A.T. Winfree, "The geometry of biologicai time", Springer Verlag, Berlin, 1990.

21) M. Kuckuck, "L'Univers, etre vivent", Librairie Kundig, Geneve, 1911.

22) 3. Adair, S.A. Touse and P.J. Melling, American Ceramic Society Bulletin, 66, 1490, 1987.

23) H.K. Henish, "Crystals in gels and Liesegang rings", Cambridge University Press, Cambridge, 1988.

23) G. Runge, "Der Bildungstrieb der Stoffe, Oranejburg, 1855.

25) G. Venzi, J. Ross, "Nucleation and colloidal growth in concentration gradients (Liesegang rings)," J. Chem. Phys., 77 (3), pp. 1302-1307, 1982.

26) M. Gaie, "Diffraction, beauty and commerce", Physics World, pp. 24-28, 0cL.

1989.

27) W. Gebhardst, Verk. d.d. Zool. Ges., 22, 175, 1912.

28) H. Meinhardt, "Models of bioiogicai pattern formation", Academic Press, London, 1982.

29) A.M. Turing, "The chemical basis of morphogenesis" Phil Trans. R. Soc., B 237, pp. 37-72,1952.

30) S. Kondo, R. Asai, "A reaction-diffusion wave on the skin of the marine angelfish Pomachantus", Nature, voI. 376, pp. *765-768,* 1995.

31) N.G. Rambidi, A.V. Maximychev, "Moiecular image processing devices based on chemical reaction systems, 4: Image processing operations performed by active media functioning in the oscillating mode». Advanced Materials for Optics and Electronics, vol 5, pp. 233-241, 1995.

Electrochemical Behavior and Electromechanical Actuation of Polyaniline in Non-aqueous Electrolytes

Benjamin R. Mattes
Santa Fe Science and Technology
3216 Richards Lane, Santa Fe, NM 87505, USA

Due to their properties of being lightweight and low operational voltages, use of conducting polymers in the development of electrochemical actuators has been an attractive topic in recent years. This type of actuator relies upon the application of an electrochemical stimuli to change the oxidation level of the polymer, which results in the ingress and egress of counterions to satisfy the neutrality and thereby its volume. The majority of research into conducting polymer actuators to date has been carried out in aqueous electrolytes. However, several disadvantages associated with aqueous electrolytes (e.g. narrow electrochemical window and fast electrolyte evaporation) and conducting polymers in aqueous media (e.g. degradation at high potentials) have been confirmed to be the main factors limiting the lifetime of conducting polymer based electromechanical actuators. Therefore, use of non-aqueous electrolytes with a high boiling point, a low vapor pressure, a high dielectric constant and a wide electrochemical window would be advantageous for the fabrication of stable and durable conducting polymer actuators. In this work, we investigated the effect of dopant anion on the electroactivity and electro-mechanical bending actuation of gilded polyaniline bilayers in propylene carbonate, and then fabricated a solid-state polyaniline bending actuator.

Freestanding polyaniline films used to fabricate the actuators were prepared from emeraldine base dissolved in N-methyl-2-pyrrolidinone (NMP). After acid doping, these films generally have conductivities between 1-10 S/cm and consequently the applied voltage would decreases along the length of the polymer film. Therefore, the EB films were gilded using commercially available gold leaf (thickness approx. 5(m) by applying a 2 wt % EB/NMP solution to one side of the polyaniline film and then carefully applying one layer of the gold leaf. With the attachment of a thin gold layer on the back, a uniform potential distribution in the polyaniline films could be achieved. The gilded EB films were doped in 1 M acidic aqueous solutions for 24 hours and then dried under dynamic vacuum for 24 hours to remove any water.

The electroactivity of conducting polymers in the electrolytes used plays an important role in determining their actuation properties. Electrochemical behavior of gilded doped polyaniline films in 1 M lithium perchlorate/propylene carbonate from –0.4 to +0.8 V vs Ag/Ag+ was performed using an EcoChemie pgstat30 potentiostat with a three-electrode system. It was found that the electroactivity of doped polyaniline films in propylene carbonate was strongly determined by the solubility of doping acid anion in the electrolyte. We investigated a range of acids for the doping of the polyaniline films, and according we could classified the acids into two groups based on the solubility of the dopant anion in propylene carbonate. The polyaniline films doped with group 1 acids (i.e. HClO4, HBF4, CF3COOH, HPF6 and CH3SO3H) showed well-defined electroactivity due to the fact that the dopant anion was soluble in the propylene carbonate electrolyte. On the other hand, for acids whose corresponding anions were insoluble in the electrolyte, labeled group 2 acids (i.e. HCl, HNO3, H2SO4, CF3SO3H, C6H5SO3H), showed little or no electroactivity in the electrolyte. This was confirmed to be due to the difficult expulsion of dopant anion into the electrolyte.

In bending actuation measurements, a gilded polyaniline film was partially immersed into the propylene carbonate electrolyte. The sample was connected to the potentiostat using a gold-plated alligator clamp without teeth. The polyaniline film was imaged using a video camera, and a transparent protractor was placed over the image on the TV screen so that bending angles could be measured (to an accuracy of less than 1 degree). The bending angle was recorded manually during potentiodynamic stimulation from -0.4 V to 0.8 V vs Ag/Ag+ at a scan rate of 5 mV/s. As expected, the action performance of the doped polyaniline films is related to the electroactivity of the film in the propylene carbonate electrolyte. For the polyaniline films doped with group 1 acids, good actuation of the glided film was observed. The highest bending angle (990) was obtained for the CF3SO3H doped polyaniline film. However, for films doped with group 2 acids, no bending actuation was observed due to the difficult expulsion of the dopant anion.

Electrochemical AC impedance measurements were used to investigate the relationship between polyaniline actuation and its faradic and capacitive behavior for the gilded polyaniline films doped with group 1 acids. This measurement was performed in 1 M LiClO4/propylene carbonate electrolyte at different potentials between 0.05 Hz and 100 kHz using an amplitude of 10 mV for the sine wave. It was found that the capacitive behavior of the polymer was the major contributor to bending actuation of polyaniline in non-aqueous electrolytes.

Finally, a solid-state polyaniline bending actuator was fabricated from two identical gilded CF3SO3H doped polyaniline films, as this material displayed the highest bending angle. A PMMA/PC/EC/ LiClO4 gel electrolyte was sandwiched between these two gilded polyaniline bilayers. The applied voltage needed to operate our prototype actuator was around 0.8 V, which was much lower than that of ~5 V that was used for the previously reported by Kaneto et al1-2. Bending was achieved as soon as the voltage was applied (about 250 for the first cycle) and then increased slightly for the following cycles for our prototype. The bending degree of our actuator (~400) was about the same as that of the previously reported actuator and the bending time of our prototype was only 12 to 15 seconds even with an applied voltage of 0.8 V. From the best result obtained for the previously reported actuator (Vapp = 5 V, bending degree = 400, bending time = 2 minutes), the actuation speed can be estimated as 0.30/sec, while that of our actuator was 2.50/sec (i.e. 8 times faster).

References

K. Kaneto, Y. Min and A.G. MacDiarmid, US Patent #5,556,700 (1996).
Y. Min, A.G. MacDiarmid, K. Kaneto, Polymer Mater. Sci. Eng., (1994) 71, 713-714.

ABSTRACT (DARPA/ONRIFO Electro-active Polymer Workshop)

FROM FLY VISION TO ROBOT VISION

Nicolas Franceschini
C.N.R.S., Neurocybernetics Research Group, Laboratory of Neurobiology
31 Chemin J. Aiguier, MARSEILLE (France)
ENFranceschini@lnb. cnrs-mrs.fr

Flies are miniature seeing creatures that use a host of smart sensors for immediate action upon the steering. They navigate swiftly in the most unpredictable environments, avoiding obstacles without resorting to any sonars or laser range-finders. They process their sensory signals on-board without being tethered to a supercomputer. A fly is equipped with " only " about 1 million neurons and it views the world with no more than 6000 pixels. And yet this humble flyer can attain a level of performance beside which present-day mobile robots look quite puny.

We studied the neurobiological principles involved in motion detection using a technique of single neuron recording combined with optical microstimulations of single photoreceptor cells on the retinal mosaic (rev.1). In this way we attained the functional diagram of an Elementary Motion Detector (EMD), from which we derived a miniature analog electronic circuit for sensing directional motion (2). We then conceived a robot that would guide itself visually on the basis of such biology-derived EMD's (3). This Robot-Fly ('robot-mouche') was equipped with a genuine compound eye and 118 EMD's that would sense the optic flow field in the azimuthal plane and control the steering so as to avoid obstacles while the (12 kg) robot was running at a relatively high speed (50cm/s) (4). Simulation studies showed that such a robot can automatically adjusts its speed to the density of obstacles present in the environment, because the radius of vision appears to be proportinal to speed (5). Further studies showed that the same principles of motion detection can be used to guide a flying robot (6), have it follow a rough terrain and land automatically (7). The principle was validated on-board a miniature helicopter system (with collective pitch but without a swashplate) equipped with a camera eye, fly EMD's, and an inertial system. The whole rotorcraft (0.8 kg), which is mounted at the the tip of a whirling arm, has only 3 degrees of freedom (7) and reaches speeds up to 6 m/s.

In two other projects, we studied the benefits of a controlled microscanning, like the one we recently discovered in flies using single unit recording on the behaving animal (8). One of the principles inspired by our biological findings was implemented onto a 0,7 kg wheeled robot that succeeded in avoiding the (contrasting) walls of an arena in spite of the very low resolution of its eye (24 pixels) (9). The second principle was implemented onto a miniature (0.1 kg) twin-engine, twin-propeller aircraft which, while hanging from a 100µm wire attached to the ceiling, can fixate a target and track it regardless of its distance (up to 2.5 m) and contrast (down to 10%). This latter project also exemplifies how two sensory modalities, visual and inertial, can be fused to improve the stability and performances of micro air vehicles - which are difficult to control due to their small mechanical time constants.

The biorobotic approach we followed since 1985 appears to be fruitful in two ways. On the one hand one can glean interesting ideas, opening to novel questions about the utility and working of natural microsystems. On the other hand this approach opens up to the design of autonomous, sensory-motor vehicles and micro vehicles that can capitalize on the million-century experience of biological evolution.

References :

[1] N. Franceschini, A. Riehle, A. Le Nestour, Directionally Selective Motion Detection by Insect Neurons In: Facets of Vision, (Eds D.G. Stavenga & R.C. Hardie), Springer, Berlin, pp. 360-390, (1989)

[2] N. Franceschini, C. Blanes, and L. Oufar, Appareil de mesure passif et sans contact de la vitesse d'un objet quelconque
Dossier Technique ANVAR/DVAR N° 51 549, Paris, (1986).

[3] J.M. Pichon, C. Blanes, N. Franceschini, Visual guidance of a mobile robot equipped with a network of self-motion
sensors
In: Mobile Robots IV (Eds. W.J. Wolfe and W.H. Chun) Proc. S.P.I.E. 1195, Bellingham, U.S.A., pp. 44-53 (1989)

[4] N. Franceschini, J. M. Pichon, C. Blanes, From insect vision to robot vision
Phil Trans Roy Soc Lond B 337, pp. 283-294, (1992)

[5] N. Martin, N. Franceschini, Obstacle avoidance and speed control in a mobile vehicle equipped with a compound eye
In: Intelligent Vehicles, E. Masaki (ed.) M.I.T. Press, Cambridge, U.S.A.. 381-386 (1994)

[6] F. Mura, and N. Franceschini, Visual control of altitude and speed in a flying agent,
In: Proc From Animals to Animats, (eds. D. Cliff and P. Husbands), Cambridge, pp. 91-99, (1994).

[7] T. Netter, N. Franceschini, Neuromorphic optical flow sensing for nap-of-the earth flight.
In: Mobile robots XIV, SPIE Vol. 3838, Bellingham, USA, pp. 208-216 (1999)

[8] N. Franceschini, R. Chagneux, Repetitive scanning in the fly compound eye
In: Proc Göttingen Neurobiology Conf. (1997)

[9] F. Mura, N. Franceschini, Obstacle avoidance in a terrestrial mobile robot provided with a scanning retina
In:Intelligent Vehicles II (Eds M. Aoki and I. Masaki), pp. 47-52 (1996)

[10] S. Viollet, N. Franceschini, Visual servo-system based on a biologically-inspired scanning sensor
In: Sensor fusion and decentralized control II, SPIE Vol. 3839, Bellingham, USA, pp. 144-155 (1999).

Sensorimotor technologies: from biology to artificial systems (and viceversa).

Giulio Sandini, Giorgio Metta, Francesco Panerai, Lorenzo Natale, Riccardo Manzotti

LIRA-Lab – DIST – University of Genova – Italy

Abstract

This talk will present some aspects of sensorimotor coordination implemented in a humanoid robot named Babybot [1, 2]. The main scientific issue studied is the development of sensorimotor coordination in humans and Babybot represents a physical result of such studies. Beside describing the overall objective of our research we will focus on some technologies which we believe are relevant for sensorimotor coordination both from an engineering and from a scientific perspective.
In particular we will describe:

1) The use of simulated elastic actuators and their control for manipulation.
2) The use of retina-like visual sensors and their peculiarities with respect to visuo-motor coordination.
3) The use of inertial sensors for image stabilization and eye-head coordination.
4) The use of acoustic information and visuo-acoustic integration for sound localization.

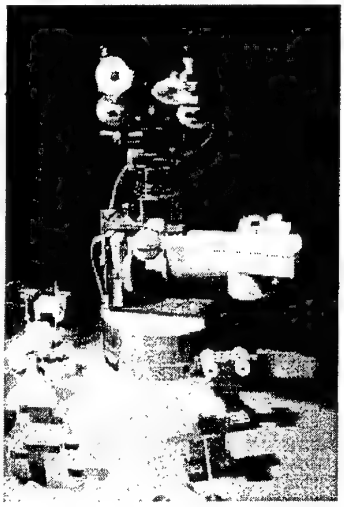

Figure 1: Babybot

In Figure 1 to the left the overall view of Babybot is presented. The robot is composed of a 4 d.o.f. arm-torso, a 5 d.o.f. head. The control of the robot arm is performed by simulating elastic actuators according to a model proposed by Bizzi et. al. known as "force fields". According to this schema, the control of the limbs is obtained by combining motor primitives coded by neurons at the level of spinal cord. The sensorimotor coordination task chosen as reference is that of "reaching" under visual control. Babybot peculiarity is the fact that this action is learned starting from a few initial reflexive behaviors similar to those found in newborn humans. Learning is performed by exploring the visuomotor space and by observing the position of the end-effector with respect to the fixation point. Vision is driven by a combination of color, motion and disparity information.
The visual system is based on retina-like cameras which are characterized by a space-variant resolution mimicking the distribution of photoreceptors in the human retina. Density of photoreceptors is highest in the center (limited by the particular technology used) and decreases monotonically toward the periphery of the Field of View (FOV). The resulting image is, consequently a compromise between resolution, amplitude of the FOV, and number of pixels. Such space-variant image is peculiar because it allows high-resolution tasks using the central region while maintaining a lower resolution part providing relevant information about the background. Such arrangement is advantageous, for example, for target tracking: the wide peripheral part is useful for detection while the central part takes over during the tracking and performs with the highest accuracy.
Of all possible implementations of space-variant sensors what will be described in this paper is the so-called *log-polar* structure [3-5]. In this schema a constant number of photosites are arranged over concentric rings (the polar part of the representation) giving rise to a linear increase of the receptor's

spacing with respect to the distance from the central point of the structure (the radius of the concentric rings).

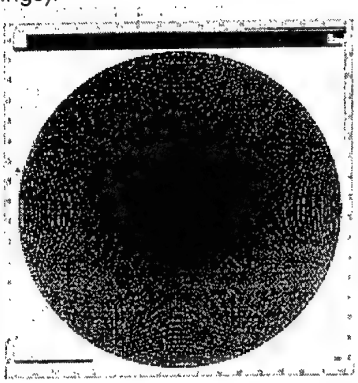

Figure 2: Layout of receptor's placing for a log-polar structure composed of about 100 rings with 250 pixels each.

A possible implementation of this arrangement is shown in Figure 2. Because of the polar structure of the photosensitive array and the increasing size of pixels in the periphery, retina-like sensor, do not provide images with a *standard* topology

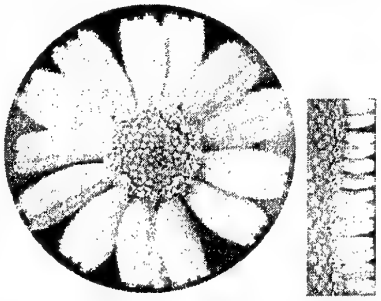

Figure 3: *Retinal* (left) and log-polar (right) image of a flower.

Because of the polar arrangement and space variant structure of the sensor the output image is represented in a so-called log-polar format where rings are mapped to vertical lines and radii are mapped to horizontal lines (see Figure 3). As far as motor control is concerned the main advantage related to the small number of pixels and the comparatively large FOV, is the fact that for some important visual tasks images can be used as if the all image was high resolution and, at the same time the lower resolution in the periphery provides vital information to understand what is happening in the field of view. Typically, for example, in target tracking where the fovea allows precise positioning of the tracking device and periphery allows the detection of moving targets. This peculiarity is exploited to control the robot head of *Babybot* (see [1, 2]). In this implementation a log-polar sensor with less than 3000 pixels is used to control in real-time the direction of gaze of a 5 degrees of freedom head using a Pentium PC. Particularly relevant is the possibility of controlling in a simple way the vergence angle of the stereo-head [6] as well as the integration of visual and inertial information for image stabilization [7, 8].

Figure 4: The artificial vestibular system

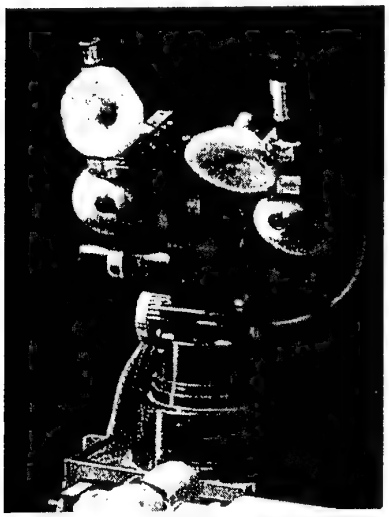

Figure 4: Babybot's head showing the eyes (blue) and the asymmetric ears.

In the initial stages of sensorimotor development, vision cannot really stabilize images sufficiently. Also for adults, image stabilization is obtained by integrating visual and inertial information thought a reflex called *vestibulo ocular reflex* (or VOR). In order to exploit this reflex we developed an inertial sensor (based on a rotational accelerometer produced by Murata) proving angular velocity around three orthogonal axes modeling the Semicircular Canals of human vestibular system.

This sensor was used to study the role of inertial stabilization in the development of oculomotor control. Results showing the role of VOR during development will be presented.

Finally the study of sound localization has been studied from two perspectives: 1) to implement a system able to locate sound sources on the basis of bi-aural information; 2) to investigate the role of vision in refining the sound localization map. The biological bases are derived from the auditory system of the barn owl. Estimates of displacements in the horizontal plane are obtained through a measure of time difference while in the vertical plane the intensity

difference due to the asymmetric configuration of the "ear lobes" is used. In Figure 5 the head of Babybot is shown. The ears are the two asymmetric conic pads on the top.

The results obtained during our study [9] were used, besides studying the implementation of a complex, adaptable system, to investigate aspects of human sensorimotor development. In that respect, some of the inspiration we got from biology has been used to test and propose different theories that should be tested on biological systems. Among them: 1) the role of VOR in the development of vergence control; 2) the role of vergence in tuning the gain of VOR; 3) the role of "neural noise" during the tuning of eye-head-hand coordination; 4) the effect of a low-resolution visual sensor in tuning saccades; 5) the role of the expansion component of optical flow for vergence and fusion. These are still a few examples of what we believe could be an important tool to study human behavior, namely, the implementation and use of biologically inspired artificial systems.

References

1. Sandini, G., G. Metta, and J. Konczak. *Human Sensori-motor Development and Artificial Systems.* in *AIR&IHAS '97.* 1997.
2. Metta, G., G. Sandini, and J. Konczak, *A Developmental Approach to Visually-Guided Reaching in Artificial Systems.* Neural Networks, 1999. **12**(10): p. 1413-1427.
3. Weiman, C.F.R. and G. Chaikin, *Logarithmic Spiral Grids for Image Processing and Display.* Comp. Graphic and Image Process.,, 1979. **11**: p. 197--226.
4. Sandini, G. and V. Tagliasco, *An Anthropomorphic Retina-like Structure for Scene Analysis.* Computer Vision, Graphics and Image Processing, 1980. **14**(3): p. 365-372.
5. Schwartz, E.L., *A Quantitative Model of the Functional Architecture of Human Striate Cortex with Application to Visual Illusion and Cortical Texture Analysis.* Biological Cybernetics, 1980. **37**: p. 63-76.
6. Capurro, C., F. Panerai, and G. Sandini, *Dynamic Vergence using Log-polar Images.* International Journal of Computer Vision, 1997. **24**(1): p. 79-94.
7. Panerai, F. and G. Sandini, *Oculo-Motor Stabilization Reflexes: Integration of Inertial and Visual Information.* Neural Networks, 1998. **11**: p. 1191-1204.
8. Panerai, F., G. Metta, and G. Sandini, *Visuo-inertial Stabilization in Space-variant Binocular Systems.* Robotics and Autonomous Systems, 2000. **30**(1-2): p. 195-214.
9. Metta, G., *Babyrobot: A Study on Sensori-motor Development*, in *Dipartimento di Informatica, Sistemistica e Telematica.* 1999, University of Genoa (PhD Thesis): Genova, Italy.

TACTILE FLOW: DOES IT EXIST, IS IT USEFUL, AND HOW?

ANTONIO BICCHI
PASQUALE SCILINGO
Centro E. Piaggio, Universita di Pisa, Italy

ABSTRACT

In the analysis of human and artificial vision, optical flow has been widely recognized to be crucial in fast sensorymotor coordination and feedback. Optical flow is basically an abstraction of raw data coming from the sensor (retina or camera), that extracts information on the relative velocity of the sensor and the visual target by observing how fast the target image grows in time. Different image sequences may have identical optical flow, so that there is a loss of information. However, optical flow of artificial images can be easily computed, and this information has been successfully used in several applications (for instance, in estimating the time-to-contact for automobiles proceeding in a line, thus enabling collision avoidance strategies). On the other hand, experimental evidence has been obtained through Functional M.R.I. techniques that some cortical areas are specifically excited by optical flow, thus proving that it is deeply rooted in human psychophysics.

In this talk, we will inquire into the existence of a similar concept in a different sensorial domain, that of tactile perception. The goal of such investigation is twofold: on one side, there is a fundamental interest in the psychophysics of a less-explored perceptual channel such as touch; on the other hand, many possible fallouts may ensue in disciplines where a sensorial substitution and simplification would be important: haptic displays for VR and prosthetics are two examples.

In particular, we are interested in establishing whether a description of "tactile flow" can be given that i) codifies important information for manipulation operations; ii) is amenable to implementation in haptic displays and/or prosthetics, and iii) has a connection to the psychophysics of touch in humans.

Some of these questions have a positive answer, while others are still open, even though we have encouraging preliminary results. We will show how tactile flow can be defined in terms of the displacement of iso-stress curves on the surface of bodies in contact at varying the overall compression force, and how this definition is consistent with the "Contact Area Spread Rate" observed under increasing load. Through extensive psychophisic testing, we also established that CASR (hence tactile flow) conveys to humans an information on the softness of the object being probed by a finger. We will also illustrate some technological implementations of both actuators and displays of tactile flow information, and will highlight their limitations and the requirement for new sensitive/active materials that might allow to exploit the potentials of tactile flow displays in applications.

Forming active structures with embedded sensors.

Yuka Yoshioka[1], Paul Calvert[1] and Mousa Ghaemi[2]
[1]University of Arizona, Materials Science and Engineering, Tucson, AZ
[2]Mazandaran University, Iran

Introduction

An animal can be thought of as a complex composite containing regions that act as actuators, sensors and power supplies in addition to the mechanical support structure. In principle a synthetic composite could also be built with these functions combined into a monolithic object. Recent developments in layerwise processing suggest how this might be achieved.

Solid freeform fabrication is a family of rapid prototyping methods that build a material layer-by-layer to form a final shape. This approach allows more freedom of design than conventional molding, for instance a loose ball inside a closed box or a set of movable meshed gears can be formed. In biological growth, solids form through chemical reaction between soluble species in a layer-by-layer process. This suggests that freeform methods could also be applied to processes where solids are formed by chemical reaction. Conventional molding methods are incompatible with the large shrinkages of most chemical solidification reactions, so that only fibers and films can be made. If the structure is built in layers, the shrinkage can be accommodated as the layers form. Also, as in biology, it becomes natural to design parts from several different materials and to connect these via compositional gradients rather than sharp interfaces.

Building a crude organism would require resolution at the scale of about 10 microns. Most current freeforming methods allow resolution down to about 100 microns with a limited materials set. Microcontact printing and related methods allow much higher resolution, down to about 1 micron but effectively are restricted to one layer [1]. There is much current interest in ink-jet printing methods which could provide the required 10 micron resolution while allowing many layers to be deposited [2].

In both synthetic and biological structures, it is useful to keep in mind a distinction between design and patterning. Phase separation, crystallization and aggregation processes can give rise to patterns in two- and three-dimensions on a scale, from millimeters to nanometers, which reflect the kinetics of the separation and diffusion processes. To form working devices or organisms, we need to build to a non-recurring design, which may include patterned elements. If we seek to adopt biomimetic processes, we will need to exploit self-assembling structures and patterns but within an overall design. In biology there are many examples of patterns forming at the nanometer level but most designs are on the scale of individual cells, a few tens of microns. There are structures, such as sensing hairs, which are much finer but the spacing between them is still on the 10 micron scale.

Previous work on embedded sensors

In the past we have used freeforming techniques to incorporate optical fiber sensors into epoxy resins in order to monitor curing and water uptake. The aim was to make a system that was a simple as possible as a model for a potential network of freeformed optical waveguides formed integrally with the resin. A silica fiber was embedded to terminate slightly below the polymer surface. Ambient light was collected through the resin layer and near-IR spectroscopy used to monitor the state of the resin [3]. Whilst it is effective this system depends on an impracticably large spectrometer attached to the part.

Polyvinylidenefluoride piezoelectric stress sensors were built into freeformed resin parts and used to monitor external stress and curing. Such sensors were also built into composite honeycomb-core composite panels. The output of the embedded piezoelectric was compared with that from an external instrumented impactor. The embedded sensor showed evidence of delamination occurring below the surface of the panel during the impact [4, 5].

Since these methods depend on introduced, preformed sensors, they really do not lend themselves to forming the sensor network concurrently with the part. It is possible to use freeforming methods to write conducting lines and carbon-polymer ink chemical sensors. What has been lacking so far is a simple, write-able stress sensor that could be built into a freeformed part in large numbers. This could be used to provide the kind of control that is available to insects during motion from the network of proprioceptors distributed across the cuticle.

Recent work in our laboratory on hydrophilic epoxy gels suggests that very effective write-able strain sensors could be formed from conducting gel composites. This is discussed in more detail below. We have also recently succeeded in inkjet printing multilayer structures, such that fine-scale sensing structures could be incorporated into freeformed objects using a combined processing technology.

Epoxy hydrogels as microactuators and sensors

Rapid response and reinforced structures are strongly needed in muscle-like actuators which change their structure and physical properties by external signals. Miniaturization is one of the approaches toward the development of polymer devices, since the speed of the volume change is proportional to the square of the gel size. Ionizable polyelectrolyte-hydrogel has long been studied as an actuator material [6]. In past work, we made electrically-driven actuators based on an asymmetric stack of acrylic acid and acrylamide hydrogel. The different response of the two surfaces resulted in a linear contractions and expansion, rather than bending, when current was passed [7]. We wanted to make sub-millimeter scale versions of these actuators but it is difficult to carry out controlled free radical polymerizations on this small scale. Condensation routes to gel

actuators have not been explored and highly crosslinked amine-epoxy networks are expected to give enough strength for practical use.

In this study, a small drop of cationic polyelectrolyte gel was prepared by the crosslinking of trifunctional polyetheramines with ethylene glycol diglycidyl ether. In aqueous solution at alkaline pH, the amines are essentially uncharged and hydrogen bonding interactions cause the volume collapse. Addition of an acid will generate positive charges on amine groups and this charge repulsion causes swelling. Subsequent immersion in water results in even greater swelling. The complex response of these materials to pH and metal ions will depend on crosslink density and ionic strength of the medium. Here two types of polyetheramines, which have different molecular weight, are used. Each of them produces large deformation (20-30 %) and respond in about 5 minutes with sub-millimeter thick stacks. They have been used to make small actuators based on electrically-induced volume changes.

Gels were prepared by crosslinking of Jeffamine (Huntsman Chemical Co.) and ethyleneglycol diglycidylether in aqueous or methanol solution. The molar ratio of epoxide in EGDGE to $-NH_2$ in Jeffamine was adjusted to give different densities of ionizable groups. 15-30 wt% of sucrose was added into solution to prevent collapse of the gels during polymerization and 5-10 wt% of fumed silica was added to prevent the monomer solution from flowing off the substrate before curing. The polymer precursor was heated at 70°C for several hours. Finally, sucrose loaded gel particles were washed thoroughly with distilled water. Gel drops (approx. 50 micron) were made by extrusion freeform fabrication on a platinum-coated silicon substrate and their swelling response to pH change and to electrical stimulation was determined [8, 9]. The gels are swollen at low pH where the excess amine groups become ionized.

In the course of this work, it was realized that these gels could be used as strain sensors. Small dots were formed with about 15 vol% of carbon black. In response to applied pressure, figure 1, fluid was extruded from the gel, reducing the volume and so increasing the conductivity. In addition, figure 2, the fluid loss resulted in a potential difference between an electrode in the gel and an external electrode, figure 2. These sensors have the advantage of being highly sensitive to stress and to being readily formed by freeforming or printing methods.

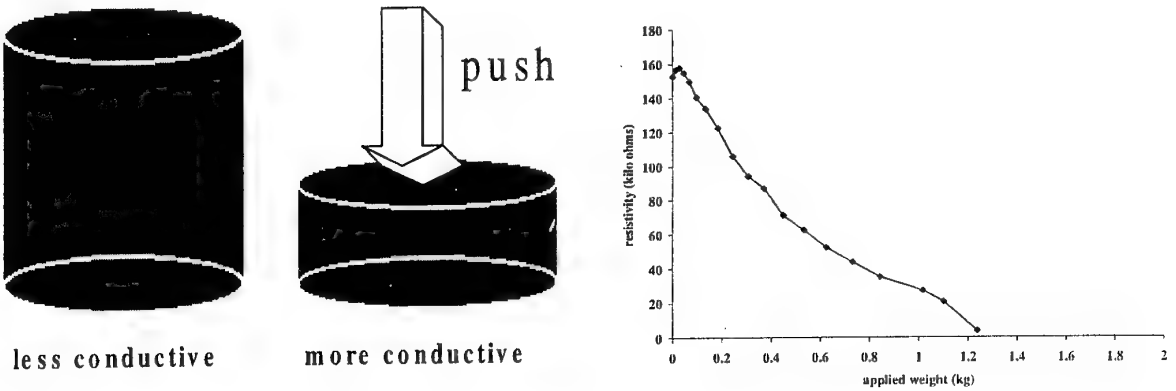

Figure 1: Schematic of a carbon-filled hydrogel strain sensor and response of resistance of an epoxy-amine gel.

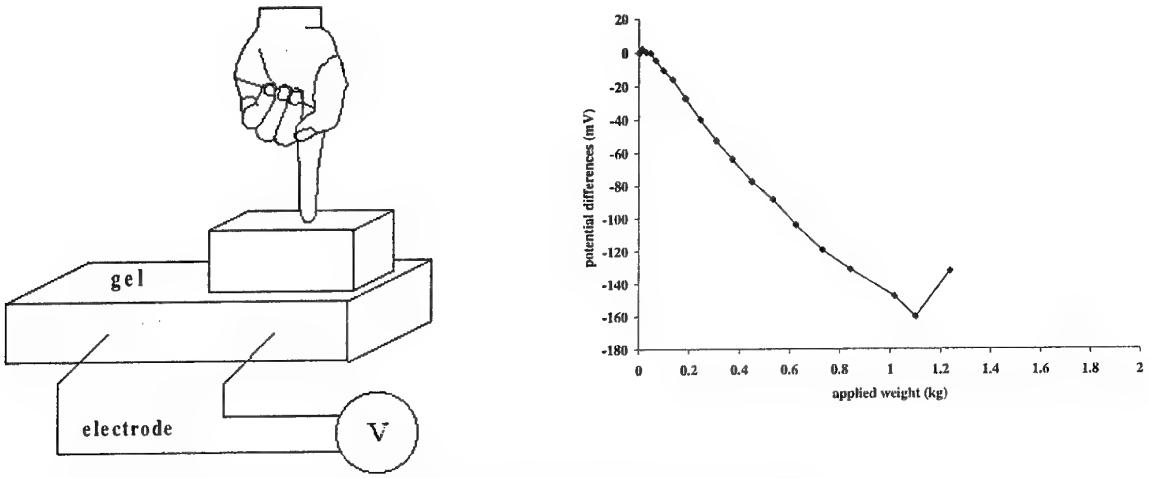

Figure 2 Potential difference response of a hydrogel to strain

Inkjet printing of structures and devices

A wide range of materials can be inkjet printed. Almost all current applications concern single layers of a material printed from solvent or suspension. There is need for a rapid direct-write technology that can be used to form devices of low temperature materials, including organic semiconductors, polymers and biopolymers. These will require several layers of different materials to be overprinted. There will also be pressure for much higher resolution than that obtainable with current printers. As well as the devices being organic, much of the need is for them to be formed on flexible polymeric substrates. The low surface energy of polymers makes the wetting more difficult and the flexing of the substrate implies a need for toughness in the device materials.

When ink is printed onto a non-adsorbent surface, it will tend to bead up, rather than form a uniform layer. In printing on transparencies, this can be controlled by use of a swelling polymer layer, a transparent but porous layer and a roughened surface. If a material is to be built from many deposited layers then these wettability questions must be resolved for inks on a previous layer of ink.

Printing of multiple ink layers onto a hard surface, with a drying time between layers, will result in redissolution, resuspension or remelting of each previous dry layer of ink in the new liquid. A mechanism is needed to harden or insolubilize each layer before the next one is deposited. Examples given above include UV curing and thermal treatment. This can also be achieved by printing a pair of inks that react to form a solid layer, by curing or by the sol-gel reaction. In addition, this insoluble layer may be dense or may be a layer of porous matrix that will take up an active material. It is thus quite possible, through combinations of materials chemistry, to either form a single layer through the interaction of several inks or to form a stack of solid layers.

Many device technologies depend on uniform insulating layers separating active components. However, inkjet printed layers often contain pinholes. Several groups have found it difficult to prevent shorting between layers. A good understanding of the formation of pinholes in printed layers will certainly be necessary if the technique is to be used for device manufacture.

Resolution is being addressed aggressively in the context of photoprinting but here the issue is partly a tradeoff between drop size and speed, which would not necessarily affect printing of devices. While droplet diameter will decrease from the current 20-30 μm, the constraints arising from viscous flow through a small hole would seem to make unlikely direct printing to linewidths of less than 10 μm. There is certainly the possibility of using controlled wetting on patterned surfaces to reduce linewidth, although it remains to be shown how this could be applied to subsequent layers of a more complex structure. In making any direct comparison between inkjet printing and photolithography, it should be kept in mind that multilayer printing methods are more truly three –dimensional and should allow many more layers to be added. Assuming ink with a solids volume fraction of about 10%, layer thicknesses are of the order of a few microns.

One clear materials challenge is that of attaining high conductivity metal electrodes. A printed nanoparticle layer would also need good particle-particle contact to reach high conductivity but nanoparticle suspensions have surfactant layers on the particle surface. The metal precursor route is successful but requires temperatures that are too still high for many active materials and substrates. In addition the electrode layer has to be strongly adherent and flexible. The same issues arise if it is desired to print layers with a high dielectric constant, with a strong piezoelectric response or with semiconducting properties; the properties of a film made by low temperature chemistry are usually much inferior to those of an evaporated or sintered material.

In a search for higher resolution than is obtainable by freeforming, we have been depositing gels by inkjet printing with a view to treating the gel layers with mineralizing solutions. The ideal "inks" for such a process would be pairs of water-soluble polymers or monomers that gel rapidly when printed in successive thin layers.

Dilute solutions of polydimethyldiallylammonium chloride ("Very low molecular weight", Aldrich Chemical Co.) and polystyrenesulfonate were printed sequentially onto glass slides using a modified HP Deskjet 1200 printer. The polymer rapidly redissolved when the slide was immersed in water. A wet anneal was carried out on the printed films at 70C over a water reservoir. The film then became insoluble in water but slowly detaches from the slide when immersed. Replacing the anionic polymer with the sodium salt of a maleic acid-styrenesulfonic acid copolymer allows the film to remain attached to the glass through subsequent immersion in water. The films still detach in water if deposited on polyester substrates.

A similar approach has been used to print films of sub-micron alumina particles by making a dispersion of alumina with the anionic polymer and then overprinting with the cationic polymer. Again the film will disperse if immersed in water as deposited but becomes insoluble after annealing overnight. Figure 3 shows the structure of such an alumina film bound by a cation/anion polymer gel. This approach has also been used to make films of epoxy resin from a water-soluble amine and a water-soluble diepoxide. IR studies of films deposited on silicon show that in this case the gelling reaction occurs during deposition. Figure 4 shows IR difference spectra of a 5 layers of epoxy resin (glycerol diglycidyl ether) printed from a 5% aqueous solution and the same material overprinted with 5 layers of a 5% solution of triethylene tetramine.

A single printed layer of 5% solution results in a film thickness of about 25 microns which would then become a liquid epoxy film of approximately 1 micron once the water is lost. Diffusional mixing of small molecules in aqueous solution on this scale would be expected to take about 5 minutes at most. Hence, A single layer may form by diffusion followed by reaction or two layers separated by a barrier if reaction prevents further diffusion, as illustrated in figure 5. In this case, the epoxy/amine films seem to be substantially reacted as they are deposited, both as alternating single layers of epoxy and amine and as alternating stacks of five layers of each. Also, no IR changes are seen on subsequent annealing.

In the case of the gelation of cationic and anionic polymers, the combination of slow diffusion and rapid complex formation presumably leads to the formation of a skin but no further gelation during the short time the system takes to dry. Annealing in a humid environment allows further gelation until an insoluble layer is formed.

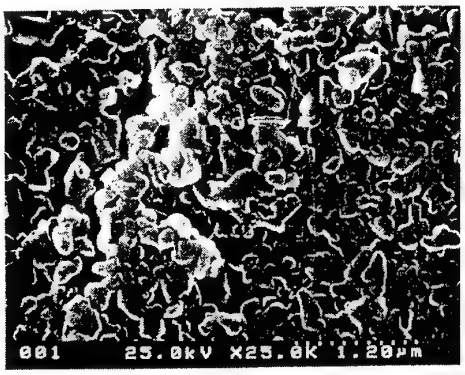

Figure 3. Alumina layer formed by printing 0.18 micron powder (Sumitomo Co.) with anionic polymer dispersant and cationic polymer solution.

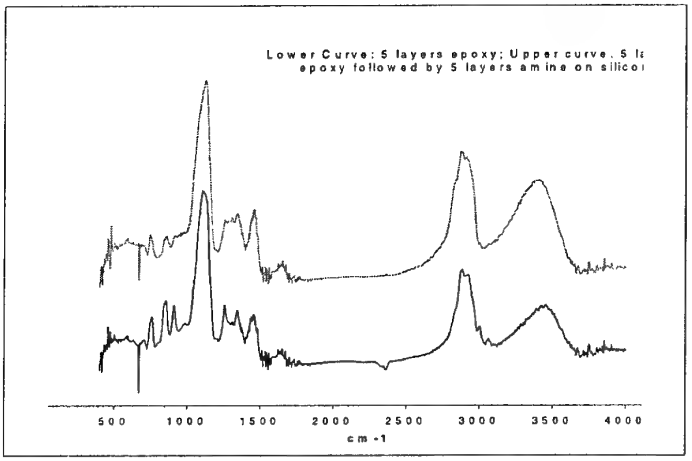

Figure 4. IR absorbance spectra of 5 layers of epoxy (lower) and 5 layers of epoxy followed by 5 layers of amine (upper), silicon substrate subtracted.

Inkjet printing of water-soluble epoxy and amine allows thin solid films to be built up rapidly. Printing solutions of cationic and anionic polymers allows self-assembly to insoluble gels if the films are annealed in a humid atmosphere. The same approach can be applied to combinations of ceramic powders, modified with ionic dispersants, and ionic polymers.

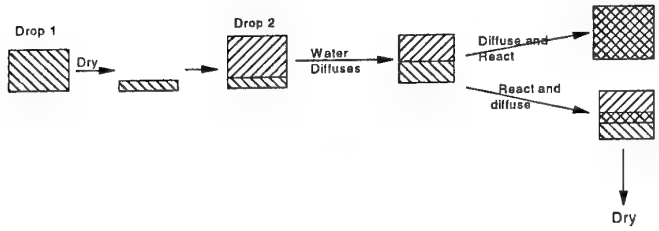

Figure 5: Print and react model.

Conclusions

Recent advances in freeforming and other similar multilayer printing methods make it possible to conceive of designing integrated objects containing structural elements, sensors, actuators and power sources.

References

1. Xia, Y. and Whitesides, G., "Soft Lithography", *Annual Review Of Materials Science* 28, 153-184, 1998.

2. Fan, H., Lu, Y., Stump, A., Reed, S., Baer, T., Schunk, R., Perez-Luna, V., Lopez, G. and Brinker, C., "Rapid prototyping of patterned functional nanostructures", *Nature* 405, 56-60, 2000.

3. Calvert, P., George, G. and Rintoul, L., "Monitoring of cure and water uptake in a freeformed epoxy resin by an embedded optical fiber", *Chem. Mater.* 8, 1298-1301, 1996.

4. Calvert, P. D., Denham, H. B. and Anderson, T. A., " Free-form fabrication of composites with embedded sensors.", *Proc. SPIE-Int. Soc. Opt. Eng. (Sensory Phenomena and Measurement Instrumentation for Smart Structures and Materials)* 3670, 128-133, 1999.

5. Denham, H. B., Anderson, T. A., Madenci, E. and P. Calvert, "Embedded PVF2 sensors for smart composites", *SPIE Proceedings* 3040, 138-147, 1997.

6. Calvert, P."Electroactive polymer gels" in *Electroactive Polymer (EAP) Actuators as Artificial Muscles - Reality, Potential and Challenges* (eds. Bar-Cohen, Y.) (SPIE Press, Vol. PM98, 2001) pp. 123-138.

7. Liu, Z. and Calvert, P., "Multilayer hydrogels as muscle-like actuators", *Adv. Mater.* 12, 288-291, 2000.

8. Yoshioka, Y. and Calvert, P., "Electrically stimulated hydrogel as microactuators", *PMSE Preprints (ACS)* 84, 335-336, 2001.

9. Yoshioka, Y. *Introducing Epoxy Based Hydrogels As Electrically Driven Muscle-Like Microactuators* (University of Arizona, 2001).

TEXTILES AS A COMMUNICATION PLATFORM

Barry Holcombe
CSIRO Textile and Fibre Technology
Belmont, Australia

Background

Over the next decade or so, clothing seems destined to be transformed from its present role as a passive protector against the elements and a fashion statement into an integral element of lifestyle-related activities. Undoubtedly fashion will remain important but the focus will shift strongly in the direction of functionality. Wearable electronics products with in-built consumer electronics such as the Levis ICD+ jacket are already a reality and groups such as Philips Research are heavily involved in projects that propose to use clothing as the platform for a range of communication, computing and entertainment accessories or to monitor the physiological functions of the wearer.

At the moment, both commercial and prototype wearable electronics systems use discrete 'deconstructed' devices located in pockets throughout the clothing and connected by conventional wiring technologies. Similarly textile-based physiological sensing systems currently involve copper wiring as the connecting medium.

Tactile properties such as stretch and recovery, drape and handle are fundamental aesthetic requirements of apparel textiles. The incorporation of elements such as copper wire within garments increases stiffness and reduces elasticity. Whilst this may be acceptable in outer garments such as jackets, it would be more noticeable in underwear or items worn near the skin and impact negatively on wearer comfort. In the longer term, it is desirable and inevitable that there be seamless integration of these devices with their textile substrates. Both connections between components and interfacing with the real world are likely to be based on conductive pathways using modified textile products such as fibres or polymer films and coatings rather than copper.

The textile industry currently uses several major technologies to assemble fibres into fabrics, each of which produces unique aesthetic and mechanical characteristics. In the short term, the incorporation of additional functional requirements such as conductivity will only be possible by manipulating these existing technologies and adding functionality to the basic textile requirements of wearer comfort, drape, handle, durability and washfastness. In the longer term, it is likely that the textile manufacturing pipeline will undergo substantial change as the extent of functionality increases and new technological developments are adopted.

Functionality is relatively new to the textile industry. Much of the development of 'functional' textiles has been in the area of active sportswear where the technical knowledge of consumers is relatively high and more attention is given to differentiation. Properties such as uni-directional sweat transport, thermal insulation and water repellency with breathability have been achieved through innovative approaches to fabric construction. Some of these concepts can be extended to accommodate the new demands of wearable electronics and sensing systems.

Fabric formation processes

Textiles are essentially 3-dimensional arrays of fibres held together by interlacing and frictional forces or by inter-fibre bonding. The manufacturing pipelines used in their production can be grouped into three main areas: non-woven, weaving and knitting. Each produces structures with quite different physical and aesthetic properties that make them suitable for particular end-uses. Non-wovens involve random entanglement of individual fibres. For weaving and knitting, fibres are first converted into yarns which are then assembled in defined structures.

Non-wovens

The simplest and cheapest fabric manufacturing technology is the non-woven route where a web of fibres is prepared and then either systematically entangled or chemically bonded. Entanglement can be either transverse penetration by a bed of needles or high-pressure water jets. Bonding can be with adhesives or thermal fusion at interfibre contact points. The resulting product is a two-dimensional fibre lattice with mechanical properties similar to those of felts. They are mainly used for industrial applications such as filters, disposables, geo-textiles and medical products. They have poor elasticity and are not often used for apparel, although they are sometimes used as liners in garments such as jackets.

It is conceivable that a non-woven liner could be used as the networking platform of a garment. Conductive yarns could be incorporated into the fibre web prior the interlacing process in both longitudinal and transverse directions or even defined 2-dimensional configurations to access specific locations within a garment panel. The technology to achieve this does not exist currently but it would require only relatively minor modification to existing machinery.

Wovens and knits

Yarn formation

The other two primary fabric manufacturing technologies are based on yarns. Natural fibres are harvested in discrete 'staple' lengths and twisted or 'spun' to produce a stable structure held together by fibre-to-fibre friction. Synthetic fibres are extruded as continuous filaments. Continuous filament yarns are quite dead in handle and are often bulked or texturised to give them softer handle. They can be cut into staple form and spun with the same technologies used for natural fibres to achieve some of the characteristics of natural fibre yarns. The main requirement in converting fibres or filaments into yarns is the achievement of sufficient strength to withstand the stresses of further fabric assembly processes. Secondary issues include softness, flexibility, appearance and other aesthetic characteristics. Both technologies can be manipulated to combine different fibres or filaments within the same yarn or fabric.

In the spinning processes used in the manufacture of yarns from staple fibres, two or more different fibres can be intimately blended during yarn formation. A slight modification of the process can be used to produce core-spun yarns consisting of a core of one fibre type wrapped by a covering or sheath of another. The core can also be in the form of continuous filaments. Thus it is possible to have the whole yarn as an integral conducting unit, or as an insulated conductor in which a conductive core is surrounded by an insulating sheath. A recent development of the extrusion process for synthetic filaments is the production of bi-component fibres consisting of two different polymers within the same fibre-cross-section. The application of the concept has thus far been limited to the development of yarns with unusual handle characteristics, but it is quite conceivable that it could be used to produce a yarn with a conductive core and an insulating sheath. The yarns used for woven and knitted fabrics are manufactured with slightly different levels of elasticity to accommodate the different strains imparted during each method of fabric formation.

Woven structures

Woven fabrics consist of two groups of yarns (the warp and weft) interlaced at right angles in a regular pattern that typically repeats after two or more yarns in both directions. Complex patterns are possible but are generally used to produce decorative effects rather than specific properties. The yarn interlacing patterns of woven structures make it difficult to bury a yarn so that it is not exposed at some point on both faces of the fabric. It is possible to alternate fine and coarse yarns so that one effectively projects higher than the other, or to increase the complexity of the weave pattern to produce thicker fabrics in which a yarn

can be kept from the surface. However such fabrics are quite heavy and stiff and generally used for engineered mechanical structures rather than apparel.

In terms of conducting paths within woven fabrics, conducting elements can only be incorporated in wovens in the directions in which the yarns are oriented, i.e. at right angles. A technology known as triaxial weaving interlaces yarns at an angle to the longitudinal direction of manufacture but this is only used for specialised engineering fabrics.

Knitted structures

Knitting is by far the most flexible of all fabric manufacturing technologies. Yarns are interlaced by looping one through another effectively forming chains of loops. There are two different knitting system; warp knitting and weft knitting. The main difference between them is the direction in which the yarns forming the loops are predominantly oriented. Although the yarn normally follows a quite curvilinear configuration in the structure, it is possible to use technologies known as laying-in and striping to incorporate yarns either longitudinally or transversely to the direction of fabric manufacture. One great advantage of knitted structures is that the technology is very flexible and the change from one structure to another is relatively quick, making the development process much simpler.

One area where there has been quite a lot of fabric structure development is active sportswear. At the performance end of this market consumers are quite technically aware and prepared to pay a premium for a product that they believe delivers technical benefits. An important technical focus is moisture management – transporting perspiration from the skin to the outside of the garment to maximise evaporation efficiency and removal of metabolic heat. By controlling fibre surface energy, fibre diameter and structure from fabric face to back it is possible to engineer a liquid gradient between the faces so that any perspiration picked up off the skin preferentially migrates to the outside of the fabric. Such fabrics are true 3-dimensional in both structure and performance. Another example of a 3-D textile structure is the 'Fastskin' swimsuit. This is a fabric with a surface profile modelled on the dermal denticles of the skin of the shark and claimed to improve the hydrodynamic flow over the body of swimmers.

Laminates

One of the most useful means of incorporating functionality into textiles is adhesive lamination. This process is used to bond two and sometimes more layers of fabric together, or to incorporate a membrane of some form. It is widely used in the manufacture of fabrics for rainwear in which a breathable polymer membrane that may be only 10μm thick is fixed to one face of a fabric, providing resistance to liquid penetration but allowing vapour to pass relatively easily. In some instances a second fabric is laminated to the other face of the membrane for protection against mechanical damage.

Membranes are either the microporous type based on stretched PTFE film, microporous polyurethane, solid hygroscopic polyurethane or polyester based polymers. The hygroscopic types (often described as hydrophilic) swell in the presence of moisture so that their vapour diffusion coefficient reduces.

In building a functional textile assembly containing physical devices or electrical circuits, the desired items could be sandwiched between two layers of fabric and thus protected both electrically and mechanically. Membranes could be used as the substrate onto which printed circuit tracks and other items could be deposited prior to lamination to a backing fabric. Membranes are quite flexible and robust, and some have elasticity comparable with that of most textile materials.

Fabric physical properties

In any merger of textile materials and functional technologies, one of the main constraints is that the normal textile behaviour is retained. Properties such as drape, elasticity and handle are fundamental to the subject comfort of garments and any technology that interferes significantly with these properties will be disadvantaged in terms of consumer acceptance, regardless of the functional benefit. For example, the thermal and vapour resistance of textile materials is linearly related to fabric thickness. The incorporation of a particular functionality that increases thickness may make the garment too uncomfortable to wear, regardless of its other benefits. In high activity conditions most body heat is lost through the evaporation of

perspiration, so that impermeable objects or layers within the textile assembly or thick composite fabrics will impact directly on vapour resistance and could make the garment unacceptably hot and uncomfortable in some conditions.

One of the most important properties of textiles that contribute to wearer comfort is stretch. Much of the extension of fabrics under load results from the straightening of yarns and fibres within the structure. The lattice structure of non-wovens provides less opportunity for re-arrangement, hence the characteristic stiffness of these structures. The interlacing of the yarns in woven fabrics results in about 5-20% more length than the dimensions of the fabric but in most woven structures this interlacing is quite densely compacted and the opportunities for stretch are limited – typically less that about 5%. With knitted fabrics, the yarn path length may be several times that of the fabric length, so that stretch in knitted structures can be in excess of 100%. This varies with the nature of the structure and its packing density.

The ability of Lycra fabrics to conform easily to the body surface and maintain good skin contact makes them ideally suited for textile-based strain and physiological monitoring systems. It is worth noting that Lycra fabrics in fact contain very little elastomer – typically less than 10%. Most of the fabrics generically described as Lycra are predominantly nylon, so that the chemistry of the application of conducting polymers to these fabrics must take this into account.

The addition of elastomers such as Lycra does not add stretch to fabrics. The maximum stretched dimensions of a fabric containing Lycra are the same as those of the base structure without Lycra. Elastomers increase elasticity by virtue of the fact that they cause the fabric structure to contract relative to the same fabric without elastomer, effectively making more yarn available for straightening when a load is applied. A fabric that would normally have 10% stretch might end up 10% smaller in length and width when elastomer is added during manufacture, so that its available stretch becomes 20%. The elastomer increases to force needed to extend the fabric and this can be varied by varying the fineness of the elastomeric filaments.

It is unlikely that the development of textile substrates with new forms of functionality will require textile structures that cannot be achieved with existing basic fabric formation technologies. It is simply not necessary as the range of structures available with these technologies is enormous. The challenge is to think laterally to apply these technologies in new ways. It is unlikely that fabric structure will be the main constraint in development in this area. Issues such as physical durability and resistance to laundering of conducting or semi-conducting polymers and other functional add-ons over the life of the garment pose far greater challenges in the short term.

Conclusion

The great flexibility of commercial fabric manufacturing processes offers an almost infinite variety of ways in which functionality based around electronics can be incorporated within clothing.

Up until now much of the evolution in textile structure has been driven by fashion - the need to differentiate each new season's product range, however differentiation is in terms of aesthetics rather than processing technologies. The technical textiles industry has contributed more to fabric structure development because of its need for fabrics with defined mechanical properties to meet specific end-use criteria. Needless to say, the merging of electronics and textiles will involve major changes to the textile processing pipeline and to a large extent the rate of evolution of this area will depend on how quickly the textile industry adapts to the new demands placed on it. At this point in time, the pressure is coming from the consumer products market rather than the textile industry itself and it is only a matter of time before this pressure escalates considerably. The textile industry is very traditional, extremely conservative and slow to change, mainly because it is very price-sensitive and capital investment is large. It is likely the tremendous opportunities for value adding posed by new end uses such as wearable electronics will change all this.

At this point in time there are a number of directions that the merging of textiles and electronics could take in terms of the technological processes involved. Only two things are certain: this merger will happen, and the textile industry will never be the same again.

ACTIVE DRESSWARE: WEARABLE HAPTIC SYSTEMS

D. De Rossi, F. Lorussi, A. Mazzoldi, E.P. Scilingo
Centro "E. Piaggio", Faculty of Engineering, University of Pisa, Pisa (Italy)
Piero Orsini
Unita Operativa Neurologia Azienda Ospedaliera Pisana, Ospedale Cisanello, Pisa, Italy

Introduction

Artificial sensory motor systems granting the power to reach out and interact with illusory objects and granting the objects the power to resist movement or to manifest their presence are now under development in a truly wearable form using an innovative technology based on electroactive polymers.

The integration of electroactive polymer (EAP) materials into wearable garments could endow them with strain sensing and mechanical actuation properties. Moreover, recent developments of "all polymer" devices are directed towards active electronic components (transistors) and batteries, thus providing in perspective all essential instrumental functions (sensor, actuator, processor, power supply) in materials and forms which could be integrated into fabrics.

The development and implementation of haptic garments has necessarily to rely on knowledge of biological perceptual processes which is, however, scattered and fragmented. Integration of different afferent and efferent muscular responses and commands to build up complex functions such as proprioperception, kinesthesia, stereognosis and haptics is far out of reach given our present understanding of perception.

Nevertheless, the combined use of new polymeric electroactive materials in the form of fibers and fabrics with emerging concepts of a biomimetic nature in engineering sensors and data analysis, pseudomuscular actuator control and computational biomechanic design may not only provide new avenues towards the realization of truly wearable haptic interfaces, but also clues and instrument to better comprehend human manipulative and gestual functions.

Applications

In the this context, we are designing an active and sensorized glove for virtual reality and rehabilitation.

Elastic textile fibers covered with an epitaxial layer of polypyrrole have been used to fabricate gloves sensorized with an array of strain sensors made of piezoresistive fabric patches. A pseudo-3D graphic interface has also been realized (Figure 1 and Figure 2) [1].

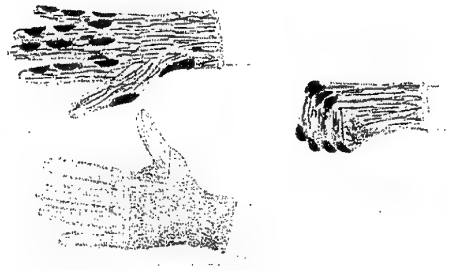

Figure 1. Sensor placements on glove

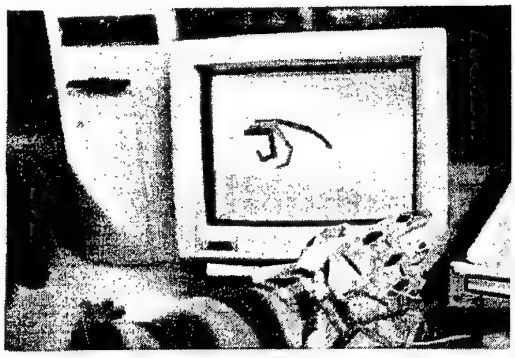

Figure 2 Sensorized glove and pseudo-3D graphic interface

Polypyrrole-lycra fabric is utilized to monitor mechanical strains, and we have characterized its response to external stresses. To do this we performed several mechanical tests, where a sensor sample is submitted to step strains in stretching with increasing amplitude and the induced variation of resistance is recorded. In Figure 3 a block diagram of the system used to characterize the fabric sensor is illustrated. An electromagnetic shaker is driven and controlled by an electronic interface connected to a computer and the relative electrical resistance variations are registered.

Several experiments were performed to calculate an important parameter describing piezoresistive properties of the conducting fabric: the gauge factor. To do this we exerted successively small increments of uniaxial stretching along two orthogonal directions in the plane of the fabric. The calculated gauge factors, $GF = (\Delta R/R)/(\Delta l/l)$, are $GF// = -13.25$ and $GF\perp = -12.5$ along the warp and the fill respectively (Figure 4). It is worth noting that the GF value of this fabric is negative, rather high and very close to that of nickel.

Fiber actuators, made with conducting polymer (CP) or electrostrictive polymers (ELS) [2,3], are under fabrication and their actuation properties will be quantified in order to realize the active components of the glove (Figure 5).

Incorporation of fiber actuators into piezoresistive coated fabrics enables either hand gesture caption and tensing-relaxation actions through a sensory-motor wearable exoskeleton.

A strain amplification system based on all-fiber technology has also been conceived to enhance fiber actuator stroke [2]. When a small voltage difference is applied on the active element its volume increases and the radial strain as reflected as a upon the longitudinal shortening of the mesh.

In this configuration the relative shortening of the mesh can be as high as 30% with a gain factor of about 10 between the strain of the fiber bundle and the relative shortening of the mesh (Fig. 6). This technical solution can be utilized to achieve both tangible shortening of the actuator and useful contractile force. Detailed calculations have been performed in the eyes of geometrical considerations and force generation capabilities

Fiber actuation technology still needs considerable work, and substantial imporvementsare are foreseen in perfomances in the near future.

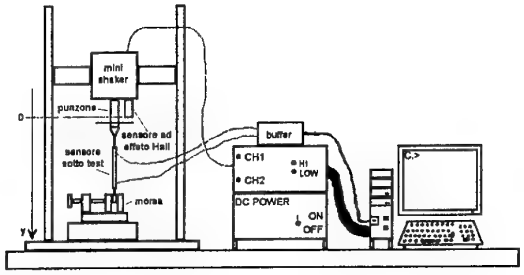

Figure 3. Overall system used to impose mechanical stresses on the sensor fabric.

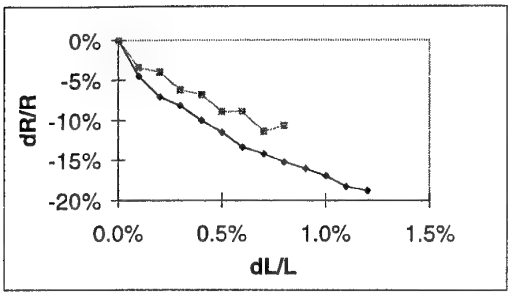

Figure 4. Resistance variations vs elongation of two rectangular samples.

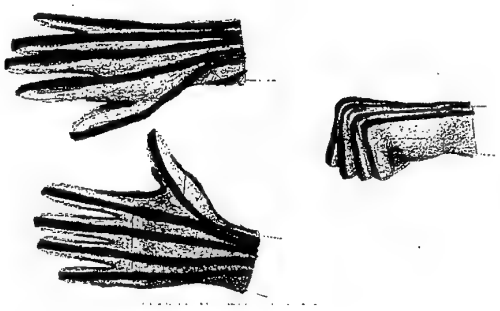

Figure 5. Actuator placement

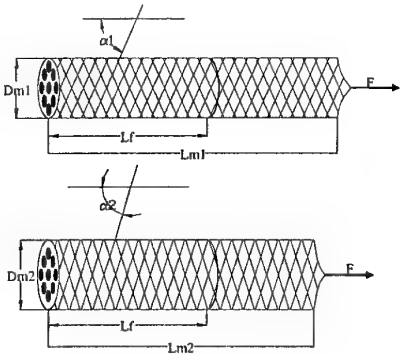

Figure 6. Scheme of strain amplifier

Fiber actuators, made with of a polyaniline (PANi) core, a solid polymer electrolyte jacket (SPE), and a copper (CU) wire counterelectrode located on the outer surface of the SPE have been fabricated and their actuation properties quantified in order to realize the active components of the glove (Fig. 7 and Fig. 8).

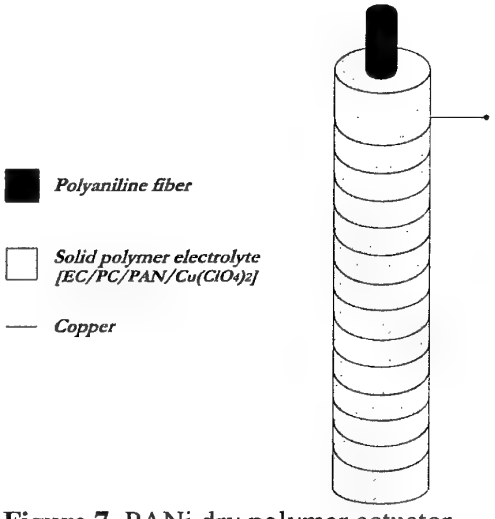

Figure 7. PANi dry polymer actuator

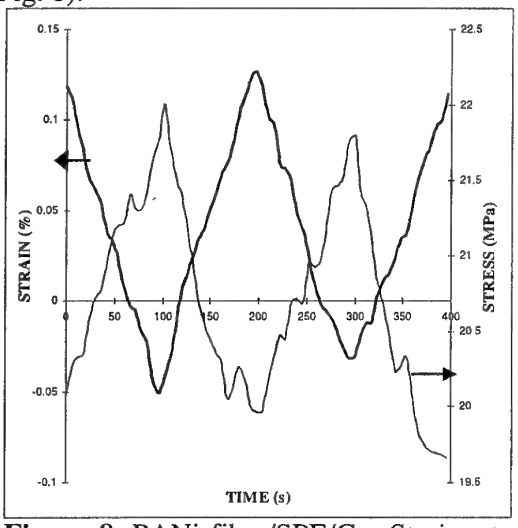

Figure 8. PANi fiber/SPE/Cu: Strain, stress and potential during square wave potential drive (-1 to +1 V between electrodes)

Virtual and augmented reality are areas of application which would benefit from the disclosed technology. Post surgery hand rehabilitation procedures are an additional targeted application area.

Conclusion

EAPs can be of fundamental importance in the field of anthropomorphic robotics, micro-robotics and bioengineering as they represent advantages over traditional actuation.
The aim of our work is to build a low cost wearable device able to record human posture and gesture, which can be worn for a long time with no discomfort and produces a continuous stream of data on movements of a subject.
In this context, we are developing a sensorized active glove in our laboratory. The gloves could be interesting in the area of virtual and augmented reality and of post surgery hand rehabilitation procedures
The actuators and sensors were first characterized to determine their properties, and to enable the actuator to be used in the glove with a correct interpretation of data relative to textile resistance variations.

REFERENCES

1 D. De Rossi, F. Lorussi, A. Mazzoldi, E.P. Scilingo, P. Orsini:, "Active dressware :wearable proprioceptive system basedon electroactive polymers", *5th International Symposium on Wearable Computers - ISWC2001* (Zuerich, Ch, October 2001)

2 D. De Rossi, Federico Lorussi, A. Mazzoldi, W. Rocchia, E.P. Scilingo: "Strain amplified electroactive polymer actuator", *Electroactive Polymer Actuators and devices (EAPAD), Part of 8th Annual International Symposium on Smart Structures and Materials* (Newport Beach, CA, USA, March 2001)

3 G. Pioggia, F. Di Francesco, C. Geraci, P. Chiarelli, D. De Rossi, "An human-like android face equipped with EAP artificial muscles to endow expressivity", *Proc. SPIE's Electroactive Polymer Actuators and Devices Conf., 8Th Smart Structures and Materials Symposium,* Newport Beach, USA, March 2001

Conducting Organic Polymer Gas Sensors – QSAR Studies of Sensor Performance

Richard A. Bissell[1], Krishna Persaud[2] and Paul Travers[1]
1. Osmetech plc, Electra House, Electra Way, Crewe CW1 6WZ, UK.
2. DIAS, UMIST, PO Box 88, Manchester, M60 1QD, UK.

Abstract. The behaviour of polyalkylterthiophene gas sensors can be described by Quantitative Structure-Activity Relationships. Linear correlations with analyte boiling point are observed. For the materials studied the general conclusions are i) polar compounds are more sensitively detected than nonpolar analyte types, ii) there is little marked size or shape selectivity towards a group of analytes which share the same functional group but differ widely in secondary structure, e.g. homologous and non-homologous alcohols, iii) changing the dopant ion has a large effect on *absolute* sensor sensitively but does not markedly affect the *relative* sensitivity towards different analyte functional groups (alcohols > esters > hydrocarbons). The model and the general conclusions are considered to applicable to other types of conducting organic polymers (COPs).

1. Background to QSAR in biology

Quantitative Structure-Activity Relationships (QSAR) [1] are used in biology to correlate the physiological action of organic compounds with their physico-chemical descriptors. Historically the most important descriptor in these studies has been the octan-1-ol/water partition coefficient as developed by Corwin Hansch in the early 1960s [2]. He recognised the importance of partition effects in any attempt to describe the properties of compounds in a biological system. The reasoning being that in order for a compound to exert an effect on a system it must first reach its site of action. Since biological systems are composed of a variety of more or less aqueous phases separated by membranes, measurement of partition coefficients in a suitable system of immiscible solvents might provide a simple chemical model of partition steps in the biosystem.

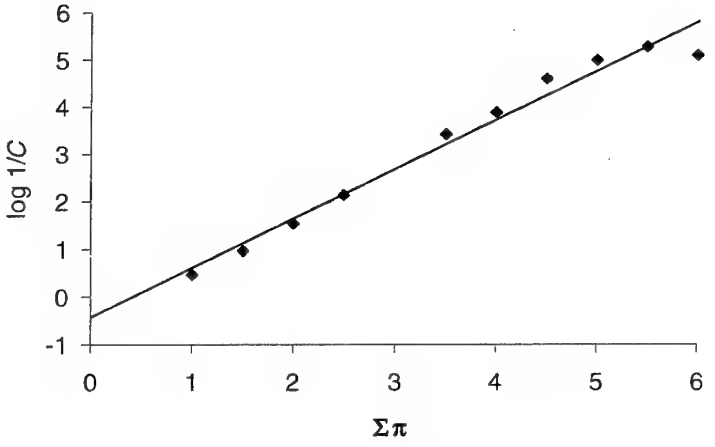

Figure 1. Anaesthetic activity ($\log_{10} 1/C$) where C is the alcohol concentration necessary to produce a standard anaesthetic effect against hydrophobicity as measured by octan-1-ol/water partition coefficients ($\Sigma\pi$)for a series of alcohols

A famous example of early QSAR is seen in the linear relationships between the narcotic action of organic compounds and their oil/water partition coefficients [3]. Figure 1 shows the relationship between the anaesthetic activity of a series of alcohols (ethanol to dodecanol) and their octan-1-ol/water partition coefficients (*C* is the alcohol concentration necessary to produce a standard anaesthetic effect).

2. QSAR in human odour detection

The primary step in human odour detection is the partition of odourant molecules from the vapour phase into the aqueous layer overlying the nasal epithelium. Such physical sorption effects are primarily determined by the vapour pressure (and hence boiling point) of the analytes. Consequently for a homologous series of simple molecules the human odour detection thresholds may be expected to show QSAR characteristics with respect to analyte boiling point. Figure 2 shows the $\log_{10}$(1/mean human olfactory detection threshold (ppm)) *vs* boiling point relationship for a series of homologous straight chain alcohols ranging from methanol to octanol. The error bars represent one SD unit in the standardised results reported by at least two, and up to 20, authors [4].

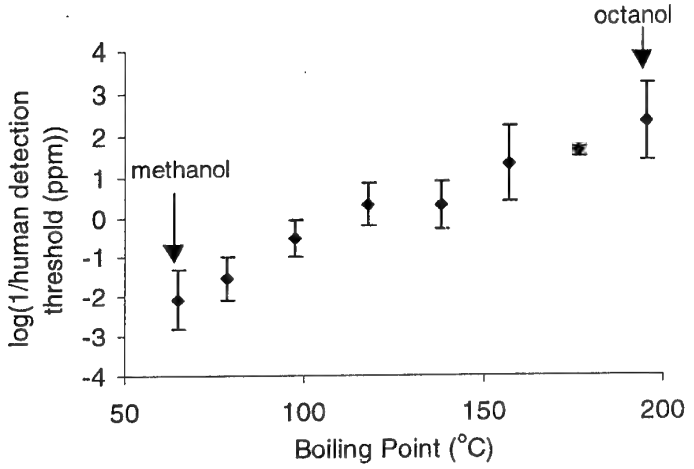

Figure 2. Plot of log(1/mean human olfactory detection thresholds) versus the boiling point of a homologous series of straight chain alcohols ranging from methanol to octanol.

3. Background to conducting polymer gas sensors

Conducting organic polymers (COPs), typically polypyrrole (PP), have been widely used as sensing elements for the detection of volatile organic chemicals (VOCs) [5]. Whilst the mechanism of sensor action [6] has received some attention, little work has been done to correlate COP sensor responses with analyte physico-chemical parameters. Such correlations would enable the prediction of COP sensor responses to untested analytes as well as providing a more complete description of COP sensor performance for studies of sensor mechanism. In the case of surface acoustic wave (SAW) gas sensor devices it has been shown that sensor responses can be correlated to analyte boiling point [7]. Establishing the correlation was facilitated by the ease with which partition coefficients can be obtained from SAW sensor responses. For COP sensors, however, no

similar results have been reported to date, perhaps due to the different physical properties measured and the complex transduction processes [8-10] involved.

In this paper we report linear relationships between steady-state COP sensor responses and analyte boiling point for groups of analytes which share the same functional group. The COP materials investigated are of the polyalkylthiophene (PAT) type. Very few reports on the use of doped PATs in gas sensing have been published [11]. PATs are attractive materials for applications in molecular electronics [12] because of their stability in both the doped and undoped states, and good processability.

4. Theoretical background and the boiling point model in COP gas sensors

4.1 *Relationship between gas partition coefficient and analyte boiling point*

The theory of molecular partition between the gas phase and a condensed phase is well established in the field of gas liquid chromatography (GLC) [13]. The partition coefficient, K, is defined as

$$K = C_c/C_v \tag{1}$$

(where C_c is the concentration of the vapour in the chromatographic stationary phase and C_v is the concentration of the vapour in the carrier gas phase). K depends on the solubility of the vapour in the polymer which in turn is a function of the saturated vapour pressure of the vapour and the strength of the vapour-polymer interactions [7]. In GLC studies the partition coefficient has been shown to follow the well-known expression [13]

$$K = RT(\rho_1/M_1)/(\gamma_2 p_2) \tag{2}$$

Where ρ_1 and M_1 are the density and molecular weight of the stationary phase, respectively, p_2 is the saturation vapour pressure of the solute vapour and γ_2 is the coefficient of interaction between vapour and polymer ($\gamma_2 = 1$ for ideal solutions).

The following approximate expression, based on Trouton's rule and the Clausius-Clapeyron equation relates p_2 and boiling point T_b

$$log\ p_2 \approx 7.7 - T_b(t/2.303RT) \tag{3}$$

where t is the Trouton constant for the vapour.

Combining equations 2 and 3 yields

$$\log K = a + bT_b \tag{4}$$

The parameters a and b in Equation 4 are defined as $a = \log (RT/\gamma_2) - 7.7 + \log (\rho_1/M_1)$ and $b = t/(2.303RT)$. For an ideal vapour-polymer solution at a given temperature, constant a is a function of the polymer alone (through the term ρ_1/M_1, $\gamma_2 \approx 1$), and constant b of analyte alone (through the parameter t, which is in the range 85-90 $J \cdot mol^{-1} \cdot K^{-1}$ for non-hydrogen bonding vapours [16]). Deviations from ideality arise when $\gamma_2 \neq 1$ due to specific vapour-polymer interactions.

4.2. *Conducting organic polymer (COP) sensor responses and VOC partition coefficients*

It can be assumed that the sensor response is proportional to the concentration of the analyte gas dissolved in the polymer:

$$\Delta R = \%dR/R = C_c \cdot k_t \tag{5}$$

where ΔR is the percentage change in resistance of the COP sensor upon exposure to the VOC, C_c is the concentration of VOC dissolved in the polymer and k_t is a 'transduction constant' indicating the sensitivity with which the amount of the partitioned analyte is translated by the polymer film into a resistance change.

By combining equations 1 and 5 the following equation is obtained

$$K = (\Delta R / k_t) / C_v \quad (6)$$

Since the transduction mechanism is complex, it is not possible at present to directly calculate k_t. However, studies by Kunugi *et al* [14] of simultaneous mass and resistance changes in polypyrrole films upon exposure to a homologous series of alcohols (methanol-butanol) have shown that i) for each alcohol the relative mass change was proportional to the relative resistance change, which is consistent with equation 5, and ii) that the relative resistance change per adsorbed molecule on the PP film was essentially constant across the series of alcohols investigated. This implies that the *transduction constant, k_t, is the same across this series.*

If the gas concentrations that induce a fixed level of response in the sensor are obtained then equation 6 reduces to

$$K \propto 1/C_v \quad (7)$$

Where C_v is the gas concentration required to produce a fixed level of response in the sensor for a series of compounds which share the same functional group, e.g. alcohols. Finally by combining equations 4 and 7 the following expression is obtained

$$\log (1/C_v) = A + a + bT_b \quad (8)$$

where A is an arbitrary constant which depends on the response value chosen in equation 6 and is equal to $\log (\Delta R \cdot k_t)$.

5. Comparison of QSARs from biology and COP gas sensors

Equation 8 is of the same form as that plotted in Figures 1 and 2 from empirical studies of response in biological systems. In both cases, the mechanism of interaction of the drug/organism or VOC/gas sensor is complex, but overall the process is governed by non-specific physico-chemical partition, which can be described by simple QSARs.

6. Experimental

The sensors investigated comprise a pair of thin (~1μm) gold electrodes vapour deposited on a ceramic substrate with a separation of 250 μm. A *p*-xylene solution (8 mg/mL) of poly(3,3″-didecyl-2,2″:5′,2″-terthiophene) - subsequently referred to as DEC - was cast over the electrodes and subsequently doped electrochemically with 0.1M solutions of Bu_4NPF_6, $Bu_4NCF_3SO_3$ and Bu_4NClO_4 in acetonitrile. The sensor materials are referred to as DEC/dopant ion. DEC was characterised by ^1H nmr spectroscopy and gel permeation chromatography (M_w = 22,900, M_n = 8,050). The thickness of the films are 1-3 μm. Resistance changes at 35.0 (±0.05) °C in air (relative humidity 50%) on exposure to sample vapours were monitored using an Aromascan analyser (A32S) and proprietary software. Analyte gas samples were generated at 22.0 (±0.1) °C. Accurate gas concentrations (± 2%) were generated by diluting saturated vapours using a custom built automated gas blending rig. All transfer tubes were teflon. The percentage steady-state change in sensor resistance (%dR/R) was measured at four gas concentrations with

three repeats at each concentration. The data thus obtained were fitted using a polynomial function (R^2 values typically > 0.9). The gas concentration required to give a response of 0.25 %dR/R was calculated from the calibration curve. In all cases this response value lay in the linear range of sensor responses and was at least three times greater than the minimum reliably detected signal (ca. 0.05% dR/R). All data are averages of three sensors.

A total of 27 analytes were investigated and are listed in Table 1.

Chemical class	Compounds investigated
alcohols	methanol, ethanol, propanol, pentanol, hexanol, octanol, propan-2-ol, 3-methyl-1-butanol, butan-2-ol, cyclohexanol, 2-methylpentan-2-ol, 2-ethyl-1-hexanol
esters	ethyl hexanoate, butyl acetate, ethyl acetate, ethyl butyrate, ethyl octanoate, isoamyl acetate
aromatic hydrocarbons	mesitylene, *o*-xylene, *p*-xylene, toluene, ethylbenzene, butylbenzene
aliphatic hydrocarbons	octane, decane, dodecane

Table 1. Compounds investigated in study

7. Results and discussion

7.1 *Features of the sensor response*

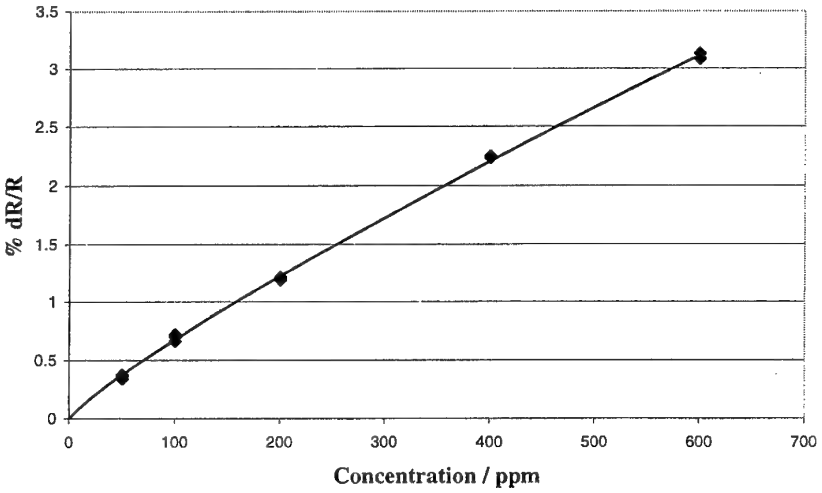

Figure 3. Percentage change in steady-state resistance of DEC/ClO_4 in response to various concentrations of propanol (three repeats at each concentration).

All the sensor responses to all the analytes reported in this paper were reversible and positive, i.e. resistance increased upon exposure to the vapour and returned to a steady baseline value after exposure was ended. A typical relationship between steady-state sensor response and gas concentration (in this case propanol vapour) is shown in Figure 3. The calibration plot is almost linear over the entire concentration range tested, which is typical of all the sensor/analyte profiles.

7.2. *Response to alcohols and the boiling point model*

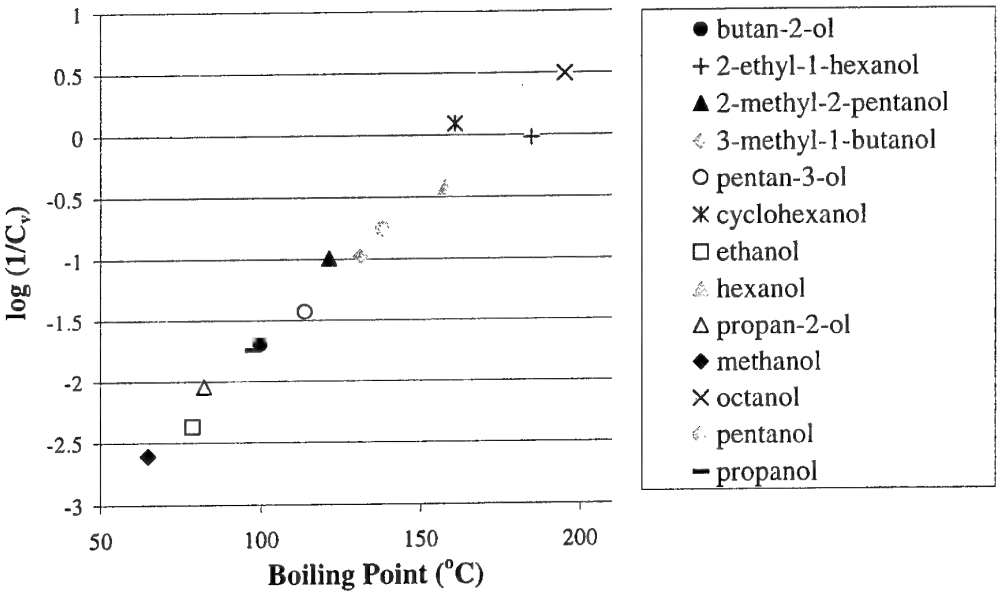

Figure 4. Log ($1/C_v$) *vs.* T_b for sensor DEC/ClO_4 in response to a variety of alcohols.

Figure 4 shows a plot of log($1/C_v$) *vs.* T_b (see equation 8) for sensor DEC/ClO_4 in response to a variety of alcohols including primary, secondary, tertiary and cyclic species spanning a wide range of boiling points. It is evident that a linear correlation is observed. The correlation is strongest if only homologous primary alcohols are considered (R^2= 0.99, n=6) but the inclusion of non-homologous species does not greatly reduce the correlation (R^2=0.97,n=13).Thus it is apparent that the sensor does not discriminate between alcohols of widely differing size and shape. An exception is perhaps the cyclic alcohol, cyclohexanol, for which for all the sensors studied gave larger signals than expected. This observation may be related to the lower entropies of vaporisation of cyclic compounds relative to their open-chain counterparts [16].

Figure 5 displays the responses of DEC doped with a variety of counter ions to the same series of alcohols. It is clear that the linear log ($1/C_v$) – T_b correlation in figure 4 is not limited to one particular dopant ion. The linear relationships in Figure 5 have similar gradients but show more variation in the intercepts. The former observation is predicted by the boiling point model which states that ideally the gradient is not dependent on the polymer type but is related to the Trouton constant (entropy of vaporisation) of the analyte (see Section 2). Calculation of Trouton's constant from the gradients in Figure 3 provides reasonable values in the range 96-121 $J \cdot mol^{-1} \cdot K^{-1}$ (literature values for alcohols range between 102 and 112 $J \cdot mol^{-1} \cdot K^{-1}$ [16]).

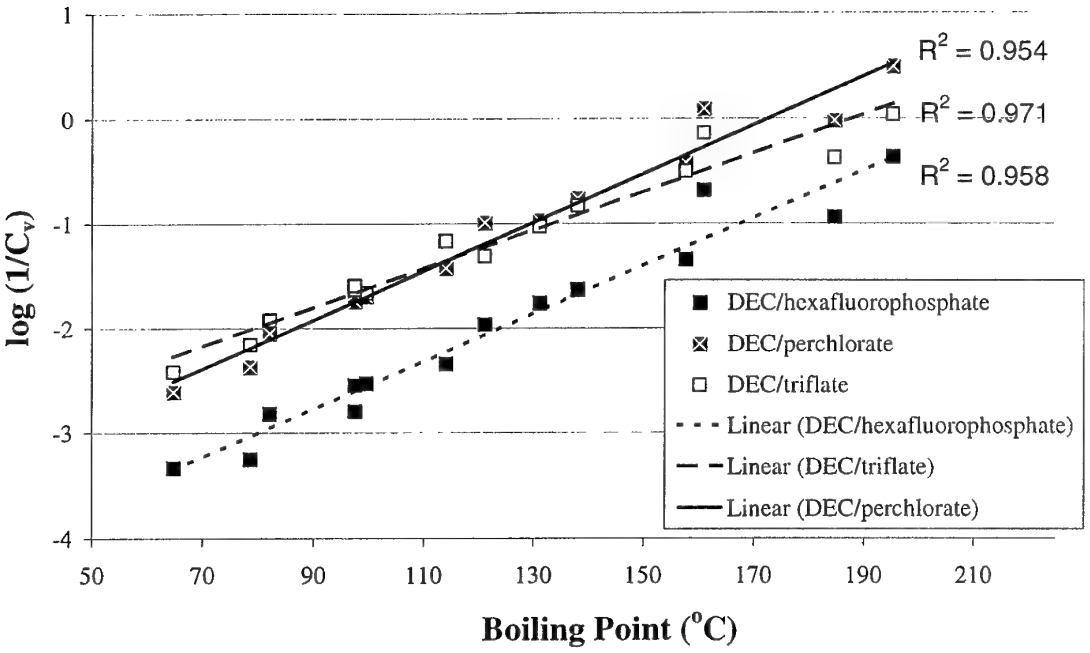

Figure 5. Log ($1/C_v$) *vs.* T_b for variously doped DEC in response to a variety of alcohols.

Since the gas concentrations in Figure 5 are the values required to generate a fixed sensor response (0.25% dR/R), the lower the required vapour concentration the more sensitive is the sensor. The variation in the intercepts in Figure 3, therefore, indicates that the sensors have different sensitivities to alcohols. The fact that the dopant ion affects the sensitivity of COP sensors is well known [15], although it is clear that in the present example improved sensitivity does not result in increased sensor selectivity for different alcohols.

7.3. *Responses to other analyte classes*

Figure 6 shows that the linear log ($1/C_v$) – T_b correlation is observed for other analyte types as well as alcohols. Further, in the studied boiling point range, the sensitivity order of sensor DEC/ClO_4 towards the analyte classes investigated is alcohols > esters > aromatic hydrocarbons ≈ aliphatic hydrocarbons. Similar observations were made for DEC sensors doped with hexafluorophosphate and triflate. The sensitivity order is consistent with the expected relative partition coefficients of the four analyte classes with a polar material since polar molecules are expected to have larger free energies of interaction than non-polar molecules. In the present model this is reflected in a non-ideal coefficient of mixing ($\gamma_2<1$) of polar vapours with the polymer (equation 4). The gradients of the relationships in Figure 4 are very similar to each other since the entropies of vaporisation of most non-strongly hydrogen bonding liquids are roughly constant (Trouton's rule).

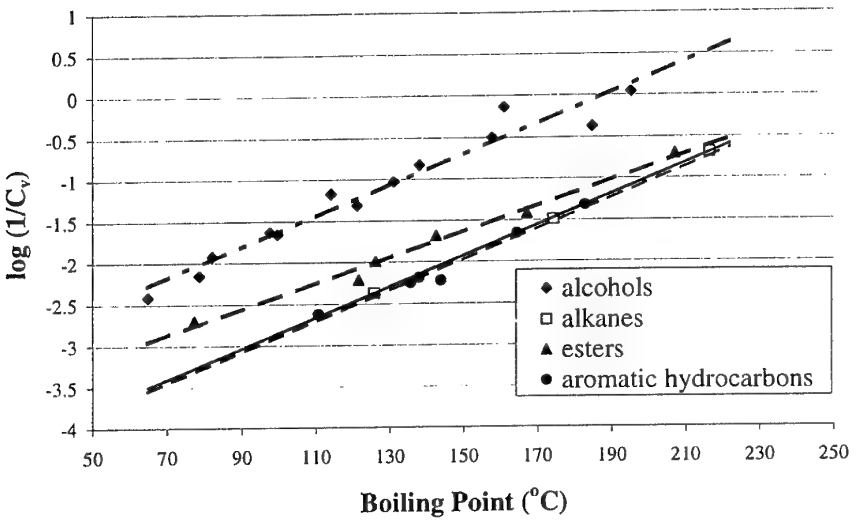

Figure 6. Log ($1/C_v$) *vs.* T_b for sensor DEC/ClO_4 in response to four functional groups.

8. Summary

A simple QSAR relating the performance of COP gas sensors to analyte boiling point has been derived. The model has been tested for a polyalkylthiophene material (DEC) doped with various counter ions. The steady-state changes in electrical resistance of the material upon exposure to multiple concentrations of 27 vapours covering four different chemical groups has provided support for the model. The general conclusions of the study are that i) DEC is more sensitive to polar rather than nonpolar analyte types, ii) DEC does not display marked size or shape selectivity towards a group of analytes which share the same functional group but differ widely in secondary structure, e.g. homologous and non-homologous alcohols, iii) changing the dopant ion in DEC has a large effect on *absolute* sensor sensitively but does not markedly affect the *relative* sensitivity towards different analyte functional groups (alcohols > esters > hydrocarbons). The model and the general conclusions are considered to applicable to other types of COPs.

References

[1] Livingstone D, 1995 Data Analysis for Chemists, Oxford University Press, New York

[2] Hansch C, Muir RM, Fujita T, Maloney PP, Geiger F, and Streich M 1963 J.Am. Chem. Soc. 85 2817-24

[3] Hansch C, Steward AR, Iwasa J and Deutsch EW 1965 Molecular Pharmacology 1 205-13

[4] Devos M, Patte F, Rouault J, Laffort P and Van Gemert LJ 1990 Standardised Human Olfacory Thresholds, Oxford University Press, New York

[5] Hatfield J V, Neaves PI, Hicks P J, Persaud K C and Travers P 1994 Sens. Actuators B - Chem. 18 221-8

[6] Slater M S, Paynter J and Watt E J 1993 Analyst 118 379-84
[7] Patrash J P and Zellers E T 1993 Anal. Chem. 65 2055-66
[8] Blackwood D and Josowicz M 1991 J. Phys. Chem. 95 493-502
[9] Slater M S, Watt E J, Freeman N J, May I P and Weir D J 1992 Analyst 117 1265-70
[10] Gardener J W, Bartlett P N and Pratt K F E
1995 IEE Proc.-Circuits and Devices Syst. 142 321-33
[11] DeWit M, Vanneste E, Blockhuys F, Geise HJ, Mertens R and Nagels P 1997 Synth. Met. 85 1303-4
[12] Bao Z, Rogers J A and Katz H E 1999 J. Mater. Chem. 9 1895-1904
[13] Littlewood A B 1970 Gas Chromatography (New York:Academic) 44-121
[14] Kunugi Y, Nigorikawa K, Harima Y and Yamashita K
1994 J. Chem. Soc. Chem. Commun. 873-4
[15] Topart P and Josowicz M 1992 J. Phys. Chem. 96 7824-30
[16] Schwarzenbach R P, Gschwend P M and Imboden D R
1993 Environmental Organic Chemistry (Wiley-Interscience) Chapter 4

An optical biosensor employing tiron-immobilised polypyrrole films for estimating monophenolase activity

Krishna C. Persaud, Ramaier Narayanaswamy, Sabari Dutta[1], Subhash Padye[1]

Department of Instrumentation and Analytical Science, UMIST, PO Box 88, Manchester, M60 1QD, UK

[1]*Department of Chemistry, University of Pune, Pune 411007, India*

Abstract

Methods applicable to development of optical biosensors to measure enzyme activity in a sample are presented. The active component of a biosensor is an immobilised substrate on a conducting polymer, and the transduction process involves a measurable optical change in a conducting polymer matrix.

Introduction

Conducting polymers have been demonstrated to be useful as immobilising agents for biological components of biosensors [1]. There are few reports of biosensors capable of measuring enzyme activity using an immobilised substrate rather than measurement of an analyte using an immobilised enzyme. We investigated methods applicable to optical biosensors to measure enzyme activity in a sample, where the active component of a biosensor is an immobilised substrate on a conducting polymer, and the transduction process involves a measurable optical change in a conducting polymer matrix. Here we describe the development of an optical biosensor which involves immobilising tiron (1,2 dihydroxybenzene,3,5 disulphonic acid disodium salt monohydrate) as the enzyme substrate in a polypyrrole matrix for the determination of enzyme activity using an optical fibre assembly. The polypyrrole film along with the substrate tiron is electropolymerised on ITO (indium tin oxide) glass. When this film comes in contact with the solution containing phenol oxidase enzyme, the tiron is converted into the o-quinone, which forms a colored product and the optical change is observed by measuring the reflectance at 590 nm (Figure 1). The incorporation of tiron into the polypyrrole matrix offers some distinct advantages such as stable matrix for immobilisation of a substrate that is accessible to the enzyme activity. The presence of the enzymes in the polypyrrole film can also be easily confirmed by cyclic voltammetry (CV). The optrode has been further utilised to measure the amount and stability of tiron in the film and to evaluate the application in the measurements of enzymes from fruits such as apples by determining the monophenolase activity.

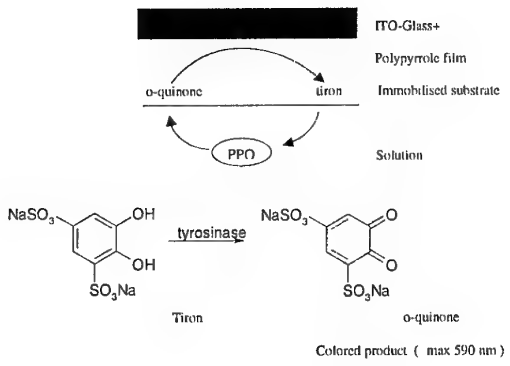

Figure 2 Strategy for an optical biosensor based on immobilised Tiron

Materials and Methods

Pyrrole (Sigma-Aldrich Co) was distilled under vacuum prior to use and stored at 4°C. Mushroom tyrosinase (E.C. 1.14.18.1 having activity of 2060 Umg-1) was stored at 4°C. Apple polyphenol oxidases were extracted from red apples and partially purified by using several sequential phase partitionings with TX-114.

Instrumentation:

The spectrophotometric studies were carried out on a Ocean Optics PC1000 spectrometer with a wavelength range 330 - 780nm. The light source used was a tungsten-halogen lamp. The polymer films were placed inside a specially designed flow-cell incorporated with a bifurcated randomised 32 optical fibre bundle for measurement of changes in reflectance. The flow cell was 0.2 ml in volume. The exterior of the cell was painted black to avoid any stray light affecting the measurements. Amperometric measurements were performed with a Princeton Applied Research (Princeton,NJ,USA) PAR 270 electrochemical system using a 15 ml electrochemical cell. The experiments were carried out using a conventional three-electrode system with the ITO-glass as the working electrode and a platinum wire as the auxiliary electrode. All the potentials quoted here were relative to an Ag-AgCl (saturated KCl) reference electrode, which was used for the measurements.

Immobilisation procedure:

Polypyrrole film incorporating tiron was formed in situ. The electrolyte 0.1 M KCl, aqueous 0.49 M pyrrole and 4 mg/ml (12mM) of tiron in 0.1 M of the phosphate buffer were mixed together to give the desired concentration and then the solution mixture was purged with nitrogen for 10 mins to remove any O_2 from the solution. A three electrode voltammetric cell was used for all electropolymerisation procedures. The ITO glass was used as the working electrode, while platinum foil was used as the auxiliary electrode with Ag/AgCl used as the reference electrode. The electropolymerisation of pyrrole was performed with a potentiostat using a potential of +0.65 V for a period of 5 mins. The polymer formed was rinsed several times with distilled water to remove any weakly bound tiron molecules after electropolymerisation. The electrode was then placed in a freshly nitrogen purged electrolyte solution. The amount of substrate present in each of the polypyrrole film was determined separately by the tyrosinase assay.

Tyrosinase assay:

Catalytic activity of mushroom tyrosinase was spectrophotometrically determined. To a piece of tiron-polypyrrole film (1mm x 2mm), 2 ml of 0.1M phosphate buffer (pH = 6.5) was added followed by the addition of 0.3mg/ml of mushroom tyrosinase (618 U/ml). After incubation at 30°C for 30 min, the amount of quinone produced in the film was determined by measurement of the optical density at 590 nm using the Ocean Optics spectrophotometer.

Kinetic data analysis:

The values of K_m and V_{max} for different substrates were calculated from triplicate measurements of v (velocity of the reaction) for each [S](S=substrate). The reciprocals of the variances of v were used as weighting factors in the nonlinear regression fitting of v vs [S] data to the Michaelis Menten equation. The accuracy of the method was characterised from 10 replicate measurements for known amounts of mushroom tyrosinase enzyme, leading to the evaluation of the limits of detection and maximum activity measurable. The kinetic data analysis was carried out by using linear and nonlinear regression fitting.

Results

We succeeded in immobilising the substrate Tiron onto a polypyrrole matrix, on indium tin oxide glass. The reflectance spectrum of the polymer matrix exhibits very few bands indicative of pure and highly conjugated polypyrrole film (Figure 2). A strong π^* band at 560 nm can be regarded as an indication of the average conjugation length in the polymer, since longer segments of planar chains would be expected to have more delocalisation and smaller energy differences between valence and conduction bands. Bands at 447 and 465 nm are possibly due to the C3-substitution of the polymer backbone [2]. On immobilising the substrate tiron onto the polypyrrole film discrete peaks are obtained which are evident of the presence of a redox site, which are different for the polymers. The narrower peaks are considered to

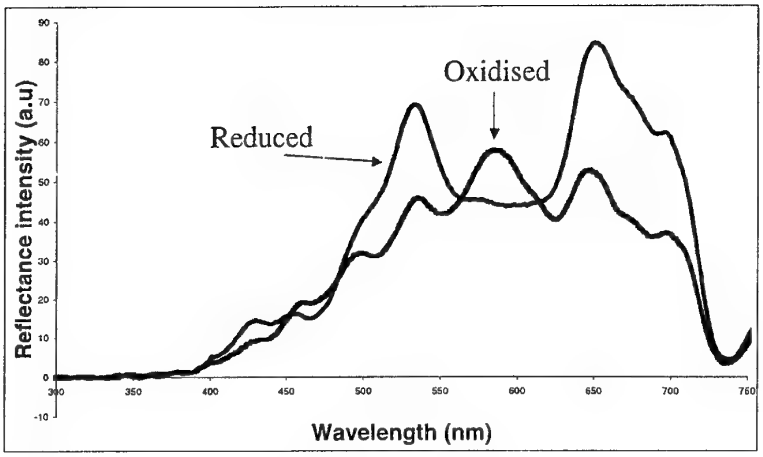

Figure 3 Reflectance Spectra of Reduced and Oxidised Tiron immobilised in polypyrrole

be an evidence of co-operative host–guest interactions. Bipolarons are the dominating species in the immobilised films where the substrate is inserted into the rigid host structure without changing the strong bonds in the host lattice. Since polypyrrole is a one-dimensional polymer the ions are envisaged as being associated in positions adjacent to the chain, rather than being incorporated on sites inside a lattice [3].

Changes in the spectrum occurs with interaction with the enzyme (Figure 2). Spectral changes in aqueous solutions containing 0.3 mg ml^{-1} of tyrosinase enzyme in 0.1 M phosphate buffer, pH 6.5, at intervals of 5 min over a period of 15 min have also been monitored. There is a decrease in the reflectance intensity as the formation of quinone intermediates increases with time. Various concentrations of tiron were immobilised into the polypyrrole film.

The presence of tiron in the polypyrrole film was verified by cyclic voltammetry. The enzyme activity using the polypyrrole–tiron film is confirmed by the catalytic conversion of immobilised substrate to quinones by the enzyme. The incorporation of tiron into the polypyrrole matrix offers some distinct advantages such as stability, enzyme accessibility and longer shelf-life. The electrode was calibrated against known activities of enzyme (Figure 3). The optrode had a K_m of 3.3 mM for apple phenol oxidase and has been further utilised for measurements of the monophenolase activity in apple juices.

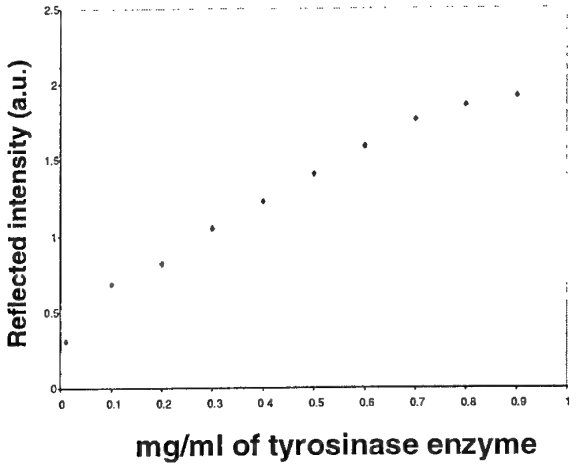

Figure 4 Calibration of electrode against known amounts of enzyme. Tyrosinase in the activity range 20.6 - 144.2 U/ml have been determined with the sensor system studied.

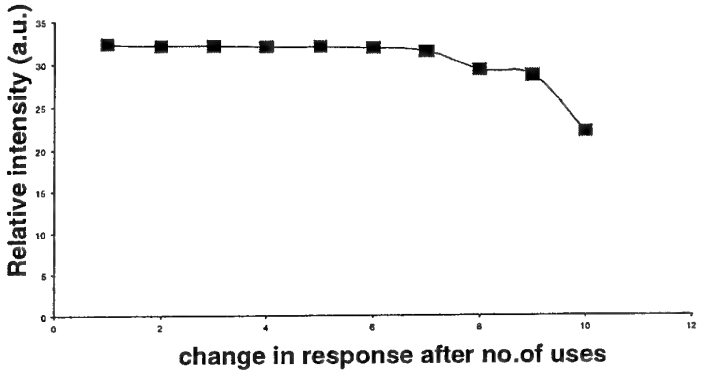

Figure 5 Re-use of electrodes: there was a fall off of activity after 5 to 6 assays

The electrode was re-usable for about five to six assays, then became subsequently less active as shown in Figure 4.

Immobilised tiron is a good metal chelator and therefore it was essential to investigate the inhibition of tyrosinase by the metal ions. Very high concentrations of $FeCl_3$ (600 mM) cause 94% inhibition of the tyrosinase activity whereas 50% inhibition (IC50) occurs at a concentration of 372 mM. The kinetics of the enzyme inhibition were studied employing much lower concentrations of $FeCl_3$ (0–100 mM). Metal ions such as Cu 2+ are poor inhibitors of the enzyme at lower concentrations.

References

1. S.B.Adeloju and S.J.Shaw Anal Chim Acta, 281(1993) 611-615.

2. S. Furukawa, S.Tazawa, Y.Fiujii and I. Harada, Synth. Met, 24 (1988) 329-332.

3. S. Skaarup, K.West, B. Zachau-Christiansen and T. Jacobson , Synth. Met, 51 (1992) 267-275.

DNA BIOSENSOR FOR THE DETECTION OF TOXICANTS

M. Mascini

Dipartimento di Chimica, Universita' degli studi di Firenze, Via G. Capponi 9, 50121 Firenze, mascini@unifi.it
http://www.chim.unifi.it/ana/

Introduction

In environmental pollution monitoring it is becoming a general opinion that chemical analysis by itself does not provide sufficient information to assess the ecological risk of polluted waters and wastewater [1,2,3]. For instance the U.S. EPA and the European Union require that industrial and urban wastewater effluents reach certain limits of non toxicity before the effluent is discharged into the environment. Moreover, since surface waters frequently are the collecting reservoir of municipal and industrial wastewaters, toxicity, as a quality parameter, is also required by many legislations.

In precedent papers [4,5,6] we proposed the use of electrochemical DNA biosensors as screening test of environmental toxicants. The disposable electrochemical biosensor was based on the immobilization of double-stranded DNA on the surface of graphite screen-printed electrodes (SPE) and on the use of voltammetry to investigate the electrodic surface. The changes in the DNA redox properties (i.e. the oxidation of the guanine base) were monitored in order to study the interactions between DNA and analyte. Moreover if electroactive compounds were present in the sample, they were determined and identified by their electrochemical redox properties.

In this paper we have reported the DNA biosensor analysis of toxicants in real samples such as waste and surface water samples. The same samples were also analysed by a commercial toxicity test, the Toxalert® 100, based on the bioluminescence inhibition of the bacterium *Vibrio Fisheri.* The *Vibrio Fischeri* bioluminescence test is a standard toxicity test widely recognised by many legislations. This test is directly linked to the vitality of the bacterial cell. A toxic substance cause changes to the cellular state (i.e. damage to the cell wall, cell membrane, the electron transport chain, enzymes, cytoplasmatic constituents); these changes are rapidly reflected in a decrease in the bioluminescence signal that can be measured with a photomultiplier in a luminometer.

Even if more than 20 aquatic toxicity tests are reported in the 20th edition of the Standard Methods for the Examination of Water and WasteWater [7], we chose this assay since bacterial bioluminescent assays are rapid, reproducible and cost effective tests; moreover many of the other bioassays are not routinely applicable. In this paper we also reported the results obtained during different Technical Meeting, organised by the Environment and Climate Program of the European Commission, that had the specific purpose of achieving a step in the use and implementation of biosensors in field conditions, and thus demonstrating that DNA biosensor and electrochemical instrumentation are in line with the requirements of in situ measurements.

Materials and Methods

Apparatus and reagents

Electrochemical measurements were performed with an Autolab PGstat 10 electrochemical analysis system, with a GPES 4.5 software package (Eco chemie, Utrecht, Holand), in connection with a VA-Stand 663 (Metrohm, Milan, Italy). The planar, screen-printed electrochemical cell (1.5 cm x 3.0 cm) consists of a carbon working electrode, a graphite counter electrode and a silver reference electrode. The procedure and reagents to make screen-printed electrodes were elsewhere reported [8]. The graphite working screen-printed electrode surface is 3 mm in diameter. Each electrode is disposable.

The luminometer Toxalert® 100 and all the reagents to perform citotoxicity tests were kindly provided from Merck (Darmstadt, Germany).

Sodium acetate, sodium chloride, acetic acid potassium chloride, sodium dihydrogen phosphate, ethanol, ethylacetate were purchased from Merck (Darmstadt, Germany).

Double–stranded calf thymus DNA, Triton X100, were from Sigma (Milan, Italy).

Real Sample Collection

The Water Supply Company of Florence (Acquedotto comunale di Firenze) provided for river Arno water samples and for wastewater samples from two different wastewater treatment plants of the town of Florence. The sampling was carried out during spring 2000.

River water samples were preconcentrated by passing 1L of river water through an Isolute ^{TM} column Solide-Phase-Extraction (SPE). The extracted organic compounds were eluted using 500 µL ethyl acetate. The samples obtained were dried, then 5 mL of a 2% NaCl solution is added. This final solution is used to perform the analysis with the Toxalert® 100 and with the biosensor using the reported procedure.

Wastewater treatment plant's sampling was performed before (influent) and after (effluent) the treatment, both the plants receive mainly urban waste water. All the plants use biological treatment.

Influents and effluents samples were collected as 24 h composite samples, by treatment plants operators. Samples were stored in Pyrex borosilicate glass bottles at 4°C. Before the analysis, the waste water samples were filtered using single-use syringe filters, pore size 0.45 µm, obtained from Sartorious (Florence, Italy). To perform the analysis with the Toxalert® 100, the pH of the samples were adjusted at the neutral range then the samples are ready to be tested. To analyse the

samples with the DNA biosensor, a concentrated acetate buffer solution was added to 5 mL of sample obtaining a final concentration of 0.25 M.
Wastewater samples were also collected during the Bioset technical meeting [9, 10]. The analyses were performed in situ with the biosensor and repeated in the laboratory some days later using also the Toxalert® 100. Sample preservation was accomplished by storing bottles at 4°C immediately after sampling and during the transportation.

DNA biosensor

The biosensor was developed by immobilising double stranded Calf Thymus DNA at fixed potential (+ 0.5 V *vs.* Ag screen-printed pseudo-reference electrode, for 120 s) onto the screen-printed electrode surface. During immobilisation step, the strip was immersed in acetate buffer solution containing 20 ppm of double stranded Calf Thymus DNA. Then a cleaning step was performed by immersion of the biosensor in a clean acetate buffer solution, at open circuit condition. The incubation step was performed just placing 100 µl of the sample solutions onto the surface of the graphite working electrode. After 2 min. the sensor was washed, immersed in acetate buffer and a square wave voltammetric scan was carried out to evaluate the oxidation of guanine residues on the electrode surface. The area of the guanine (around +1 V *vs.* Ag screen-printed pseudo- reference electrode) was measured. Potentially toxic compounds present in water or wastewater samples can be evaluated by changes of the electrochemical signal of guanine. We estimate the DNA modification with the value of the percentage of response decrease (R%) which is the ratio of the guanine peak area after the interaction with the analyte (GPA_s) and the guanine peak area after the interaction with the buffer solution (GPA_b): $R\% = [(GPA_s / GPA_b) - 1] \times 100$.
The toxicity of a sample can be determined within 8 minutes.
The electrode surface was pretreated applying a potential of +1.6 V for 3 min.
The supporting electrolyte for the voltammetric experiments and for any step in the biosensor set up was acetate buffer 0.25 M pH 4.7, KCl 100mM.
Square Wave voltammetry parameters were: frequency: 200 Hz, step potential: 15 mV, amplitude: 40mV, potential range 0.2-1.2 V vs. Ag-pseudoreference electrode.

Toxalert® 100 Procedure

In all the experiments the osmolality of all standard and samples solutions was adjusted to 2% NaCl for the optimal reagents performance. To express the toxicity we have used the percentage of inhibition (%I), determined by comparing the response given by a saline control solution to that corresponding to the sample as function of the incubation time. For all the experiments we used an incubation time of 30 min. Therefore the bioluminescence inhibition is determined by:
$I\% = [(I_{0c} - I_f)/I_{0c}] \times 100$
where I_{0c} is the corrected value of luminescence intensity of the control test suspension in RLU (relative luminescence unit) and I_f is the luminescence intensity of the test sample after the contact time of 30 min. in RLU [11].

Results and Discussion

Figure 1 and 2 show the comparison of the samples analysis with the DNA biosensor and with the Toxalert® 100. In figure 1a were reported the influent samples and in figure 1b the effluent samples collected in a treatment plant of Florence. It is important to underline that both the methods show the same trend with each kind of sample. Analysing the influent samples we observed high level of citotoxicity with the Toxalert® 100 and also with the biosensor we had high values of response decrease. Analysing the effluent samples we observed the same trend with both the method, and a lower toxicity effect than that observed with the influent samples. Nevertheless with the Toxalert® 100 we have high values of inhibition, always higher than 20% and included between the 40-80%, thus we defined that these samples presented moderate to acute toxicity. The response decrease with the biosensor was always included between 10 to 50%, and only one samples was higher than 60%. Thus these samples can be defined as low to moderate toxic. Classical chemical parameters such as COD, BOD_5, and TOC were not correlated with the results obtained with both the procedure, as expected, since they describe the total amount of organic matter but don't discriminate between toxic or not toxic compounds.
In figure 2 were reported the results of both tests on the samples collected and analysed during the Bioset Technical Meeting (5-7th April 2000) held in Barcelona. Also on these samples we observed the same trend.

Analysis of river samples

In figure 3 were reported the analysis of river water samples, collected in the town of Florence. The toxicity of these samples was very low, and just one sample was defined toxic, since, according to the Toxalert 100 supplier's notes, only inhibition values over 20% can be attributed to a toxic compound. The analysis with the DNA biosensor show the same trend.

Conclusion

DNA biosensors are interesting devices for toxicity screening test. Results of real samples analysis show that the DNA biosensor give results in trend with other official methods. Moreover, it is important to underline that this is a cheaper and more rapid test (10 min) than other already on the market.

Figure 1

a)

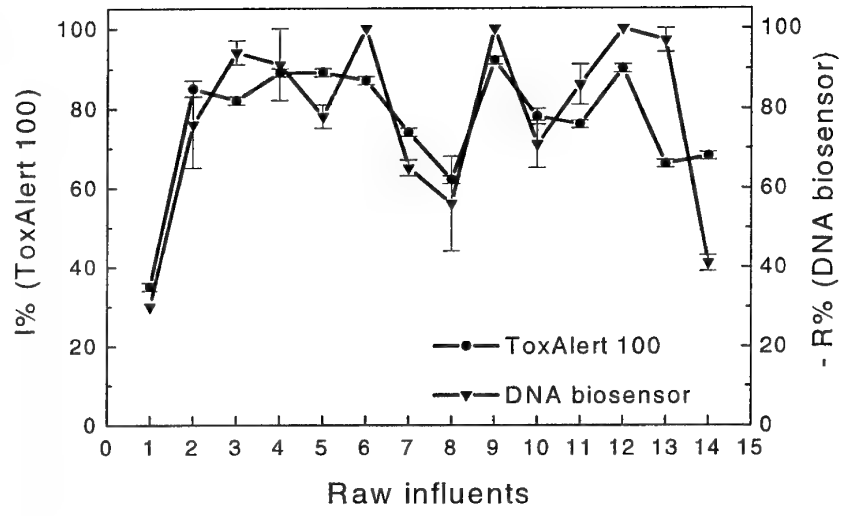
I% (ToxAlert 100)
- R% (DNA biosensor)
ToxAlert 100
DNA biosensor
Raw influents

b)

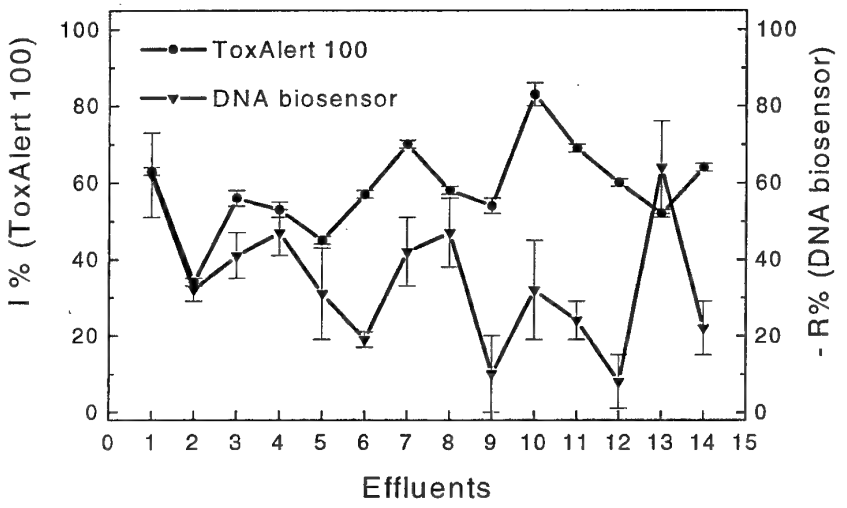
I % (ToxAlert 100)
- R% (DNA biosensor)
ToxAlert 100
DNA biosensor
Effluents

Figure 2

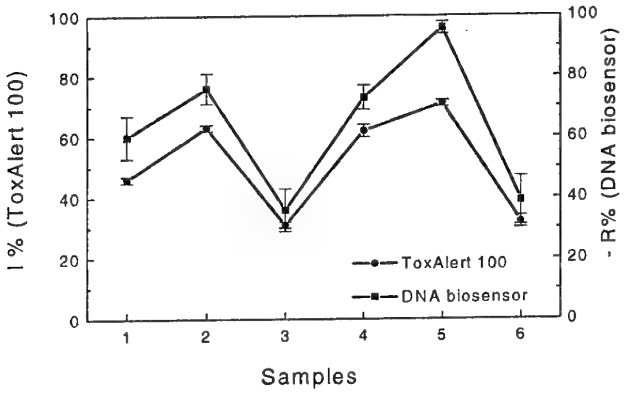

1,4 Raw influent
2,5 Influent after primary settlement
3,6 Treated water

Figure 3

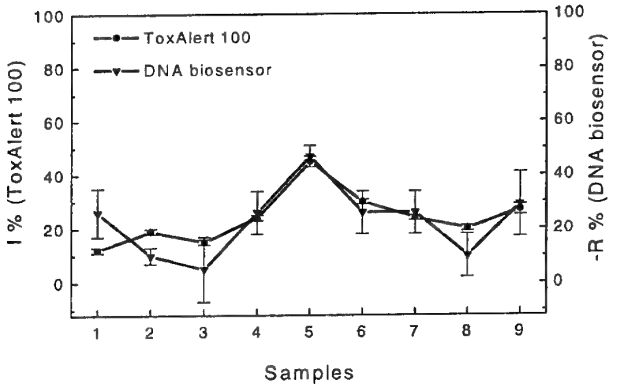

References

1. M. Castillo, M.C. Alonso, J. Riu, M. Reinke, G. Kloter, H. Dizer, B. Fischer, P.D. Hansen, D. Barcelo, Analytica Chimica Acta, 20451, 1-13, 2000
2. M. Castillo, D. Barcelo, Anal. Chem., 1999, 71, 3769-3776
3. M. Farre, M.J. Garcia, L. Tirapu, A. Ginebreda, Barcelo D., Analytica Chimica Acta, 427, 181-189, 2001
4. Marrazza G., Chianella I., Mascini M., Analytica Chimica Acta, 387, 1999, 297-307
5. Chiti G., Marrazza G., Mascini M., Analytica Chimica acta, 2001, 427, 155-164
6. Mascini M., Palchetti I., Marrazza G., DNA electrochemical biosensors, Fresenius J. Anal. Chem., 369/1, 2001, 15-22
7. Standard Methods for the Examination of Water and WasteWater, 20th edition,
8. A. Cagnini, I.Palchetti, I. Lionti, M. Mascini, A.P.F. Turner, Sensors and actuators B 24-25, (1995), 85-89
9. BIOSET: Final Report, Biosensors for evaluation of the performance of waste water treatments works, Barcellona, april 5-7th 2000, Editors D. Barcelo, J. Dachs and S. Alcock, Barcellona, Spain 2000
10. Technical Workshop on genotoxicity biosensing, TECHNOTOX, May 8-12 2000, Mol, Belgium, Draft
11. Toxalert® 100 Operating Manual, Merck, 2000

Measuring Biochemical Parameters On-Line: Key Challenges and Future Potential

Professor Dermot Diamond

Associate Director, NCSR, Dublin City University, Dublin 9, Ireland

Introduction

There are many reasons why the on-line measurement of biochemical parameters is of major interest at the present time. The interface between wireless communications technologies, materials science and sensors/biosensors promises revolutionary approaches to performing analytical measurements in completely new ways. The market 'push' of these technologies is being felt right across the discipline of analytical science, in areas as diverse as environmental monitoring to food quality assurance, to clinical diagnostics. While the technology sector is currently going through a downturn, there is no doubt, that the integration of wireless communications and mobile computing spearheaded by the 'bluetooth' initiative [i], will spawn new concepts in personal communications. While the initial focus is on audio and video information, it is equally clear, that the wireless communications infrastructure and technologies currently emerging will rapidly seek other sources of valuable information. For example, the concept of 'ubiquitous computing', which envisages 'intelligence' and wireless communications embedded into all sorts of objects - chairs, carpets, desks, fridges, washing machines, television sets, industrial plant machinery, analytical instruments, clothing, packages, watches etc. [ii,iii]. In order to realise the full potential of this concept, these objects will have to incorporate a sensing capability. In other words, ubiquitous computing will require a 'ubiquitous sensing' front end, so that previously 'dumb' objects can begin to understand and interpret what is happening in their immediate environment, and make this information available to remote user through a variety of platforms (cell phones, pagers, personal organisers, laptop PCs, desktop PCs). Part of this vision will be targeted at ways to gather information about the health status of individuals.

The Building Blocks of Ubiquitous Sensing

Conventionally, monitoring units consist of a sensor targeted at a specific measurand, some circuitry to look after signal digitisation and perhaps localised storage, and a cable to communicate with a basestation (e.g. a laptop PC) as illustrated in Figure 1. Current technology enables sensors to be integrated with wireless communications technology that frees the sensors from the base station. Interest in such 'free-standing' monitoring units is growing rapidly in environmental monitoring, as it offers the potential for developing 'environmental nervous systems' based on large-scale integrated networks of these devices that can detect, warn and, in its ultimate manifestation, initiate remedial action to minimise damage arising from pollution incidents [iv].

Developments in the environmental and food monitoring areas provide useful indicators for the potentially enormous benefits of this emerging hybrid of science and technology [v].

Impact of Biomedical and health Monitoring

With respect to biomedical and health monitoring, current activities can be divided roughly into three areas;

Point-of-need diagnostics: developments in optics and reagent handling mean that many diagnostic tests can now be packaged into hand-held units, and the results of the test made available to remote locations using consumer-based communications technology. For example reagents can be deposited in a very reproducible manner as dots to provide a matrix of tests for a particular condition. The data from the tests can be automatically transmitted to a palm-type device or cell phone and relayed to healthcare specialists at remote locations (Figure 2). In this manner, individuals can take more personal responsibility for their treatment (where this may extend over months or even years), and, at the same time, specialists are kept up to date with the condition of the patient.

Wearable (non-invasive) Sensing: Computers are now small and light enough to be worn. Components are now being integrated into fabrics, leading to truly wearable systems that are completely innocuous to the wearer. New types of human-computer interface are emerging that are compatible with these 'wearables', such as VDUs and speakers integrated into spectacles (Figure 3). Sensors that track body movements have been around for some time, but new developments in conducting polymers means that these molecular strain gauges can be made an integral part of the fabric itself, rather than attached to it, as is the case with conventional devices. This means that specific locations in a garment can be made 'active' in terms of ability to monitor movement. These garments can already pick up breathing and heartbeat/pulse, and, integrated with micro-dimensioned gyroscopes and wireless communications units, can provide important information about the general health of the wearer. Garments such as the 'smart bra' [vi] have already shown the way forward (Figure 4). This approach can be readily adopted for remotely monitoring the breathing and/or pulse of aged people or young infants in real-time. This is an attractive place to initiate research into wearable diagnostics, as the sensors are rugged and reliable, and the measurements are not in-vivo. A step towards wearable biochemical measurements is the use of the 'smart watch' (Figure 5) that samples and analyses sweat for common electrolytes (Na^+, K^+, Cl^- etc.). Another non-invasive approach is to measure blood oxygen transcutaneously [vii].

In-Vivo Biochemical Monitoring: The area of in-vivo monitoring of important biochemical parameters has been most developed in the area of acute treatment, where devices need only function for a few days at most. There are still considerable barriers to the use of implantible sensors for more extended periods of time, despite the tremendous success of devices such as hearing aids

and pacemakers, which can be left in-situ for years. The key difference is that all chemical sensors and biosensors require intimate contact with the sample at a sensitive membrane or film in order to provide information about the target species, whereas pacemakers can be completely encapsulated within a protective, inert shield. The surface characteristics of these membranes/films rapidly change on exposure to body fluids such as blood that are rich in diagnostic information. Hence the response characteristics of the sensors also rapidly change, leading to a need for regular recalibration, which in turn complicates how they function, and how they are packaged. For example, how are standards to be incorporated safely, and how are standards to be regularly switched into contact with the sensor in place of the body fluid?

The Future?

The challenges outlined above are clearly significant, but exciting advances in materials science, nanotechnology, molecular chemistry and biology, and surface characterisation techniques (e.g. scanning microscopy and molecular spectroscopy) will provide researchers with powerful new tools which will undoubtedly lead to major breakthroughs. Nature shows us the way, with its exquisite molecular receptors and signalling processes linked to sophisticated multi-layer feedback systems. Materials that can regenerate or self-assemble into complex entities using templates activated through chemical signals remains an elusive, but exciting goal. Molecules that can selectively recognise target species and signal the binding event are already well known [viii]. Coupling these characteristics with the ability to move in the direction of a chemical gradient, and scavenge energy from their environment will be defining achievements on the road to 'autonomous' molecular devices. They will be designed with specific tasks in mind. For example, distinguish, locate and deliver a payload to diseased tissue, or identify and combat harmful viruses and bacteria (Figure 6). These 'artificial antibodies' or 'Nanobots' have the potential to render the conventional drug application and monitoring cycle obsolete, and hence entirely revolutionise the healthcare industry [ix]. Rather than the nanomachines of the artists impression, these are likely to be much simpler molecular structures that can nevertheless perform the extraordinary tasks outlined above.

Conclusions

For invasive sensors to be justified, they have to meet extremely demanding specifications (e.g. function for several years unattended). The preference for a non-invasive approach suggests that sweat may be a possibility as a sample fluid. However, it is not generally known which important health markers are present in sweat, and if they are, what their concentrations might be, and how these concentrations relate to systemic (blood) concentrations. Furthermore, sweat is only intermittently available, and amounts vary considerably from person to person. However, there is no doubt that developments in technology, and demands from healthcare will create enormous opportunities for wearable sensors that can deliver unique information about the health of the wearer.

The real challenge is in identifying which sensor(s) to go for in a proof-of-principle investigation of wearable sensors - a success in this area would generate confidence in the entire concept.

Ultimately, however, the really exciting science will happen at the molecular level, but this will require long-term 'blue skies' projects that are driven by a revolutionary vision, rather than relatively short-term gain.

Acknowledgements

Paper presented submitted at the DARPA-ONRIFO meeting: 'Electroactive Polymers and Biosystems: New Directions in Electroactive Polymer Materials for Biomemetic and Biointereactive Processes', Pisa, Italy, August 2001. Support from ONRIFO is gratefully acknowledged.

Figures

Figure 1: In conventional monitoring units, the sensors (right) are linked to the basestation (laptop) via a lead. In wireless based systems, there is no need for expensive shielded cables, and the sensors can be freely located anywhere within the transmission distance of the unit

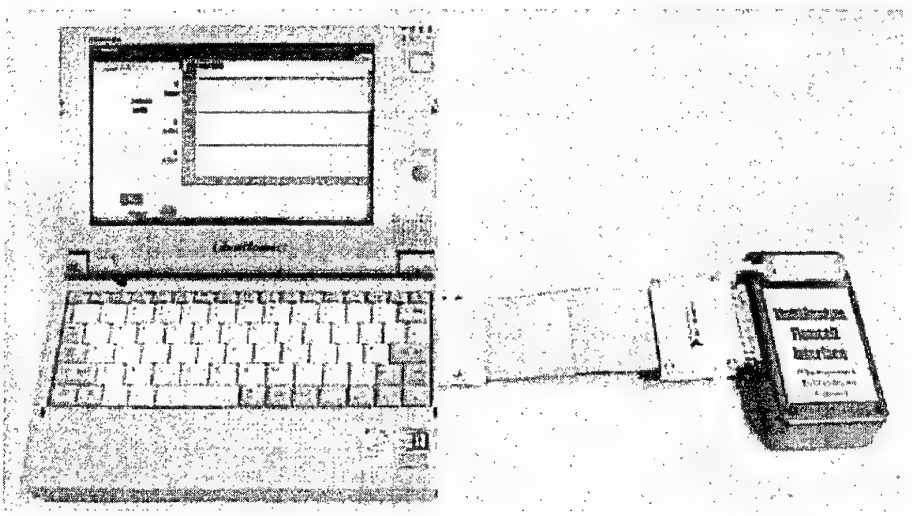

Figure 2: Diagnostic test results can be passed to consumer communications units such as Palm Computers or GSM Phones. Specialists can respond with general advice or make specific changes to therapy. The patient does not have to visit an outpatient centre as often as before. The picture (left) shows a UV-VIS spectrometer built into a HP-Jornada Palm-Computer which could provide a platform for performing home-based analytical measurements (see www.oceanoptics.com for more details). On the right, an image of the recently launched 'Active EEG' remote cardiac monitoring unit based on a Palm Pilot Platform. See www.activecenter.com for more information

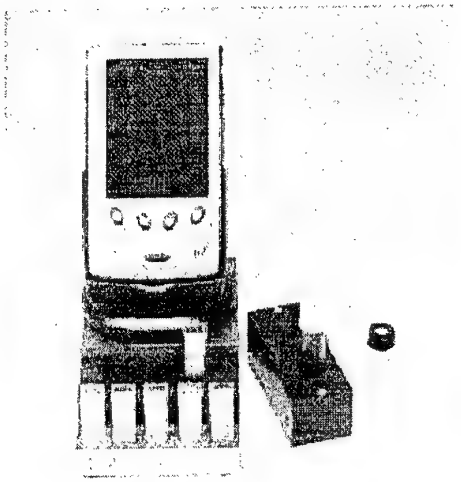

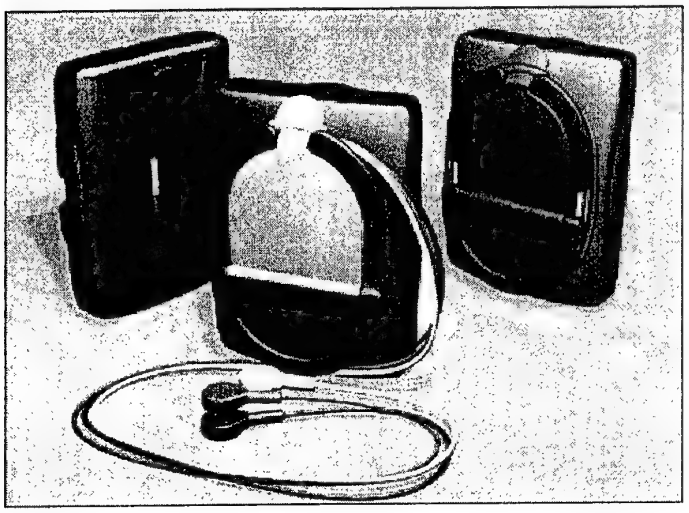

Figure 3: IBM Wearable Computer with VDU eyepiece (left) and (right) VDU integrated into spectacles via a prism that directs the visual signals into the eye (MicroOptical Corporation)

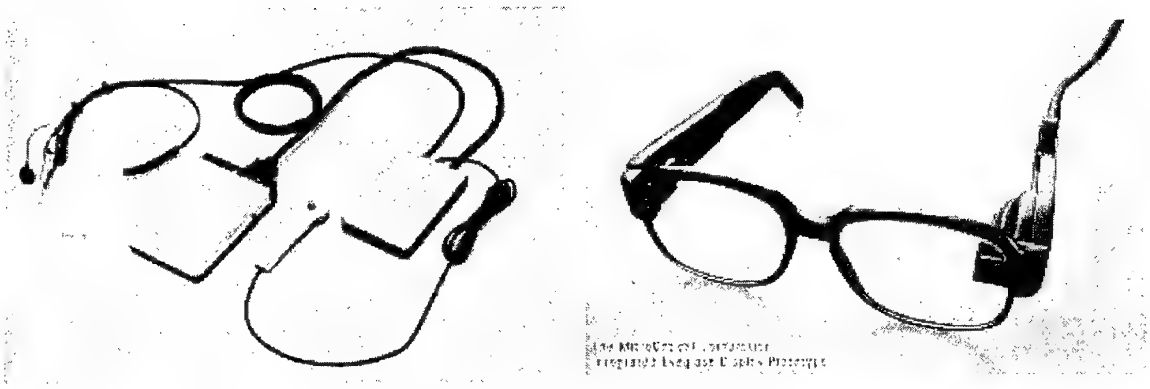

Figure 4: 'Smart Bra' with molecular strain gauges based on conducting polymer integrated into the shoulder straps and chest region can provide information on breathing and breast bounce during sports activity via wireless telemetry unit (picture provided by Prof. GG Wallace and Dr. Julie Steele, University of Wollongong).

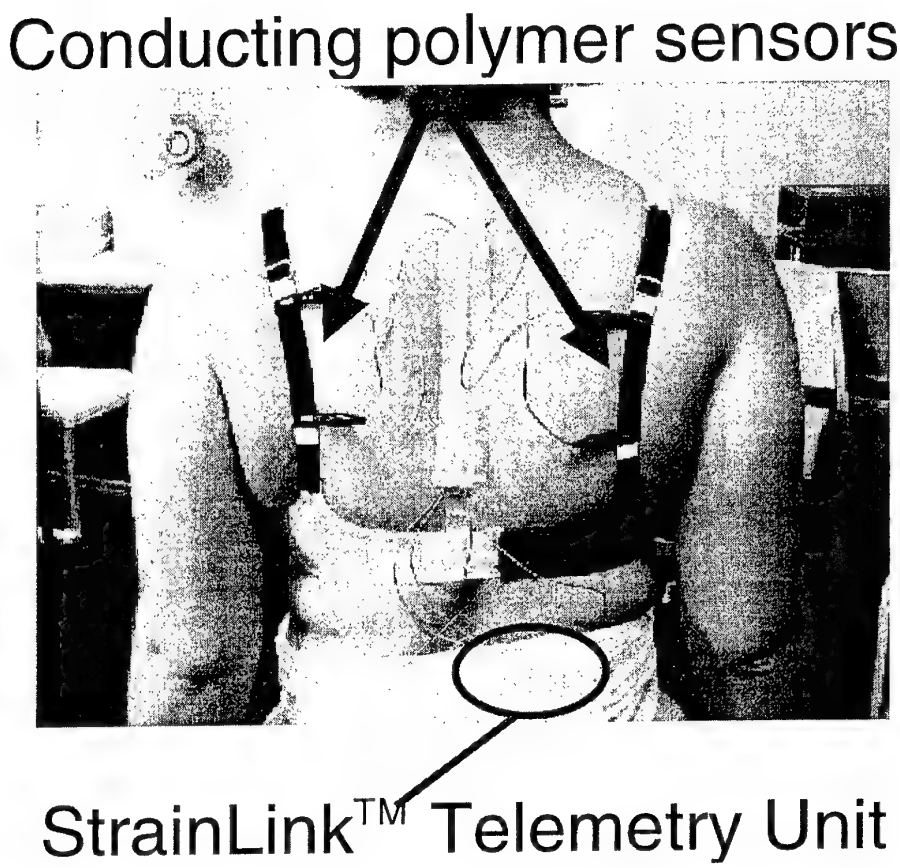

Figure 5: WESCOR Sweat sampling 'watch' with integrated flow channel containing two sensors (Na^+ and Cl^-). Bluecore RF communications platform shown for size comarison.

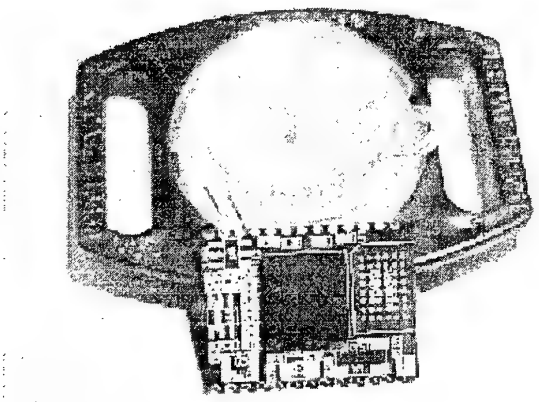

Figure 6: Molecular gearing systems such as these functionalised carbon nanotubes (left) enable control of movement at the atomic level (www.nsa.nasa.gov/groups/nanotechnology). The ultimate vision is to construct molecular machines (right) that can exist autonomously within the body and aid the immune system in identifying and destroying dangerous entities as depicted in this futuristic illustration by Jeff Johnson (http://www.foresight.org/Nanomedicine/Gallery/).

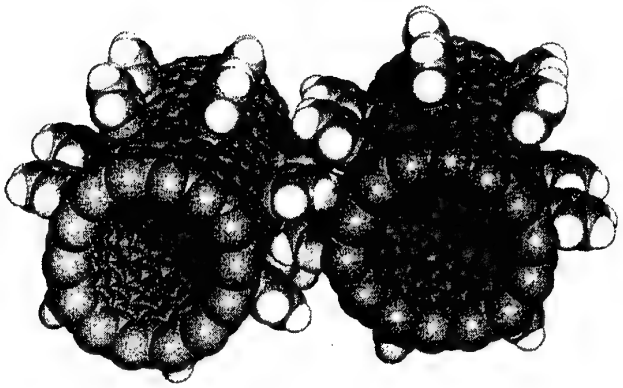

References

i See the website www.bluetooth.com for more information.

ii 'Smart rooms', Alex Pentland, Scientific American, 274, No. 4, (1996) 68-76.

iii Bradley J. Rhodes, Nelson Minar and Josh Weaver, The Proceedings of The Third International Symposium on Wearable Computers (ISWC '99), San Francisco, CA, October 18-19 1999, pp. 141-149.

iv 'Towards Autonomous Environmental Monitoring Systems', M Sequeira, M Bowden, E Minogue and D Diamond, Talanta, (2001) (accepted for publication).

v 'Temperature Logging of Fish Catches Using Autonomous Sensing Units', K McAteer, D Raftery and D Diamond, Trends Food Science and Technology, 11 (2001) 291-295.

vi 'Breast Bounce, Brassiere Straps and Conducting Polymers: A Novel Approach to Assessing Dynamic Loading' K-A Bowles,. J.R Steele, J Wu, D. Zhou, G.M. Spinks, P.C Innis and G.G. Wallace, ESM Munich, Germany, 2-6 August 2000.

vii 'Non-Invasive Oxygen Monitoring Techniques', JA Wahr and KK Tremper, Critical Care Clinics, 11 (1) (1995) 199-217.

viii 'Calixarenes: Designer Ligands for Chemical Sensors', D Diamond and K Nolan, Anal. Chem., 73 (2001) 22A-29A

ix 'Say "Ah!" - Nanorobots the size of bacteria might one day roam people's bodies, rooting out disease organisms and repairing damaged tissue', RA Freitas, SCIENCES (New York) 40: (4) (2000) 26-31

DESIGN, ACTUATION AND FABRICATION ISSUES IN MICRO-ENDOSCOPY

P. DARIO, A. MENCIASSI, C. STEFANINI
MiTech Lab, Scuola Superiore Sant'Anna, Pisa, Italy
dario@arts.sssup.it

The increasing popularity of minimally invasive surgery (MIS) and therapy (MIT) generated a strong need for smaller and smaller medical tools with enhanced diagnostic capabilities and high dexterity. However, the design, actuation and fabrication of miniature and micro-machines (autonomous or semiautonomous) for MIS and MIT are very challenging issues, requiring new theoretical models and new technologies. This new area of engineering which deals with the design of machines with size ranging between 10 mm and about 10 □m (or less) is known as "biomedical micro-engineering".

As a mechatronic system, a micro-machine integrates harmonically mechanisms, actuators, sensors, embedded control, power supply and user interface in a smart, compact and small device. But the design rules, the simulation tools and the fabrication technologies of micro-machines are quite different from those used with normal-size machines. One cannot develop micro-machines simply by "scaling down" the standard rules, tools and technologies of traditional mechanical engineering; moreover, if the micro-machine is for biomedical applications, this effort becomes even more challenging.

The actuation of autonomous micro-endoscopes is not a trivial problem: besides the scaling laws which affect the actuators effectiveness in the micro-domain, the human body is a very aggressive -and at the same time a very delicate- environment, which cannot tolerate all possible actuators. No existing actuators look ideal for micro-endoscopy. Electromagnetic motors are too large to be used in wireless configurations, while small micromotors (with diameter less than 2 mm) have not enough torque or require reduction gears. Shape memory alloys have a favourable force/mass ratio, but they need high currents to be actuated and they are difficult to control. Piezoelectric actuators generate high forces but they have low stroke and generally needs high voltage. Hydraulic and pneumatic actuators are quite common in medical actuators, but they require an external supply and are not easily miniaturizable. Electro-active polymers (EAPs) could be good candidates for "on board" actuation of micro-endoscopes: they require low voltage and current; they can generate large strokes and forces, depending on their different composition. Currently, EAPs are not completely reliable, but they represent definitively a future important resource.

In this presentation, we discuss basic problems encountered in the design and actuation of micro-machines for micro-endoscopy, different technologies used to fabricate them, and some examples of biomedical micro-machines being developed in various laboratories, including the authors' one.

Two case-studies will be presented: the first one is the development of an innovative micro-endoscopy system for the inspection of the entire gastrointestinal tract; the second one concerns the design of a micro-endoscope for neurosurgery, endowed with a complex system of hydrodynamic actuators.

Micro-endoscopy of the gastrointestinal (GI) tract is a very "hot" topic. Several researchers are working on miniaturised endoscopes and swallowable capsules for GI endoscopy. An Israelian company, Given Imaging Ltd's, has produced a wireless swallowable capsule which is capable of obtaining real images of the small intestine for diagnosis of small bowel disorders in humans (http://www.givenimaging.com). Locomotion of this capsule is entirely due to natural peristaltic movements of the GI tract: no active locomotion is performed.

On the other hand, locomotive means are extremely important to stop the devices at any point for a "better look" or to navigate to an area of interest for therapeutic procedures: the capsule without locomotion cannot be considered a clinical device. In the authors' laboratory, mini- and micro-endoscopes that can propel semi-autonomously or autonomously in some parts of the gut are being developed in the framework of a project funded by the Intelligent Microsystem Center in Seoul

(http://www.microsystem.re.kr). Starting form large (25 mm in diameter, 150 mm in length) prototypes with external pneumatic actuation, we developed smaller prototypes (12 mm in diameter, 30 mm in length) actuated by external motors and we are designing now real wireless devices with on board actuators.

The second case-study, the micro-endoscope for neurosurgery is even more challenging and long-term, from a clinical point of view: the propulsion is generated externally in a controllable way by the operator, but the endoscope must advance without touching - and consequently damaging - the spinal wall and the environment around. The actuation strategy for keeping the micro-endoscope in the right direction is an interesting micro-engineering topic, which involves many critical issues in terms of safety, physical parameters to be monitored (temperature developed by the actuators, required power supply, etc.) and biocompatibility.

NanoStructures Group at Media Lab Europe: Technologies and Solutions for the Future

Marc in het Panhuis and Andrew Minett[1]

Media Lab Europe, Sugar House Lane, Bellevue, Dublin 8, Ireland
Tel: +353 1474 2800, Fax: +353 1474 2809, E-mail: mihp@media.mit.edu

Media Lab Europe (MLE) is a new innovation centre located in the centre of Dublin, Ireland. It will "invent the future" by replicating the innovative and entrepreneurial operating model of the world-renowned Media Laboratory at Massachusetts Institute of Technology (MIT) in Boston, USA. Like the MIT Media Laboratory, Media Lab Europe is adopting an interdisciplinary approach to the way in which new technologies can impact on people's lives and environments.

Media Lab Europe's overall goal is to enhance quality of life through research and education focused at sustainable, human centred design in technology, science and the arts. It is also expected to foster greater levels of innovation and entrepreneurship, through development of a parallel incubator/accelerator unit.

The innovation teams at MLE have a focus ranging from Time and Attention (technologies for our scarcest human resources), Sustainable Development (renewable energy sources), ContemPLAYtion (playing to learn, impressive environments), Common Cents (mobile context aware e-commerce applications), Connectedness (personal area networks, tactile displays) and Building Blocks (nanostructures).

The NanoStructures Group founded by Marc in het Panhuis is part of Building Blocks with overlapping projects in ContemPLAYtion and Connectedness.

The mission statement of the group is to develop technologies and solutions for future Nano-Bio-Medical applications. Upon admission to a hospital several invasive operations are performed. Needles are used to extract blood in several quantities, in some cases the cardiovascular systems is checked. This causes discomfort for the patient. The main aim of the group is to develop a bio-compatible multifunctional medical assessment device (see figure 1) to assess a patient without discomforting them. This nano-scale device will be able to assess for example, glucose and red blood cell levels from within the body, through a connection to a blood vein. A nanoscale pump will allow blood to flow through the nano-channel

[1] Currently at Max-Planck Institute for Festkorper Forschung in Stuttgart, Germany

towards the sensing part of the device. The nanosensing units consist of carbon nanotube bundles which act as electrodes. The bundles in each of the sensing units will be chemical functionalised to selectively bind to one particular type of molecule. The presence of, for example glucose molecules can then be electrochemically detected. The assessment data is transported through wire-less technology. The device will operate through molecular electronics.

This device will allow non-invasive monitoring of a person's health. It can automatically alarm a general practitioner if for example glucose levels become to high. It can also be employed to assess the health of a soldier on tomorrow's battlefield.

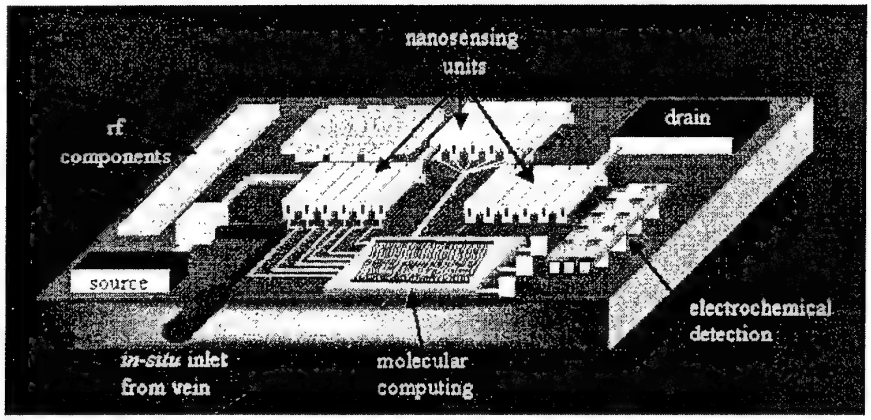

Figure 1: Schematic of the bio-medical multifunctional assessment device.

Most of the current research projects are working towards solutions that can be incorporated in this device. A novel nanotransistor device has been proposed which uses charge flow in conjugated materials (i). It is switched off simply by breaking the effective conjugation between adjacent carbon atoms and hence limiting current flow. Single walled carbon nanotubes (SWNT), with metallic properties, act as interconnects for the switching region (SR), which contains a single molecule. This

SR has polar elements, which make it susceptible to an electric field, and this property can be used to switch the transistor between ON and OFF states. By applying a voltage to the gate electrode an electric field will be set up. The SR will respond to this field, changing its orientation. Depending on the molecular orientation the device will then be in the ON or OFF state.

The first step (on this very long path) towards the device shown in figure 1 is to build a nano-scale sensing device that can selectively detect glucose in an aqueous solution. Single walled carbon nanotubes were deposited across two electrodes on a silicon wafer. Scanning electron microscopy (SEM) images (figure 2) show the presence of single tubes and bundles on the substrate (ii). E-Beam lithography was employed to contact the ends of the tubes.

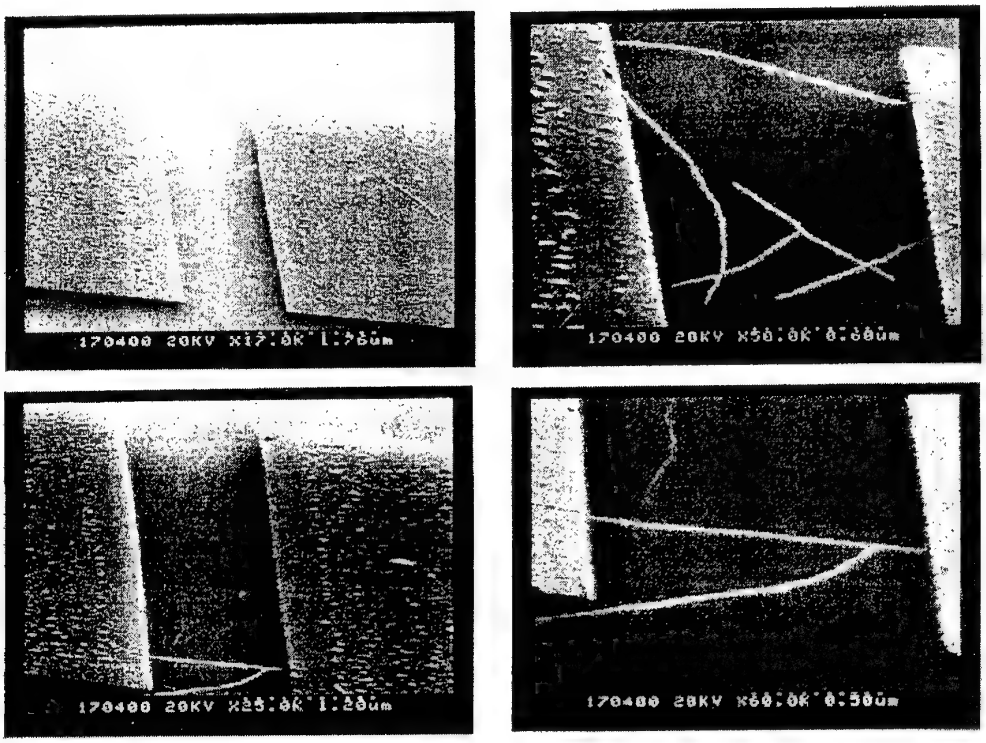

Figure 2: SEM pictures of nanotubes across electrodes.

The entire area except for the gap between the electrodes would then be insulated with PMMA for example, so only the nanotube would be in contact with the solution. This will enable us to start to gather electrochemical information about different molecules absorbed onto the nanotubes.

Increases in both sensitivity and time of detection can be expected compared to macro or micro sensing devices. The nanotube also provides an exceptional material for functionalisation or chemical modification. For example, coating in conducting polymers or covalent attachment of functional groups such as enzymes, antibodies or proteins are currently being pursued.

In addition to the medical assessment project there is also research such as the Tactile Display (Tactus) and Science-Visualisation (Sci-Vi) projects, which involves collaboration with several other innovation groups.

The goal of the Tactus project is to realize a dream, to create a refreshable, versatile tactile display capable of rendering a range of tactile effects from fine textured surfaces to tactile maps and graphs. Existing commercially available haptic display devices render virtual objects by simulating contact forces. Surface geometries and textures are rendered as changes in force perceived at the tip of an infinitely fine stylus probing the virtual environment. The haptic display device is, in effect, a tool that mediates the experience of touching a texture directly – like feeling a surface by stroking it with a pencil instead of with a fingertip. By creating a programmable, refreshable tactile display, we hope to provide the ability to render virtual textures that can be felt not just by the fingertip but by the whole hand.

Media Lab Europe is also committed to promoting and further educating the general public about science. One of the main problems of explaining Nanotechnology to non-science educated people is the scale at which this technology operates. Scientists are now able to manipulate objects which are one million times smaller than the tip of a pen. The Sci-Vi project involves developing an immersive environment which will enable people to "feel" the nanoworld. Using this environment people will be able to push and pull molecules around in the nano-world. Alternatively it could be used to assemble nano-scale devices. The essence of this project is to couple a nano-scale microscope with force feedback and virtual reality to break down the barriers of science and open a previously closed world to the imagination of the general public.

---

i M. in het Panhuis, J.N. Coleman, P.L.A. Popelier, B. Foley, R.W. Munn and W.J. Blau, submitted 2001.

ii A. Minett and M. in het Panhuis, unpublished results.

Haptic devices for minimally invasive surgery

Enzo Pasquale Scilingo* Antonio Bicchi*‡ Danilo De Rossi*†

(*) Centro "E. Piaggio", Facoltà di Ingegneria, Pisa, Italy
(‡) Dept. of Electrical Systems and Automation, University of Pisa,Italy
(†) Istituto di Fisiologia Clinica del C.N.R., Pisa, Italy
E-mail: pasquale, bicchi, derossi@piaggio.ccii.unipi.it

Abstract— In the last years the surgical approach to pathologies is shifted from traditional open surgery to the use of less invasive means. These minimally invasive alternatives offer many advantages: less pain, scarring and recovery time for the patient, as well as reduced health-care costs. Nevertheless they suffer from some limitations due to loss of tactile perception by surgeon during the operation. He can only see biological organs through a computer's monitor and touch them by means of elongated surgical tools. We have proposed and realized several solutions to this problem. First, we focused our efforts on the identification of rheological properties of biological tissues, and to do this we designed a sensorization system to be applied on a surgical forceps able to acquire signals relative to force applied on tissues manipulated and deformation induced. By elaborating suitable models, distinctive parameters of biological tissues have been evaluated. Next step has been to design an actuator, duly controlled, capable to simulate tissues compliance. Several devices and different control strategies have been considered: a linear solenoid interfaced to the sensorized tool, a miniaturized rotational solenoid integrated onto surgical tool, a pneumatic kinesthetic display and a pneumatic haptic interface. All devices design has been guided by principles of simplicity, inexpensiveness and effectiveness. Finally an innovative haptic interface based on magnetorheological fluid has been studied and realized. This fluid is a suspension of micron-sized, magnetizable particles in a synthetic oil. Exposure to an external magnetic field induces in the fluid a modification in rheological behaviour changing it into a near-solid in few milliseconds. Just as quickly, the fluid can be returned to its liquid state with the removal of the field. We built a device containing MR fluid and we verified the possibility of using it to mimic the compressional compliance of biological tissues. A further psychophysical validation using samples of bovine biological tissues has been performed in order to assess performances of the device MR fluid-based. Also, devices based on conductive polymers are under investigation, in particular electroactive catheters and polymeric fibers, that can be used in applications for minimally invasive surgery, have been studied.

I. Introduction

Nowadays diagnostic and therapeutic methods in the medicine aim to reduce discomforts for the patient. Surgery joins to this tendency and, in confirmation of this, approach to pathologies is shifted from traditional open surgery to the use of less invasive means. Minimally invasive surgery, in fact, proposes to reduce the traumatic effect of some surgical operation [2]. It offers many advantages: reduction of risks, disfigurement, and patient pain, shorter immobilization (about 24 hours), shorter hospitalization (about 2-24 hours) and an earlier return at work (about 7 days). These advantages lead to a total health care cost reduction for commercial and governmental institutions as well as for the patient [3]. Nevertheless, the minimally invasive surgery is still afflicted with important limitations. One of the most important is the surgeon loss of both tactile and kinesthetic sensibility due to the transmission mechanism of the elongated tools. The surgeon may operate only using long tools, visualizing abdominal environment through a monitor. The absence of a direct touch restricts the application of this technique only to some specific fields. The lack of tactile sensibility, in particular, limits the discrimination tissue's compliance and viscosity. These effects are so relevant that it can be very difficult to discriminate the anatomical nature of the manipulated tissue [6].

Here we present several solutions to this problem. First, we focused our efforts on the identification of rheological properties of biological tissues, and to do this we designed a sensorization system to be applied on a surgical forceps able to acquire signals relative to force applied on tissues manipulated and deformation induced. Several models have been considered and the best one has been chosen by comparing theoretical data with experimental results. In this way, distinctive parameters of biological tissues have been evaluated. Signals acquired have been used to control an actuator able to give back to surgeon the lost tactile perception. To that end we designed and realized different actuators, duly controlled, capable to simulate tissues compliance. Several devices and different control strategies have been considered: a linear solenoid interfaced to the sensorized tool, a miniaturized rotational solenoid integrated onto surgical tool, a pneumatic kinesthetic display and a pneumatic haptic interface. All devices design has been guided by principles of simplicity, inexpensiveness and effectiveness. Finally an innovative haptic interface based on magnetorheological fluid has been studied and realized. This fluid is a suspension of micron-sized, magnetizable particles in a synthetic oil. Exposure to an external magnetic field induces in the fluid a modification in rheological behaviour changing it into a near-solid in few milliseconds. Just as quickly, the fluid can be returned to its liquid state with the removal of the field. We built a device containing MR fluid and we verified the possibility of using it to mimic the compressional compliance of biological tissues. A further psychophysical validation using samples of bovine biological tissues has been performed in order to assess performances of the device MR fluid-based. Also, devices based on conductive polymers are under investigation, in particular electroactive catheters and polymeric fibers, that can be used in applications for minimally invasive surgery, have been studied.

II. Sensory system and kinaesthetic display

As a first attempt to solve the abovementioned problem, we realized a sensorized prototype of a laparoscopic forceps able to realize real time data acquisition and analysis [1]. To measure the applied force and the position of the jaws, we employed strain gauges and an optical position

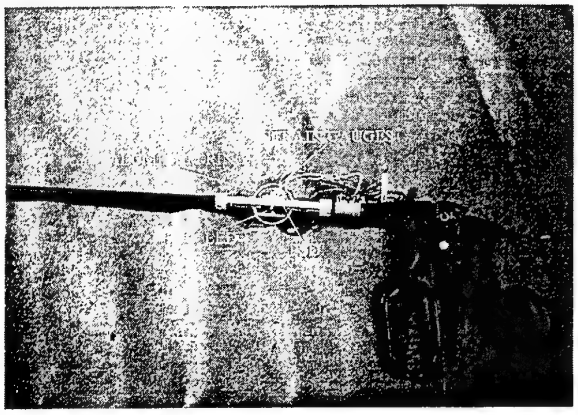

Fig. 1. Sensorized surgical tool.

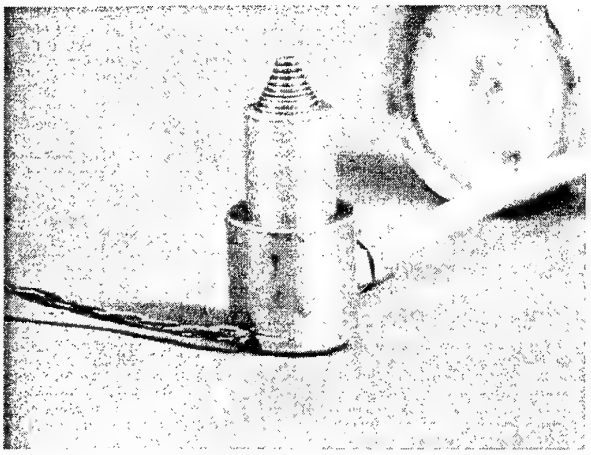

Fig. 2. The physical setup of the haptic display.

sensor device (see Figure 1). An 8 bit microcontroller with 8 A/D inputs, an asynchronous and a synchronous serial port, three 8 bit input-output digital ports was used to acquire sensors signals.

In a preliminary validation phase with skilled minimally invasive surgeons, the graphic display did not show completely satisfactory. This is mostly due to the disparity of the sensorial modality used for display from the one the surgeon is trained to, i.e. kinesthetic and tactile. We have realized a display (see Figure ??), which at first was only kinesthetic, designed to provide the surgeon with a haptic sensation of the compliance of manipulated tissues. The display is comprised of a linear actuator, a spring, and a linear position encoder. The actuator is realized by a piston fitting into a solenoid, being its vertical stroke limited by the spring. The inputs of the haptic display are the force exerted on the piston and the current flowing into the solenoid. The outputs is the variation of the piston position with respect to the equilibrium position. The operator force is opposed by the spring's force and by the piston inertia, while the magnetic force generated by the current flowing into the solenoid may concur with the operator force to make the device appear "softer" than the spring itself.

Although the performances of the kinesthetic display are good and the experimental results encouraging, according to the work of Srinivasan and LaMotte[4], both tactile and kinesthetic information are necessary for discriminating the softness of materials. Motivated by this we designed a sensory and actuatory system able to replicate a haptic sensation.

III. Haptic displays

Aware of difficulties to realize a matrix system we concentrated our efforts to realize a single element sensor and actuator. Our design was inspired by the mechanism of tactile perception, where the human finger exerting an increasing force on manipulated objects, the contact area between the object and the fingerpad grows in size in relation to compliance of the object. Our goal was to replicate this behaviour designing and realizing a display, associated with a suitable sensory system, able to provide it.

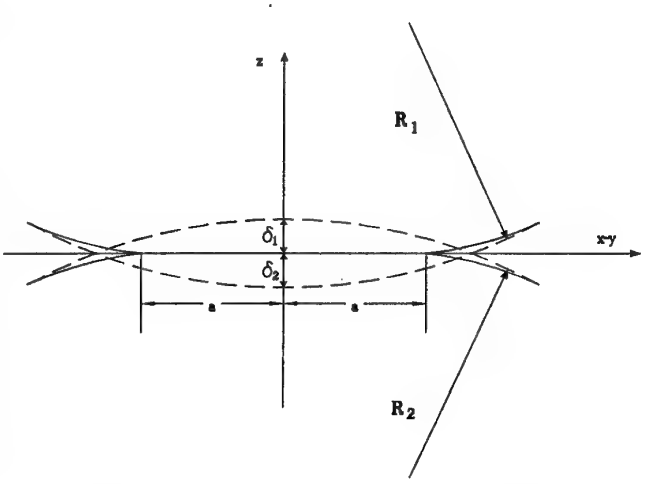

Fig. 3. Behaviour in the region of contact of two bodies.

A. Pneumatic display

A.1 The CASR conjecture

Observation of haptic exploration of objects in humans, such as described in the psychophysical literature ([4], [5]) and by everyday experience, definitely shows that kinesthesia alone can not supply sufficient information for most haptic tasks, and that tactile information is instrumental. However, tactile information in humans is extremely rich in content and purposes, and it might not be the case that all its richness is actually necessary to discriminate softness of different materials, which is our ultimate goal in this research. As an example, it is easily verified that, up to some indesirable "haptic illusions", softness discrimination is not affected by the finger touching the surface of a specimen at different orientations; nor is it very sensitive to the location of the contact area on the finger surface. These observations lead to consider haptic discrimination of softness as fundamentally invariant with translations and rotations of

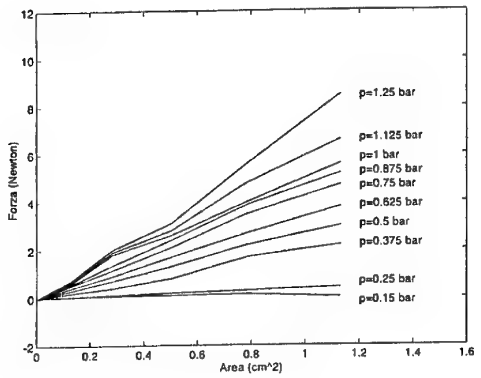

Fig. 4. Characterization of the haptic display.

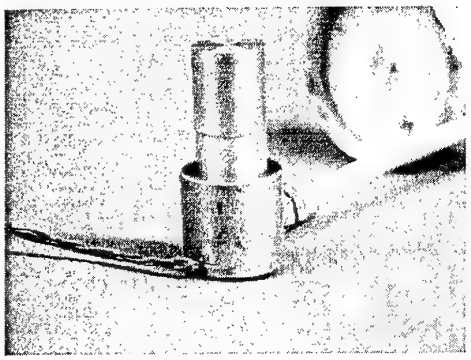

Fig. 5. Appearance of the kinesthetic display used in the experiments.

the contact area.

One may go further on this line of reasoning, and find other aspects of fine cutaneous imaging available to humans, to be scarcely relevant to haptic discrimination of softness. For instance, the actual *shape* of the contact zone between the finger and the object does not seem to be by far as relevant as the *area* of the zone itself. More precisely, we conjecture that a large part of haptic information necessary to discrimate softness of objects by touch is contained in the law that relates overall contact force to the area of contact, or in other terms in the rate by which the contact area spreads over the finger surface as the finger is pressed on the object. We call this relationship the Contact Area Spread Rate (CASR).

A first prototype of haptic display realizing the CASR conjecture is pneumatically driven. The display is comprised of a linear concentric cylinders able to run one inside the other, like a telescope (see Figure 2). By lowering the central cylinder, having an area A_0 down to Δh the finger of the user encounters a surface $A_1 = A_0 \Delta A$; and by pushing down again, after Δh the finger interacts with a surface increased $A_2 = A_1 \Delta A$ and so on. If we impose a constant pressure p_0, the display opposes to user's finger a force $F_0 = p_0 A_0$ at first step and $F_i = p_0 A_i$ at next steps. In Figure 4 you can see the characterization of the display experimentally identified. So by controlling the pressure with a pneumatic servo valve we can replicate the behaviour Force versus Area of manipulated tissues evaluated early.

A.2 Experimental results

To validate, at least preliminarly, the CASR hypothesis, we devised and executed several psychophysical experiments, which have been conducted in our laboratory with the help of volunteers using the CASR sensing and displaying equipment described above. For comparison purposes, a purely kinesthetic display is used in some experiments. In order to minimize the impact on psychophysical experiments of the different technology and appearance of the kinesthetic display with respect to the CASR haptic display, the former device has been realized by covering the CASR display with a hollow cylinder, whose upper base is flat and rigid (see fig.5).

A.3 First Experiment: Recognition Rate

The experiment consisted in measuring the capability of 15 volunteers to recognize 5 different items by touching a remote haptic system. Recognition rates using direct exploration, a kinesthetic display, and the CASR paradigm have been compared.

A.4 Second Experiment: Consistency of Perception

An experimental protocol was designed to assess the consistency of users' perception from the haptic and kinesthetic displays. By this protocol, volunteers were required to tune (through instructions given to an assistant) the regulation of the air pressure in the inner chamber of the haptic display, while comparatively exploring a given specimen and the display itself, at their will. The assistant himself was blind to what display was being used. Subjects used the same finger for probing the specimen and the display in turns. The tuning procedure was interrupted when the volunteer was subjectively satisfied with the degree of resemblance of the perception from the display and the specimen, and the corresponding pressure level in the display recorded as the perceived optimal tuning parameter.

A completely analogous series of experiments were performed replacing the haptic display with the kinesthetic display. Subjects were aware about which type of display was being used. The experiment was repeated five times by each of the 15 volunteers for the five different specimens and for the two types of display. Experiments with the two displays and the five specimens were executed in mixed order, to equally distribute effects of test fatigue in volunteers. Results show that haptic display is more effective than kinaesthetic display.

A.5 Third Experiment: Perceptual Thresholds

Important parameters in the psychophysics of perception are absolute and differential thresholds, i.e. the minimum

level of intensity of a stimulus capable of evoking a sensation, and the minimum intensity difference between two stimuli that allows the subject to distinguish between them. In the case of haptic discrimination of softness, absolute thresholds are rather difficult to measure, and not as relevant to applications as differential thresholds. We focussed therefore on the assessment of the latter parameter.

The differential threshold of a perceptual stimulus, or, as it is often called, the *just noticeable difference* (JND), is a figure reflecting the fact that people are usually more sensitive to changes in weak stimuli than they are to similar changes in stronger or more intense stimuli (for instance, one would probably notice a difference in weight between an empty paper cup and one containing a coin, yet probably a difference between a cup containing 100 coins and one containing 101 would not be noticed). The German psychophysicist Weber suggested the simple proportional law $JND = kI$, indicating that the differential threshold increases with increasing intensity I of the stimulus; the constant k is referred to as Weber's constant. Although more recent research indicates that Weber's law should only be regarded as a rough characterization of human sensitivity to changes in stimulation, it approximates reality well in the middle range of stimuli (the JND tends to grow more slowly in the low and high range of reference stimuli). Average values of Weber's constants are available in the psychophysical literature for most common perceptual channels, among which the two most relevant to our purposes here is for $k = 0.013$ for diffused tactile stimuli, and $k = 0.136$ for punctual tactile stimuli (this numbers indicate the rapid saturation of receptors involved in single–point tactile perception).

In the evaluation of the JND of the CASR haptic display comparatively with the kinesthetic display, the stimulus is represented by the device compliance, and hence the stimulus intensity can be identified with the pressure level in the device. The 15 volunteers were asked to touch the haptic display regulated at a constant reference stimulus, and familiarize with the corresponding compliance by probing the device. Afterwards, the device was regulated at slowly increasing pressures, until the subject, who kept probing the device, would detect a difference in compliance. The difference between the corresponding value of pressure and the reference value was then recorded. All subjects repeated the experiment twice for six different levels of reference pressure, equally spaced in the operating range of the device. The sequence of experiments was randomized. The same procedure was then applied to the kinesthetic device.

The mean JND and its standard deviation for each reference stimulus and display type were calculated for each subject, and these data averaged over the 15 subjects. Results are presented in fig.6, along with the corresponding error bars.

Both diagrams are pretty much linear in the medium range, where Weber's constant can be evaluated as ca. $k = 0.09$. Though not as good as diffused cutaneous tactile perception, both displays show a slower growth of JND than single-point stimuli. The average JND of the haptic

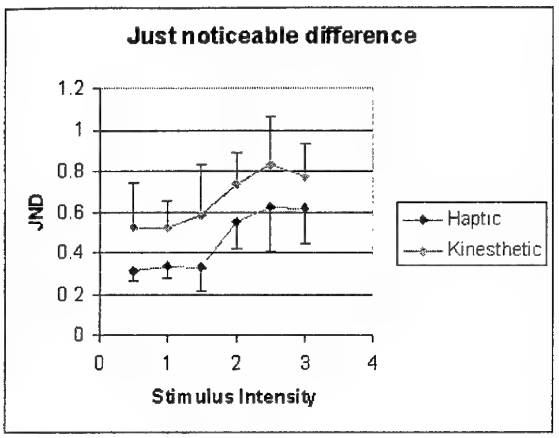

Fig. 6. JND versus the intensity of reference standard stimulus for the CASR display and the purely kinesthetic display. Each data point represents the average of 30 trials (2 trials by 15 subjects). Error bars (segment lengths are equal to half the average of standard deviations for the 15 subjects) are superimposed to data.

and kinesthetic displays are 0.46 and 0.66 stimulus units, respectively. The haptic display allows subjects to discriminate differences in compliance 30% more finely than the kinesthetic display.

A.6 Fourth experiment: Psychometric function

The psychometric function is another measure of sensorial resolution widely used in psychophysical studies. The experiment consists of asking volunteers to compare the apparent compliance of the CASR display in two successive trials. During the first trial, the display is regulated to a standard value S of compliance (i.e. of air pressure in the inner chamber), while during the second a different value X is set. Fifteen volunteers were asked to decide whether X was "harder" than S, and the number of positive answers divided by the total number of answers is denoted by $P\{X > S\}$. As X is varied from values lower to values higher than S, the *psychometric function* is obtained as

$$F_S(X) = P\left\{X > S|_{(S,X)}\right\}. \qquad (1)$$

In the ideal case of an infinitely fine resolution in the sensory channel, the psychometric function would be a step function ($F_S(X) = 0, X < S$, $F_S(X) = 1, X > S$). A diagram of the psychometric functions obtained with the CASR haptic display and the kinesthetic display is reported in fig.7. The discrepancy between the ideal step function and the experiments can be measured by the sum of the squares of deviations from the ideal, stepwise curve, namely by the figure

$$D = \sum_{i=1}^{4} P_i^2 + \sum_{i=5}^{8} (1 - P_i)^2$$

It can be observed that the haptic display curve is closer to the ideal behavior ($D = 0.87$) than the kinesthetic display ($D = 0.52$).

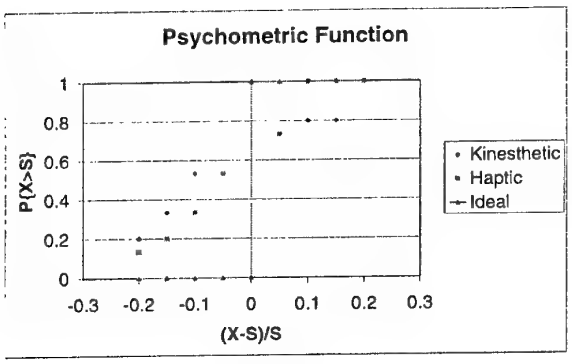

Fig. 7. Psychometric function of the CASR display. The reference stimulus S corresponds to an air pressure of 0.5 bar in the displays, i.e. in the middle of the operating range of the devices. Each data point represents the average of 30 trials (2 trials by 15 subjects).

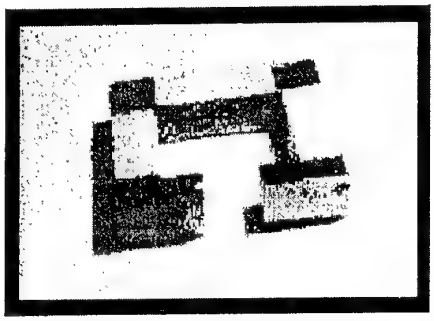

Fig. 8. The core of the electromagnetic device used.

B. Magnetorheological display

Magnetorheological (MR) fluids are materials that respond to an applied magnetic field with a change in rheological behaviour. Typically, this change is manifested by the development of a yield stress that monotonically increases with applied field. Just as quickly, the fluid can be returned to its liquid state with the removal of the field. MR fluids are already present on the market but their application field is restricted to devices such as valves, brakes, clutches, dampers. In order to apply a magnetic field on the MR fluid specimen we designed and built an electromagnet. Design process steps were to design a low reluctance steel flux conduit to guide and focus magnetic flux into region of MR fluid ; maximize the magnetic field energy in this region and minimizing the energy lost in the other regions. To do this we positioned MR fluid in the air-gap of an electromagnet with three coils in series composed by 2400 turns of copper wire with 0,8 mm in diameter, such that the maximum current flowing in it is 1,26 A sufficient to produce magnetic field of our interest. In fig. 8 is reported the core of the electromagnetic device used.

B.1 Experimental results

At first we proceeded with a psychophysical investigation. In this phase we selected six sample of bovine biological tissues: brain, myocardium, spleen, liver, lower limb muscle and lung. Each sample has been reduced to the same size of the MR fluid specimen in order to remove artefacts due to differences in test conditions. Volunteers were asked to manipulate at the same time using both hands the biological tissue sample and the MR fluid specimen duly excited with magnetic field. The magnetic field was changed on volunteers' suggestion till a good resemblance in compliance was attained. When volunteers perceived the same tactile sensation from both biological tissue sample and MR fluid specimen, the corresponding magnetic field was recorded. Tests were repeated more times for each volunteer in order to calculate the average magnetic field necessary to excite the MR fluid specimen and to induce a compliance similar as much as possible to corresponding biological tissue sample. Results were encouraging, but for the myocardium, lower limb muscle and lung where the analogy was not satisfactory. This is due to the fact that the magnetic field intensity needed to induce a compliance similar to these biological tissues, is beyond saturation of the MR fluid we used.

IV. Conclusions

It has been firmly established in the psychophysical literature that the ability of discriminating softness by touch is intimately related to both kinesthetic and cutaneous tactile information in humans. In replicating touch with remote haptic devices, there are serious technological difficulties to build devices for sensing and displaying fine tactile information. In this paper, we presented several solution of devices able to convey enough information to allow satisfactory discrimination of softness.

References

[1] A. Bicchi, G. Canepa, D. De Rossi, P. Iacconi, E. P. Scilingo: "A sensorized Minimally Invasive Surgery Tool for detecting Tissutal Elastic Properties", *Proceedings of the 1996 IEEE International Conference on Robotics and Automation*, Minneapolis, Minnesota - April 1996 pages 884-888.

[2] K. A. Zuker, W, W.W. Bailey, T. R. Gadacz and A.L. Imbembo. Laparoscopic guided cholecystectomy. *Am J. Surgery*, 161:36-44, 1991

[3] A. Cuschieri and G. Berci. *Laparoscopic Biliar Surgery*. Blackwell Scientific Pubblications, Oxford, GB, 1993

[4] M. A. Srinivasan and R. H. LaMotte, "Tactile Discrimination of Softness",*Journal of Neurophysiology*, Vol. 73, No. 1, pp. 88-101, Jan 1995.

[5] S. J. Lederman and R. L. Klatzky: "Sensing and displaying spatially distributed fingertip forces in haptic interfaces for teleoperator and virtual environment studies", Presence, 1998 (in press).

[6] R. D. Howe, W. J. Peine, D. A. Kontarinis, and J. S. Son. Remote palpation technology. *IEEE Eng in Medicine and Biology Magazine*, 14(3):318-323,1995

[7] K. L. Johnson, "Contact mechanics", chapter 4, Cambridge University Press 1985.

AN ANDROID HEAD TO TASTE SUBSTANCES AND TO ENDOW EXPRESSIVITY

D. De Rossi, G. Pioggia

Abstract

Electroactive polymer artificial muscles (EAP) can be used to mimic human muscles. Exploiting these properties we are developing in our laboratory a human-like Android unit able to replicate human facial expressions. The Android is equipped with linear actuators and is made up of a sophisticated multisensing acquisition system able to detect rheological and organoleptic properties of food. After the data analysis, the Android looks like a man who tastes similar substances. It develops expressions mimicking humans response to the same foodstuff. In this paper we will present the design and relevant features of the muscles and the performance of the Android.

Human anatomy and mechanical studies were needed to build up the carbon fiber composite holding structure. Location and electromechanical characteristics of EAP actuators were investigated. It holds sensors, artificial skin and actuators to obtain suitable expressions, dividing the chewing phase, performed by a dedicated actuator, from the expressive phase. This was achieved through the different amplitude of the actuators' force elongation and driving conditions.

Introduction

Mimicry is one of the most complex comunication way. The human face permits nonverbal expression and man can communicate moods, emotions and feelings. Each of us has experienced the uplifting effect of a clown-face or a baby's smile. If a sad person incites our help, we try to cheer the person with a warm facial affect. The properties of EAP allow the development of a humanlike face capable of replicating these idioms. Such an undertaking involves reproducing human facial complexities with a limited array of EAP actuators. In the Android head system of University of Pisa, the goal is to mimic human anatomy with 25 actuators attached to a graphite fiber composite skull, from which they manipulate an artificial skin. The form of the human skull was modified to suit project needs. Analysis of muscles was conducted to identify the requirements for various expressions. Location and electromechanical characteristics of EAP actuators have been investigated, with first attempts at actuation successful. Actually, the state of present technology has enabled the design of some artificial faces but it did not improve the expressivity set and neither the dynamics. In fact, the products on the market are very limited and their expressivity is the combination of a few simple movements that makes them like technological toys.

Exploiting the features above described, we are developing in our laboratory this human-like Android unit with the capability to taste substances. In fact, it would be able to mimic human expressions in response to the same food tasting analysis. As above mentioned, the Android is equipped with twenty-five artificial muscles, twenty-four dedicated to endow expressivity and one to perform the chewing phase, and will be supported by a sophisticated array of sensors and data acquisition system. Data will be acquired by different acquisition cards, stored in a personal computer and analyzed through a dedicated neural net. A new driver system that was designed and developed at Centro "E. Piaggio" in Pisa activates the Android. More, the head can be designed looking like any desired face.

Our Android will be aided by neural networks (ANN) and it will use sensors to detect rheological and organoleptic properties of food to determine the consistency and quality of the particular substances that are analyzed. A conductive polymer electronic nose consisting of tactile sensors will be added as well as a strain gauge and high-resolution acoustic sensors to analyzed the chewed substances. After the data analysis, the Android looks like a man who tastes similar substances. It develops expressions mimicking humans response to the same foodstuff. This was achieved through the different amplitude of the actuators' force elongation and driving conditions. Figure 1 shows the whole block scheme of the Android. It consists of a drivers unit, an acquisition unit and the physical structure. Before describing the details of this project, an examination of human facial anatomy is necessary.

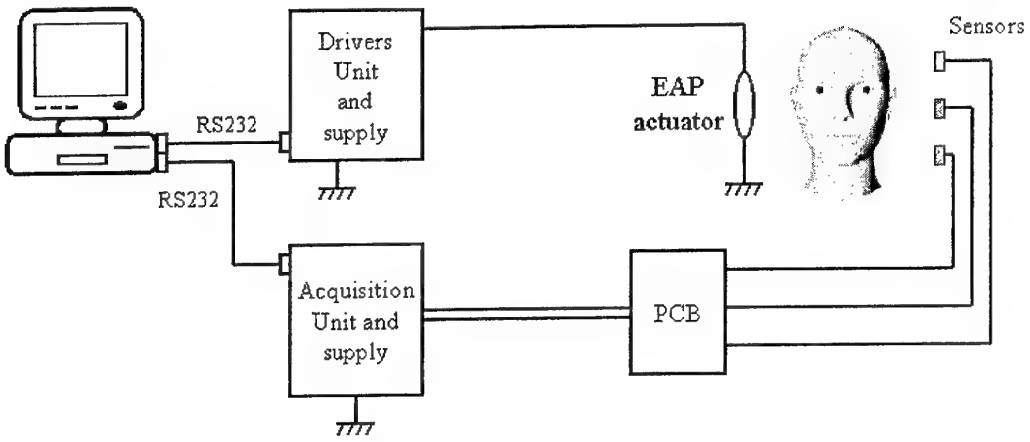

Figure 1 – Schematic of the Android

1. HUMAN FACIAL ANATOMY

Figure 2 shows the muscles responsible for facial expression. The muscles mimicked in the Android face can be divided in five groups: *epicranius muscle*, *muscles of the eyelids*, *muscles of the lips*, *auricularis muscles* and *muscles of the nose.* In humans, all aforementioned muscles are controlled via the facial nerve. First discussion will be focused on the first three muscle groups, the primary contributors to facial expressions. The *epicranius muscle* is a thin structure that stretches onto the braincase. It is formed by the *frontalis muscle* in the front side, the *occipital muscle* in the backside and by the *galea aponeurotica* in the medium region. The *frontalis muscle* is flat and has a quadrilateral shape; it starts from the boundaries of the *galea* up to the skin in proximity of the eyebrow and the upper nose. The *frontalis muscle* contracting moves up the scalp and wrinkles the forehead. The *occipital muscle* is also a flat plate that starts from the backside of the *galea aponeurotica* down to 2/3 of the lateral upper line of the nape. This muscle with its contraction moves back the scalp. The *galea aponeurotica* is a *fibrous lamina* that covers the vault and the lateral regions of the skull. It has a quadrilateral shape, where the upper boundaries are greatly connected to the cutaneous derm. The *frontalis muscle* starts from its front boundaries, the *occipital muscle* from its back boundaries and from its lateral boundaries the *auricularis anterior muscles*. The muscles of the eyelids include the *orbicularis oculi muscle* and the *corrugator supercilii muscle*. The *orbicularis muscle* has an elliptic ring shape around the *palpebral rima*. It is possible to note *orbital*, *palpebral* and *lachrymal* parts. The *orbital* part is the most developed and forms almost complete ring around the eyelids. From the lateral corner of the eye some little fasciculus comes down to the cheek and to the *zygomaticus muscle*. The *palpebral* part is contained into the thickness of the upper and lower eyelids; its fibers take origin from the *medium palpebral ligamentum*. The *lachrymal* part is located more deeply; it is divided in two fasciculae, where respectively the upper and lower eyelids come to the *palpebral* part of the muscle. The *orbicularis muscle* by its contraction performs the closing of the *palpebral rima*, directs the tears to internal angle of the eye and dilating the *lachryma sac* helps their downflow. The *corrugator supercilii muscle* is a thin plate with lower concavity located nearby the eyebrow. It starts from the medium limits of the *supercilii arch* up to the derm; its location is deeply into the *frontalis muscle* and into the *orbitalis* part of the *orbicularis oculi muscle*. Its contraction moves down the skin of the eyebrow. The muscles of the lips include the *zygomaticus muscle*, the *buccinator muscle*, the *triangular muscle*, the *square muscle of the lower lips* and the *orbicularis oris muscle*. The *zygomaticus muscle* starts from the lateral surface of the zygomatic bone up to the derm and to the *labial mucous* nearby the *commissure*, where fibers start to the *orbicularis oris muscle*. By its action it moves up and down the *labial commissure*. The *buccinator muscle* is a fleshy plate that constitutes a large region of the cheek. It starts nearby the molar teeth, its fasciculus come up to the *labial commissure*, where fits deeply into the derm and into the *mucous*. In proximity of the *commissure insertion* some fibers intersect so that some upper fasciculus come to the upper lips, while others come to the lower lips; these fasciculus contribute to the formation of the *orbicularis oris muscle* of the mouth. The *buccinator muscle* contracting shifts behind the *labial commissure* and sticks the cheeks and the lips to the *dental alveolus arch* helping the chewing phase. The *triangular muscle* is located below the *labial commissure*, it starts from the external face of the jaw, its fasciculus come up inserting in part into the derm of the *commissure* and in part into the upper lips where form part of the *orbicularis oris muscle*. Its contraction moves down the *labial commissure*. The *muscle square of the lower lips* is located more deeply with reference to the *triangular muscle*. It starts nearby this last one up to insert into the derm and into the membrane of the lower lips. Its movement consists of shifting below and laterally the lower lips. The *orbicularis oris muscle* is one of the mainly constituents of the lips, it is an elliptical ring placed around to the *buccal rima* and has an external and an internal part. The

external one is peripheral and includes fasciculus coming from some mimic muscles like *buccinator* and *triangular*; these fasciculus form two half rings that have their center in the *commissure* and their tips onto the median line of the lips. Fasciculus of this external region insert into the labial skin nearby the median line and nearby the skin that covers the back part of the contour of the nose and the back part of the *depressor septi nasi muscle*. The internal part of the *orbicularis oris muscle* is formed by a ring placed in proximity to the free edge of the lips. This ring is composed of the upper and lower lips intersecting in the *commissure*, running deeply into the skin and the *mucous*. By this movement the *orbicularis oris muscle* reduces and closes the *buccal rima* and puts out the lips.

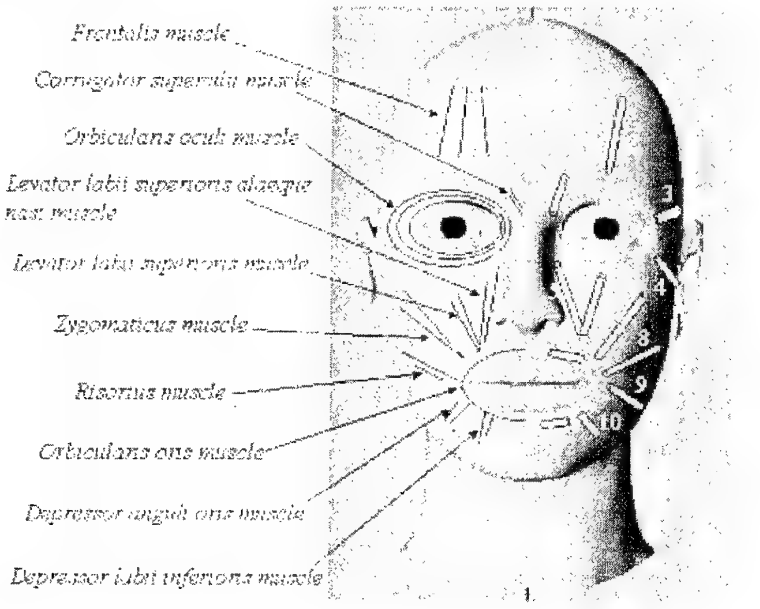

Figure 2 - Principal facial muscles that allow us to make expressions and location of the mimic EAP artificial muscles.

2. THE ANDROID FACE

With reference to figure 1, the Android face is constituted by a personal computer, in which the control software is implemented, a unit containing the drivers, an holding structure, the artificial skin and the array of electroactive actuators. The driver unit is connected to the personal computer via a RS232 serial interface. The actuators are jointed between the holding structure and the artificial skin.

The holding structure is a syntetic resin reproduction of a skull and of the top section of the backbone. This structure is designed to lodge the actuators and holds the artificial skin; it is crossed by the supply cables to allow the positioning of the actuators tangentially to the skin. The artificial skin was hand made by means of a plaster cast that allows to build a mould. A silicone rubber is melted inside the mould and after the solidification it will be the artificial skin.

The drivers unit consists of a shielded box holding seven cards, one supply for the EAP actuators up to 3 kV and one supply (5 V) for the logic controls. The unit was realized with a modular design to improve flexibility and possible future features. Each card holds a programmable microprocessor, four driver and each driver has a standard RS232 serial interface. The protocol is organized on three bytes: the first for the address (0..255), the second one for the desired position (0..255) and the last one for the information of moving rate (0..255). The baud rate is 57.6 Kbaud with a command execution rate of 520 μs, all the actuators are driven within 12.5 ms. The microprocessor acquires the informations about the desired deformation of the actuator and the rising time and forces the polymer. An electronic comparator and an encoder will be added to obtain a closed loop control; at the moment an encoder suitable for our purpose is under development and the control is performed in open loop. The actuators are controlled using various force amplitudes mimicking accuracy and dynamics of the human muscles. Our aim was to model the EAP actuators into the control system in terms of surface shape modifications that are needed to create the desired facial expressions. For this reason human expressions were acquired by motion capture sequences. We acquired perceptions and expressions directly from a man model, stored the patterns, and managed them to effectively adapt actual expressions and provide information as input for the driver unit. We obtained matrix of data for three expressions (happiness, disgust and uncertainly) and a chewing phase, where the columns are the actuators and the rows are the scan rate. Data are percentage of deformation of the actuators in ascii format. A program reads the data selected and drives the serial port and the drivers unit. By this way this control system drives simultaneously all the twenty-five actuators of the Android allowing to conduct both facial expression and chewing motion.

The data acquisition unit consists of 16 electronic nose sensors, 10 strain gauges, 2 microphones and a dedicated electronics. An electronic nose has a section to acquire data from sensors. The first section is a CPU-controlled current generator, which produces different currents that supply each of sensors and it can drive up to 16 conductive polymer

and/or metal oxide sensors. It contains 16 independent user customizable polarization interfaces, composed by 4 D/A converter DAC8420, 16 operational preamplifiers and 16 scaling resistors (Rs). The operational amplifiers contain four OP400 chips. The converter has a resolution of 2.44mV or 1.22 μA, a settling time of 6 μs, a maximum output voltage of 10V and it can drive up to 5mA. The nose can drive a maximum current of 2.5mA and use sensors with intrinsic resistance ranging from 500 W to 1 MW. The second section of the system consists of 16 independent sigma-delta A/D converter circuits. For the strain gauges, commercial cards are used to aliment them and acquire data whereas a common audio PC card drives the microphones.

3. EAP CONFIGURATION

In order to develop a system suitable for the EAP actuators that simulates the movements of the natural muscles and therefore the human expressivity, we designed an array of electroactive artificial muscles that represents a model of the mimic activities. We used EAP as artificial muscles that, referring to the natural muscles, are different in number and positioning but not in functionality. In fact, we tried to endow almost all the motion phases and expressivities of a human face by the lowest number of actuators. With this aim we analyzed only the muscles that endow a good contribution to the expressivity, overlooking others that have less influence like the *transverse part of nasalis muscle*. We used twelve muscles for half a face and one to perform the movement of the jaw, in total twenty-five muscles. Figure 2 shows the mimic EAP artificial muscles model.

Corrugator supercilii muscle (actuator #1) – The functionality of this muscle was mentioned earlier and it is needed to provide both longitudinal and transversal deformations. Generally, this muscle deformation along the longitudinal axis causes expansion in the transversal direction allowing filling adjacent regions. The use of an electrostatically stricted polymer (ESSP) as actuator (see example in Figure 3) allows generating the required longitudinal movement, however the use of swelling ionic polymer metallic composite (IPMC) layers is also being considered under the current study.

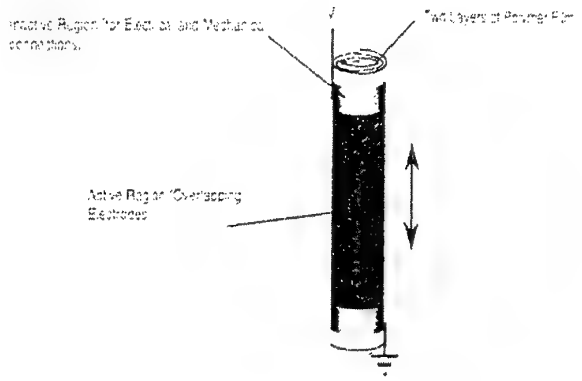

Figure 3 - Schematic of an electrostatically stricted polymer layer (ESSP) actuator

Frontalis muscle (actuator #2) – The function of this muscle can also be emulated by using an ESSP linear actuator that is placed near the *corrugator*. The synergy of these two muscles allows inducing facial deformations due to contraction in the upper *orbicularis* regions. In human this muscle is a large strip, and it is emulated using an extended actuator over the entire eye region with a series of constraint links to the skull and the artificial skin. This actuator is used to induce linear deformation over the whole forehead.

Orbicularis oculi muscle (Actuator #3) – This muscle is simulated with an actuator that is next to the eye region but it is not exactly emulated since it represents a muscle that covers a large region surrounding the human eye. Its shape is a curve and can't be reproduced with linear actuators. To emulate it there are two possibilities, where the first one is to simulate its function using an ESSP actuator that is placed in position number three. This actuator can be used to emulate movements by pulling on the artificial skin and compressing it in the *orbicularis* region. Using these actuators the eye can be partially closed and opened in synergy with the *zygomaticus muscle*, and thus expressing happiness and surprise. Another alternative, which is also under a current study, is to use a diaphragm EAP actuator wit a hole that contains the simulated eye and eyelids. This actuator consists of dielectric elastomers stretched onto a rigid circular frame made of a plastic material.

Palpebral rima (Actuator #4) – This muscle is also difficult to emulate with an EAP actuator but the use of actuator number four allows addressing the need to express sadness by pulling on the lateral region. Again, an ESSP can be used to simulate the required linear actuator.

Levator labii superioris alaeque nasi muscle (Actuator #5) – Actuator #5 allows controlling the labial region by inducing force near the nose area towards the internal direction with reference to the *nasal fossa*e. This actuator needs to be used in synergism with actuator #6, the *zygomaticus minor muscle*, which has the same function, but has a 40° degrees shift. Its particular position allows one to raise and externally bend the lips. In human these two muscles are used

synchronous with the *levator labii superioris muscle*, but in this anthroid case this muscle can be overlooked because its function can be obtained by forces from actuators #5 and #6 and these too can be made of ESSP linear actuators. The *zygomaticus major muscle* is also located in the zygomatic region, but towards the outside and it allows rising the *labial commissure* to express happiness. To emulate this muscle actuator #7 is used and its location is similar to the human equivalent while it is located subcutaneously Actuator #8, which represents the functions of the *buccinator muscle*, is placed in a different location that the biological equivalent. Here it is located at the jaw area to allow pulling and conduct chewing but it is not easy to operate it. Modifications where made to allow locating a planar actuator parallel to the jaw at the fixed braincase structure using an IPMC. This actuator is operated similar to the EAP dust-wiper using an artificial skin that is constrained at its top. To complete the upper labial mimic we an actuator was designed to emulate the *orbicularis oris muscle*. This actuator was not designed to operate like a single muscle, but as a coordinated set of three ESSP actuators representing #9, #11 and #12. The synergic movement of these actuators enables reproducing the movement of this complex muscle. Actuator #11 provides the contraction of the upper labial region, actuator #9 provides the reduction of the mouth corners and actuator #12 provides the reduction of the lower region of the lips. This latter actuator, however, does not conduct a longitudinal movement and it is designed to produce labial curving and to do so an ESSP actuator is placed at a subcutaneous location to induce the required curving on the artificial skin. The last actuator that was designed is #10 and it represents the *square muscle of the lower lips* and it is used to pull in the lower region of the lips. This actuator is constructed using an ESSP actuator that is fitted directly into the jaw. To obtain a human appearance, a holding structure was constructed using a plaster copy of a human skull, which was modified to achieve the desired functional and aesthetic features. The plaster allowed coupling the actuators and provided the necessary links. Initial efforts were focused on the lower jaw system and the ability to conduct rotation, even though human expressivity consists of longitudinal, transversal and rotational movements. This capability allowed chewing with the aid of a single actuator where the condyle was fixed to the head by a joint pin allowing the jaw to rotate on this axis. The *fossa* of the *condylar process* was strapped to minimize surface deformation and avoid complications of the mechanism and maintain low weight of the structure. At the current phase, the EAP actuators that are used exhibit low force, which is insufficient to induce expressivity. Efforts are underway to reduce the weight of the structure using graphite/epoxy composite materials for the structure and enhanced EAP actuators. Further, the *mylohyoid line* of the jaw was linking to the *nasal fossae* using an actuator. Also, the *infratemporal fossa* was closed to reserve room for the *temporal muscles* and the jaw was widened to allow that the actuator #8 to perform longitudinal and linear movements.

4. EAP SPECIFICATION

Organic materials have shown to be useful to create new actuator capable to react to physical, chemical or electrochemical stimuli. This kind of actuators are useful for all tasks that do not require a high degree of precision but versatility and complexity of operation. For this reason they can be of fundamental importance in the field of anthropomorphic robotics, micro-robotics and bioengineering. Electroactive polymers (EAP) show drastic change of electron conductivity and electromagnetic absorption spectra associated to changes of ionic doping inside the polymer. For these characteristics conducting polymers are potentially useful in many interesting applications [1].

Recently it has been shown that π-conjugated electroactive polymers can exert tremendous forces, hundreds of time greater than those of natural muscle, and that they undergo volume changes with noticeable variation of elastic moduli when ionic species are forced by electrodiffusion to penetrate inside their network. The electrochemomechanical energy conversion has been studied from experimental point of view [2,3] and a model elucidating how the doping process influences the polymer molecules has been proposed [4]. EAPs usually operate with lower strain (1-10%) than gels, but still higher than piezoelectric polymers. Since energy conversion in π-conjugated EAP is mainly diffusion limited [3,4] the response time "τ" can be reduced by assembling the EAP actuator into very thin elements. Polymer gels have received much attention since the fifties and more recently they have been used to build prototypes of muscle-like actuators, chemical valves, drug delivery systems, etc. [11]. They usually yield larger strain (50% and more) and lower forces than EAP, but comparable with natural muscles. Energy conversion in gels also involves diffusion processes [12,13] so that the dimension of the contracting element is a crucial constraint in order to obtain an acceptable time response. Given that for a thin gel fibre, strip or membrane $t \propto a^2 f / \pi^2 \mu$ [9], (where μ is the shear elastic modulus and f is a frictional parameter expressing the interaction between interstitial fluid and polymeric matrix) a response time of a second is achieved for majority of gels with a physical dimension a equal less than 10 μm.

In early attempts, metal electrodes were positioned in contact with gels, more recently polymer gels with interpenetrating EAP network have been proposed [11,14,15]. These configurations make use of electrochemical reactions at electrode surface to modify the ionisation state of polyelectrolyte gels. Electro-kinetic effect [16] and change of the red-ox state of polymer matrix groups [17,18] are also useful to induce volume and permeability changes in gels. However the mechanical degradation of thin contracting elements and the electrically triggered chemically fuelled electrochemomechanical conversion are unsolved problems which limit the application of gel as actuators.

Recently, EAP have shown to be a simple actuating system with good performance and working life. They actually constitute a closer to market product among linear non conventional actuators.

In our laboratory we tested a planar rectangular electrostatically stricted polymer layer (ESSP) actuator. The experimental set-up to test the actuator was designed to reproduce as much as possible the lodging of the actuator on the skull. It is composed by a isotonic position transducer, a signal amplifier, a plotter, an high voltage supply and a function generator. All these instruments are driven by a personal computer. The position transucer consists of a 10 cm long lever, where is linked the actuator under test, and of a moving counterweight. By this system is possible to control the force induced to the sample. Its resolution is 0.01g and it has a maximum load of 15g. The core of the signal amplifier is the Analog Device integrated circuit AD624, that is an high precision and low noise device. Plotter allows to draw the signal collected in a time scale. The high voltage needed to supply the designed actuators, we used an high precision HV-DC Bertan device. It can supplies up to 30kV with currents in the range 0-0.5mA. The function generator is an electronic card based on the integrated device XR-2206 able to manage frequecies in the range 0.1-1MHz. Our goal is to quantify the amount of the longitudinal strain under a continuous stimulus in a finite time interval and to point out the force per unit area in function of the voltage. Figure 4 shows the logitudinal strain vs the voltage supply. It is possible to note that the strain grows while increasing the voltage, the maximum strain is around 7% through 22V/μm for 1 minute. This result is good in comparison to the constraints superimposed to the actuator. Figure 5 shows the force/m^2 produced by the actuator vs voltage against the gravity. These results are preliminary, in fact we are investigating the viscoelestic behaviour of the electroactive material that is not weighed up. Figure 6 shows a picture of the Android.

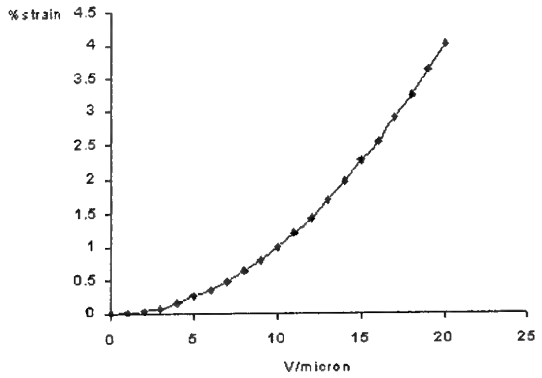

Figure 4 – Strain versus Voltage for the actuator under test

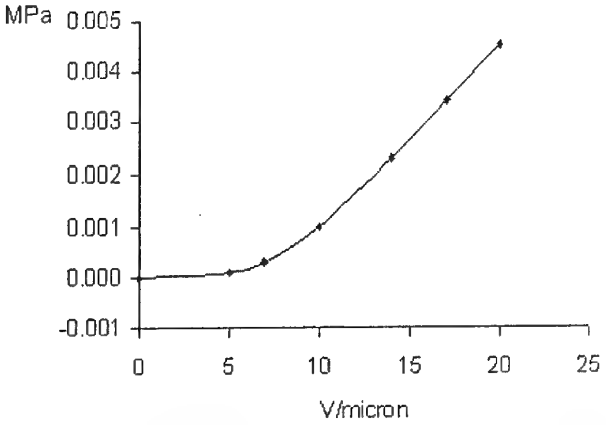

Figure 5 – Force/m^2 versus Voltage for the actuator under test

Figure 6 – The android

CONCLUSION

The EAP can be of fundamental importance in the field of anthropomorphic robotics, micro-robotics and bioengineering representing so many advantages over traditional actuation. Exploiting these properties we are developing in our laboratory a human-like Android unit able to replicate human facial expressions. This face could be a first important step towards the application of EAP in animatronics.

REFERENCES

1) Baughman R., H., and Sacklette L., W., *Science Applications of Conducting Polymers,* Salaneck W., R., et al., Ed., Adam Higler, New York, 47-61, (1991).

2) Pei Q., and Inganas O., *Adv. Mat.*, 4, (1992).
3) Chiarelli P., et al., *Polym. Gels & Net.*, 2, 289-97, (1994).
4) Tanguy J., et al., *J. Electrochem. Soc.: Electrochem. Sci. & Tech.*, 134, (1987).
5) Biot M., A., J. *Appl. Phys.*, 26, 182-5, (1955).
6) Chiarelli P., and De Rossi D., *J. Int. Mat. Systems & Structures*, 396-417.(1992).
7) Tanaka T., and Filmore D., J., *J. Chem. Phys.*, 70, (1970),
8) Chiarelli P., and De Rossi D., *Progr. Coll. Polym. Sci.*, 78, 4-8,(1988).
9) Peters A., and Candau S., J., *Macromolecules*, 21, 2278-82, (1988).
10) Chiarelli P., et al., *Biorheology*, 29, 383-98, (1992).
11) Osada Y., *Adv. Polym. Sci.*, 82, 28, (1987).
12) Eisenberg S., R., and Grodzinsky A., J., *J Biomech. Eng.*, 109, 83, (1978).
13) De Rossi D., et al, *Trans. Am. Soc. Artif. Intern. Organs*, 22, 157-62, (1986).
14) Umezawa K., et al., *Polymer gels*, De Rossi et al. Ed. Plenum press, New York, 195-203, (1991)
15) Gilmore K., et al., *Polym. Gels & Net.*, 2, 135-43, (1994).
16) Suzuki, Proc. Int. Symp. on *Polym. Gels: Fundamental and Intelligent Applications*, Tsukuba, 18-20 September (1989).
17) Kuhn W., et al., in : *Size and shape changes of contractile polymers*, Wasserman A. Ed., Pergamon press, New York, 46-49, (1960).
18) Yoshino K., et al., *Jap. J. of Appl. Phys.*, 28, 490-2, (1989)
19) Bar-Cohen Y., (Ed.), *Proceedings of the SPIE's Electroactive Polymer Actuators and Devices Conf.*, 7th Smart Structures and Materials Symposium, Vol. 3987, ISBN 0-8194-3605-4 (2000) pp 1-360.
20) Bar-Cohen Y., "Electroactive polymers as artificial muscles – Capabilities, potentials and challenges," Handbook on Biomimetics, NTS inc., Japan, Aug 2000
21) Bar-Cohen, Y., (Ed.), *Proceedings of the SPIE's Electroactive Polymer Actuators and Devices Conf.*, 6th Smart Structures and Materials Symposium, Volume 3669, ISBN 0-8194-3143-5, (1999), pp. 1-414.
22) Baughman R.H., C. Cui, A. A. Zakhidov, Z. Iqbal, J. N. Basrisci, G. M. Spinks, G. G. Wallace, A. Mazzoldi, D. de Rossi, A. G. Rinzler, O. Jaschinski, S. Roth and M. Kertesz, "Carbon Nanotune Actuators," Science, Vol. 284, (1999) pp. 1340-1344.
23) Full, R.J., and Tu, M.S., "Mechanics of six-legged runners." J. Exp. Biol. Vol.148, pp. 129-146 (1990).
24) Pelrine R., R. Kornbluh, Q. Pei, and J. Joseph, "High Speed Electrically Actuated Elastomers With Strain Greater Than 100%," Science, Vol. 287, (2000) pp. 836-839.
25) Zhang Q. M., V. Bharti, and X. Zhao, "Giant electrostriction and relaxor ferroelectric behavior in electron-irradiated poly(vinylidene fluoride-trifluorethylene) copolymer," *Science*, Vol. 280, pp.2101-2104 (1998).

LIST OF PARTICIPANTS:

	SPEAKERS:		SPEAKERS:
Ahluwalia, Arti	Arti Ahluwalia Centro "E. Piaggio", Faculty of Engineering, University of Pisa, Via Diotisalvi 2, 56126 Pisa, Italy Tel: ++39-050-5536369 Fax: ++39-050-550650 E-mail: Arti.Ahluwalia@ing.unipi.it	Baughman, Ray	Ray Baughman Honeywell Inc. 101 Columbia Road Post Office Box 1021 Morristown New Jersey, 07962-1021 USA Tel: ++1-973-455-2375 Fax: ++1-973-455-5991 or 5570 E-mail: ray.baughman@honeywell.com
Beebe, Dave J.	Dave J. Beebe Department of Biomedical Engineering UW-Madison 1410 Engineering Drive rm 274 CAE BLDG Madison, WI 53706-1608 USA Tel: ++1-608-262-2260/3013 (rm273), 5112 (rm 70); cell ++1-608-516-9552 Fax: ++1-608-265-9239 E-mail: dbeebe@engr.wisc.edu http: //mmb.bme.wisc.edu	Bicchi, Antonio	Antonio Bicchi Centro "E. Piaggio", Faculty of Engineering, Uiniversity of Pisa Via Diotisalvi 2 56126 Pisa Italy Tel: ++39-050-5536369 Fax: ++39-050-550650 E-mail: bicchi@ing.unipi.it
Bissel, Richard	Richard Bissel Osmetech plc, Electra House, Electra Way Crewe CW1 6WZ UK Tel: Fax: E-mail: rbissel@umist.ac.uk	Cancedda, Ranieri	Ranieri Cancedda Centro di Biotecnologie Avanzate/Istituto Nazionale per La Ricerca sul Cancro - e Dipartimento di Oncologia, Biologia e Genetica, Università di Genova - Genova Italy Tel: Fax: E-mail: cancedda@ermes.cba.unige.it
Chiarelli, Piero	Piero Chiarelli Institute of Physiology, CNR, Pisa, Via G. Moruzzi Pisa Italy Tel. ++39-050-315-2470 Fax: E-mail: ramsete@piaggio.ccii.unipi.it	Dalton, Joan	Joan Dalton Naval Research Laboratory, 4555 Overlook Avenue, SW Washington, DC USA Tel: ++1-202-767-2264 Fax: ++1-202-767-4470 E-mail: sanday@anvil.nrl.navy.mil

Dario, Paolo	Paolo Dario Scuola Superiore Sant'Anna, Via Carducci 40 56100 Pisa Italy Tel: ++39-050-883111 Fax: ++39-883-225 Dario@arts.sssup.it	De Rossi, Danilo	Danilo De Rossi Centro "E. Piaggio", Faculty of Engineering, Uiniversity of Pisa Via Diotisalvi 2 56126 Pisa Italy Tel: ++39-050-5536369 Fax: ++39-050-550650 E-mail: derossi@piaggio.ccii.unipi.it
Diamond, Dermot	Dermot Diamond National Centre for Sensor Research – NCSR, School of Chemical Sciences Dublin City University Dublin 9 Ireland Tel: ++353-1-7005404 Fax: ++353-1-70048021 E-mail: dermot.diamond@dcu.ie	Dittmar, Andre	Andre Dittmar LPm Insa Lyon-ORGA, Bat 401 20 av. A Einstein, 69621 Villeurbanne Cedex France Tel: ++33-472438986 Fax: ++33-472438987 E-mail: dittmar@univ-lyon1.fr
Franceschini, Nicolas	Nicolas Franceschini CNRS, Neurocybernetics Research Group, Laboratory of Neurobiology 31 Chemin J. Aigueir Marseille France Tel: ++33-491164129 Fax: ++33-491220875 E-mail: ENFranceschini@LNB.cnrs-mrs.fr	Galli Resta, Lucia	Lucia Galli Resta Istituto di Neurofisiologia CNR Area della Ricerca CNR Via Giuseppe Moruzzi 1 56100 Pisa Italy Tel: ++39-050-315-3215/3158 Fax: ++39-050-315-3220 E-mail: galli@in.pi.cnr.it
Grattarola, Massimo	Massimo Grattarola Dipartimento Biofisica e Elettronica-DIBE, Università di Genova Via Opera Pia 11/a 16145 Genova Italy Tel: ++39-010-3532761/4 Fax: ++39-010-3532133 E-mail: gratta@dibe.unige.it	Holcombe, Barry	Barry Holcombe Textile and Fibre Technology CSIRO - Belmont Australia Tel: Fax: E-mail: Barry.Holcombe@mail.bigpond.com
in het Panhuis, Marc	Marc in het Panhuis Nanostructure Group Media Lab Europe - - - Tel ++353-87-9483565 Fax: E-mail: mihp@media.mit.edu http: www.medialabeurope.org	Inganas, Olle	Olle Inganas Biomolecular and Organic Electronics, IFM, Linkoping University 58246 Linkoping Sweden Tel: ++46-13-281231 Fax: ++46-13-288969 Mobile: ++46-70-5380981 Home: ++46-131022891 Fax home: ++46-13238639 E-mail: ois@ifm.liu.se http: //www.ifm.liu.se/biorgel/

Jeronimidis, George	George Jeronimidis Centre for Biomimetics, Department of Engineering Reading University 1 Earley Gate Whiteknights Reading, RG6 2AY UK Tel: ++44-118-9318582 Fax: ++44-118-9313327 E-mail: g.jeronimidis@reading.ac.uk	Kane-Maguire, Leon	Leon Kane-Maguire Intelligent Polymer Research Institute, Department of Chemistry, University of Wollongong Northfields Avenue Wollongong NSW 2522 Australia Tel:++61-2-4221-3127 Fax: ++61-2-4221-3114 E-mail: Maguire@uow.edu.au
Kornbluh, Roy	Roy Kornbluh SRI Inernational - - USA Tel: Fax: E-mail: kornblu@erg.sri.com	Madden, John	John D. Madden Bioinstrument Laboratory Department of Mechanical Engineering Massachusetts Institute of Technology 3-147 77 Massachusetts Avenue Cambridge MA 02139 USA Tel: Fax: e-mail: jmadden@MIT.EDU
Mascini, Marco	Marco Mascini Dipartimento di Chimica Via Gino Capponi 50121 Firenze Italy Tel ++39-55-2757274 Fax: ++39-55-2476972 E-mail: Mascini@cesit1.unifi.it http: www.igiene.unifi.it/Chimica/sensori	Mattes, Ben	Ben Mattes SFST 3216 Richard Lane Santa Fè, NM 87505 USA Tel: ++1-505-474-3535 Fax: ++1-505-474-9489 E-mail: mattes@sfst.net
Mazzoldi, Alberto	Alberto Mazzoldi Centro "E. Piaggio", Faculty of Engineering, University of Pisa Via Diotisalvi 2 56126 Pisa Italy Tel: ++39-050-5536369 Fax: ++39-050-550650 E-mail: alberto@ piaggio.ccii.unipi.it	Mussa-Ivaldi, Sandro	Sandro Mussa-Ivaldi Department of Physiology, Department of Physical Medicine and Rehabilitation, Northwestern University Medical School, and Sensory Motor Performance Program Rehabilitation Institute of Chicago - USA Tel: ++1-312-238-1230 Fax: ++1-3112-503-5101 E-mail: sandro@northwestern.edu or sandro@nwu.edu http: //www.northwestern.edu/nuin/faculty/Mussa-Ivaldi_F/ http: //manip.smpp.nwu.edu/4

Parrish, Phil	Phil Parrish Office of Naval Research International Field Office 223 Old Marylebone Road London NW1 5TH UK Tel: Fax: E-mail: pparrish@onrifo.navy.mil	Paul Calvert	Paul Calvert Dep. of Materials Science and Engineering, University of Arizona, AML 4715 E. Fort Lowell Rd Tucson AZ 85721 USA Tel: ++1-520322-2994 Fax: ++1-520-322-2993 E-mail.: calvert@engr.arizona.edu
Persaud, Krishna	Krishna Persaud Department of Instrumentation and Analytical Science, DIAS, UMIST, PO BOX 88, Sackville Streey Manchester, M60 1QD UK Tel: ++44-161-200-4892 Fax: ++44-161-200-4879 E-mail: kcpersaud@umist.ac.uk	Picasso, Bruno	Bruno Picasso Department of Mechanical Engineering Università di Cagliari Piazza d'Armi 09123 Cagliari Italy Tel: ++39-070-6755702 Fax: ++39-070-6755717 E-mail: picasso@zot.unica.it
Pollack, Gerald	Gerald Pollack University of Washington Box 367962 Washington Seattle WA 98195 USA Tel: ++1-206-685-1880 Fax: ++1-206-685-3300 E-mail: ghp@u.washington.edu	Rath, Bhakta B.	Bhakta B. Rath Materials, Science and Componentes Technology Directorate Naval Research Laboratory-NRL Code 6000 Washington DC 20375-5321/43 USA Tel: ++1-202-767-3566/2538 Fax: ++1-202-404-1207 E-mail: rath@uthopia.nrl.navy.mil
Rudolph, Alan	Alan Rudolph DARPA, Defense Science Office 3701 North Fairfax Drive Arlington VA 22203-1714 USA Tel: ++1-703-696-2240 Fax: E-mail: arudolph@darpa.mil	Sanday, Carlos	Carlos Sanday Naval Research Laboratory, 4555 Overlook Avenue, SW Washington, DC USA Tel: ++1-202-767-2264 Fax: ++1-202-767-4470 E-mail: sanday@anvil.nrl.navy.mil
Sandini, Giulio	Giulio Sandini DIST Università di Genova - Genova Italy Tel. Fax: E-mail: sandini@dist.unige.it	Sands, Randy	Randy Sands 20504 Riggs Hill Way, Brookeville MD USA Tel: Fax: E-mail: rrsands@pipeline.com

Scilingo, Enzo Pasquale	Enzo Pasquale Scilingo Centro "E. Piaggio", Faculty of Engineering, University of Pisa Via Diotisalvi 2 56126 Pisa Italy Tel: ++39-050-5536369 Fax: ++39-050-550650 E-mail: pasquale@ piaggio.ccii.unipi.it	Shahinpoor, Mohsen	Mohsen Shahinpoor Artificial Muscles Research Institute, School of Engineering & School of Medicine University of New Mexico Albuquerque NM 87131 USA Tel: ++1-505- 277 3966 Fax: ++1-505- 277 1571 E-mail: Shah@mail.unm.edu
Suzuki, Makoto	Suzuki Makoto Department of Metallurgy, Material Science and Material Processing CIRTU, Graduate School of Engineering, Tohoku University Aoba-yama 02 Sendai 980579 Japan Tel: ++81-22-217-7303 Fax: ++81-22-217-7203 E-mail: msuzuki@argon.material.tohoku.ac.jp	Uwe Meyer, Jorg	Jorg Uwe Meyer Department Sensor System / Microsystems Frauhnhofer Institut IBMT Ensheimer Strasse 48 66386 St. Ingbert Germany Tel: ++49-68941980 150 Fax: ++49-68941980 400 E-mail: uwe.meyer@ibmt.fhg.de http: www.ibmt.fhg.de
Vincent, Julian	Julian Vincent Department of Mechanical Engineering Faculty of Engineering and Design University of Bath Bath BA2 7AY UK Tel: ++44-1225-826933 Fax: ++44-1225-826928 E-mail: J.F.V.Vincent@bath.ac.uk	Wallace, Gordon	Gordon Wallace Intelligent Polymer Research Institute, Department of Chemistry, University of Wollongong Northfields Avenue Wollongong NSW 2522 Australia Tel: ++61-2-4221-3127 Fax: ++61-2-4221-3114 E-mail: gwallace@uow.edu.au
West, Keld	Keld West The Danish polymer Centre Risoe National Laboratory DK-4000 Roskilde Denmark Tel: Fax: E-mail: Keld.West@risoe.dk	Yamauchi, Takeshi	Takeschi Yamauchi. Department of Mechanical Engineering Faculty of Engineering and Design Universiy of Bath Bath BA2 7AY UK Tel: ++44-1225-826933 Fax: ++44-1225-826928 E-mail: Takeshi.Yamauchu@virgin.net Or T.Yamuchi@bath.ac.uk
Rocchia, Walter	Walter Rocchia Centro "E. Piaggio", Faculty of Engineering, University of Pisa Via Diotisalvi 2 56126 Pisa Italy Tel: ++39-050-5536369 Fax: ++39-050-550650 E-mail: rocchia@ piaggio.ccii.unipi.it	Vozzi, Giovanni	Giovanni Vozzi Centro "E. Piaggio", Faculty of Engineering, University of Pisa Via Diotisalvi 2 56126 Pisa Italy Tel: ++39-050-5536369 Fax: ++39-050-550650 E-mail: rocchia@ piaggio.ccii.unipi.it